WRDC-TR-89-4095

IMPROVED TOUGHNESS ALLOYS BASED ON TITANIUM ALUMINIDES

M.J. Blackburn

M.P Smith

United Technologie Corporation
Pratt & Whitney
West Palm Beach, Florida 33402

26 October 1989

Final Technical Report for Period August 1985 thru March 1989

Approved for Public Release; Distribution Unlimited

MATERIALS LABORATORY
WRIGHT RESEARCH DEVELOPMENT CENTER
AIR FORCE SYSTEMS COMMAND
WRIGHT-PATTERSON AIR FORCE BASE, OHIO 45433

DISCLAIMER NOTICE

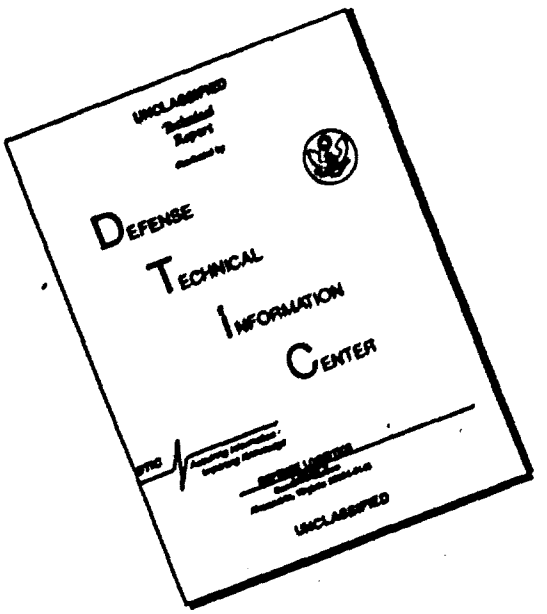

THIS DOCUMENT IS BEST QUALITY AVAILABLE. THE COPY FURNISHED TO DTIC CONTAINED A SIGNIFICANT NUMBER OF PAGES WHICH DO NOT REPRODUCE LEGIBLY.

NOTICE

WHEN GOVERNMENT DRAWINGS, SPECIFICATIONS, OR OTHER DATA ARE USED FOR ANY PURPOSE OTHER THAN IN CONNECTION WITH A DEFINITELY GOVERNMENT-RELATED PROCUREMENT, THE UNITED STATES GOVERNMENT INCURS NO RESPONSIBILITY OR ANY OBLIGATION WHATSOEVER. THE FACT THAT THE GOVERNMENT MAY HAVE FORMULATED OR IN ANY WAY SUPPLIED THE SAID DRAWINGS, SPECIFICATIONS, OR OTHER DATA, IS NOT TO BE REGARDED BY IMPLICATION, OR OTHERWISE IN ANY MANNER CONSTRUED, AS LICENSING THE HOLDER, OR ANY OTHER PERSON OR CORPORATION; OR AS CONVEYING ANY RIGHTS OR PERMISSION TO MANUFACTURE, USE, OR SELL ANY PATENTED INVENTION THAT MAY IN ANY WAY BE RELATED THERETO.

THIS TECHNICAL REPORT HAS BEEN REVIEWED AND IS APPROVED FOR PUBLICATION.

William R. Kerr
Processing and High Temperature
Materials Branch

Norman M. Geyer, Acting Chief
Processing and High Temperature
Materials Branch
Metals and Ceramic Division

FOR THE COMMANDER

Norman M. Tallan
Director
Metals and Ceramics Division

IF YOUR ADDRESS HAS CHANGED, IF YOU WISH TO BE REMOVED FROM OUR MAILING LIST, OR IF THE ADDRESSEE IS NO LONGER EMPLOYED BY YOUR ORGANIZATION PLEASE NOTIFY WRDC/MLLM, WRIGHT-PATTERSON AFB, OH 45433-6533 TO HELP MAINTAIN A CURRENT MAILING LIST.

COPIES OF THIS REPORT SHOULD NOT BE RETURNED UNLESS RETURN IS REQUIRED BY SECURITY CONSIDERATIONS, CONTRACTUAL OBLIGATIONS, OR NOTICE ON A SPECIFIC DOCUMENT.

Unclassified
SECURITY CLASSIFICATION OF THIS PAGE

REPORT DOCUMENTATION PAGE

Form Approved OMB No. 0704-0188

1a. REPORT SECURITY CLASSIFICATION: Unclassified	1b. RESTRICTIVE MARKINGS
2a. SECURITY CLASSIFICATION AUTHORITY	3. DISTRIBUTION/AVAILABILITY OF REPORT: Approved for Public Release; Distribution Unlimited
2b. DECLASSIFICATION/DOWNGRADING SCHEDULE	
4. PERFORMING ORGANIZATION REPORT NUMBER(S): FR-20760	5. MONITORING ORGANIZATION REPORT NUMBER(S): WRDC-TR-89-4095
6a. NAME OF PERFORMING ORGANIZATION: United Technologies Corp. Pratt & Whitney; 6b. OFFICE SYMBOL (If applicable)	7a. NAME OF MONITORING ORGANIZATION: Materials Laboratory (WRDC/MLLM) Wright Research Development Center
6c. ADDRESS (City, State, and ZIP Code): Pratt & Whitney-Florida Operations P.O. Box 109600 West Palm Beach, FL 33410-9600	7b. ADDRESS (City, State, and ZIP Code): Wright-Patterson AFB, OH 45433-6533
8a. NAME OF FUNDING/SPONSORING ORGANIZATION; 8b. OFFICE SYMBOL (If applicable)	9. PROCUREMENT INSTRUMENT IDENTIFICATION NUMBER: F33615-85-C-5030
8c. ADDRESS (City, State, and ZIP Code)	10. SOURCE OF FUNDING NUMBERS

PROGRAM ELEMENT NO.	PROJECT NO.	TASK NO	WORK UNIT ACCESSION NO.
62102F	2420	01	70

11. TITLE (Include Security Classification)

Improved Toughness Alloys Based on Titanium Aluminides

12. PERSONAL AUTHOR(S)
Blackburn, Martin J.; Smith, Michael P.

13a. TYPE OF REPORT	13b. TIME COVERED	14. DATE OF REPORT (Year, Month, Day)	15. PAGE COUNT
Final	FROM 85/08/12 TO 89/03/12	89/10/26	223

16. SUPPLEMENTARY NOTATION

17. COSATI CODES		
FIELD	GROUP	SUB-GROUP
	11	06
	Materials	Metallurgy

18. SUBJECT TERMS (Continue on reverse if necessary and identify by block number)
Titanium Aluminides, Powder Metallurgy, Gas Turbines, Rapid Solidification, Fracture Toughness, Engines, Turbines (JG)

19. ABSTRACT (Continue on reverse if necessary and identify by block number)

Alloy development programs over the past decade have identified alloys, based on the compound Ti_3Al (alpha-two) with tensile and creep properties that indicate applications at temperatures as high as 760C (1400F) should be possible. However, rather low values of toughness and impact resistance at temperatures less than 260C (500F) lead to concerns over component durability during assembly and service. The objective of this program was to improve the toughness of Ti_3Al based alloys. In Phase I, solid solution modifications (Task 1), development of a tough second phase (Task 2), and formation of rare earth oxide dispersions by rapid solidification (Task 3) were investigated. Task 4 evaluated a combination of those alloys and processing techniques from the first three tasks. In Phase II, three alloy systems were selected for scale-up and extensive mechanical property testing.

Titanium Aluminide

20. DISTRIBUTION/AVAILABILITY OF ABSTRACT	21. ABSTRACT SECURITY CLASSIFICATION
☒ UNCLASSIFIED/UNLIMITED ☐ SAME AS RPT ☐ DTIC USERS	Unclassified

22a. NAME OF RESPONSIBLE INDIVIDUAL	22b. TELEPHONE (Include Area Code)	22c. OFFICE SYMBOL
William R. Kerr	(513) 255-9834	WRDC/MLLM

DD Form 1473, JUN 86 Previous editions are obsolete

19. Abstract (Continued)

For conventionally processed ingot metallurgy alloys, higher niobium levels, up to 18 a/o, increased strength, ductility and toughness but resulted in marginal creep resistance. Substitution of 1-2% molybdenum restored creep resistance at a slight toughness loss. Optimum processing for toughness was an isothermal beta reduction followed by quenching into 815C (1500F) molten salt for 30 minutes. Phase blending of a high strength and high toughness alloy powder could double the toughness of a brittle alloy, but resulted in low ductility and elevated temperature properties. Rare earth additions in rapidly solidified alloys yielded no property improvements in alpha-two alloys and those produced generally exhibited low ductility and elevated temperature properties.

Three alloys from the Ti-Al-Nb-Mo system were selected for Phase II scale-up. Toughness values as high as 28 MPa$\sqrt{\text{meter}}$ (25 ksi$\sqrt{\text{inch}}$) were achieved. The optimum property balance was found in the Ti-24Al-17Nb-1Mo alloy system.

FOREWORD

This is the final Technical Report (P&W Report FR-20760) covering work performed under Contract F33615-85-C-5030 for the period 12 August 1985 through 12 March 1989.

The investigation was conducted by Materials Engineering (CT) of Pratt & Whitney, East Hartford, Connecticut under the technical direction of Mr. W. R. Kerr, WRDC/MLLM, Wright-Patterson Air Force Base, Ohio.

Dr. M. J. Blackburn was the Program Manager and Mr. M. P. Smith was the responsible engineer. Metallographic support was provided by Mr. C. A. Barrasso, Mr. A. R. Geary and Mr. T. E. Kenney. Electron microscopy was conducted by Mr. Jim Lin and Mr. G. W. Levan. Samples were prepared by Mr. S. Russo. Ingot preparation was performed by Mr. W. J. Maynard. Thanks are extended to Ms. N. A. Giampolo for typing and editorial assistance.

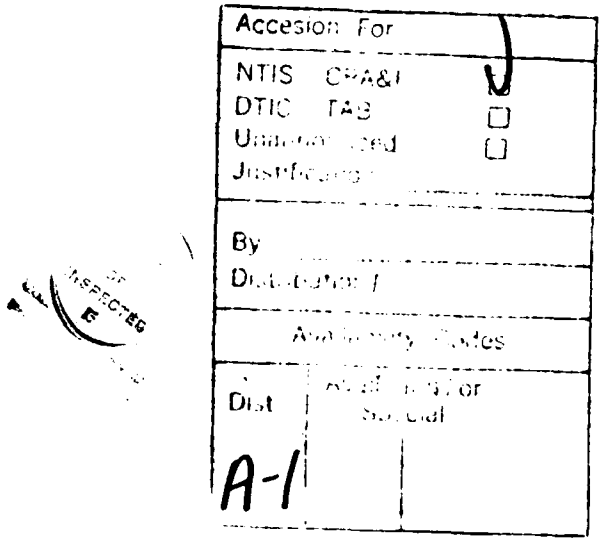

TABLE OF CONTENTS

TABLE OF CONTENTS
(CONTINUED)

LIST OF ILLUSTRATIONS

LIST OF ILLUSTRATIONS
(CONTINUED)

LIST OF ILLUSTRATIONS
(CONTINUED)

LIST OF ILLUSTRATIONS
(CONTINUED)

LIST OF ILLUSTRATIONS
(CONTINUED)

LIST OF ILLUSTRATIONS
(CONTINUED)

LIST OF ILLUSTRATIONS
(CONTINUED)

LIST OF ILLUSTRATIONS
(CONTINUED)

LIST OF TABLES

LIST OF TABLES
(CONTINUED)

LIST OF TABLES
(CONTINUED)

1.0 INTRODUCTION

High performance gas turbine engines depend on materials which are strong, light and able to operate at high temperatures. In the past, major advances in engine technology have been associated with the applications of nickel and cobalt base superalloys and the conventional alpha-beta titanium alloys. Development of alpha-beta titanium alloys has improved high temperature capability to the point where high compressors in advanced engines utilize these lightweight materials. Further extension of the use of lightweight materials to higher temperature structures in the turbine or afterburner sections of the engine is highly desirable; however, current titanium alloys offer only limited scope for improvement without a major breakthrough in alloy design and processing. Materials based on the intermetallic compound Ti_3Al have been evaluated which could offer considerable advantage over conventional alloys in high temperature environments. For example, design analysis and payoff studies have indicated significant weight savings can be achieved in a wide range of engine applications. In general, turbine rotor weight savings from 30 to 40 percent (three to five percent of engine weight) would be achieved with widespread application of titanium aluminides in rotating hardware; engine weight savings of up to sixteen percent could be achieved in fighter engine applications in static structures such as vanes, cases and bearing supports. Beyond the immediate and obvious savings in engine weight, it is possible to translate these benefits into significant fuel savings with attendant effects on operating costs.

The development of alloys based on the Ti_3Al phase has reached an interesting stage. Some current alloys meet many of the strength and ductility goals originally established in the 1970's. However, a barrier to extensive use of these alloys remains the rather low toughness and impact resistance exhibited at temperatures less than 260°C (500°F). If these problems can be overcome, it is possible that aluminide applications could be extended to many critical rotating components in gas turbine engines.

2.0 PROGRAM SCOPE AND APPROACH

2.1 Background

At the inception of the development program on the titanium aluminides, program goals were set based on advanced gas turbine engine property requirements. Previous investigations[1-4] conducted by Pratt & Whitney have defined a small region in the Ti-Al-Nb system that met the strength, ductility and creep rupture goals for Ti_3Al base alloys. The results of these alloy screening studies can be represented in the ternary diagram shown in Figure 1, which illustrates the rather limited compositional range in which acceptable room temperature ductility can be combined with the required stress-rupture capability. The alloy Ti-25Al-14Nb* in the center of this region was used as the base for additional alloy studies. Alloys formulated with vanadium in the 2-4% range as a replacement for niobium exhibited comparable properties and were desirable from a cost and density standpoint, but reductions in environmental resistance eliminated such alloys from extensive consideration. Another interesting addition has proved to be molybdenum which seems to increase both the stiffness (modulus) and stress-rupture properties.

At present, the "best" alloy that has been evaluated in any detail is Ti-25Al-10Nb-3V-1Mo. The tensile and rupture properties of this alloy compared program goals as shown in Figure 2a. Figure 2b shows the toughness and impact values measured for the same alloy which paint a less encouraging picture and certainly suggest that handling during assembly and maintenance of parts made from the alloy could be a problem.

*All values are in atomic percent unless otherwise specified.

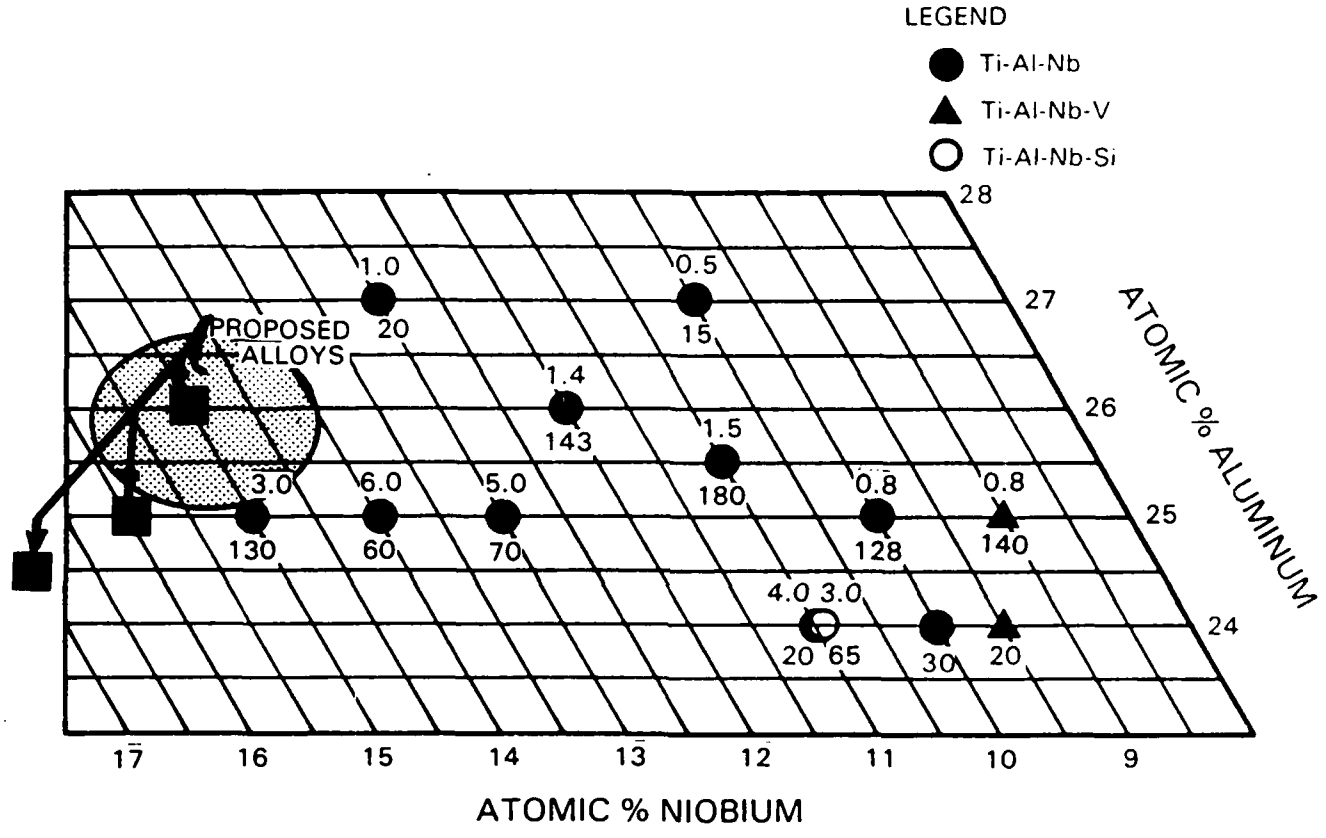

Figure 1

Room temperature tensile ductility (top number) and 1200°F/55 ksi stress-rupture life (bottom number) of forged and solution treated Ti-Al-Nb -(X) alloys showing proposed compositional region to be investigated for solid solution compositions.

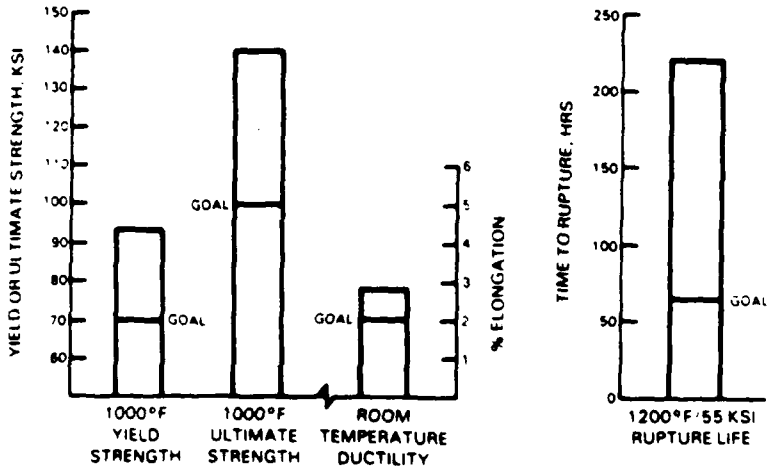

Figure 2(a)

Comparison of tensile properties and creep rupture properties of forged and solution treated Ti-25Al-10Nb-3V-1Mo alloy vs. program goals (tensile strength = to Ti-6Al-2Sn-4Zr-2Mo and creep rupture = to Inconel 718).

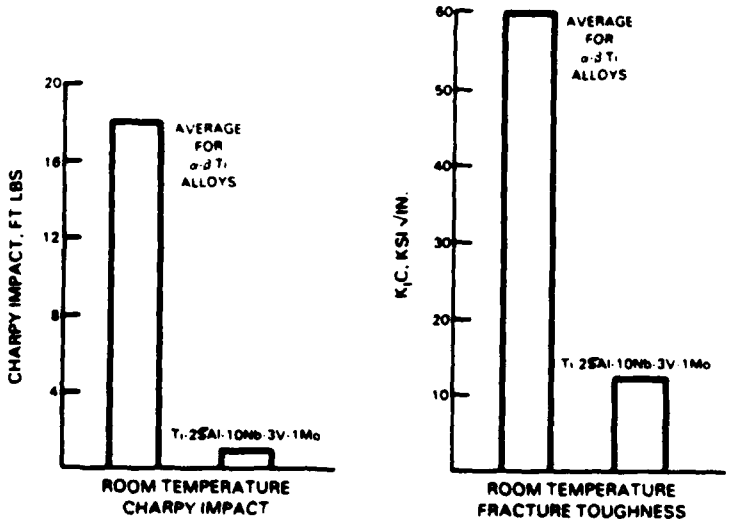

Figure 2(b)

Notched Charpy impact strength and fracture toughness of forged and solution treated Ti-25Al-10Nb-3V-1Mo compared to properties of conventional alpha-beta alloys.

2.2 Program Objective

The objective of this program was to investigate methods of improving the toughness of alpha two alloys with the goal of increasing values to 33 MPa$\sqrt{\text{meter}}$ (30 ksi$\sqrt{\text{inch}}$) without compromising high temperature properties. To achieve this, a two phase effort was conducted. Phase I consisted of four tasks; the first three evaluated methods of improving the toughness of alloy by:

- o Solid solution modification (Task 1)
- o Utilizing a tough second phase (Task 2)
- o Creating fine, stable dispersions by rapid solidification methods (Task 3)

Task 4 combined the best features of these three approaches into a single alloy series. Phase II scaled up the three best materials and processes from Phase I and characterized the mechanical properties of these alloys in some detail.

2.3 Program Approach

2.3.1 Phase I, Task 1: Solid Solution Alloys

We should note that the alloys considered to be most promising are two phase consisting of an alpha-two (Ti_3Al base hexagonal) and beta (body centered cubic) phase although the former predominates. Thus, this task concentrated on methods that could improve the toughness of the alpha-two phase or current phase mixtures. An assumption made in much of the following discussion of alloying strategies is that tensile ductility is related to toughness. In a general sense, this is true, but some of the potential complications are clearly illustrated by relationships in conventional titanium alloys. In these alloys, acicular alpha:beta structures have lower ductility but better toughness than an equivalent

equiaxed alpha:beta phase distribution. It can be noted that optimizing toughness within the aluminides has never been attacked systematically basically because of the preoccupation with the ductility of the alloys. By analogy with conventional titanium alloys, the toughest Ti_3Al structure would be anticipated to be a relatively coarse acicular structure; however, relatively early heat treatment studies have shown that the most ductile alpha-two structure was a very fine acicular structure. The analog of this in conventional titanium alloys would be anticipated to have quite low toughness (for example work conducted at P&W with very similar structures in Ti-6Al-4V produced by the Howmet CST^R process have shown that the fine structure has about half the toughness of more conventionally beta processed material).

Examination of the alloying directions that could improve the toughness of the alpha-two phase reveal that the only two systems that have been shown to exhibit ductility in the "single" phase condition are Ti-Al-Ga and Ti-Zr-In-Al[1]. In the former case, the phase Ti_2Ga is present in the ductile alloy and in the latter a phase mixture of DO_{19} and $L1_2$ lattices occur. Both Ga and In are rather expensive and, therefore, alloys containing large amounts of the elements are not feasible economically. However, it was considered worthwhile to see if smaller gallium additions would have a large impact on the properties of current alloys.

Another factor that has influenced ductility is the oxygen content of alloys; the lower the levels of this element, the higher the ductility at ambient temperatures. As the prospect for low oxygen electrolytic sponge fades, it is apparent that the best the industry can do at present is to hold a level of 0.06% (wt.) oxygen in small experimental heats and a higher value in larger heats. Earlier studies showed that levels of approximately 0.03% could more than double ductility at room temperature[3]. An experimental heat with quite high oxygen levels (0.19 w/o) was the basis of an experiment aimed at reducing the level by the addition of lanthanum. The experiment was at least partially successful

in that elongation at room temperature showed a two-fold increase. It was not clear if the effect arose from effective oxygen gettering or from the grain refinement that was also observed. The use of lanthanide and rare earth additions for either or both reasons was deemed worthy of reinvestigation.

Carbon was another interstitial element that was evaluated in a limited way, in the initial stages of titanium aluminide development. In alloys based on the alpha-two phase, addition of up to 0.7 a/o carbon appeared to improve strength while having a neutral effect on ductility[1]. Addition of up to 0.2 a/o carbon was found to improve creep resistance in gamma base two phase alloys[5]. The conventional alloy IMI 834 also contains carbon to improve processability by "flattening" the thermal approach to the alpha-beta:beta transition, thus permitting the creation of microstructures with small amounts of equiaxed phase present. Since the present alpha-two alloys are similar in many ways to the high creep strength conventional alloys, we felt that this could be a potential approach for thermomechanical processing. Therefore, carbon additions were included in the Task 1 screening trials. Subsequent independent work performed concurrently with the program showed little advantage for an alpha-two:beta microstructure; thus, the need for carbon to control alpha-two content was not pursued.

The other class of alloying elements of interest are the transition metals, most of which are classed as neutral or beta stabilizing elements. Earlier studies[1-3] indicate that Zr and Hf have little or no effect of ductility, so elements in the center of the transition group appear the most attractive candidates for further alloying studies. Niobium has become the centerpiece of this study over the years and the element is surprisingly soluble in aluminides. It was, therefore, decided to evaluate if higher niobium contents can produce tougher structures.

The second part of the first task was an evaluation of thermomechanical effects on two alloys selected in Task 1. The specific process sequences such as heat treatment cycle and the forging procedure were deemed to be important. Options included isothermal or nonisothermal forging methods, the forging sequence and the final forge condition (alpha:beta or beta).

2.3.2 Phase I, Task 2: Alloying to Produce a Tough Second Phase

It is clear from the studies completed to date that the body centered cubic phase is the only viable candidate as a tough phase[1-3]. Other possibilities include, the alpha phase and an ordered $L1_2$ phase, of the Zr_3Al type, for example. Alloys can be made of the alpha/alpha-two type from both the binary and ternary (Ti-Al-Nb) systems. Although high ductility (and by implication toughness) can be exhibited by such alloys, they have two major drawbacks. First is the tendency to be unstable and to exhibit poor high temperature properties. For example, screening work at P&W has shown that Ti:20Al has almost the same stress-rupture capability as conventional titanium alloys. It is possible that <u>if</u> inert particle dispersions are effective strengtheners at high temperatures, the alpha/alpha-two systems could be revisited. The prospect of producing an ordered $L1_2$ structure phase was evaluated quite thoroughly in the early stages of the program[1] and although some success was achieved, no useful alloy appeared feasible.

Therefore, the beta phase is the only second phase that was considered for this program as a toughening agent for aluminide alloys.

There are two basic approaches for using the beta phase to produce a tougher system. The first is to simply manipulate the alloy composition to produce a greater volume fraction of the phase and thus potentially improve the overall toughness of the phase mixture. A second, more radical, approach was to define a beta composition (compatible with the alpha-two phase) with superior toughness, produce both this and an alpha two phase separately, and then mix and consolidate the two phases.

The first approach utilized simple alloy modifications to improve toughness. Molybdenum and tungsten were two obvious candidates to increase the amount of beta phase and also possibly improve the high temperature properties of the phase. Chromium was another candidate element to increase the amount of beta phase. The basic information on how much can be added was rather limited; based on Rockwell work[6], it would seem that at least two atomic percent is soluble in a single phase Ti-Al-Nb base. Thus, it seemed that levels of at least up to four or more percent could be considered in this program. The last beta stabilizer that was considered for this part of the program was copper. In the early series of alloys studied, Cu, Ni and Fe of the late transition elements were added to a number of alloys. Of these, copper in some cases appeared to enhance ductility. As programs became evermore focused on Ti-Al-Nb alloys, this potential beneficial effect was not followed up. This program evaluated the effects of copper at concentrations up to 4% range.

The other aspects of beta phases must be deduced from alloying behavior in conventional titanium-based alloys as so little work has been performed on the aluminide-base systems. Two other candidate elements that emerge from such a study are tin and silicon. Tin is added to most near beta alloys, in part for its effect on low temperature (undesirable) phase changes such as omega-phase formation and also because it appears to enhance toughness. In the case of silicon, there is some evidence that high temperature properties could be greatly improved by this element.

The second approach was to develop a method to form a beta phase and distribute this through an alpha-two matrix. It was proposed to do so using powder metallurgy methods. Obviously such a system could be metastable, but two factors made the approach workable in this case. First, the projected operating temperatures are relatively low for Ti_3Al type alloys (704-1400°F maximum) where interdiffusion will still be quite slow. By selecting specific alloys, any interdiffusion that does occur

can be tailored to prevent any deleterious interfacial alloy compositions. The first problem with the approach was to define beta alloys with an attractive property balance. Compositions of the beta phase in current aluminides were taken as a starting point. Analysis of this phase in the Ti-25Al-10Nb-3V-1Mo indicates the approximate composition is Ti-20Al-15 (Nb+V+Mo) as indicated in Figure 3. Thus, a beta phase was constructed with somewhat less aluminum and more beta stabilizing elements. The choices were not unlimited, however; ordered B2 and $L2_1$ structure can occur in these compositional areas and obviously had to be avoided. Further, if too much aluminum was removed, oxidation resistance may well be compromised. The general area of compositions that were evaluated in this program are also indicated in Figure 3. Silicon additions were considered to improve creep resistance of the beta phase. If too large a difference in creep capability exists, then the properties of the overall system could be compromised.

2.3.3 Phase I, Task 3: Dispersoid Containing Alloys

This third class of alloys suggested for this study were a rapidly solidified (RS) product. The objective was to create a uniform fine dispersion of stable particles in any alloy and in this way not only increase strength but modify plastic flow characteristics. If the slip distribution or flow dynamics could be modified correctly, then improved toughness levels could result. The approach has much in common with current programs that are modifying conventional titanium alloys with rare earth elements, notably erbium, to form very fine stable oxides[7].

Too large an increase in strength produced by a fine oxide dispersion of this rather low ductility system could cause a problem at ambient temperatures. On the other hand, if oxide dispersions are effective high temperature strengtheners, they could be very important in beta alloys where creep properties are anticipated to be low. The specific element chosen to form an oxide dispersion could include a lanthanide that tends

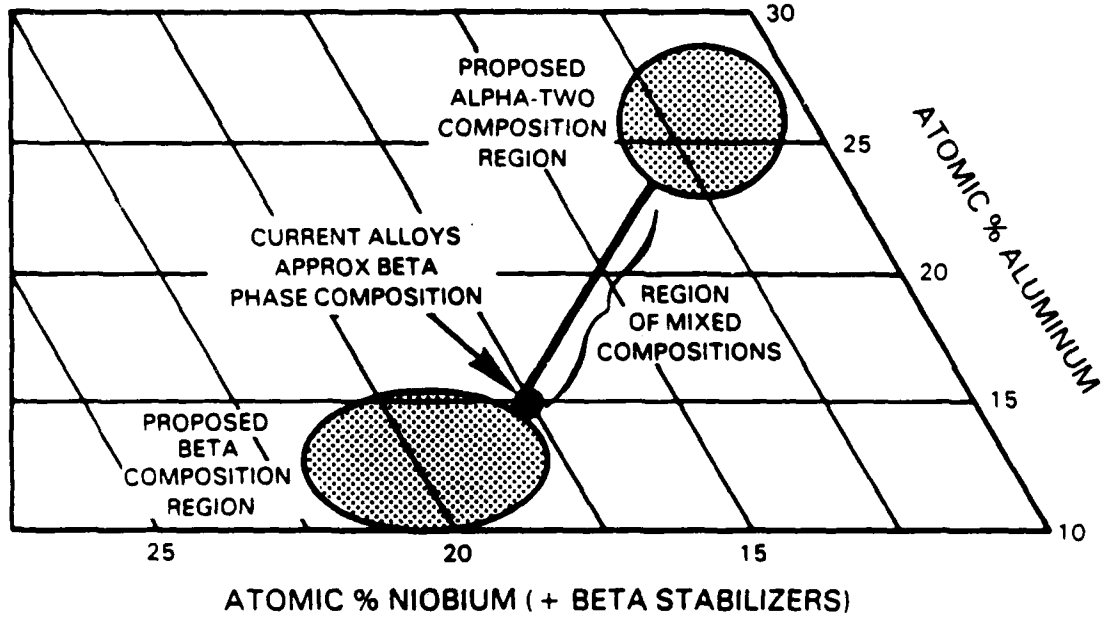

Figure 3

Proposed alpha-two and beta compositional ranges for developing alloys with a tough second phase.

to form coarser particle (probably in the melt) or erbium or other related rare earth elements which form fine dispersions. The key could be the ability to form a controlled dispersion from both a size and distribution standpoint and to insure that the selected components of the systems are compatible.

A second effect that could influence toughness was the removal of oxygen from solid solution by the formation of stable rare earth oxides. As noted above, low oxygen results in quite large increases in ductility at low temperatures.

To screen potentially useful systems, small amounts of alloys evaluated in the tasks 1 and 2, or in previous studies (Ti-25Al-10Nb-3V-1Mo for example) were doped with selected rare earth elements, etc. A limited quantity of splat was produced to evaluate the nature of dispersoid found and its thermal stability.

Based on the results of these screening studies, an alloy composition was selected for powder production.

2.3.4 Phase I, Task 4: Combination Alloys

Task 4 combined various features of the above three approaches into a single alloy series.

2.4 Phase II: Scale-Up

This phase involved selecting the three most promising alloys/processes from Phase I and conducting a fairly extensive property testing effort.

3.0 PHASE I RESULTS AND DISCUSSION

3.1 Phase I, Task 1: Solid Solution Alloys

3.1.1 Alloy Composition and Processing - Alloy Screening

The general outline of the experimental procedure for Task 1 was as follows. Alloys were formulated based on the principles outlined in section 2.3.1; see Table 1 for specifics, and ingots produced using a nonconsumable arc drop casting technique. The selected elements or master alloy were melted several times in a semicircular water cooled copper mold using a thoriated tungsten electrode to form a homogeneous hemispherical button. During the final melt, the button is superheated rapidly allowing the melt to drop into a 25 mm (1 in) diameter x 100 mm (4 in) long water cooled copper mold. A typical drop casting is shown in Figure 4. Aim and actual chemistries for Task 1 alloys are given in Tables 1 and 2.

The beta transus of each alloy was measured by metallographic examination of pieces quenched from temperatures in the range 982-1150°C (1800-2100°F). Values are listed in Table 1. The remainder of each casting was hot isostatically pressed (HIP) at temperatures approximately 27°C (50°F) below the beta transus.

The HIP castings were prepared for forging by lathe turning and chamfering the corners and coating with boron nitride as a lubricant. Forging was conducted on a 4.5 MN (500 ton) isothermal press at the P&W facility in West Palm Beach, FL. Upset was accomplished in vacuum on TZM alloy flat dies at a strain rate of 2.5 mm/mm/min (0.1 in/in/min). Temperatures were the same as those selected for HIP in order to produce a fine grained alpha-beta processed microstructure. A typical forging is shown in Figure 5.

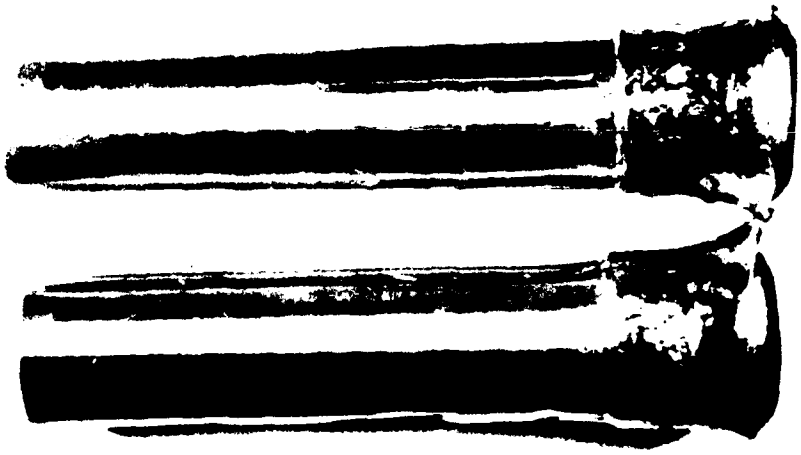

Figure 4 Mag: ~1X

Typical titanium aluminide drop casting, 25 mm (1 in) diameter x 100 mm (4 in) long. Castings are machined to a uniform diameter prior to forging.

Figure 5

Isothermally forged titanium aluminide drop casting (side upset).

Table 1

Composition and
Processing Data for
Task 1 Alloys

Alloy No.	Composition a/o (w/o)				Beta Transus Temp. °C (°F)	HIP/Forge Temp. °C (°F)	Hardness, Hv	
	Al	Nb	V	Other			As-Forged	Heat* Treated
2	25 (13.1)	10 (18.0)	-	20 (27.1) Ga	Not Determined	Could not forge	-	-
3	25 (14.1)	10 (19.5)	4 (4.3)	0.5 (1.4) La	1093-1120 (2000-2050)	1093 (2000)	408	265
4	25 (14.1)	10 (19.4)	4 (4.3)	0.5 (1.7) Er	1070-1093 (1950-2000)	1038 (1900)	350	306
5	25 (14.1)	10 (19.5)	4 (4.3)	0.5 (1.5) Ce	1150-1176 (2100-2150)	1150 (2100)	330	296
6	25 (14.3)	10 (19.7)	4 (4.3)	0.2 (0.05) C	1204-1232 (2200-2250)	1150 (2100)	363	290
7	25 (14.3)	10 (19.7)	4 (4.3)	0.4 (0.1) C	1232-1260 (2250-2300)	1150 (2100)	386	299
17	26 (14.1)	15 (28.3)	-	-	1150-1176 (2100-2150)	1150 (2100)	296	260
18	25 (13.5)	16 (29.8)	-	-	1150-1176 (2100-2150)	1150 (2100)	316	280
19	24.5 (13.1)	17 (31.3)	-	-	1120-1150 (2050-2100)	1093 (2000)	296	284

*Beta transus + 27°C (50°F)/1 hour/air cool + 815°C (1500°F)/1 hour/air cool

Table 2

Chemical Analysis Results
for Task 1 Alloys
(In Weight %)[1]

Alloy No.		Al	Nb	V	Other	O_2
3	Aim	14.0	20.0	4.3	1.4 La	0.10 max.
	Actual	14.2, 14.4	19.7, 19.5	4.6, 4.6	0.93, 0.93	0.10, 0.11
4	Aim	14.0	20.0	4.3	1.5 Er	0.10 max.
	Actual	14.0, 14.4	20.0, 19.4	4.6, 4.6	1.54, 1.64	0.079, 0.061
5	Aim	14.0	20.0	4.3	1.5 Ce	0.10 max.
	Actual	14.2, 14.5	19.2, 19.4	4.5, 4.6	1.0, 1.12	0.097, 0.080
6	Aim	14.0	20.0	14.3	0.05 C	0.10 max.
	Actual	14.1. 14.4	19.3, 19.4	4.5, 4.5	0.07, 0.06	0.086, 0.080
7	Aim	14.0	20.0	4.3	0.10 C	0.10 max.
	Actual	14.2, 14.5	19.2, 19.3	4.5, 4.5	0.12, 0.12	0.098, 0.082
17	Aim	14.0	28.0	-	-	0.10 max.
	Actual	14.3, 14.3	27.8, 27.4	-	-	0.050, 0.057
18	Aim	14.0	20.0	-	-	0.10 max.
	Actual	13.5, 13.6	29.3, 28.3	-	-	0.045, 0.057
19	Aim	13.0	31.0	-	-	0.10 max.
	Actual	13.2, 13.4	30.3, 30.5	-	-	0.051, 0.061

[1]One analysis from each casting (two castings per alloy).

It was decided to normalize microstructure for the alloys and provide a high toughness condition by solution treating all forgings at 27°C (50°F) above the beta transus followed by air cooling. The solution treated forgings were then stabilized by heating to 815°C (1500°F) for one hour and air cooling. Independent internal work on Ti-25Al-10Nb-4V alloy demonstrated that stabilization at 815°C (1500°F) resulted in good toughness with no detrimental effect on tensile or creep-rupture properties. It was also considered that this process would result in improved microstructural stability and, by maintaining a similar microstructure for all alloys, the property differences measured would focus on compositional effects.

3.1.2 Results and Discussion - Alloy Screening

Metallographic examination and hardness testing revealed that the selected heat treatment approach achieved in general, the aim of normalizing microstructure. Hardness values (Table 1) lay in a narrow range of 280-310 for all alloys. Microstructures typically consisted of relatively coarse beta grains with alpha/alpha-two platelets in a Widmanstatten array. Some grain boundary alpha-two phase was also present. The rare earth modified alloys 3, 4 and 5 (La, Er and Ce, respectively) were studied more closely to evaluate the size and distribution of the oxide particles. Examination of polished and very lightly etched specimens revealed that specimens containing lanthanum or cerium exhibited quite large dispersed particles ranging from 100-300μm in diameter, while the erbium-containing Alloy 4 had dispersed particles in the 10-30μm range uniformly distributed in the matrix (Figure 6). Microprobe analysis revealed that some of the rare earth additions did not react to form oxides. An example of this is shown in Figure 7.

Mechanical property characterization consisted of RT, 427°C (800°F), 650°C (1200°F) tensile testing; 650°C/385 MPa (1200°F/55 ksi) creep-rupture testing; and fracture toughness testing of fatigue

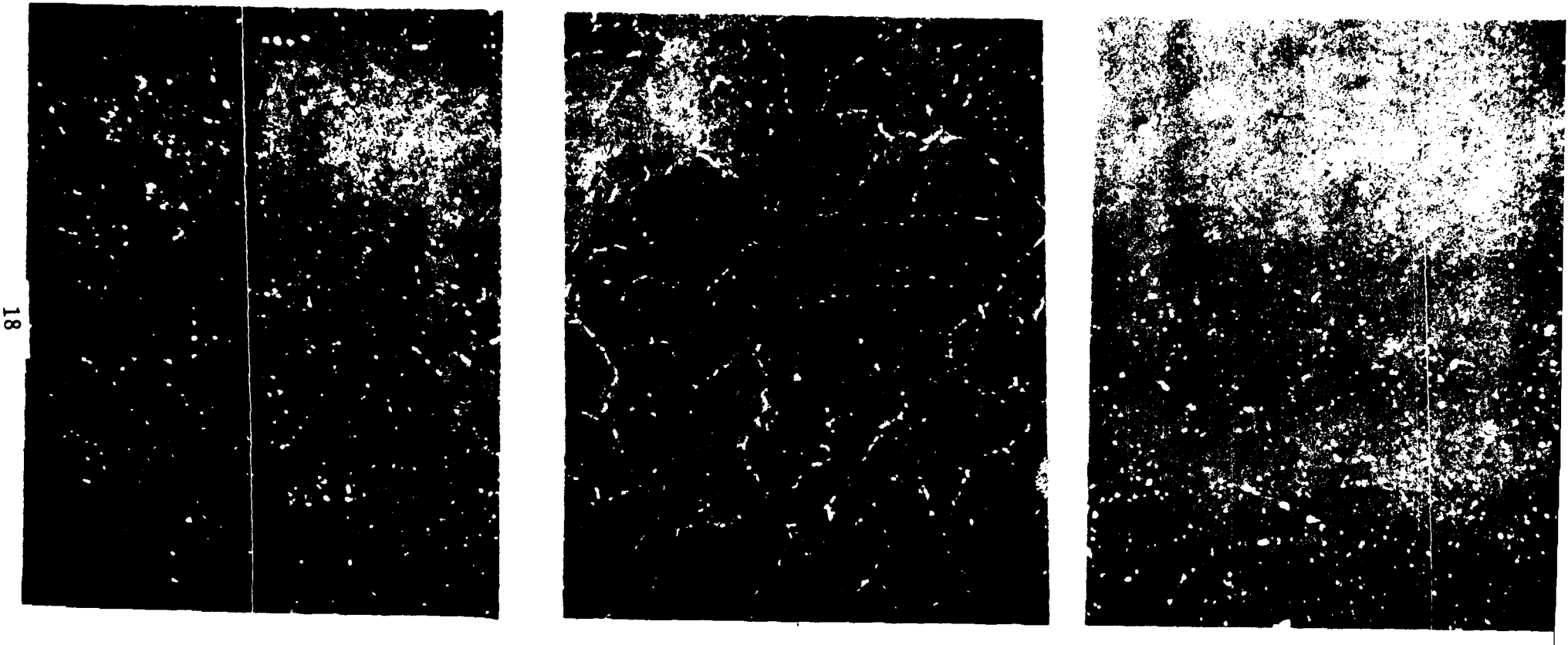

Figure 6 100X

Second phase distribution in La, Er and Ce modified Ti-25Al-10Nb-4V alloys.

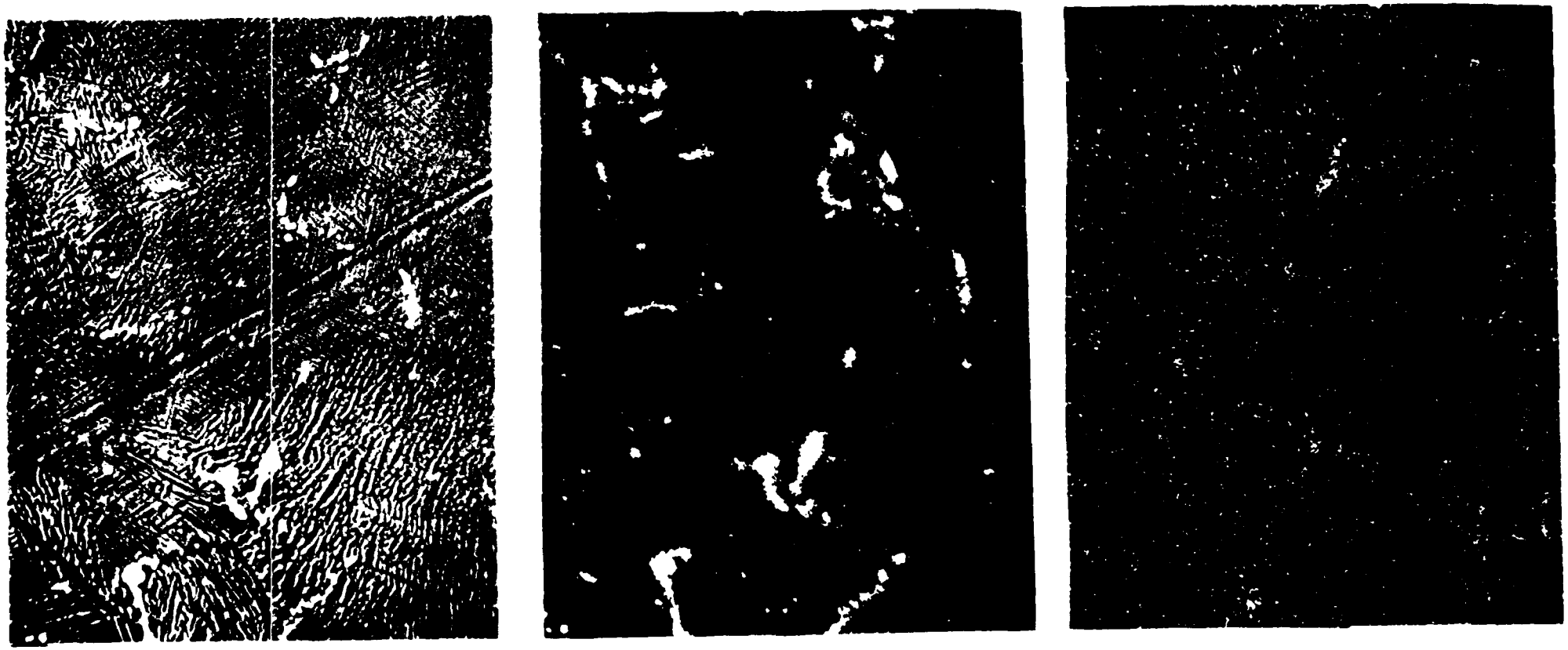

Figure 7

Erbium and oxygen distribution in forged and heat treated Ti-6Al-4V-2Nb alloy.

precracked, chevron notched bend specimens* at room temperature. Tensile data (Table 3) may be compared with the property goals shown in Figure 2 in section 2.1. None of the Task 1 alloys tested met all the strength and ductility goals.

The lanthanum and cerium-containing alloys (3 and 5, respectively) had acceptable properties at RT and 427°C (800°F) and the quite good RA values for the La modified alloy at RT should be noted. However, the lanthanum and cerium-containing alloys showed poor properties at 650°C (1200°F).

The erbium containing Alloy 4 had somewhat lower strength and ductility at room temperature, but significantly better properties at 427°C (800°F) and 650°C (1200°F) than the lanthanum and cerium-containing Alloys 3 and 5. Microprobe and SEM analysis were employed in an attempt to understand the differences. The following observations were made, based on these analyses:

- The erbium dispersoids were much finer than the lanthanum and cerium-rich particles (Figure 6b).

- The erbium dispersoids were essentially confined to the beta grain boundaries (Figure 6b).

- Fracture surfaces of the RT tensile specimens of each alloy were similar in appearance and appeared to be a mixture of transgranular and cleavage fracture (Figures 8a and 9a).

*ASTM method E399-83

Table 3

Tensile Properties of Task 1 Alloys

Alloy No.	Alloy a/o	Test Temp. °C	Test Temp. (°F)	0.2% Yield Str. MPa	0.2% Yield Str. (Ksi)	Ult. Tens. Str. MPa	Ult. Tens. Str. (Ksi)	% EL	% RA
3	Ti-25Al-10Nb-4V-.5La	21	(70)	511	(74.0)	649	(94.1)	2.8	4.0
				527	(76.4)	603	(87.4)	1.6	3.0
		427	(800)	332	(48.1)	509	(73.8)	6.5	5.3
				357	(51.7)	518	(75.0)	6.0	4.0
		650	(1200)	-	-	157	(22.7)	0.8	-
				-	-	174	(25.2)	0.7	-
4*	Ti-25Al-10Nb-4V-.5Er	21	(70)	-	-	348	(50.5)	0.67	-
				518	(75.0)	598	(86.6)	1.2	1.3
		427	(800)	372	(53.9)	671	(97.2)	9.0	10.4
				-	-	-	-	-	-
		650	(1200)	348	(50.5)	515	(74.6)	3.8	4.0
				-	-	-	-	-	-
5	Ti-25Al-10Nb-4V-.5Ce	21	(70)	520	(75.3)	617	(89.4)	2.2	-
				518	(75.0)	591	(85.6)	1.6	0.7
		427	(800)	301	(49.6)	403	(58.4	2.6	2.0
				340	(49.3)	406	(58.8)	2.3	1.3
		650	(1200)	-	-	115	(16.6)	0.5	-
				-	-	126	(18.2)	0.6	-
6	Ti-25Al-10Nb-4V-.2C	21	(70)	544	(78.8)	582	(84.3)	0.67	-
				562	(81.5)	621	(90.0)	1.1	1.4
		427	(800)	328	(47.6)	502	(72.8)	8.6	9.2
				344	(49.9)	515	(74.6)	8.9	10.4
		650	(1200)	333	(48.2)	493	(71.4)	7.3	10.4
				328	(47.6)	508	(73.7)	8.2	14.2

*Due to a machining error, only four specimens were available for alloys 4 & 17.

Table 3

Tensile Properties of Task 1 Alloys
(Continued)

Alloy No.	Alloy a/o	Test Temp. °C	Test Temp. (°F)	0.2% Yield Str. MPa	0.2% Yield Str. (Ksi)	Ult. Tens. Str. MPa	Ult. Tens. Str. (Ksi)	% EL	% RA
7	Ti-25Al-10Nb-4V-.4C	21	(70)	554	(80.3)	676	(97.9)	1.9	2.6
				594	(86.1)	708	(102.6)	1.4	2.6
		427	(800)	424	(61.4)	645	(93.5)	5.0	4.0
		650	(1200)	344	(49.9)	520	(75.3)	7.8	9.1
				344	(49.9)	550	(79.7)	9.8	10.4
				342	(49.6)	552	(80.0	8.0	9.2
17*	Ti-26Al-15Nb	21	(70)	484	(70.2)	511	(74.1)	1.3	-
				491	(71.2)	566	(82.0)	1.2	2.7
		427	(800)	343	(49.8)	635	(92.0)	8.3	5.3
				-	-	-	-	-	-
		650	(1200)	348	(50.5)	588	(85.2)	8.8	15.4
18	Ti-25Al-16Nb	21	(70)	517	(74.9)	580	(84.1)	1.0	-
				563	(81.6)	673	(97.5)	1.6	2.6
		427	(800)	421	(61.0)	660	(95.7)	8.5	9.8
				393	(57.0)	632	(91.6)	7.3	10.5
		650	(1200)	424	(61.4)	600	(86.9)	6.3	14.2
				396	(57.4)	586	(84.9)	7.3	13.0
19	Ti-24.5Al-17Nb	21	(70)	508	(73.6)	671	(97.3)	3.9	6.0
				576	(83.5)	676	(97.9)	1.8	2.7
		427	(800)	400	(58.0)	644	(93.4)	9.9	11.6
				386	(56.0)	680	(98.5)	16.2	21.4
		650	(1200)	427	(61.9)	597	(86.6)	5.5	7.9
				374	(54.2)	551	(79.8)	10.5	14.0

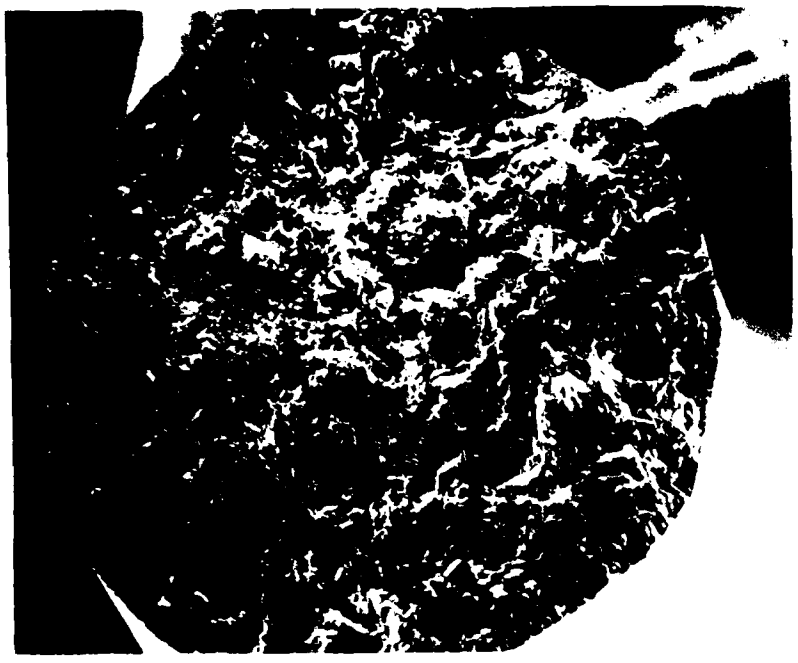

(a) 25X

(b) 25X

Figure 8

Fracture surface typical of Er containing Ti-25Al-10Nb-4V (Alloy 4). a) RT tensile; b) 650°C (1200°F) tensile. Note similar nonoriented fracture surface at both temperatures.

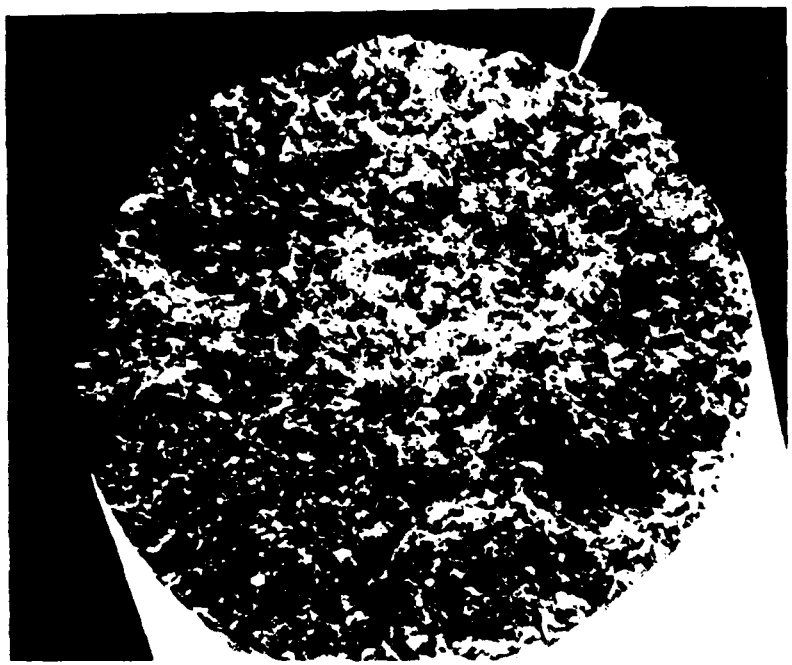

25X

(a)

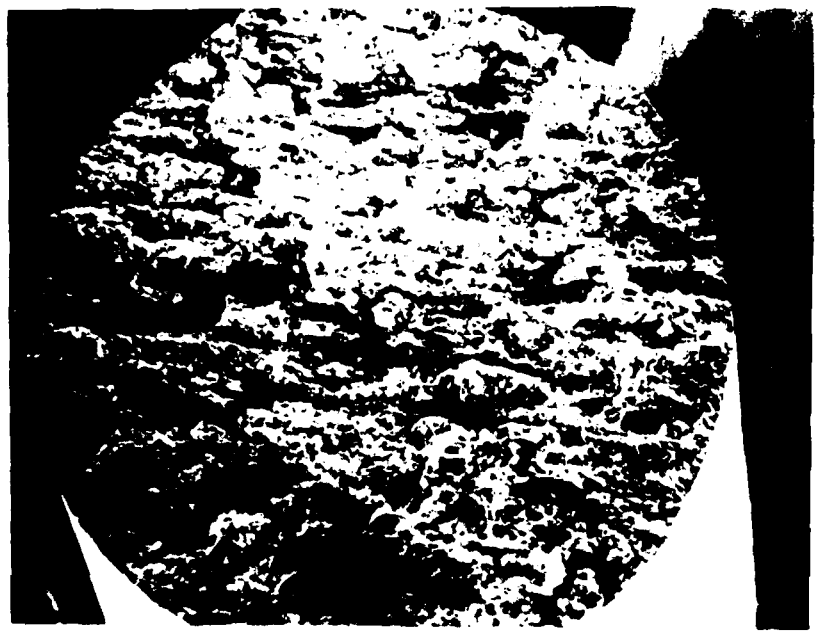

25X

(b)

Figure 9

Fracture surface typical of La and Ce containing Ti-25Al-10Nb-4V (Alloys 3 and 5). a) RT tensile; b) 650°C (1200°F) tensile. Note unusual parallel fracture ridges at 650°C (1200°F).

- At 650°C (1200°F), the lanthanum and cerium containing alloys appeared to fail along preferred planes parallel to the fracture surface. The failure planes seemed to be the beta grain boundaries formed in the cast ingot and subsequently flattened during forging. In contrast, the erbium alloy tested at 650°F (1200°F) had a similar fracture appearance as the companion room temperature specimen (Figures 8b and 9b).

The poor elevated temperature properties of the lanthanum and cerium containing alloys is believed to be caused by the massive oxide particles and/or segregation present in the prior beta grain boundaries in a region where boundary sliding is an important deformation mechanism.

The Ti-25Al-10Nb-4V alloys containing carbon additions failed to meet strength and ductility goals and were lower in strength than a similarly processed Ti-25Al-10Nb-4V alloy ring evaluated in an independent study. Of the three alloys with variations in the Al-Nb ratio, only Alloy 19 (Ti-24.5Al-17Nb) showed potential promise due to its higher strength and ductility at room and higher temperatures.

Creep-rupture data are given in Table 4. At the 650°C/385 MPa (1200°F/55 ksi) condition, it is no surprise that the lanthanum and cerium alloys ruptured on loading and the erbium alloy failed in a short time as the ultimate strengths are less than 385 MPa (55 ksi). The carbon containing alloys exhibited somewhat better rupture resistance but also fell below goal life. Only the three ternary Ti-Al-Nb alloys lasted longer than 60 hours with the Ti-26Al-15Nb alloy (No. 17) reaching an excellent life of 240 hours.

Fracture toughness data for the Task 1 alloys are also presented in Table 4. It can be seen that all alloys exceeded the 12.6 MPa$\sqrt{\text{meter}}$ (11.6 ksi $\sqrt{\text{inch}}$) value of the baseline material by at least 5.5 MPa$\sqrt{\text{meter}}$ (5 ksi $\sqrt{\text{inch}}$). The highest toughness was measured at 28.3 MPa$\sqrt{\text{meter}}$ (26.0 ksi $\sqrt{\text{inch}}$) for Alloy 19 which approaches the toughness levels exhibited by some high strength titanium alloys.

Table 4

RT Fracture Toughness and 650°C/385 Mpa
(1200°F/55 Ksi) Creep-Rupture Properties
of Task 1 Alloys

	Alloy a/o	Fracture Toughness		Creep, Life, Hours				RT Post Test	
		MPa √Meter	Ksi √Inch	0.2%	0.5%	1.0%	Rupture	%EL	%RA
3	Ti-25Al-10Nb-4V-.5La	22.4	20.6	-	R.O.L. in Radius*		-	2.0	-
4	Ti-25Al-10Nb-4V-.5Er	16.6	15.2	0.1	0.4	2.1	2.5	3.5	4.6
5	Ti-25Al-10Nb-4V-.5Ce	23.1	19.5	-	R.O.L. in Radius		-	0.3	-
6	Ti-25Al-10Nb-4V-.2C	19.9	18.3	<0.1	<0.1	<0.2	2.8	9.4	12.5
7	Ti-25Al-10Nb-4V-.4C	19.1	17.5	<0.1	<0.1	0.2	31.5	10.0	12.3
17	Ti-26Al-15Nb	19.2	17.6	0.8	13.2	71.5	246.0	4.3	5.0
18	Ti-25Al-16Nb	20.7	19.0	1.6	10.7	33.6	68.2	7.3	5.5
19	Ti-24.5Al-17Nb	28.3	26.0	1.6	10.8	36.0	62.0	4.3	11.7

*ROL = Ruptured on Loading

Task 1 of the program required that the two best alloys be selected for more complete screening of the effect of thermomechanical processing on mechanical properties. One obvious alloy was the Ti-24.5Al-17Nb (Alloy 19) composition with its high toughness and ductility, combined with adequate tensile strength and creep-rupture capability. No promising second alloy was apparent. Therefore, an alloy from Task 2, described in section 3.2.2, was selected as the second material for thermomechanical processing. The composition of this alloy was Ti-25Al-10Nb-4Mo (Alloy 15).

3.1.3 Thermomechanical Processing (TMP)

A 4 Kg (9 lb) ingot of each alloy was prepared by VAR melting for the processing trials. To produce material with a low oxygen content, the highest quality raw materials were used and the process cycle was controlled to minimize oxygen pickup.

Titanium sponge was obtained from International Titanium Inc. of Moses Lake, Washington. The sponge was high purity with low (0.05 w/o) oxygen. The sponge was specially screened through a 12 mm (0.5 in) screen to facilitate consolidation. The sponge compacted easily and exhibited very little outgassing during melting. Elemental aluminum additions were made using ALCOA high purity shot (99.999%) with less than 0.001 oxygen; however, most aluminum and niobium additions were made using a high purity 60Nb-40Al master alloy made in-house or procured from Shieldalloy. Molybdenum additions were made using high purity Mo_3Al. Oxygen content of the master alloys was less than 0.001% in all cases.

Melting of primary electrodes was conducted in a Leybold-Heraeus LH-1 model consumable arc furnace; the specific procedure used is given in Table 5. Samples for chemical analysis were drilled from top, middle and bottom locations of the ingot. A solid sample was removed from the side of the ingot for oxygen analysis. Analyzed chemical composition of the ingots is given in Table 6; the oxygen level was held below 0.10%.

Table 5

Titanium Aluminide Ingot Production Procedure

- Cut 3.8 cm (1.5 in) diameter commercially pure tubing to required length; machine end caps 0.54 cm (0.25 in) in thickness.
- Acid clean tubing and caps per POP 223 and store in clean bags or brown paper until ready to use.
- Weld bottom caps to tubes in an inert atmosphere of argon.
- Fill tube gradually with blended alloy elements and titanium sponge. Cold press using a titanium ram at 105 MPa (15 ksi).
- Weld to make primary electrode; VAR melt into 7.6 cm (3 in) diameter crucible.
- Quarter first melt electrode and reweld electrodes into a new stick.
- Remelt into 7.6 cm (3 in) diameter mold.
- Remove material for chemical analysis.

Table 6

Chemical Composition of Task 1
TMP Ingots* (W/O)

	Al		Nb		Mo		O^2	
Alloy	Aim	Actual	Aim	Actual	Aim	Actual	Aim	Actual
19	13.0	12.8	31.0	30.9	-	-	0.10**	0.07
15	13.7	12.8	19.0	18.7	7.8	7.6	0.10**	0.09

*Average of three locations
**Maximum

After double melting, the ingots were hot isostatically pressed at 1000°C (1832°F) and 105 MPa (15 ksi) for 3 hours to seal internal porosity and pipe. The HIP'ed ingots were cut into two sections and lathe turned to remove the surface and square the ends. One section of each alloy was isothermally beta forged at 1175°F (2150°F) using the 4.5 MN (500 ton) press at P&W in West Palm Beach, FL. Forging reduction was from 7.5 cm (3 in) high to 1.25cm (0.5 in). The remaining section from each alloy was isothermally beta forged using a similar reduction schedule, followed by quenching into 815°C (1500°F) molten salt for 30 minutes at Wyman-Gordon Co., Millbury, MA. A typical ingot and pancake forging is shown in Figure 10. Each pancake forging was cut into two equal pieces for heat treatment, resulting in a total of eight conditions. A summary of the eight conditions studied is given in Table 7.

Structural characterization and hardness testing was performed to give a preliminary indication of property capability. Both alloys exhibited a coarse, nearly equiaxed macrostructure after forging and air cooling off the press. This structure persisted in both the aged and resolution treated and aged conditions. In contrast, the direct off the press salt quenched forgings exhibited a finer, heavily deformed and elongated macro grain flow (Figure 11) which remained unchanged in subsequent heat treatments. While similar macro effects were noted in both alloys, there were major differences at a microstructural level. In order to facilitate discussion, each alloy will be treated separately.

Ti-24.5Al-17Nb (Alloy 19)

After forging and air cooling, Alloy 19 (Ti-24.5Al-17Nb) exhibited a very fine needle-like Widmanstatten microstructure (Figure 12a). Direct aging at 650°C (1200°F) for 8 hours resulted in no resolvable change in the microstructure (Figure 12b) and no change in hardness (both averaged Hv 360). After solution treating at 27°C (50°F) below the beta transus, the microstructure consisted of well-defined prior beta grains averaging 0.375 mm (0.0157 in) in diameter (Figure 12c) containing a coarse Widmanstatten basket weave structure. Hardness was Hv 278. Forging

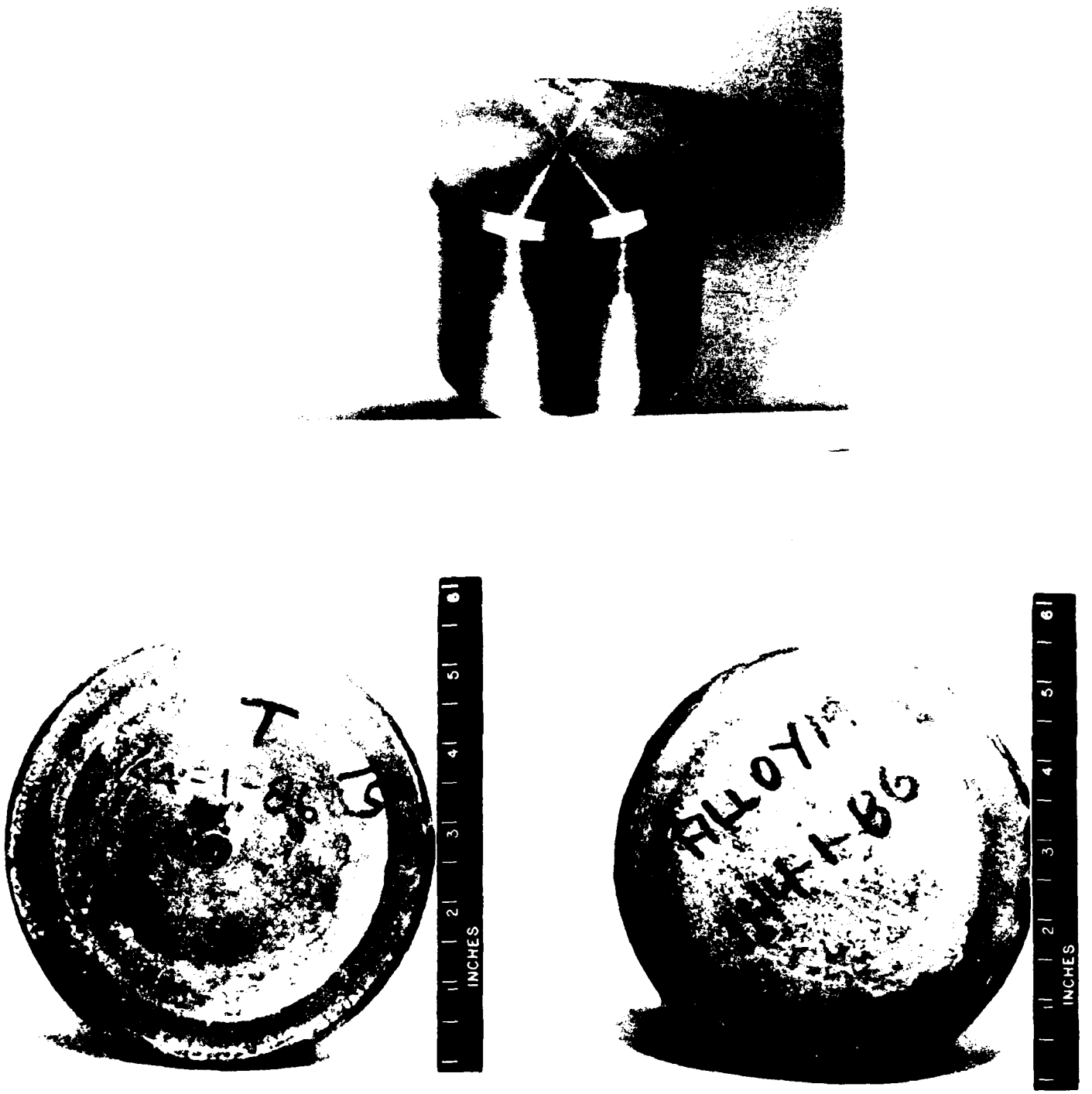

Ti-24.5Al-17Nb Alloy 19 after isothermal beta forging at 1175°C (2150°F) followed by quenching into 815°C (1500°F) molten salt for 30 min. The ingot section prior to forging is shown in top photo.

Table 7

Heat Treatment Schedule for
Task 1 TMP Alloy Study

Alloy No.	Composition	Forging Temp./Cool °C	°F		Heat Treatment
19-1	Ti-24.5Al-17Nb	1175	2150	Air Cool	650°C (1200°F)/8 hours AC
19-2	"	"	"	"	1050°C (1925°F)/1 hour AC + 650°C (1200°F)/8 hrs AC
19-3	"	"	"	Salt Quench*	As-Forged
19-4	"	"	"	"	650°C (1200°F)/8 hours AC
15-1	Ti-25Al-10Nb-4Mo	1175	2150	Air Cool	650°C (1200°F)/8 hours AC
15-2	"	"	"	"	1050°C (1925°F)/1 hour AC + 650°C (1200°F)/8 hrs AC
15-3	"	"	"	Salt Quench*	As-Forged
15-4	"	"	"	"	650°C (1200°F)/8 hours AC

*Salt quench from press to 815°C (1500°F) and hold for 30 minutes.

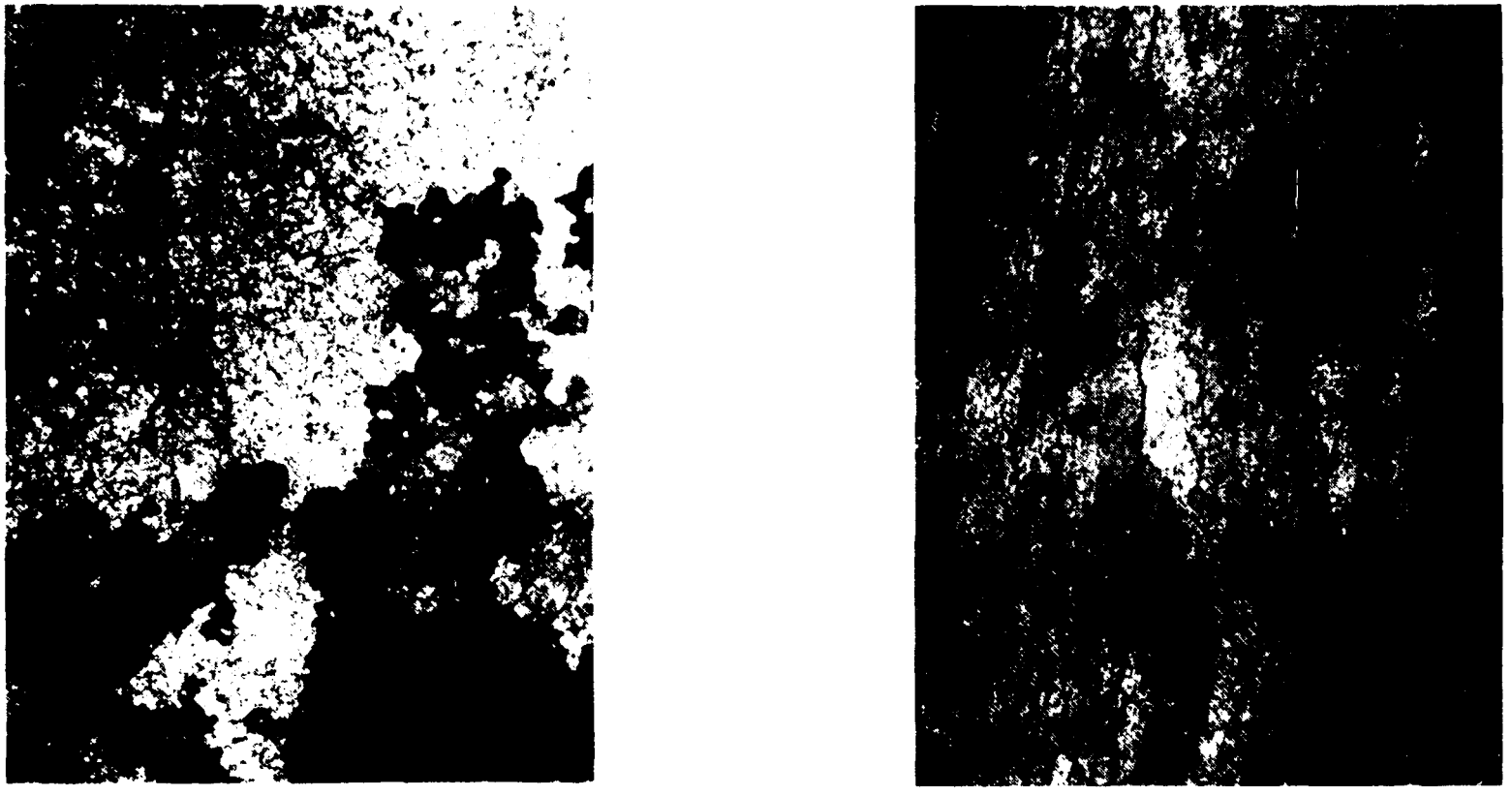

Figure 11

Macrostructure of Task I TMP forgings. a) Air cooled from press; b) Salt quenched from press.

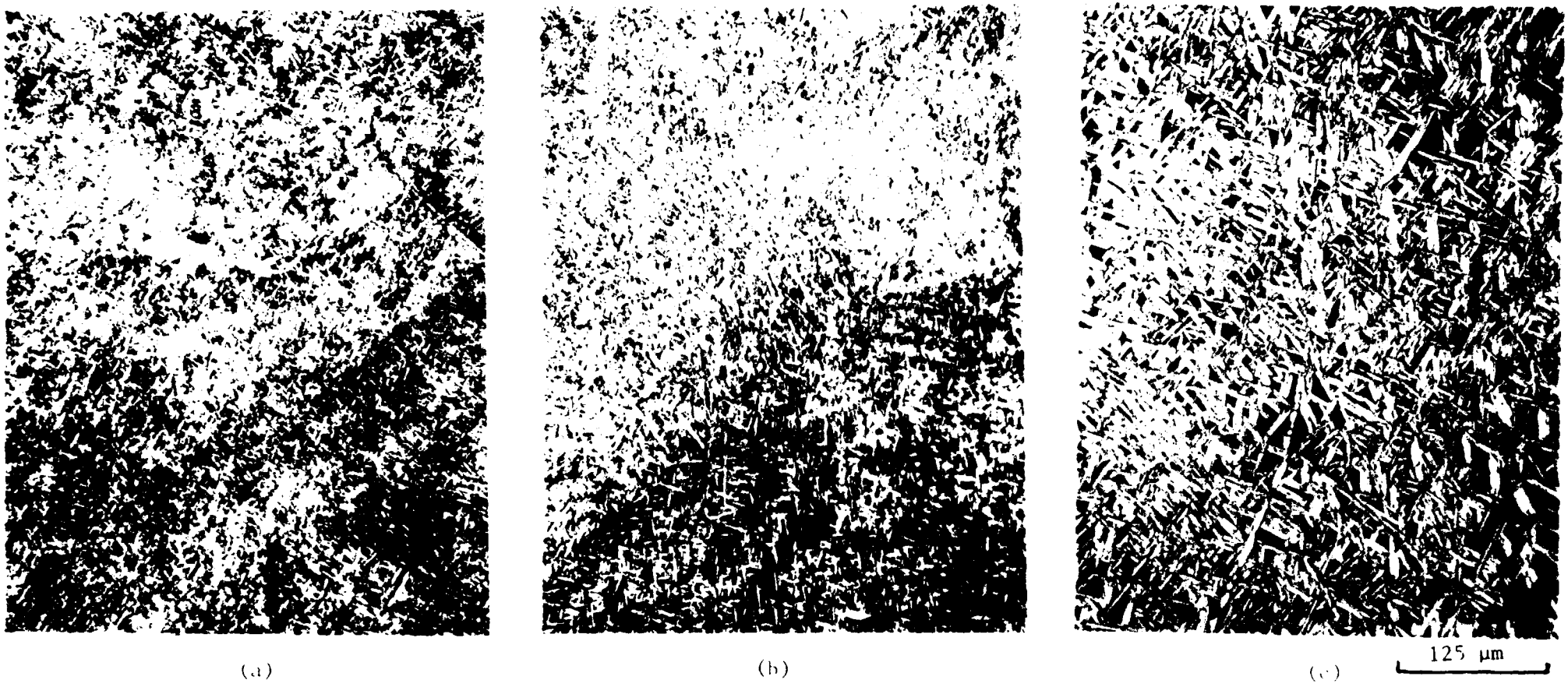

Figure 12

Microstructures of Alloy 19 (Ti-24.5Al-17Nb) pancake forging after processing. a) as-forged 1175°C (2150°F) AC; b) direct age 650°C (1200°F)/8 hours AC; STA 1065°C (1925°F)/1 hour AC + 650°C (1200°F)/8 hours AC.

followed by direct salt quenching resulted in a similar microstructure to that achieved by air cooling although the Widmanstatten needles were more numerous, slightly coarser and longer as a result of the isothermal transformation (Figure 13a). As before, samples subjected to direct aging at 650°C (1200°F)/8 hours showed little visual change (Figure 13b). Average hardness was Hv 308 for both conditions. Selected specimens were examined in more detail by transmission electron microscopy (TEM). This confirmed that there was little basic difference in the microstructure of this alloy processed by the two different techniques. However, it was shown that the alpha-two phase in the air cooled sample exhibited up to 4 w/o variation in Nb content indicating a nonequilibrium condition. In addition, small patches of fine basketweave morphology, consistent with a structure formed during continuous cooling, were found only in the air cooled material (Figure 14).

Tensile properties of the Alloy 19 series are given in Table 8. All process sequences evaluated resulted in better strength and ductility than the alpha-beta forge, beta anneal + age procedure used for screening trials. Program goals were easily met. The room temperature ductility values are among the highest ever achieved on intermediate scale titanium aluminide forgings. The major difference in properties among the four conditions was the yield strength which varied about 140 MPa (20 ksi) between the air cooled and direct aged material. Creep rupture data are presented in Table 9. All conditions met the goal life of 60 hours at 650°C/385 MPa (1200°F/55 ksi) by a narrow margin and there was very little difference in rupture capability among the various processes. Room temperature fracture toughness test data are given in Table 10. Values ranged from 20.6-28.6 MPa$\sqrt{\text{meter}}$ (18.7-26.0 ksi$\sqrt{\text{inch}}$) for the four conditions. Only one condition achieved the value of 28.3 MPa $\sqrt{\text{meter}}$ (26.0 ksi$\sqrt{\text{inch}}$) of the beta annealed specimen used in the screening study. It seems apparent that the toughness is only mildly microstructure dependent in these beta processed conditions but does correlate with tensile ductility; i.e., toughness increased as ductility increased.

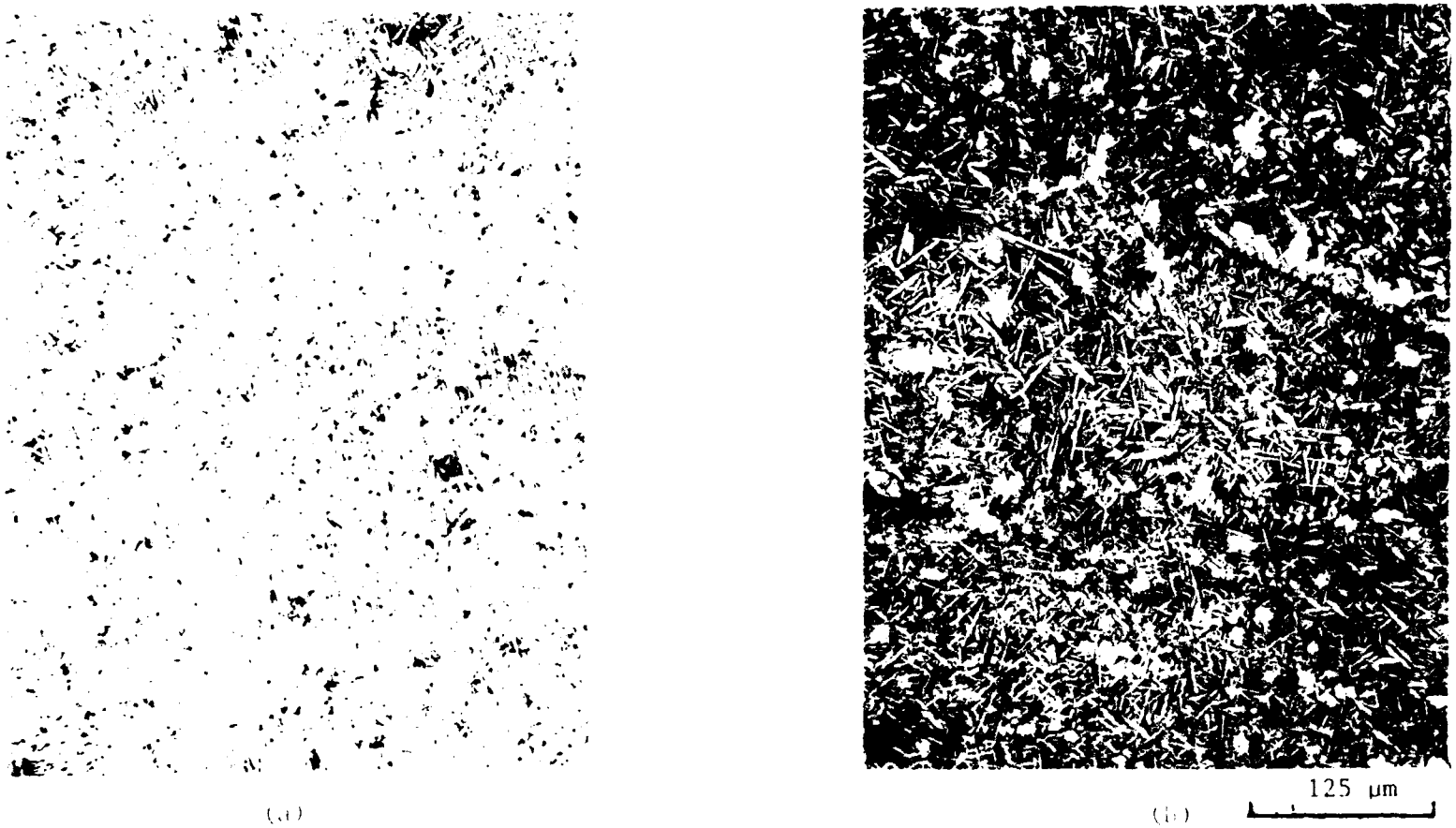

Figure 13

Microstructures of Alloy 19 (Ti-24.5Al-17Nb) pancake forging after processing. a) as-forged 1175°F (2150°F) SQ → 815°C (1500°F)/30 min.; b) direct aged 650°C (1200°F)/8 hours AC.

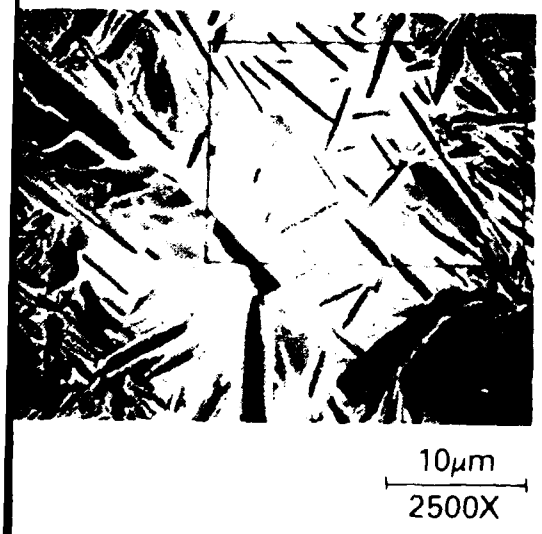

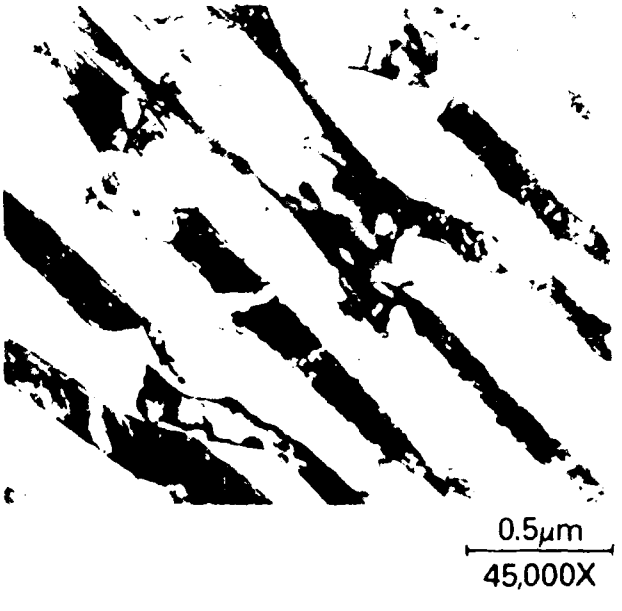

Figure 14

Microstructure of Ti-24.5Al-17Nb alloy specimens as tested. Top row, forged, air cooled plus STA; bottom row, forged, salt quenched and aged at 650°C (1200°F).

Table 8

Tensile Properties of Thermomechanically Processed Ti-24.5Al-17Nb Alloy 19

Alloy Number	Forging and Heat Treat[1]	Test Temp. °C	Test Temp. °F	0.2% Yield Str. MPA	0.2% Yield Str. Ksi	Ult. Tens. Str. MPA	Ult. Tens. Str. Ksi	EL (%)	RA (%)
19-1	1175°C DA (2150°F) Air Cool	21	70	931	134.3	1097	158.3	6.3	7.9
				975	140.7	1131	163.2	5.3	11.9
		427	800	822	118.6	1009	145.6	12.5	45.7
				856	123.5	1007	145.3	9.0	38.6
		650	1200	747	107.8	852	123.0	7.0	26.4
				692	99.6	799	115.3	5.3	19.2
19-2	1175°C STA (2150°F) Air Cool	21	70	718	103.6	989	142.7	8.6	14.3
				669	96.5	901	130.0	11.0	13.8
		427	800	552	79.7	856	123.6	19.3	51.9
				590	85.1	911	131.4	20.4	39.7
		650	1200	527	76.0	687	99.1	11.0	33.2
				534	77.1	696	100.4	10.5	25.1
19-3	1175°C AF (2150°F) SQ 815°C (1500°F) Air Cool	21	70	716	103.3	944	136.3	6.8	9.2
				751	108.4	958	138.3	6.3	9.1
		427	800	626	90.4	886	127.9	18.0	35.1
				761	109.8	865	124.8	20.9	40.2
		650	1200	552	79.7	698	100.7	9.0	30.7
				549	79.2	690	99.5	9.2	23.8
19-4	1175°C DA (2150°F) SQ 815°C (1500°F) Air Cool	21	70	755	109.0	958	138.8	5.8	7.0
				721	104.0	934	134.8	5.8	9.2
		427	800	613	88.4	875	126.2	15.4	34.0
				627	90.5	896	129.3	15.8	41.2
		650	1200	565	81.5	703	101.5	8.3	22.7
				552	79.7	727	104.9	8.6	19.1

[1] AF = As-forged
DA = 650°C (1200°F)/8 hours/AC
STA = 1050°C (1925°F)/1 hour/AC + 650°C (1200°F)/8 hour/AC

Table 9

Creep Rupture Lives of Thermomechanically Processed Ti-24.5Al-17Nb (Alloy 19)

Alloy Number	Forging and Heat Treat(1)		Test Conditions °C/MPa (°F/Ksi)	Time to (Hours) 0.2%	0.5%	1.0%	Rupt.	Post Test %EL	%RA
19-1	1175°C (2150°F) Air Cool	DA	650/385 (1200/55)	NA	NA	NA	67.7	10.6	15.5
19-2	"	STA		NA	NA	NA	50.9	8.15	12.9
19-3	1175°C (2150°F) SQ 815°C) (1500°F) Air Cool	AF		NA	NA	NA	75.8	8.62	12.4
19-4	"	DA		0.4	3.1	10.1	84.2	9.5	16.0

(1) AF = As-forged
DA = 650°C (1200°F)/8 hours/AC
STA = 1050°C (1925°F)/1 hour/AC + 650°C (1200°F/8 hours/AC

Table 10

Room Temperature Fracture Toughness of Thermomechanically Processed Ti-24.5Al-17Nb (Alloy 19)

Alloy Number	Forging Condition	Heat Treat(1)	K1C MPa$\sqrt{\text{Meter}}$	K1C Ksi$\sqrt{\text{Inch}}$
19-1	1175°C (2150°F) AC	DA	20.6	18.7
19-2	"	STA	27.6	25.1
19-3	1175°C (2150°F) SQ 815°C (1500°F)/30 min/AC	AF	26.0	23.6
19-4	"	DA	28.6	26.0

Ti-25Al-10Nb-4Mo (Alloy 15)

Forged and air cooled Alloy 15 (Ti-25Al-10Nb-4Mo) exhibited a nearly featureless microstructure and only faint grain boundaries could be seen despite heavy etching (Figure 15a). Hardness averaged Hv 380. After direct aging at 650°C (1200°F), a structure with subgrains visible within the larger equiaxed beta grains (Figure 15b) was observed. Average hardness increased to Hv 523. Solution treating and aging resulted in a fine matrix with about 10-15% needle-like alpha-two phase present (Figure 15c). Hardness in this condition was Hv 515.

The forged and salt quenched Alloy 15 microstructure is shown in Figure 16a and consists of an optically resolvable but extremely fine Widmanstatten needle-like structure with a hardness average of Hv 400. One section of the forging was aged at 650°C (1200°F). The aged microstructure exhibited no change in appearance (Figure 16b) or hardness (Hv = 413).

It was realized that the high hardness values of the air cooled Alloy 15 material would probably result in high tensile and possibly creep strength, but low ductility and thus fracture toughness. Therefore, an overaging program was initiated to determine if the alloy could be softened. Small 1.25 cm (0.5 in) square coupons were prepared, solution treated at 1050°C (1925°F) and air cooled. Aging temperatures ranged from 650°C (1200°F) to 925°C (1700°F) for times ranging from 2-24 hours. It became apparent that the alloy was very resistant to softening. It was necessary to heat the alloy to 925°C (1700°F) for two hours to effect a 100 point (Hv) change in hardness. This was apparently achieved by additional precipitation of finer alpha-two phase platelets as illustrated for the STA specimens (group 15-2) in Figure 17. Accordingly air cooled specimen blanks were given the 925°C (1700°F) overage prior to testing.

Analytical electron microscopy was again employed in order to more fully characterize the differences between the air cooled and salt quenched material. The most obvious differences in structure are summarized in

Figure 15

Microstructures of Alloy 15 (Ti-25Al-10Nb-4Mo) pancake forging after processing. a) As-forged 1175°C (2150°F) AC; b) Aged 650°C (1200°F)/8 hours AC; c) STA 1065°C (1925°F)/1 hour AC + 650°C (1200°F)/8 hours AC.

(a)

(b)

Figure 16

Microstructures of Alloy 15 (Ti-25Al-10Nb-4Mo) pancake forging after processing. a) As-forged 1175°C (2150°F) SQ → 815°C (1500°F)/30 min.; b) Aged 650°C (1200°F)/8 hours AC.

(a) (b)

Figure 17

Microstructure of Ti-25Al-10Nb-4Mo specimens from group 15-2. a) Forged, air cooled plus STA; b) After additional 925°C (1700°F) overaging heat treatment prior to testing. Note fine secondary alpha-two plates.

Figure 18. It can be seen that the air cooled material contains a higher beta phase content in which both coarse (1176°C/2150°F) and fine (925°C/1700°F) of alpha-two platelets have formed. Also a continuous film of coarse alpha-two platelets is present in prior beta grain boundaries. The beta phase was rich in niobium and molybdenum as expected, while the alpha-two phase was aluminum-rich. The level of molybdenum was quite low in the alpha-two phase and niobium was only about half that of the bulk composition level. Salt quenched Alloy 15 samples showed a much greater level of transformation. Alpha-two platelets had a higher aspect ratio and were more uniform than those in the air cooled material. The alpha-two phase distribution was primarily Widmanstatten but some small colony clusters were also visible. There was little prior beta grain boundary decoration by the alpha-two phase. Isolated areas of beta phase were present between the alpha-two platelets. Composition of the two phases were similar to the air cooled material although Mo contents had become more uniform. It is clear that the addition of molybdenum to the base Ti-Al-Nb composition causes a significant slowing of the beta-alpha-two + beta transformation, resulting in the ability to retain substantial amounts of beta phase after equivalent heat treatments.

Tensile properties of the Ti-25Al-10Nb-4Mo alloy are presented in Table 11. Forged, air cooled and aged specimens did not yield prior to fracture and had no measurable ductility up to and including 650°C (1200°F). The extreme brittleness of the material in this condition is reflected in the low fracture stresses. Specimens from salt quenched forgings exhibited much better tensile properties, although at room temperature, ductility remained quite low. Some salt quenched specimens did yield at room temperature with a strength approaching 1040 MPa (150 ksi). At 650°C (1200°F) yield strength still exceeded 690 MPa (100 ksi). Fractographic analysis was conducted on a representative air cooled and salt quenched specimen that had been tensile tested at room temperature. It was observed that the air cooled specimen exhibited large area of flat

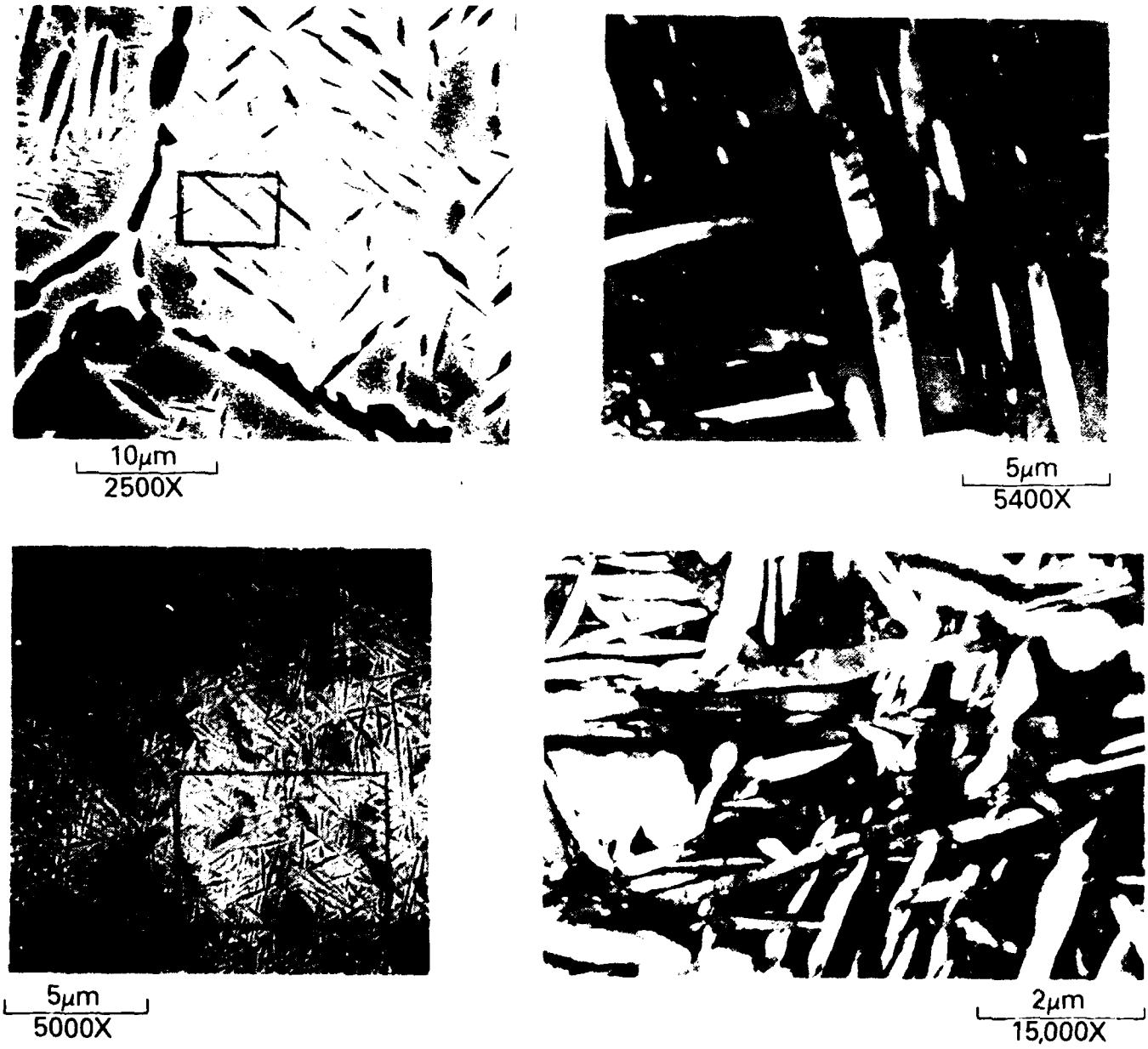

Figure 18

Microstructure of Ti-25Al-10Nb-4Mo alloy specimens as tested. Top row; forged, air cooled plus STA and 925°C (1700°F) overage. Note continuous beta matrix with alpha-two platelets; bottom row, forged plus salt quenched and aged at 650°C (1200°F). Platelets are alpha-two with small areas of beta (dark) dispersed throughout.

Table 11

Tensile Properties of Thermomechanically Processed Ti-25Al-10Nb-4Mo Alloy 15

Alloy Number	Forging and Heat Treat[1]	Test Temp. °C	Test Temp. °F	0.2% Yield Str. MPA	0.2% Yield Str. Ksi	Ult. Str.[3] MPA	Ult. Str.[3] Ksi	EL (%)	RA (%)
15-1	1175°C (2150°F) DA[2]	21	70		-	407	58.7	0	0
		427	800		-	475	68.5	0	0
					-		41.9	0	0
		650	1200		-	400	57.8	0	0
15-2	1175°C (2150°F) STA[2] Air Cool	21	70		-	441	63.7	0	0
		427	800		-	290	41.9	0	0
		650	1200		-	448	64.7	0	0
15-3	1175°C (2150°F) AF SQ 815°C (1500°F) Air Cool	21	70		-	758	109.6	0.24	0
					-	1041	150.3	0.32	0
		427	800	796	114.8	1120	161.6	13.8	25.2
				815	117.6	1090	157.2	8.9	19.2
		650	1200	806	116.3	920	132.8	4.0	9.2
				775	111.8	904	130.4	3.1	6.5
15-4	1175°C (2150°F) DA SQ 815°C (1500°F) Air Cool	21	70		-	958	138.3	0.4	0
				1021	147.4	1159	167.2	1.5	1.3
		427	800	845	122.0	1107	159.8	5.8	7.0
				822	118.6	1096	158.1	7.0	9.8
		650	1200	745	107.5	898	129.6	3.5	9.1
				721	104.1	894	129.0	3.1	14.1

[1] AF = As-forged
DA = 650°C (1200°F)/8 hours/AC
STA = 1050°C (1925°F)/1 hour/AC + 650°C (1200°F)/8 hour/AC

[2] Vacuum annealed after machining 925°C (1700°F)/2 hours/

[3] Values for 15-1 and 15-2 do not give actual "ultimate" strength

cleavage fracture while the salt quenched specimen had a rougher surface with possible cleavage on a smaller scale (Figure 19). At higher magnification, fracture surface of the salt quenched specimen appeared to exhibit quasi-ductile tearing, probably along the platelet boundaries; in contrast, air cooled material fracture surfaces were much flatter, the fracture appearing to travel rapidly through the beta phase, but leaving ridge-like striae at the alpha-two platelets. Metallographic cross sections of the two specimens were then prepared and examined. The fracture mode was similar for both; crack propagation was essentially transgranular and did not propagate along the prior beta grain boundaries (Figure 20). It is probable that the difference in properties is somewhat grain size related in that an advancing crack could progress more rapidly across large grains before changing directions. Parallel behavior has been observed for cast or beta annealed wrought conventional alloys in independent studies. Coarse grain size was shown to have a strong influence on low temperature tensile ductility and fracture occurred in an identical manner. However, based on the TEM and SEM analysis, it seems likely that the fully transformed acicular microstructure also contributed heavily to property improvement of salt quenched material.

Creep rupture data are given in Table 12. Forged and air cooled specimens failed in 10 hours or less while the salt quenched specimens had lives of 100-200 hours at 650°C (1200°F)/380 MPa (55 ksi). Air cooled material did not yield at this temperature and the fracture stress of the material was very close to the applied creep rupture stress of 380 MPa (55 ksi), which probably explains the low life. However, the behavior is in sharp contrast to that found in a similar alloy evaluated in Task 2, described in section 3.3.2. Here a coarse grained version of the alloy exhibited lives in excess of 600 hours. The difference may be attributed to heat treatment. The rather slow cooling rate from the beta phase field used in the Task 2 heat treatments resulted in more complete transformation than in the present case. Apparently, the larger amount of retained beta reduces ductility substantially causing premature brittle fracture even in a stress-rupture test.

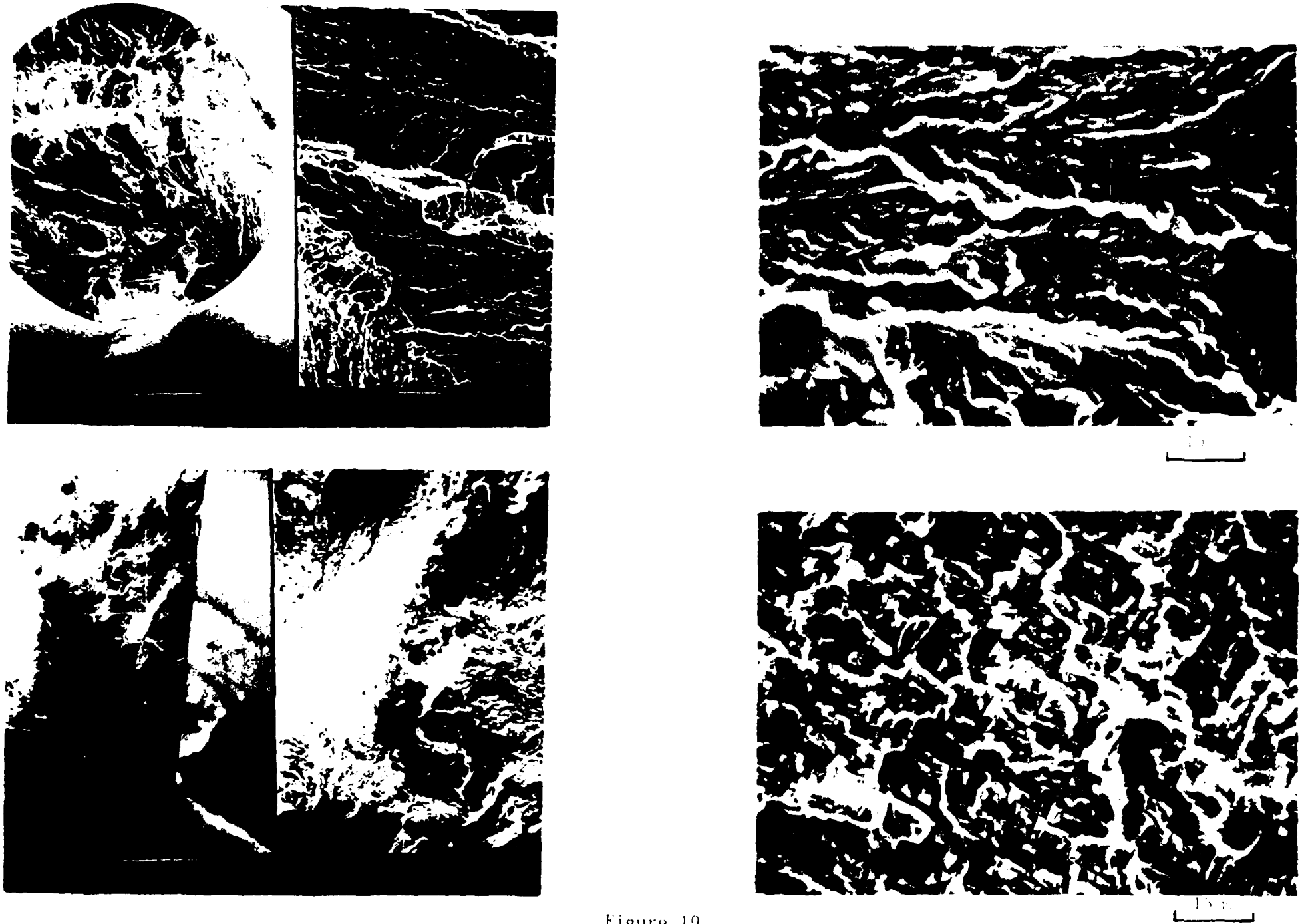

Figure 19

Fracture surface of Ti-25Al-10Nb-3Mo RT tensile specimens. Top row, AC from press, 0% ductility. Bottom row, SQ from press, 1% ductility. (Note dark areas on bottom specimen are residual Bakelite - specimen removed from mount.)

(a)

Figure 20

Microstructure of Ti-25Al-10Nb-3Mo-1V tensile specimens heavily etched and filmed under oblique light to reveal fracture mode. a) Air cooled specimen; b) Salt quenched specimen.

Table 12

Creep Rupture Lives of Thermomechanically Processed Ti-25Al-10Nb-4Mo (Alloy 15)

Alloy Number	Forging and Heat Treat[1]		Test Conditions °C/MPa (°F/Ksi)	Time to (Hours) 0.2%	0.5%	1.0%	Rupt.	Post Test %EL	%RA
15-1	1175°C (2150°F) Air Cool	DA	650/385 (1200/55)	<0.1	-	-	0.4	0.22	0.12
15-2	"	STA[2]		0.4	5.7	-	11.1	Failed in Radius	
15-3	1175°C (2150°F) SQ 815°C)	AF		0.7	14.0	63.0	120.1	2.0	7.6
15-4	(1500°F) Air Cool	DA		1.9	11.0	43.0	199.7	3.6	6.7

Table 13

Room Temperature Fracture Toughness of Thermomechanically Processed Ti-25Al-10Nb-4Mo (Alloy 15)

Alloy Number	Forging Condition	Heat Treat[1]	K1C MPa$\sqrt{\text{Meter}}$	K1C Ksi$\sqrt{\text{Inch}}$
15-1	1175°C (2150°F) AC	DA[2]	12.2	11.1
15-2	"	STA[2]	8.5	7.7
15-3	1175°C (2150°F) SQ 815°C (1500°F)/30 min/AC	AF	15.2	13.8
15-4	"	DA	13.4	12.2

[1] AF = As-forged
DA = 650°C (1200°F)/8 hours/AC
STA = 1050°C (1925°F)/1 hour/AC + 650°C (1200°F/8 hours/AC

[2] 15-1 and 15-2 were vacuum annealed at 925°C (1700°F) after machining

Room temperature fracture toughness of the Ti-25Al-10Nb-4Mo alloy was about half that of the Ti-24.5Al-17Nb alloy, ranging from 8.5-15.2 MPa $\sqrt{meter}$ (7.7-13.8 ksi $\sqrt{inch}$). Material which had been salt quenched appeared to be slightly tougher than air cooled specimens, but actual differences among the four conditions were smaller than may have been expected from the tensile behavior (Table 13).

The results of the TMP study made it clear that the alloys selected probably bracket the property balance options for this class of aluminides. The Ti-24.5Al-17Nb alloy showed an excellent combination of tensile strength, ductility and toughness but creep capability was marginal. Another attractive feature of the alloy was that good properties could be achieved with a number of process cycles. In the case of Alloy 15, the addition of 4% molybdenum is probably too high at the 10% niobium level and limits processing options which could result in a useful set of properties. The isothermal forge/salt quenching approach results in better properties and three factors may contribute. They are a finer grain size, a more complete transformation ($\beta \rightarrow \alpha_2 + \beta$) and possibly the lack of a network of grain boundary alpha-two. The alloy was about twenty-five percent stronger than the ternary Ti-24.5Al-17Nb alloy and showed about twice the creep rupture capability. Toughness was about half that of the ternary alloy. So the challenge was clear - could the ternary alloy be modified with sufficient molybdenum to increase the tensile/rupture properties while maintaining a measurable toughness level. In addition, could the modification be tailored to give a reasonable processing latitude to yield the required properties.

3.2 Task 2 - Alloying to Produce a Tough Second Phase

3.2.1 Phase I, Task 2 - Alloy Composition and Processing - Alloy Screening

Alloys for the initial portion of the task were processed and evaluated in an identical manner to those of Task 1. The aim was to formulate an alpha-two alloy with a greater amount of a tough and ductile beta phase.

Specific alloy chemistries selected and processing data are shown in Table 14. Chemical analysis results are given in Table 15 which show that aim compositions were achieved in all alloys. After HIP and forging, the heat treatment/processing approach was identical to that conducted in Task 1 alloys.

3.2.2 Results and Discussion - Alloy Screening

The alloys in this task fall into two classes and will be discussed separately. Alloys 8 through 15 are similar to current alpha-two titanium aluminide compositions with various beta stabilizing elements (W, Cr, Cu and Mo) added in an attempt to improve strength and toughness. Alloys 20, 21 and 22 were formulated with low aluminum and high niobium contents in order to produce a predominantly beta phase structure. If successful, one of these alloys would be selected as the 'tough' component of a blended powder alloy system.

Metallographic examination of the first group of alloys revealed that most exhibited microstructures consisting primarily of coarse acicular platelets, with the prior beta grains outlined by an almost continuous alpha-two film (Figures 21-24). Two exceptions were found. Alloy 11 (4% Cr) and 15 (4% Mo) had microstructures with smaller grains and much finer transformed acicular structure. These structures are interesting in that they resulted in alloys with very high tensile and creep-rupture strengths. Hardness values showed considerably more variability than the Task 1 alloys. One trend observed was that for each alloy pair, the one containing the higher amount of beta phase stabilizer had the higher hardness. Molybdenum additions appeared to result in the most potent hardening effect.

Tensile testing was conducted at RT, 427°C (800°F) and 650°C (1200°F) and results are listed in Table 16. All alloys were lower in ductility than the Task 1 alloys at approximately equivalent strength level. Alloy 15,

*Alloy also evaluated in TMP portion of Task 1

Table 14

Composition and
Processing Data for
for Task 2 Alloys

Alloy No.	Composition a/o (w%) Al	Nb	Other	Beta Transus Temp. °C (°F)	HIP/Forge Temp. °C (°F)	Hardness, Hv As-Forged	Hardness, Hv Heat Treated
8	25 (14.2)	10 (19.5)	1 (1.8) W	1150-1176 (2100-2150)	1150 (2100)	305	260
9	25 (14.1)	10 (19.4)	2 (3.5) W	1150-1176 (2100-2150)	1150 (2100)	337	311
10	25 (14.3)	10 (19.6)	2 (2.2) Cr	1120-1150 (2050-2100)	1093 (2000)	391	297
11	25 (14.3)	10 (19.6)	4 (4.4) Cr	1093-1120 (2000-2050)	1093 (2000)	428	342
12	25 (14.2)	10 (19.6)	2 (2.7) Cu	1093-1120 (2000-2050)	1093 (2000)	298	313
13	25 (14.1)	10 (19.4)	4 (5.4) Cu	1038-1070 (1900-1950)	1038 (1900)	382	355
14	25 (14.0)	10 (19.3)	2 (4.0) Mo	1093-1120 (2000-2050)	1093 (2000)	465	328
15	25 (13.7)	10 (19.0)	4 (7.8) Mo	1093-1120 (2000-2050)	1093 (2000)	445	412
20	15 (7.7)	17.5 (30.9)	-	927-954 (1700-1750)	927 (1700)	295	323
21	15 (7.4)	22.5 (38.1)	-	927-954 (1700-1750)	927 (1700)	269	294
22	12 (5.6)	20 (32.3)	3 (6) Sn 2.5 (4) Mo 0.25 (0.12) Si	982-1010 (1800-1850)	982 (1800)	309	339

Table 15

Chemical Analysis Results
for Task 2 Alloys
(In Weight %)[1]

Alloy No.		Al	Nb	W	Cr	Cu	Mo	O_2
8	Aim	14.0	20.0	2.0	-	-	-	0.10 max.
	Actual	14.1, 14.1	18.8, 18.9	2.04, 2.24	-	-	-	0.06, 0.06
9	Aim	14.0	20.0	4.0	-	-	-	0.10 max.
	Actual	14.0, 14.2	19.0, 18.9	3.8, 3.8	-	-	-	0.04, 0.045
10	Aim	14.0	20.0	-	2.2	-	-	0.10 max.
	Actual	14.3, 14.3	18.9, 19.0	-	2.0, 2.1	-	-	0.06, 0.044
11	Aim	14.0	20.0	-	4.4	-	-	0.10 max.
	Actual	14.3. 14.3	19.1, 19.0	-	4.1, 4.1	-	-	0.057, 0.065
12	Aim	14.0	20.0	-	-	2.7	-	0.10 max.
	Actual	14.1, 14.1	19.1, 18.7	-	-	2.77, 2.87		
13	Aim	14.0	20.0	-	-	5.4	-	0.10 max.
	Actual	14.1, 14.0	18.6, 17.9	-	-	5.8, 5.7	-	0.059, 0.055
14	Aim	14.0	20.0	-	-	-	4.0	0.10 max.
	Actual	14.1, 14.3	18.7, 18.4	-	-	-	4.1, 3.9	0.067, 0.066
15	Aim	14.0	20.0	-	-	-	7.8	0.10 max.
	Actual	14.1, 13.9	18.3, 18.3	-	-	-	7.4, 7.8	0.061, 0.071

[1]One analysis from each casting (two made per alloy).

Table 15

Chemical Analysis Results
For Task 2 Alloys (In Weight %)(1)
(Continued)

Alloy No.		Al	Nb	Sn	Si	Mo	O_2
20	Aim	7.7	30.9	-	-	-	0.10 max.
	Actual	7.2, 7.2	31.2, 31.3				0.10, 0.14*
21	Aim	7.4	38.1	-	-	0.10 max.	0.10 max.
	Actual	7.3, 7.1	37.1, 37.4			0.079, 0.061	0.07, 0.08
22	Aim	5.6	32.3	6.0	0.12	4.2	0.10 max.
	Actual	5.5, 5.5	32.8, 33.1	5.1, 5.0	0.15, 0.14	4.4, 4.4	0.08, 0.08

(1)One analysis per forging (two forgings per alloy).
*Out of spec.

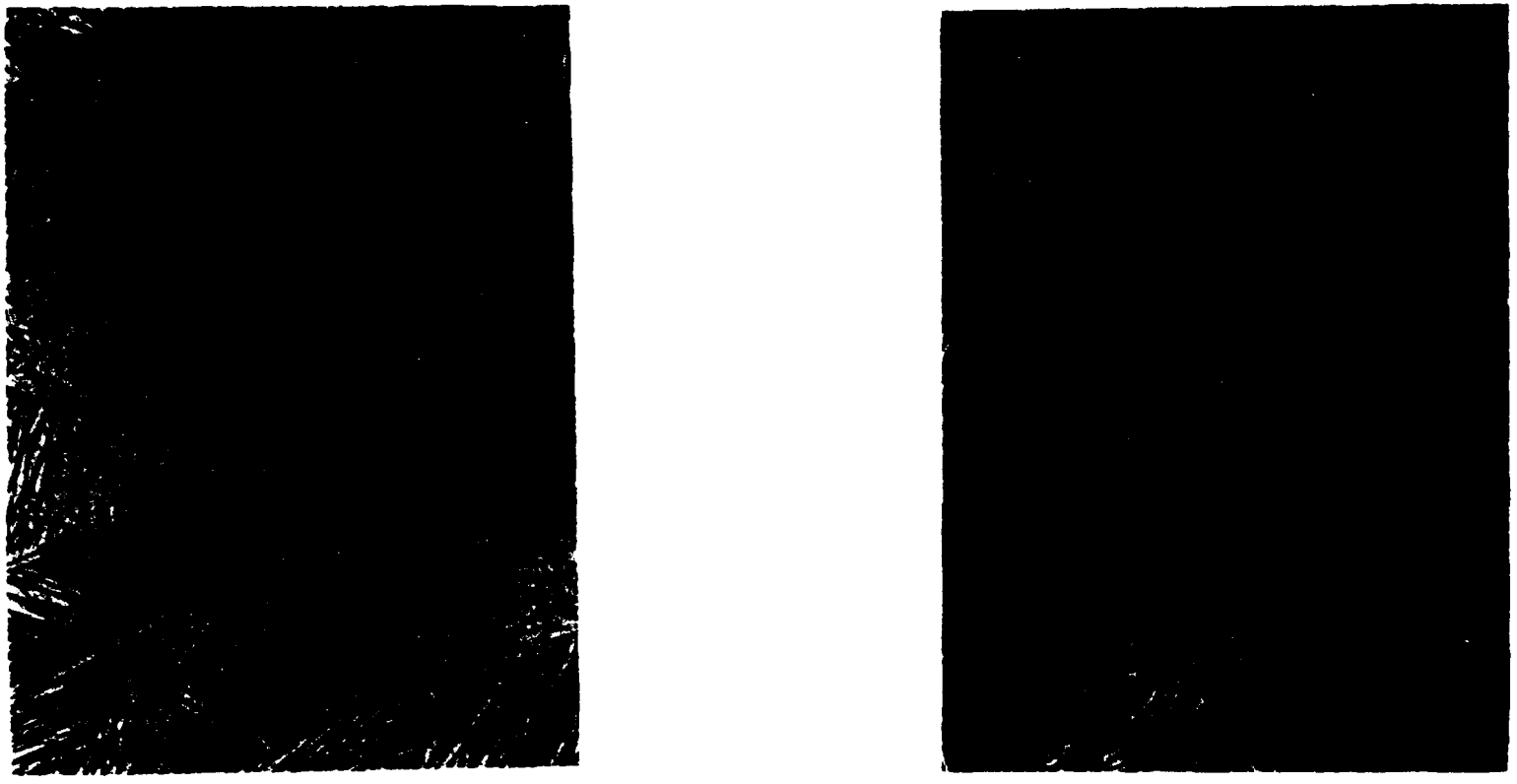

Figure 21 Mag: 250X

Typical microstructures of forged and heat treated Ti-25Al-10Nb Alloys 8 and 9 containing a) 1% W; b) 2% W.

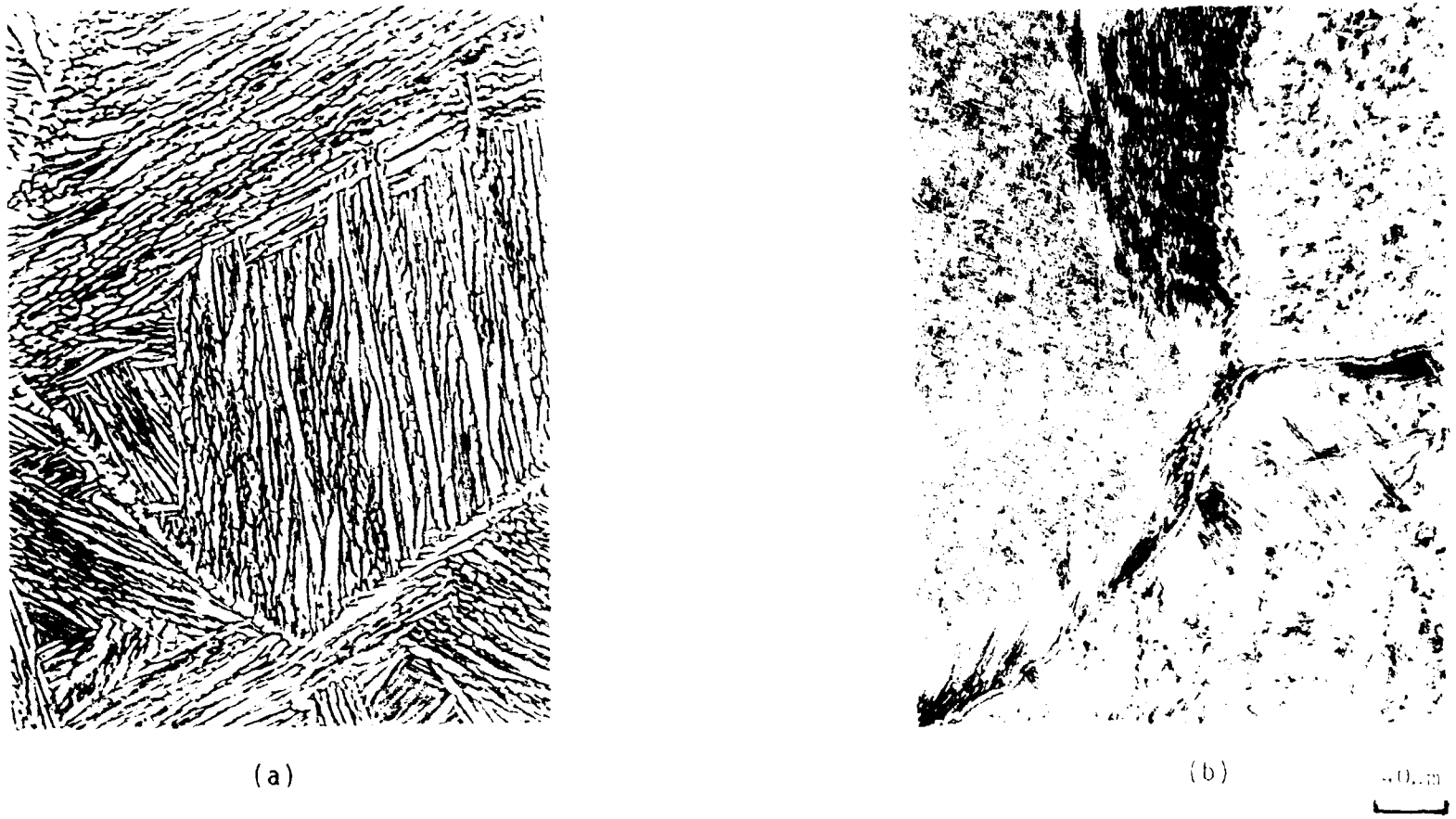

Figure 22 Mag: 250X

Typical microstructures of forged and heat treated Ti-25Al-10Nb alloys 10 and 11 containing a) 2% Cr; b) 4% Cr.

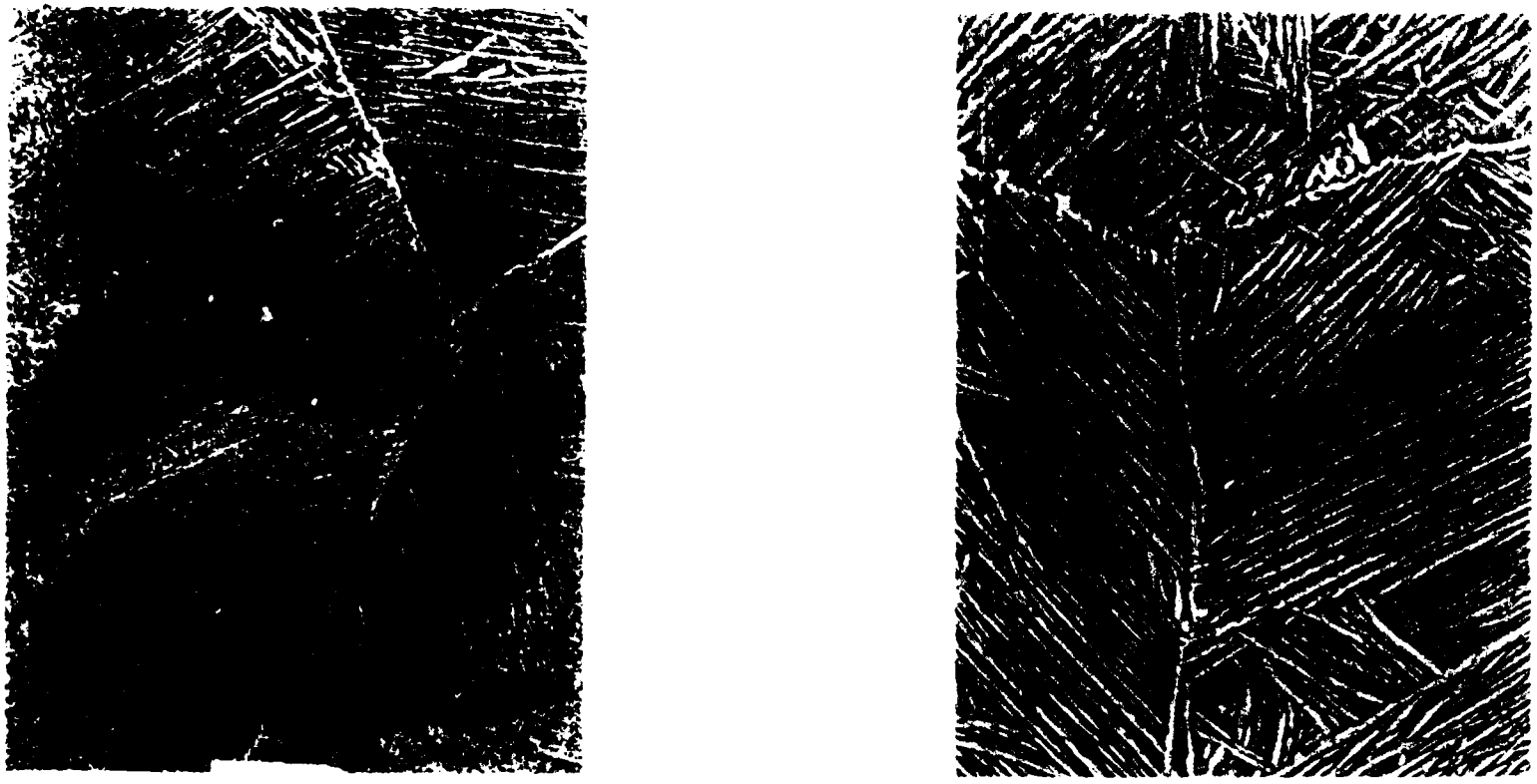

(a)

(b)

Figure 23

Mag: 250X

Typical microstructures of forged and heat treated Ti-25Al-10Nb alloys 12 and 13 containing a) 2% Cu; b) 4% Cu.

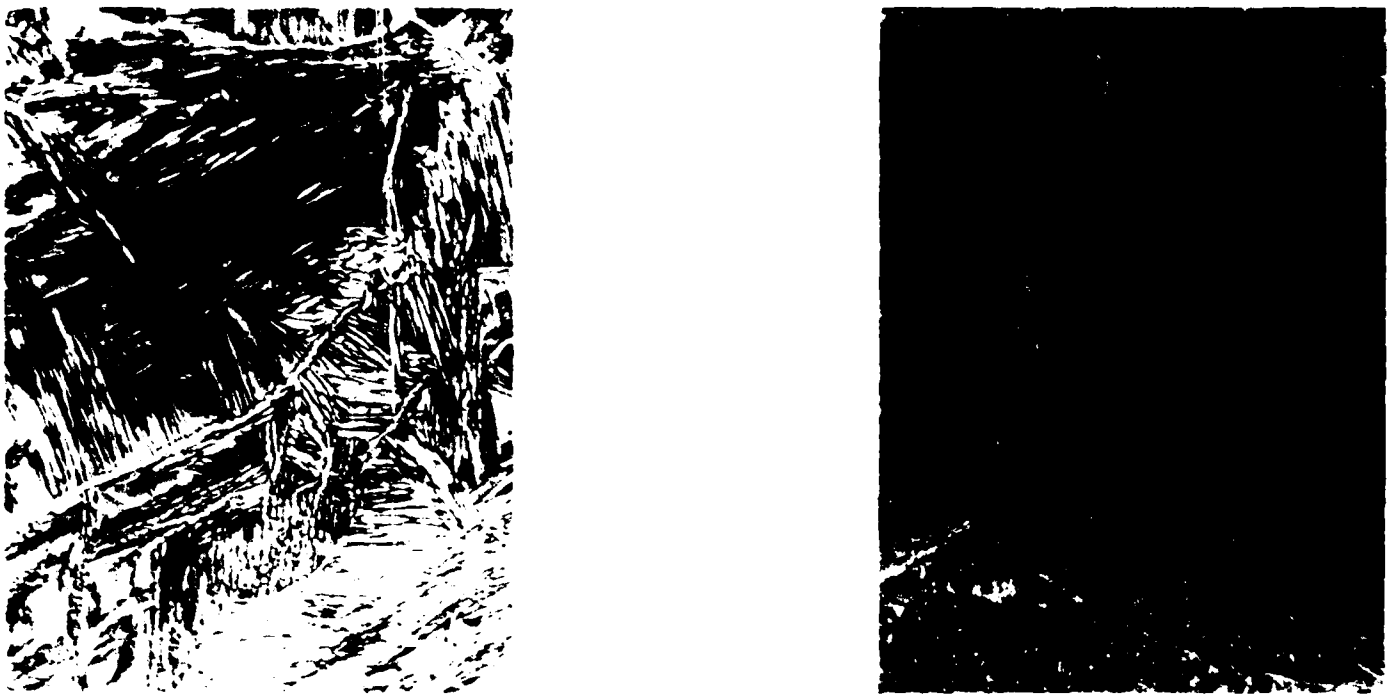

Figure 24

Mag: 250X

Typical microstructures of forged and heat treated Ti-25Al-10Nb alloys 14 and 15 containing a) 2% Mo; b) 4% Mo.

Table 16

Tensile Properties of Task 2 Alloys

Alloy No.	Alloy a/o	Test Temp. °C	Test Temp. (°F)	0.2% Yield Str. MPa	0.2% Yield Str. (Ksi)	Ult. Tens. Str. MPa	Ult. Tens. Str. (Ksi)	% EL	% RA
8	Ti-25Al-10Nb-1W	21	(70)	515	(74.6)	515	(74.6)	0.5	1.32
				498	(72.2)	514	(74.5)	1.2	-
		427	(800)	331	(48.0)	551	(79.9)	6.4	9.2
				338	(49.0)	609	(88.3)	1.0	12.9
		650	(1200)	290	(41.9)	465	(67.4)	9.3	13.1
				301	(43.6)	520	(75.4)	11.3	15.7
9	Ti-25Al-10Nb-2W	21	(70)	560	(81.2)	560	(81.2)	0.9	1.3
				-	-	535	(77.6)	0.5	0.64
		427	(800)	397	(57.9)	593	(86.0)	5.3	7.9
				391	(56.7)	648	(93.9)	8.0	9.2
		650	(1200)	370	(53.5)	549	(79.6)	5.6	9.2
				320	(53.5)	548	(79.4)	5.3	11.8
10	Ti-25Al-10Nb-2Cr	21	(70)	522	(75.7)	522	(75.7)	0.58	1.3
				528	(76.5)	557	(80.8)	0.83	-
		427	(800)	353	(51.2)	608	(88.1)	6.7	7.6
				355	(51.4)	593	(86.0)	5.5	9.3
		650	(1200)	293	(42.4)	527	(76.4)	9.3	15.6
				305	(44.2)	533	(77.2)	9.1	11.9
11	Ti-25Al-10Nb-4Cr	21	(70)	-	-	713	(103.3)	0.17	-
				665	(96.4)	735	(106.5)	0.5	-
		427	(800)	529	(76.7)	782	(113.4)	2.8	5.3
				534	(77.4)	800	(115.9)	3.0	5.3
		650	(1200)	446	(64.6)	705	(102.2)	3.6	7.3
				526	(76.2)	766	(111.1)	3.6	6.6

Table 16

Tensile Properties of Task 2 Alloys
(Continued)

Alloy No.	Alloy a/o	Test Temp. °C	Test Temp. (°F)	0.2% Yield Str. MPa	0.2% Yield Str. (Ksi)	Ult. Tens. Str. MPa	Ult. Tens. Str. (Ksi)	% EL	% RA
12	Ti-25Al-10Nb-2Cu	21	(70)	-	-	424	(61.4)	0.33	0.33
				508	(73.6)	508	(73.6)	0.58	-
		427	(800)	323	(46.8)	531	(76.9)	5.4	3.9
				324	(47.0)	522	(75.7)	4.3	5.3
		650	(1200)	285	(41.3)	467	(67.7)	7.7	13.0
				317	(45.9)	546	(79.2)	9.6	11.7
13	Ti-25Al-10Nb-4Cu	21	(70)	-	-	488	(70.7)	-	-
				-	-	529	(76.7)	0.25	1.4
		427	(800)	385	(55.8)	471	(68.3)	-	4.0
				397	(57.6)	634	(91.9)	2.7	2.7
		650	(1200)	340	(49.3)	546	(79.2)	3.3	4.0
				357	(51.8)	579	(83.4)	7.3	8.0
14	Ti-25Al-10Nb-2Mo	21	(70)	730	(105.8)	730	(105.8)	0.42	-
				698	(101.1)	728	(105.4)	0.58	1.4
		427	(800)	550	(79.7)	798	(115.6)	4.9	7.0
				531	(76.9)	768	(111.3)	4.0	7.9
		650	(1200)	469	(68.0)	678	(98.2)	4.2	10.5
				502	(72.7)	710	(102.9)	4.3	10.5
15	Ti-25Al-10Nb-4Mo	21	(70)	-	-	933	(135.2)	-	-
				1011	(146.5)	1011	(146.5)	0.25	-
		427	(800)	882	(127.9)	955	(138.4)	0.66	1.3
				831	(120.5)	941	(136.5)	0.90	1.3
		650	(1200)	829	(120.3)	874	(126.7)	0.83	2.7
				807	(117.0)	823	(119.3)	0.5	1.3
20	Ti-15Al-17.5Nb	21	(70)	861	(124.8)	964	(139.8)	5.3	9.1
				879	(127.4)	982	(142.3)	6.5	13.0
		427*	(800)	649	(94.1)	782	(113.3)	7.5	32.9
		650	(1200)	393	(57.0)	491	(71.2)	19.1	77.7
				373	(54.1)	489	(70.9)	14.8	70.8

Table 16

Tensile Properties of Task 2 Alloys
(Continued)

Alloy No.	Alloy a/o	Test Temp. °C	Test Temp. (°F)	0.2% Yield Str. MPa	0.2% Yield Str. (Ksi)	Ult. Tens. Str. MPa	Ult. Tens. Str. (Ksi)	% EL	% RA
21	Ti-15Al-22.5Nb	21	(70)	867	(125.6)	964	(139.8)	6.1	13.1
				853	(123.6)	961	(139.5)	7.3	12.9
		427	(800)	653	(94.7)	785	(113.6)	7.5	26.2
				649	(94.0)	808	(117.1)	11.2	37.7
		650	(1200)	513	(74.4)	630	(91.3)	4.5	14.0
				428	(62.0)	531	(76.9)	10.0	23.9
22	Ti-12Al-20Nb-3Sn-2Mo-.25Si	21	(70)	1038	(150.5)	1072	(155.3)	2.2	3.2
				996	(144.3)	1025	(148.6)	1.5	5.3
		427	(800)	861	(124.8)	967	(140.2)	3.3	11.1
				800	(115.9)	942	(136.5)	7.2	21.5
		650	(1200)	593	(86.0)	706	(102.4)	8.0	14.1
				582	(84.3)	722	(104.7)	14.3	14.3

*Only one specimen available for 427°C (800°F) test.

with 4% Mo*, showed high strength levels over the entire temperature range tested; however, ductility was unfortunately very low. This was the only alloy to meet the strength goals.

Creep-rupture testing at 650°C/385 MPa (1200°F/55 ksi) demonstrated that this alloy set had much better creep-rupture strength than Task 1 alloys (Table 17). Only those alloys containing copper (12 and 13) or 2% chromium (10) did not exceed the goal life. While additions of tungsten or 4% chromium were effective in promoting rupture resistance, by far the most potent strengthener was molybdenum. The lives of the molybdenum alloys were among the highest measured for an alpha-two alloy of this type, and we know that the creep rate was low. In fact, the capability of Alloy 15 lies between that of IN901 and IN718 (without density correction). Metallographic and hardness evaluation of the molybdenum containing alloys 14 and 15 was performed to evaluate their condition after over 600 hours of exposure. Hardness was found to be virtually unchanged. Alloys 14 and 15, respectively, had post exposure average hardness of Hv 312 and Hv 405, compared to pretest hardnesses of Hv 328 and Hv 412. A hardened alpha stabilized case 0.0027 mm (0.0005 in) was detected, but little or no secondary cracking occurred away from the immediate fracture. These results are encouraging as they indicate that the molybdenum containing alloys have both good environmental resistance and phase stability at 650°C (1200°F).

Room temperature fracture toughness data are also shown in Table 17. Most of the Ti-25Al-10Nb + beta stabilizer alloys showed equal or higher toughness compared to the baseline. Interestingly, even the very high strength 4% molybdenum Alloy 15 had a reasonable toughness value of 15.1 MPa$\sqrt{\text{meter}}$ (13.9 ksi$\sqrt{\text{inch}}$).

Not unexpectedly, metallographic examination of the second group of alloys revealed considerably different structures. The alloys appeared to be two phase, but the (assumed) alpha-two phase precipitates are very fine in Alloys 20 and 21 (Figure 25a, b). Alloy 22 was somewhat similar but exhibited a significant amount of light etching islands of a white

Table 17

RT Fracture Toughness and 650°C/385 Mpa
(1200°F/55 Ksi) Creep-Rupture Properties
of Task 2 Alloys

	Alloy a/o	Fracture Toughness		Creep, Life, Hours				RT Post Test	
		MPa √Inch	Ksi √Inch	0.2%	0.5%	1.0%	Rupture	%EL	%RA
8	Ti-25Al-10Nb-1W	21.0	19.3	< 0.1	0.1	0.25	131.5	4.2	17.3
9	Ti-25Al-10Nb-2W	15.6	14.3	0.4	6.2	78.1	123.9	2.5	7.9
10	Ti-25Al-10Nb-2Cr	18.9	17.3	< 0.1	0.25	1.3	16.6	7.0	12.2
11	Ti-25Al-10Nb-4Cr	No Data	-	0.3	7.5	116.0	385.2	2.6	2.9
12	Ti-25Al-10Nb-2Cu	12.9	11.8	< 0.1	0.1	0.25	3.4	10.1	20.9
13	Ti-25Al-10Nb-4Cu	13.0	11.9	< 0.1	0.15	0.3	5.9	9.0	14.3
14	Ti-25Al-10Nb-2Mo	17.5	16.1	1.1	11.9	130.8	684.6	3.2	10.9
15	Ti-25Al-10Nb-4Mo	15.1	13.9	9.1	68.0	340.0	635.2	2.7	1.5
20	Ti-15Al-17.5Nb	28.9	26.5	< 0.1	< 0.1	0.1	0.5	17.9	54.1
21	Ti-15Al-22.5Nb	42.3	38.8	< 0.1	< 0.1	< 0.2	0.9	21.1	54.5
22	Ti-12Al-20Nb-3Sn-2Mo-.25Si	17.4	16.0	< 0.1	0.2	0.9	9.7	10.3	13.5

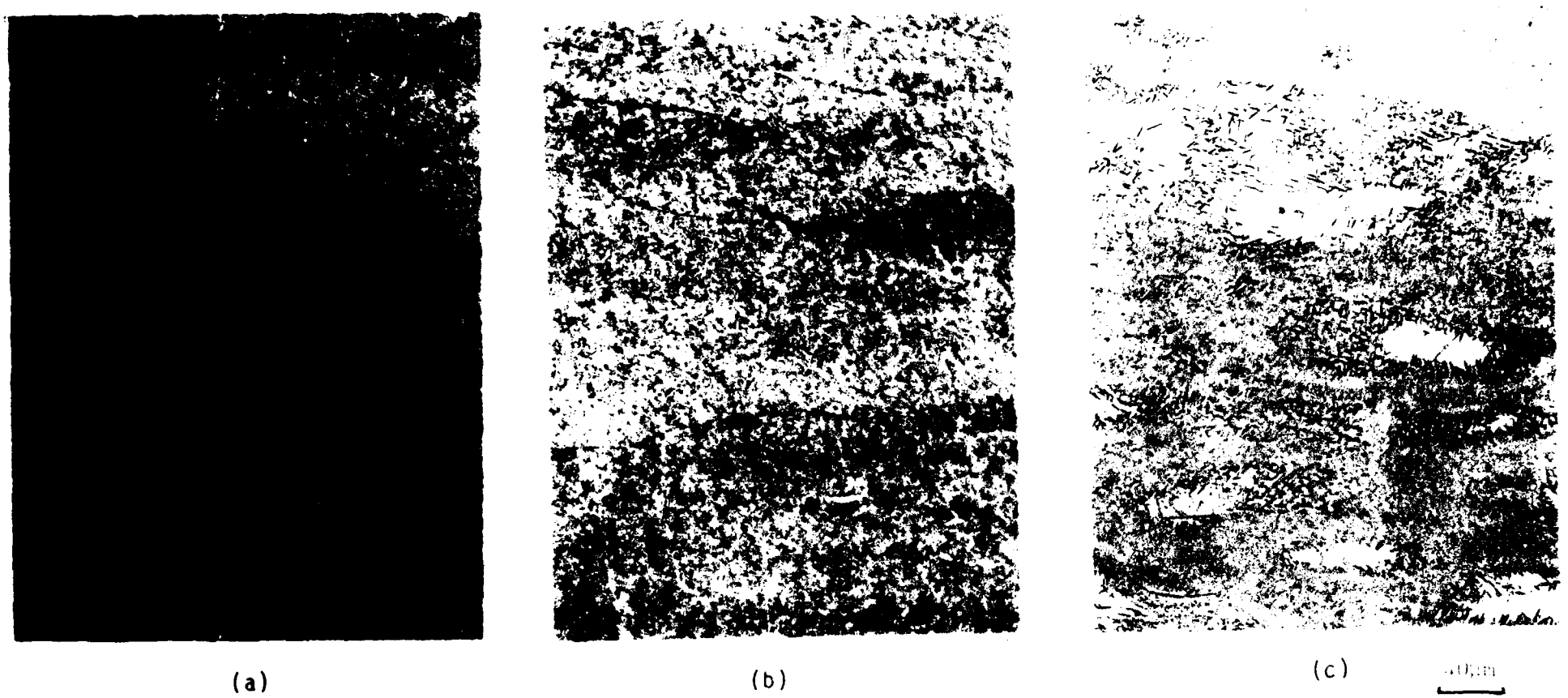

Figure 25 Mag: 250X

Typical microstructures of forged and heat treated low aluminum/high niobium alloys. a) Alloy 20, Ti-15Al-17.5Nb; b) Alloy 21, Ti-15Al-22.5Nb; c) Alloy 22, Ti-12Al-20Nb-3Sn-2Mo-.25Si.

phase, with some needle-like features within the islands (Figure 25c) which could be partially transformed beta phase. Tensile strength and ductility of the three alloys were quite high. Fracture toughness values ranged from 17.4-42.7 MPa$\sqrt{\text{meter}}$ (16.0-38.8 ksi$\sqrt{\text{inch}}$); obviously the high values are encouraging. As is quite typical for beta alloys, creep-rupture resistance was quite low, but creep ductility was excellent. The addition of tin and silicon did demonstrate an improvement in creep capability although life was still far below goal.

As stated previously, the primary aim of Task 2 was to select the best alloy from each class, convert these to powder and then blend to form a composite material. If the volume fracture, size and distribution could be optimized, it was considered that a tough material could be produced without severely compromising high temperature properties. Two alloys were obvious candidates. Alloy 15 (Ti-25Al-10Nb-4Mo) had very high tensile and rupture strength and toughness equivalent to many lower strength compositions; the "best" beta alloy was Alloy 21 (Ti-15Al-22.5Nb), with its high ductility and toughness and respectable tensile strength.

As noted in section 3.1.3, the second alloy for the thermomechanical processing study was also chosen from this group due to the lack of a second promising Task 1 candidate. The alloy selected was also the Alloy 15 composition (Ti-25Al-10Nb-4Mo).

3.2.3 Alloying to Produce a Tough Second Phase-Powder Metallurgy Approach

3.2.3.1 Ingot Melting and Conversion

Two ingots weighing about 6 Kg (13 lbs) were prepared of the selected alloys to produce sufficient powder for the study. VAR ingots were prepared in essentially the same manner as those used for thermomechanical processing in Task 1. However, due to the size requirements dictated by the powder-making process, the ingots were longer (250 mm/10 in) and smaller in diameter (75 mm/3 in) (Figure 26). The melting procedure was modified so that the three pairs of primary

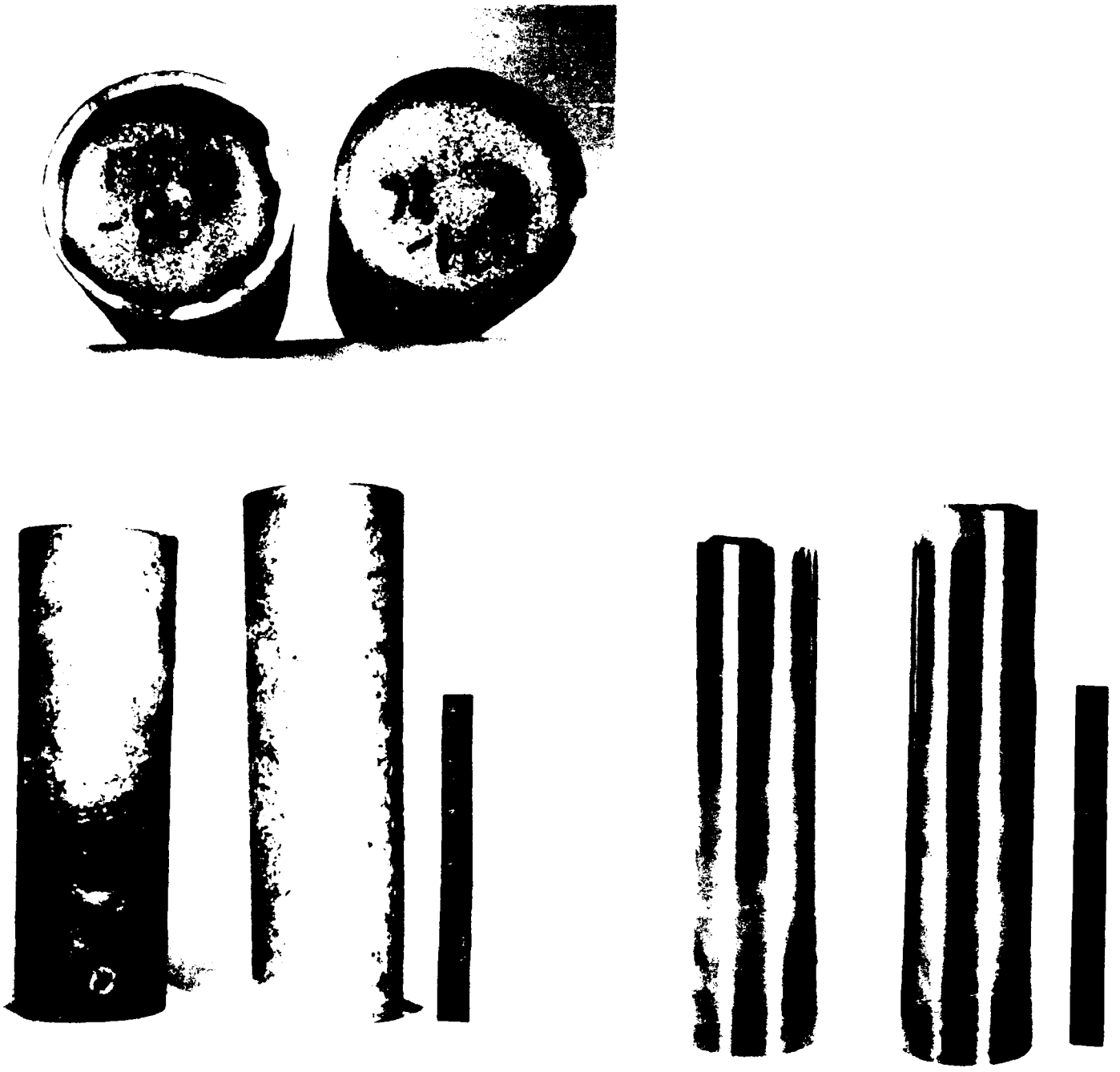

Figure 27

Typical VAR ingot prepared for Task 2 powder production. Left, as melted + HIP'ed ingots - note shrinkage of pipe cavity in ingot top; right, machined ingots prior to powder conversion.

electrodes were melted in a 50 mm (2 in) diameter crucible, welded together and remelted in a 75 mm (3 in) diameter crucible. The resulting ingots were machined to the required 63.5 + 0.00 - 0.076 mm (2.5 in + 0.00 - 0.003 in) diameter (Figure 26).

Alloy 21 (Ti-15Al-22.5Nb) presented a difficult melting problem due to its high niobium/low aluminum content. Even using a specially melted 70Nb-30Al (w/o) master alloy, about one-third of the niobium required had to be added using a different approach. Since previous studies had demonstrated that a homogeneous melt could not be achieved using elemental Nb additions, a formulation of 70Nb-30Ti (w/o) master alloy buttons were made by nonconsumable melting. Since this master alloy was not brittle, it was necessary to mill the buttons into chips and small chunks. The presence of these larger pieces was apparent when subsequent chemical analysis of the ingots revealed that the Nb matrix content was lower than the aim as a result of the presence of areas of Nb-rich segregation (Table 18). Subsequent analysis revealed that there were a small number of niobium-rich areas which persisted after powder conversion.

Alloys 15 and 21 (Ti-25Al-10Nb-4Mo and Ti-15Al-22.5Nb) were successfully converted to powder using the Plasma Rotating Electrode Process (PREP) by Nuclear Metals, Inc. of Concord, MA. Analysis of the resulting powder (Table 19) revealed that there was little chemical difference between the ingots and the powder for each alloy, although oxygen content of Alloy 15 was about 0.05 w/o higher than the maximum aim of 0.10 w/o. Examination of the electrode stubs after PREP processing revealed the Nb segregation as one of the Alloy 21 stubs; otherwise, there were no abnormalities (Figure 27). Approximately 75% of the powder yield was 80 mesh or finer, although virtually none was less than -325 mesh. Scanning electron microscopy (SEM) examination of the atomized powder of Alloy 15 revealed that the particles were spherical and homogeneous with a "soccer ball" coarse dendritic surface appearance (Figure 28). Optical metallographic examination of polished powder cross sections confirmed the structure and showed no porosity (Figure 29). Powder particles of Alloy 21 were similar but many paired particles were apparent. Occasional particles showed the Nb-rich segregates (Figures 30 and 31).

Table 18

Chemical Composition of Alloy 15 and 21
Ingots Melted for Powder Production
(In Weight Percent)

Alloy No.		Al	Nb	Mo	O	N
15	Aim	13.7	19.0	7.8	0.10*	0.04*
	Actual**	12.9	20.0	7.6	0.12	0.006
21	Aim	7.4	38.0	-	0.10*	0.04*
	Actual**	6.8	35.2	-	0.095	0.011

Table 19

Chemical Composition of Nuclear Metals Inc.
PREP Powders for Task 2
(In Weight Percent)

Alloy	Task		Average Composition Al	Nb	Mo	O	N
15	2	Aim	13.7	19.0	7.8	0.10*	0.04*
		Actual	13.0	19.0	7.7	0.15	0.05
21	2	Aim	7.4	38.0	-	0.10*	0.04*
		Actual	6.7	35.8	-	0.06	0.01

*Maximum
**Average of the two ingots

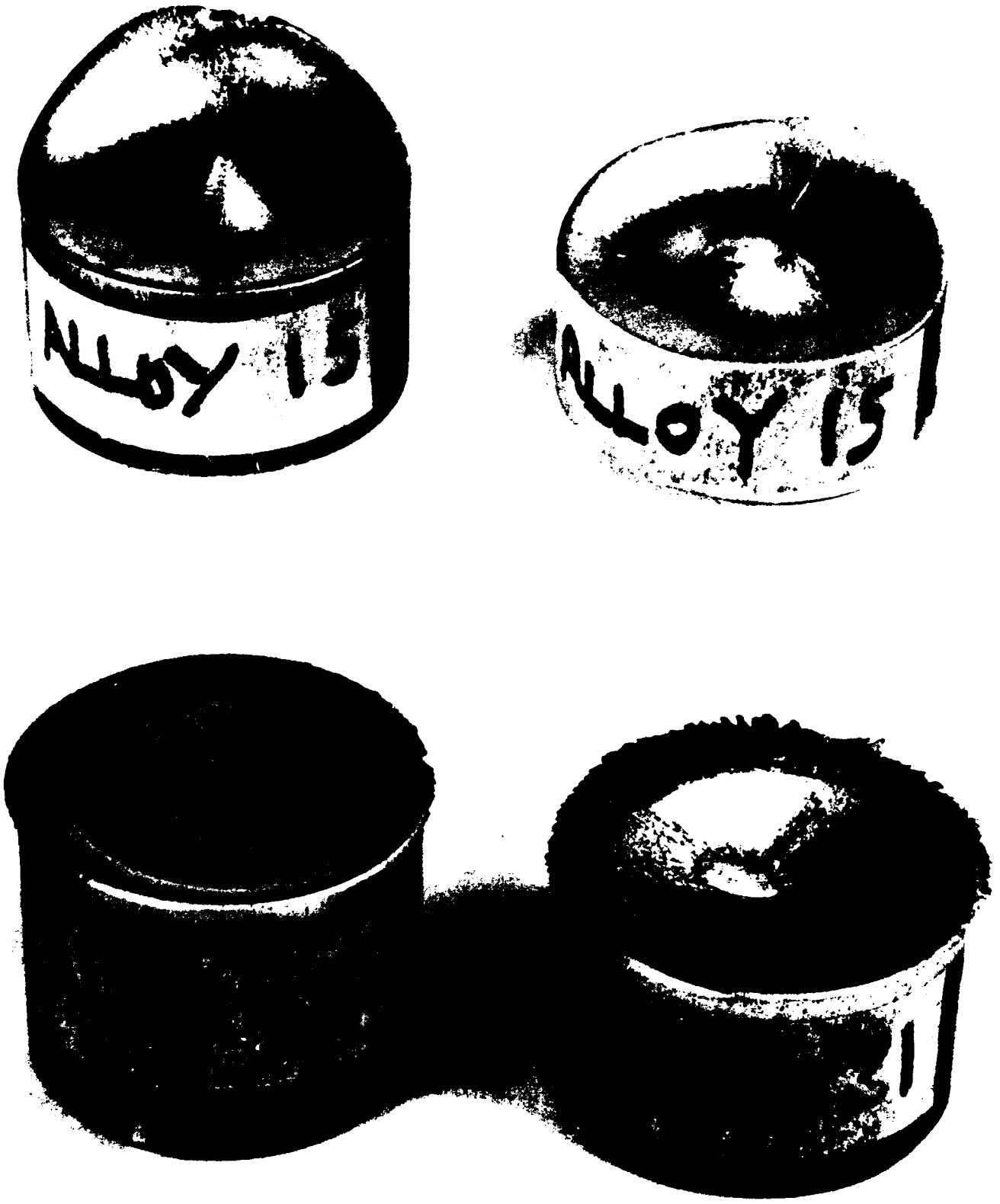

Figure 27

Ingot stubs remaining after conversion of Alloys 15 and 21 to PREP powder. Note Nb-rich area centered in lower right stub of Alloy 21.

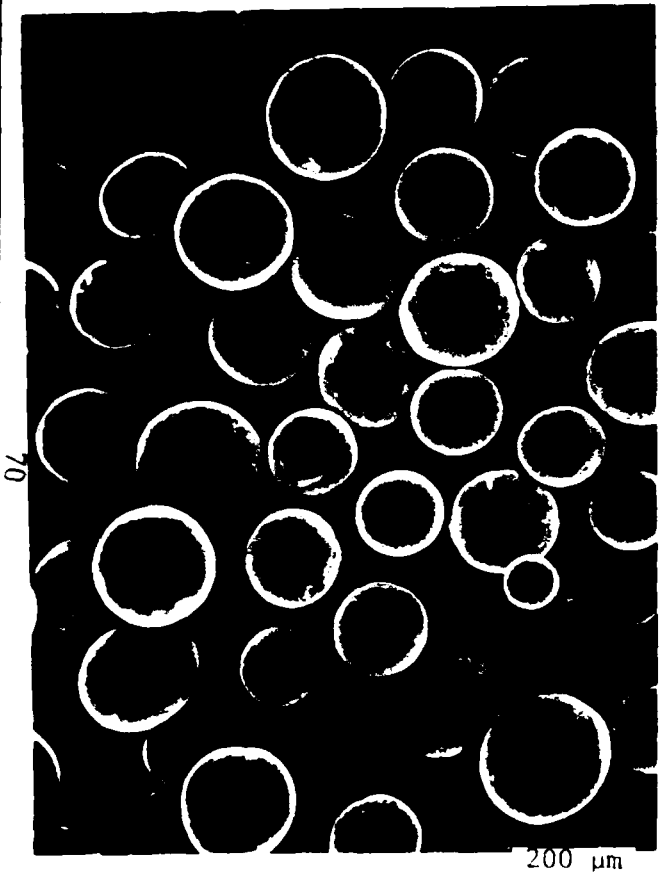

100X

500X

1000X

Figure 2a

SEM photos of Alloy 15 (Ti-25Al-10Nb-3Mo) PREP powder.

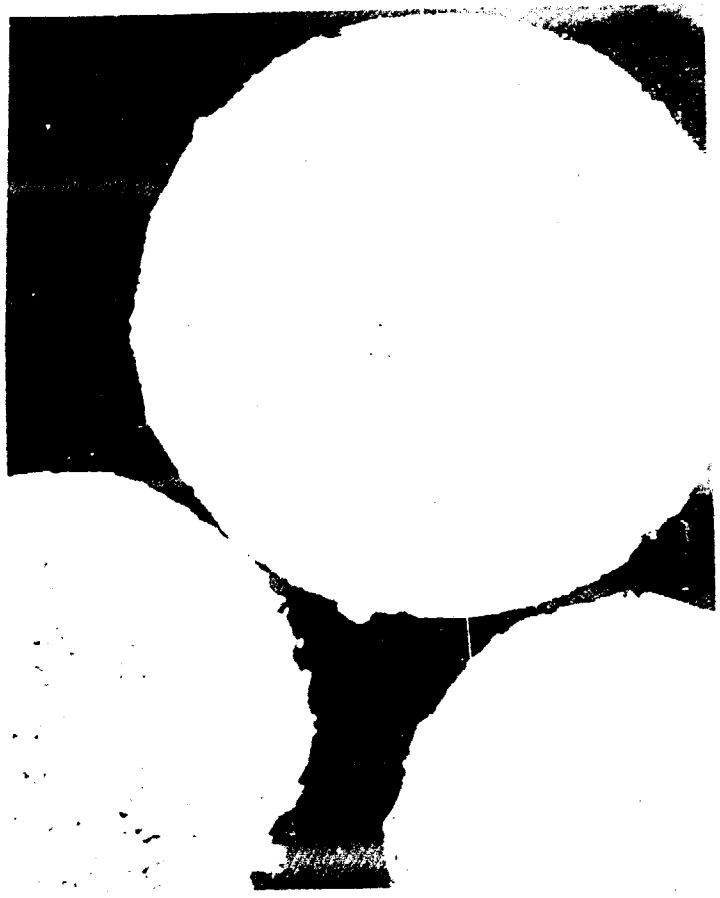

360X

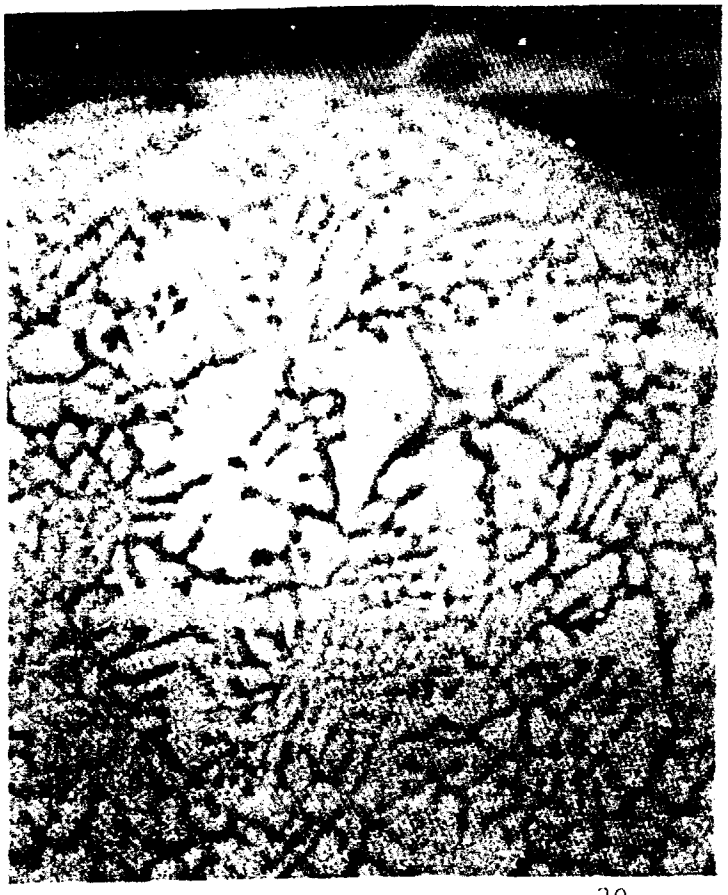

1000X

Figure 29

Microstructure of Alloy 15(Ti-25Al-10Nb-3Mo) PREP Powder as atomized.

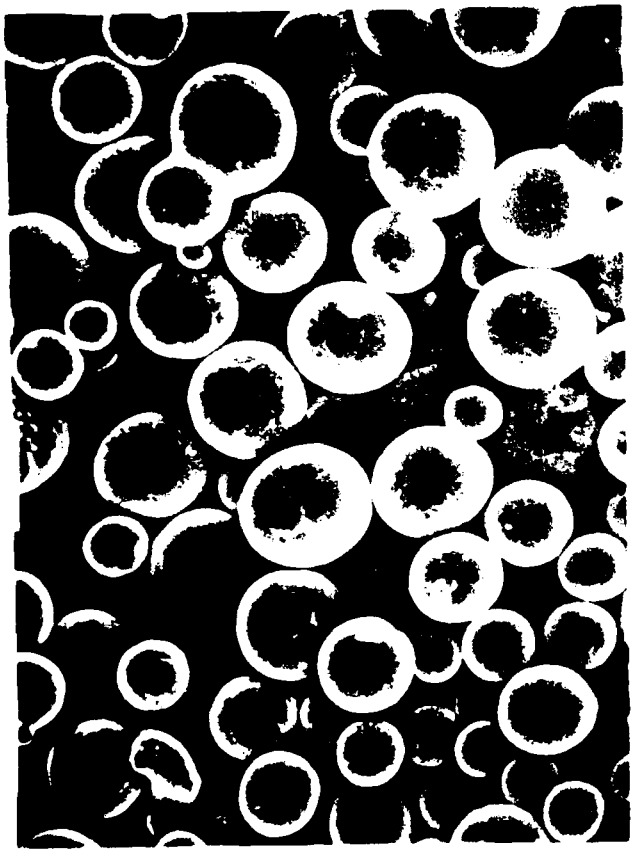

Figure 41

Microstructure of Alloy 21 (Ti-15Al-22.5Nb) PREP powder as atomized. Nominal particles shown left and particles with Nb-rich areas at right.

3.2.3.2 Consolidation

Subscale consolidation trials were performed in order to establish the general blending characteristics, microstructural appearance and reactivity of the two alloys. Fifty gram (0.11 pound) samples were made using 10 v/o and 20 v/o of Alloy 21 powder in an Alloy 15 matrix; both powders were -80 mesh. The samples were blended by vigorous agitation and rotation in a double cone vee blender, sealed in commercially pure titanium tubing and hot isostatically pressed (HIP) at 1010°C/105 MPa (1850°F/15 ksi) for two hours. Compacts were fully dense and no porosity was apparent. The sample containing 10 v/o Alloy 21 exhibited a uniform distribution of the beta alloy with little clustering (Figure 32). Reaction between the second phase and the matrix consumed approximately 25% of the second phase as shown by the interaction layer around the particles. At 20 v/o, the beta Alloy 21 began to form clusters or a semi-continuous network; matrix/second phase interaction was similar to the sample with 10 v/o Alloy 21 (Figure 33). Analysis using X-ray emission spectroscopy revealed little difference in the composition of the normal Alloy 21 particle and those occasional Nb-rich phases (Figure 34).

Eight blend and/or processing conditions were selected for evaluation (Table 20). During HIP, one container developed a leak and was unusable, thus, material was available for only seven test conditions. Three of the HIP consolidations were isothermally forged at 954°C (1750°F) with a total reduction of ≈60%. Post processing heat treatments are also listed in Table 20.

Metallographic examination at low magnification revealed that a uniform distribution of the second alloy powder was achieved. As-HIP second phase regions were equiaxed in appearance and ranged in size from 100-200 microns in diameter. Upon forging, the second phase areas were elongated in the forging direction. In the as-HIP condition and as-forged condition, the islands of second phase alloy exhibited a very fine Widmanstatten type needle structure (Figures 35a and 36a). After

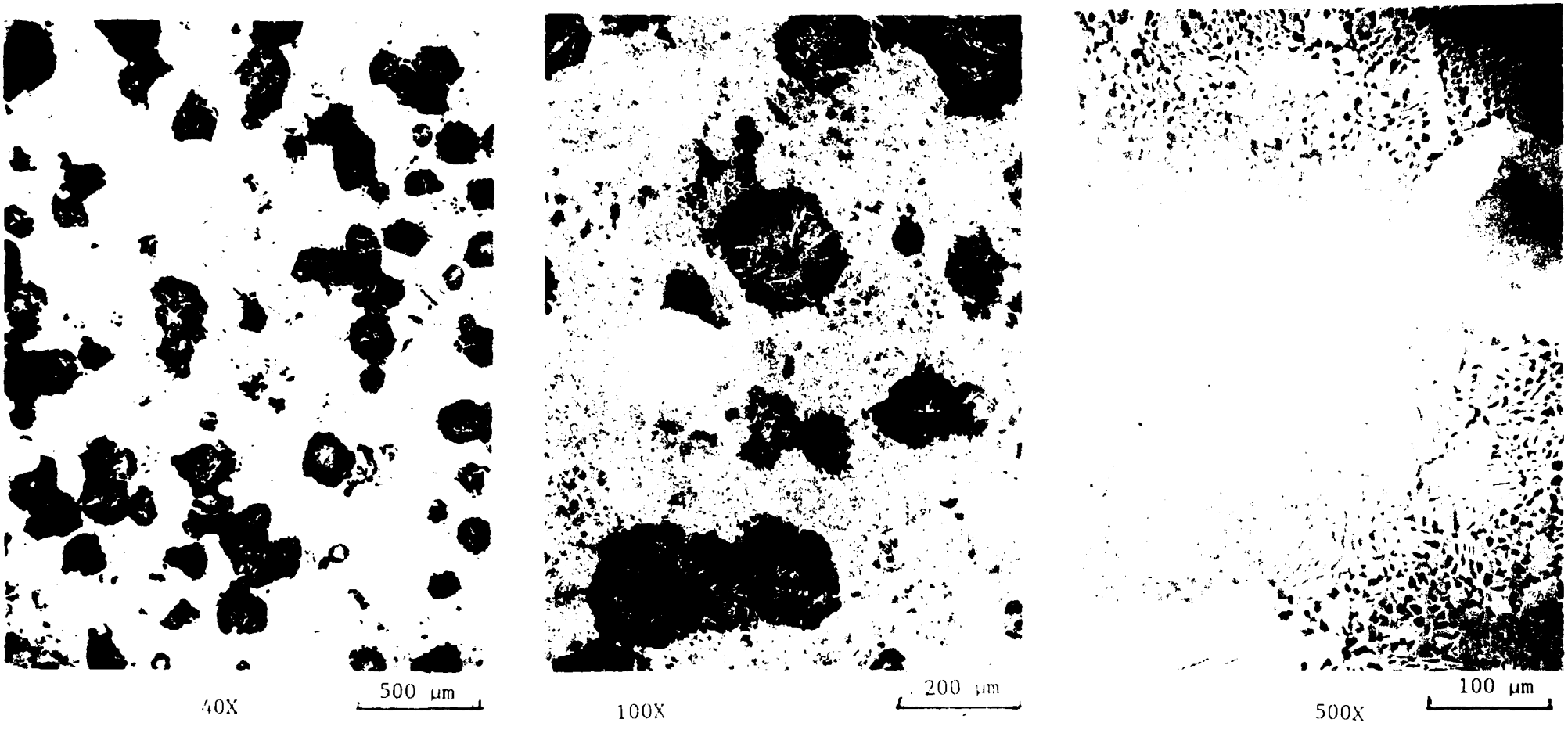

Figure 3.

Microstructure of a blend of 10% Alloy 21 (Ti-15Al-22.5Nb) in a matrix of Alloy 15 (Ti-25Al-10nb-4Mo) after 1010°C (1850°F) HIP. The white background is the matrix, the dark etching areas Alloy 21 and the small round white particles are Nb-rich Alloy 21.

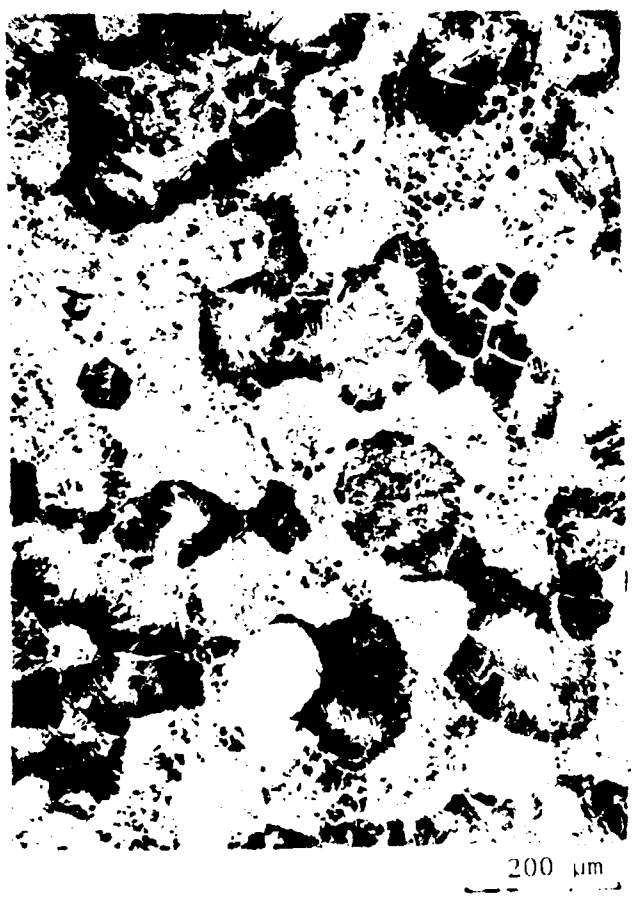

Figure 33

Microstructure of a blend of 20% Alloy 21 (Ti-15Al-22.5Nb) in a matrix of Alloy 15 (Ti-25Al-10nb-4Mo) after 1010°C (1850°F) HIP. The white background is the matrix, the dark etching areas Alloy 21 and the small round white particles are Nb-rich Alloy 21.

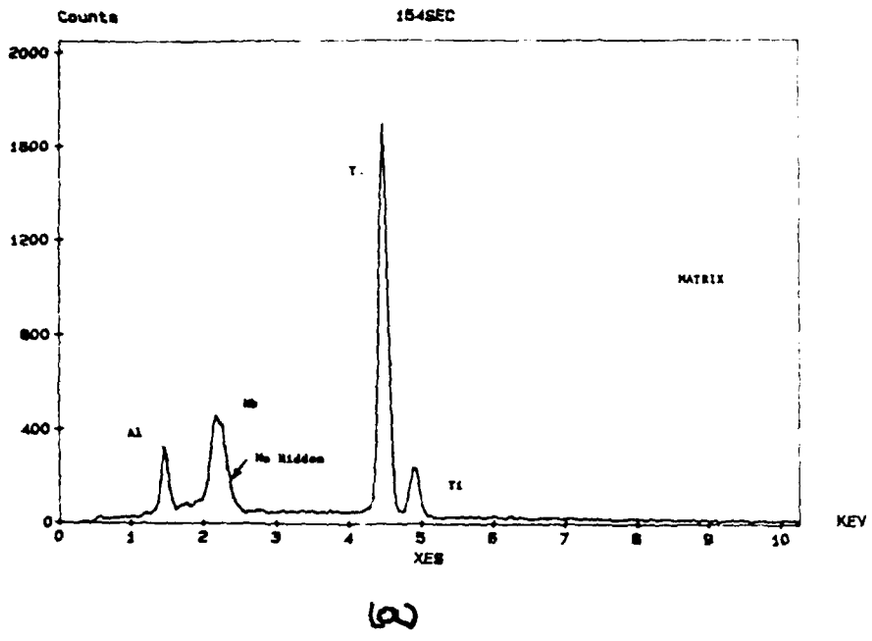

(a)

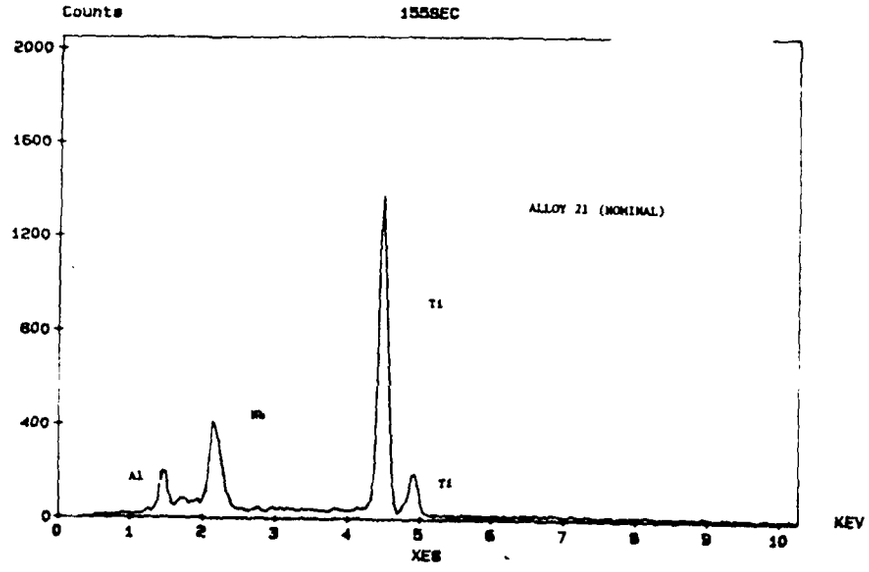

(b)

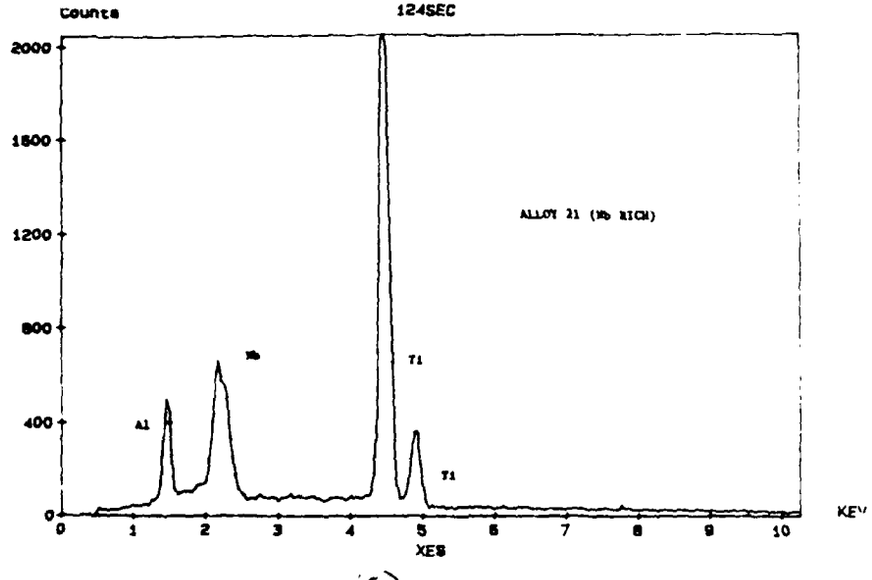

(c)

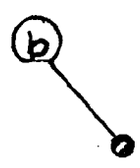

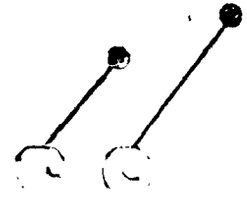

Figure 34

Analysis of composition of phases in a 10% Alloy 21/90% Alloy 15 consolidation. a) nominal matrix composition, Ti-25Al-10Nb-4Mo; b) nominal second phase Alloy 21, Ti-15Al-22.5Nb; c) Nb-rich region of Alloy 21. Note high Nb and Ti peaks from 70Nb-30Ti w/o master alloy.

Table 20

Processing Conditions for Task 2, Part 2 Alloys[1]

Sample Identity	Second Phase Amount	Particle Size	Processing Conditions
A	5 v/o	-35 +80 mesh (≈200 μm)	HIP: 1010°C (1850°F)/105 MPa (15 ksi)/ 2 hours STA: 954°C (1750°F)/1/AC + 815°C (1500°F)/4/AC
B	20 v/o	-35 +80 mesh (≈200 μm)	Same as 'A'
C	5 v/o	-140 +230 mesh (≈100 μm)	Same as 'A'
D	20 v/o	-140 +230 mesh (≈100 μm)	Same as 'A'
E	20 v/o	-35 +80 mesh (≈200 μm)	HIP: 1010°C (1850°F)/105 MPa (15 ksi)/ 2 hours Forge: ≈60% @ 954°C (1750°F) STA: 954°C (1750°F)/1/AC + 815°C (1500°F)/4/AC
F	5 v/o	-140 +230 mesh (≈100 μm)	Same as 'E'
G	20 v/o	-140 +230 mesh (≈100 μm)	Same as 'E'

[1] Material with 5 v/o -35 +80 mesh alloy for forging leaked during HIP and could not be replaced.

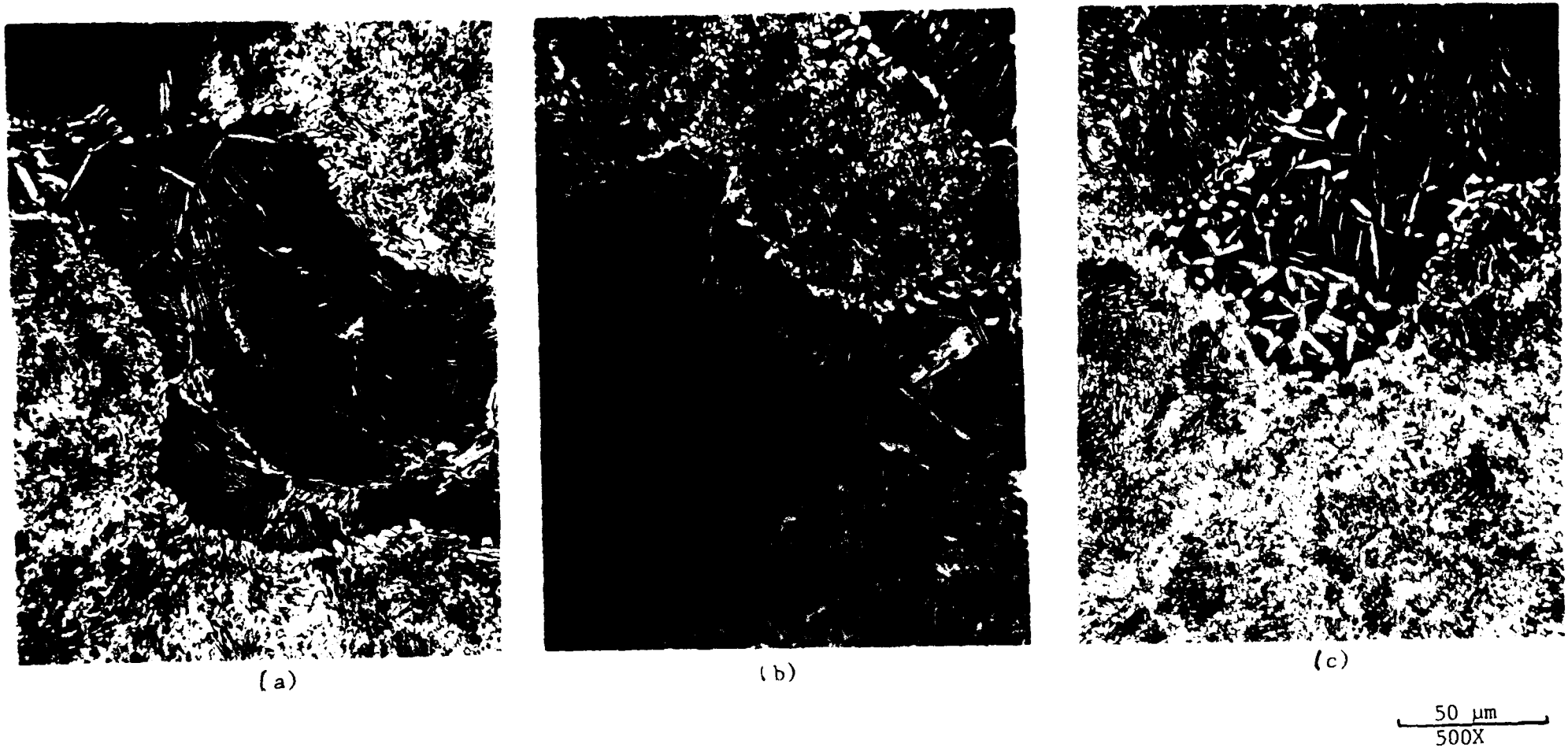

Figure 35

Microstructure of Alloy 21 islands in a matrix of Alloy 15. a) as-HIP; b, c) solution treated and aged. Note coarsening and growth of white needle-like phase.

Figure 3b

Microstructure of Alloy 21 islands in a matrix of Alloy [illegible] (a) as forged; b) forged + SIA.

Table 21

Hardness (Hv) of Task 2
Alloy Blends

Matrix: Ti-25Al-10Nb-4Mo
2nd Phase: Ti-7.5Al-38Nb

Condition	Matrix	2nd Phase
As-HIP	380	300
HIP + STA	440	325
HIP + Forge	430	350
HIP + Forge + STA	420	320

solution treating and aging, the appearance of a coarse needle-like structure in interfacial regions was observed (Figures 35b, c and 36b). Microhardness testing revealed that the second phase was 80-120 points softer (Hv) than the matrix as shown in Table 21.

Microprobe line scan analysis confirmed that interdiffusion between the second phase and the matrix extended to a depth of about 50-60 microns and resulted in the needle-like regions around the periphery of the second phase regions (Figure 37). Internal areas of the second phase displayed nominal composition of Alloy 21.

3.2.3.3 Mechanical Properties of Consolidations

Tensile, fracture toughness and stress-rupture property data are summarized in Table 22. Baseline properties for Alloy 15 were either measured or estimated from Task 1 data. It can be seen that tensile strength of the blended alloys was 34-70 MPa (5-10 ksi) lower than alloy 15 but exhibited at least equivalent and generally higher ductility over the temperature range tested. Fracture toughness levels were increased in most cases by at least 100% in the alloy blends with the second phase addition. Powder size did not appear to have a major effect, but the addition of 20 v/o second phase clearly produced a large increase in toughness. Visual examination of the tested toughness specimens revealed that fracture surface roughness increased as toughness increased (Figure 38). Forged specimens exhibited elongated, ridge-like fracture surfaces that correlated with the deformed grain structure. Scanning electron microscopy of selected specimens confirmed visual results and further revealed the crack deflection and branching caused by the second phase additions (Figure 39). On the other hand, stress-rupture capability was clearly compromised by the second phase additions. Although Alloy 21 exhibited very low rupture life during screening trials, the magnitude of the reduction in the phase mixtures is surprising.

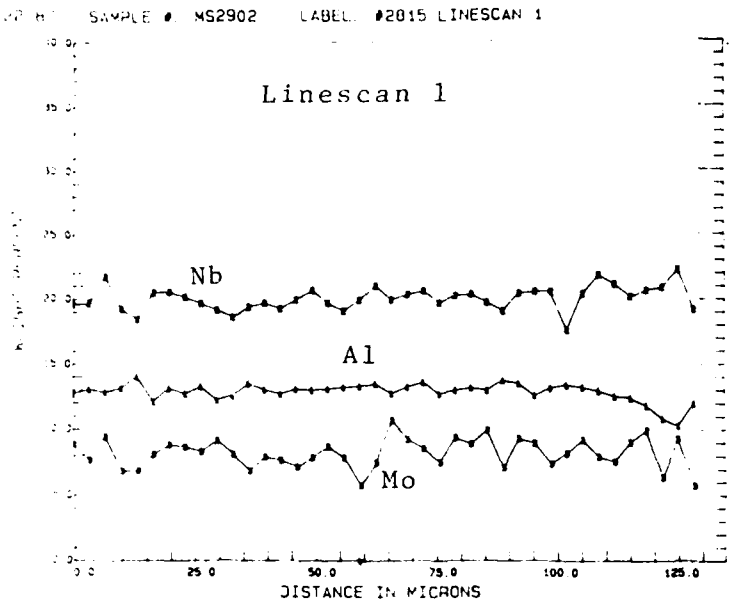

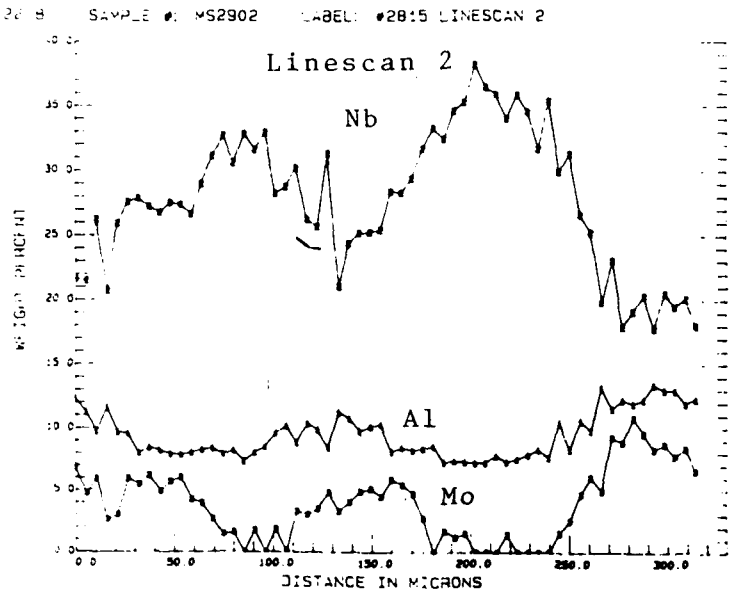

Figure 37

Electron microprobe analysis or as-forged Alloy 15 matrix and Alloy 21 powder blend. Note gradual reduction in of Al and Mo levels on line scan 2.

Table 22

Mechanical Property Summary for Task 2
Alpha-Two Alloy Phase Blends

Second Phase Size V/O	Material Condition	Test Temp. °C	°F	Yield Strength MPA (Ksi)	Ult. Tensile MPA (Ksi)	EL (%)	RA (%)	K1C MPa√M (Ksi√In)	650°C/380 MPa (1200°F/55 Ksi) Rupture Hours To Rupt.	EL (%)	RA (%)
None	HIP + STA	21*	RT	- -	345-552 (50-80)	<0.5	0*				
"		427*	800	- -	345-690 (50-100)	<0.5	0*	(6.3)	100-200*	-	-
"		650	1200	702 (101.8)	751 (108.8)		0.9	6.9			
≈200 µm 5% "A"	HIP + STA	21	RT	- -	586 (85.0)	-	-	(11.7)	12.8	1.6	-
		427	800	798 (115.7)	830 (120.3)	0.7	1.3	12.9			
		650	1200	649 (94)	704 (102)	1.1	2.7				
≈200 µm 20% "B"	HIP + STA	21	RT	- -	642 (93)	-	-	(14.3)	12.1	2.8	2.6
		427	800	748 (108.4)	794 (115)	1.0	2.0	15.7			
		650	1200	580 (84)	676 (98)	1.8	3.4				
≈100 µm 50% "C"	HIP + STA	21	RT	- -	497 (72)	-	-	(11.4)	20.2	1.7	0.6
		427	800	- -	745 (108)	-	-	12.5			
		650	1200	662 (96)	751 (106)	2.0	4.0				
≈100 µm 20% "D"	HIP + STA	21	RT	- -	759 (110)	-	-	(18.5)	19.1	1.1	2.1
		427	800	731 (106)	828 (120)	2.3	4.0	20.4			
		650	1200	600 (87)	656 (95)	3.1	4.0				
≈200 µm 20% "E"	HIP + Forge + STA	21	RT	- -	497 (72)	-	-	(16.0)	3.6	1.1	1.9
		427	800	787 (114)	828 (120)	0.8	2.0	17.6			
		650	1200	560 (81.2)	662 (96)	2.0	3.5				
≈100 µm 5% "F"	HIP + Forge + STA	21	RT	- -	567 (82)	-	-	(11.2)		No Test	
		427	800	814 (118)	828 (120)	1.0	1.3	12.3			
		650	1200	669 (97)	683 (99)	1.5	4.0				
≈100 µm 20% "G"	HIP + Forge + STA	21	RT	-	656 (85)	-	-	(15.5)		No Test	
		427	800	783 (113.5)	842 (122)	2.1	2.0	17.0			
		650	1200	607 (88)	650 (94)	6.5	9.0				

*Estimated from Task 1 data.

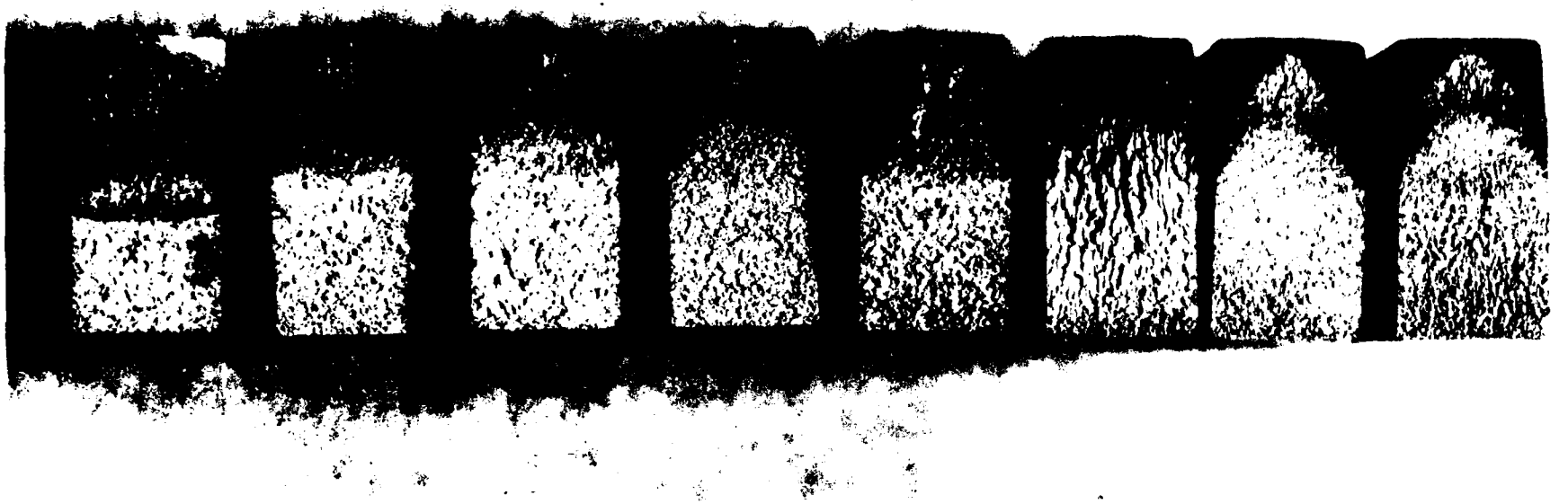

Figure 38

Fracture surface of Task 2 fracture toughness specimens showing baseline (left) and conditions A-G (L-R).

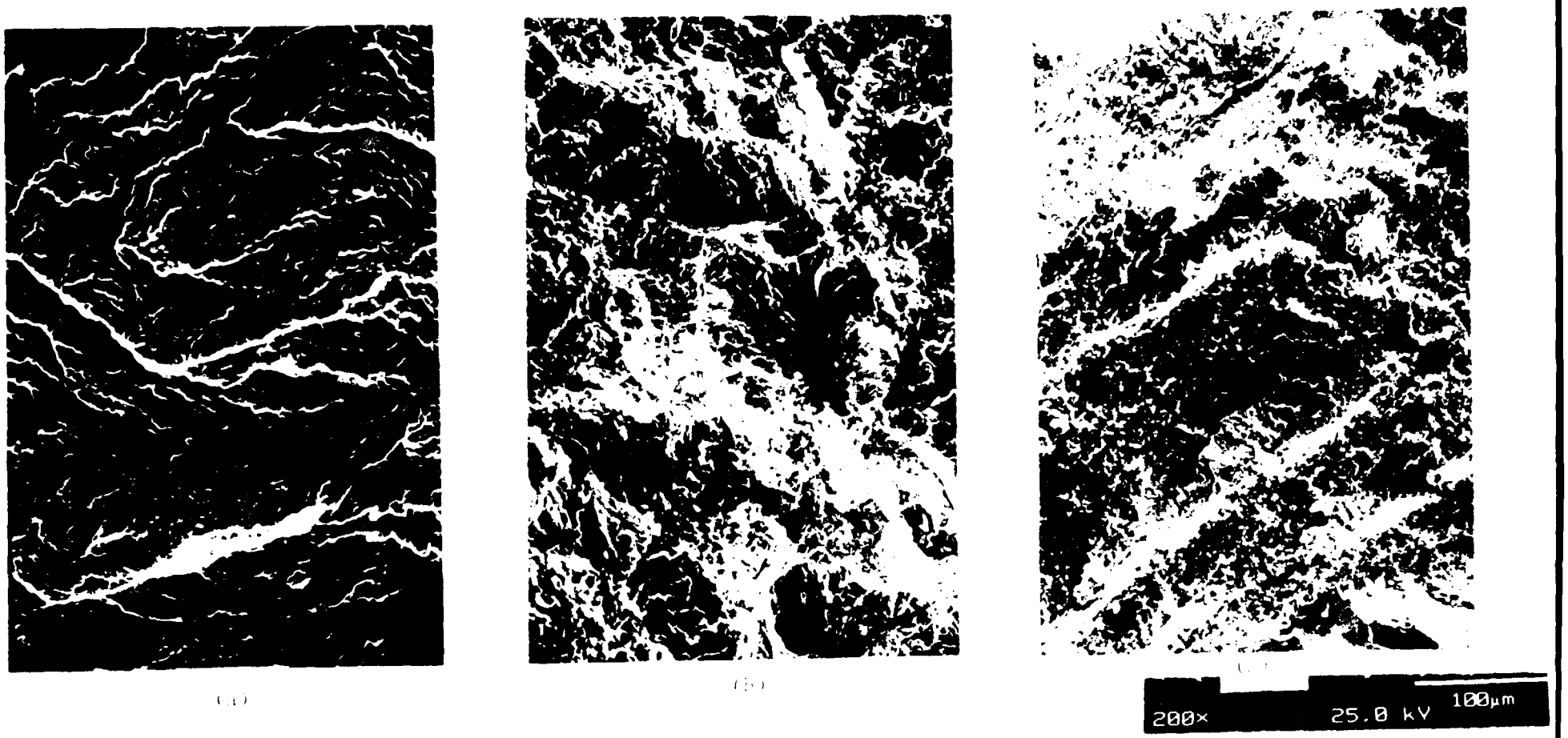

Figure 39

Fracture surfaces of Task 2 fracture toughness specimens in the rapid fracture zone: a) Baseline Ti-25Al-10Nb-4Mo; b) HIP Ti-25Al-10Nb-4Mo + 20 v/o Ti-15Al-22.5Nb; c) HIP + forged Ti-25Al-10Nb-4Mo + 20 v/o Ti-15Al-22.5Nb.

3.3 Task III - Dispersion Containing Alloys

3.3.1 Alloy Development and Processing - Rapid Solidification

The objective of this task was to create titanium aluminide alloys with dispersions of rare earth oxides to evaluate any potential for particle ductilizing and/or deoxidation of the matrix. Such dispersions have been produced by RSR methods in these and other titanium alloys by the additions of rare earth or lanthanide metals which scavenge the oxygen in the system[7-10]. Some workers have used direct addition of oxides to study the dispersion effect[6]. Alloys 3, 4 and 5 from Task 1 were selected for the study to permit a direct comparison of the behavior of the elements La, Ce and Er in both the conventionally cast and rapidly solidified conditions. The alloy Ti-25Al-10Nb-4V was selected as the baseline as a good data base existed for the alloy. Material from all the modified alloys was rapidly solidified using splat quenching. The apparatus used was developed by United Technologies Research Center, and is capable of processing 0.2 to 0.4 gram of an alloy. The cooling rate for the splats increases as the splat thickness decreases and can be varied from 10,000 C/s to 1,000,000 C/s. The melting operation is carried out under high vacuum resulting in minimal contamination. The size and shape of the product is compatible with simple bend testing.

3.3.2 Results and Discussion

Two splats were produced from the baseline alloy and Alloys 3, 4 and 5 (La, Er and Ce containing, respectively) and are illustrated in Figure 40. The base composition was quite ductile and could be bent 180° over a small radius without cracking (Figure 40a); the other alloys not only cracked in the as-splatted condition but had to be handled very carefully to avoid further cracking (Figure 40b, c and d). Sections of each alloy splat were subjected to a simulated consolidation cycle by vacuum annealing at 1000°C (1832°F) and 1250°C (2282°F) for one hour. During the heat treatment, the splats were sealed in CP titanium foil to prevent oxygen contamination of the surface. Additionally, the wrapped packets

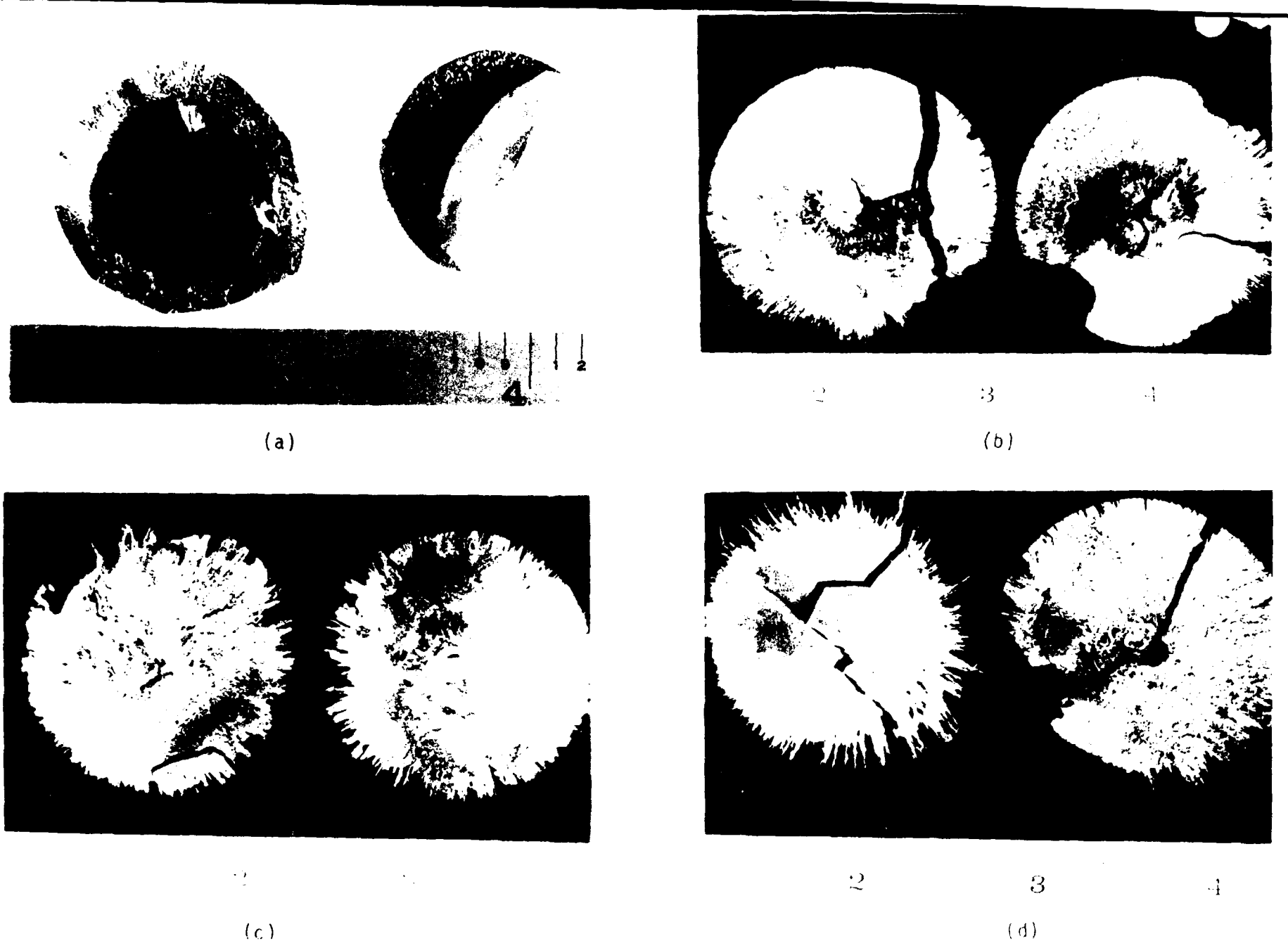

Figure 40

Titanium aluminide alloy rapidly cooled splats in the "as-splat" condition. a) Baseline alloy Ti-25Al-10Nb-4V; b) Alloy 3, Ti-25Al-10Nb-4V-.5La; c) Alloy 4, Ti-25Al-10Nb-4V-.5Er; d) Alloy 5, Ti-25Al-10Nb-4V-.5Ce.

were immersed in a titanium container filled with titanium sponge. After heating to 1000°C (1832°F), all alloys were ductile and could be bent through angles greater than 90° without failure. The alloys were less ductile after the 1200°C (2282°F) treatment but still showed some plastic behavior.

Evaluation of the baseline samples using transmission electron microscopy (TEM) revealed the presence of a single phase alloy with an average grain diameter of 8 μm (Figure 41). Microdiffraction showed that the crystal structure was BCC ordered (B2 type) with a lattice parameter a = 3.15A. After a 1000°C (1832°F) anneal, the alloy was found to have equiaxed grains 10-18 μm in diameter surrounded by a Widmanstatten structure (Figure 42). The B2 structure had transformed almost completely into an ordered hcp alpha-two phase with lattice parameters a=5.76A and c=4.58A.

Splats of alloys with La or rare earth additions exhibited an equiaxed grain structure 2-3 μm in diameter and dispersoids ranging in size from 0.01 μm to 0.06 μm (Figure 43). Microdiffraction revealed that the particles contained the expected rare earths, but only the erbium-rich particles could be directly confirmed as oxides, Er_2O_3 (a = 10.3A). The matrix in all cases was an ordered BCC phase with a lattice parameter of a = 3.15A and a very fine anti-phase domain structure, as found in the baseline alloy. Specimens annealed below the beta transus (1000°C/1832°F) showed little grain growth, but the size of the dispersoids increased substantially. The size ranges were as follows:

La: 0.3-1.2 μm
Er: 0.2-1.0 μm
Ce: 0.4-1.5 μm

A typical structure is shown in Figure 44 which again consists of alpha-two and transformed beta regions. Not surprisingly, annealing the splats above the beta transus at 1250°C (2282°F) caused the grain size to increase over tenfold to 50-60 μm and resulted in the formation of a coarse Widmanstatten structure on cooling. The dispersoids also coarsened to larger size, especially the La and Ce oxides. Size ranges values were now:

Figure 41

Microstructure of Ti-25 a/o Al-10 a/o Nb-4 a/o V in the as-splat condition. Matrix is a single phase bcc ordered (B2) structure.

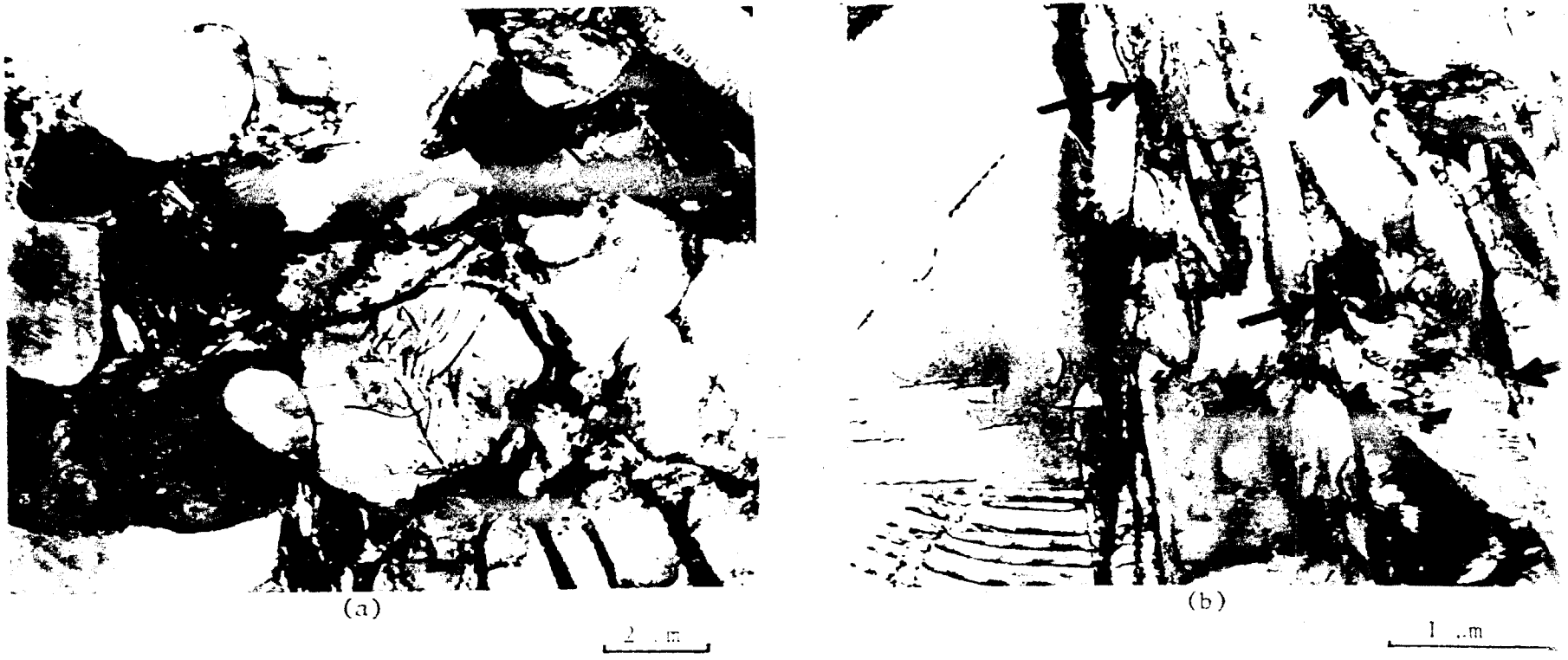

Figure 42

Microstructure of Ti-25Al-10Nb-4V in the 1000°C (1°32°F) annealed condition. a),equiaxed grains of ordered hexagonal phase (α_2); b),equiaxed grains surrounding regions of acicular Widmanstatten structure which is also predominantly ordered hexagonal (α_2)

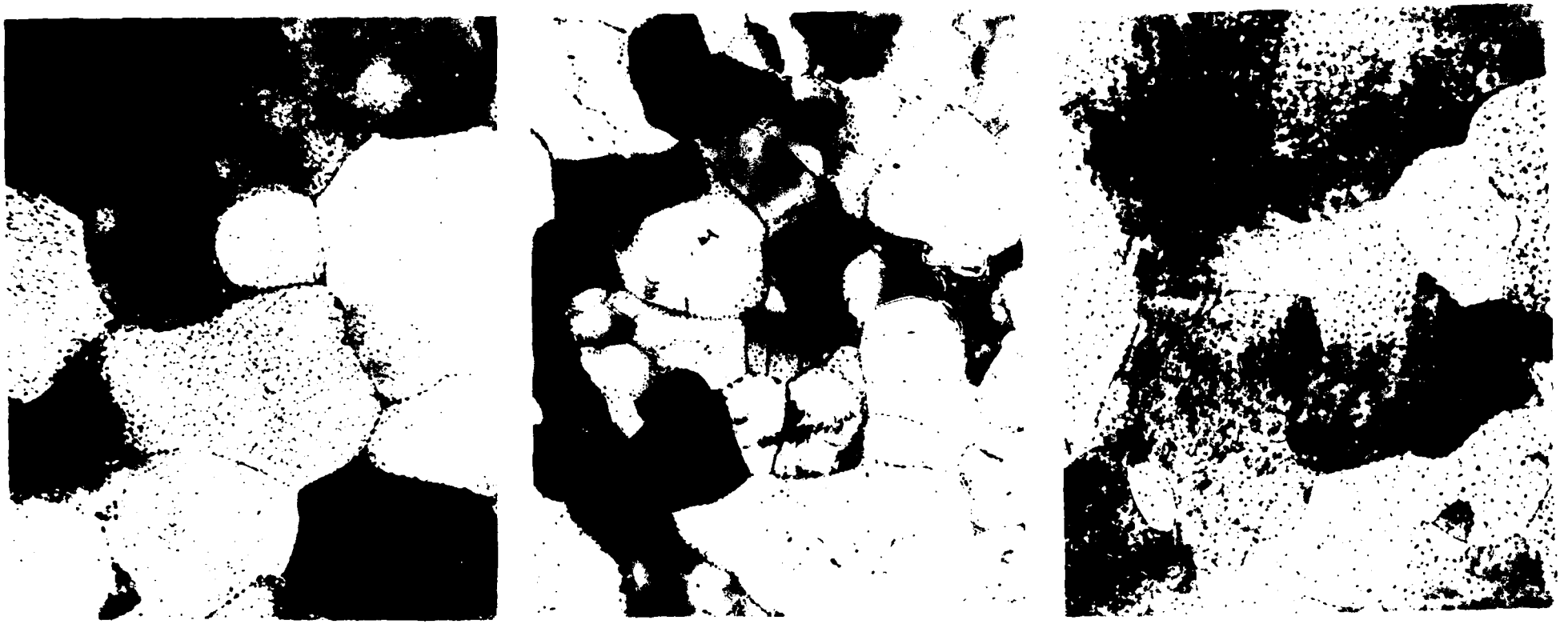

(a) (b) (c)

Figure 43 Mag: 7.5KX

Transmission electron microscope photos of thin foil titanium aluminide alloys in the as-splat condition. a) Alloy 3, Ti-25Al-10Nb-4V-.5La; b) Alloy 4, Ti-25Al-10Nb-4V-.5Er; c) Alloy 5, Ti-25Al-10Nb-4V-.5Ce.

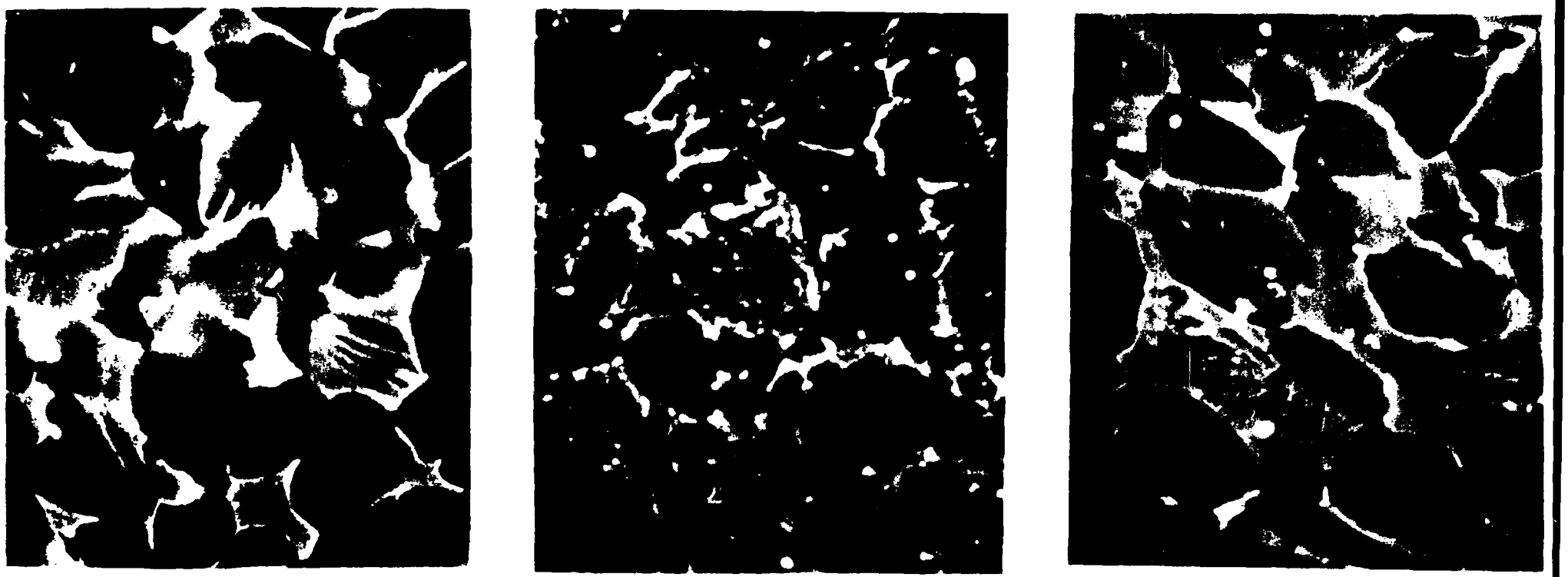

Figure ..

Microstructures of rapidly cooled dispersoid containing Ti-25Al-10[illegible]-4V splats after 1000°C (1832°F) anneal.

La: 1.0-3.0 μm

Er: 0.4-1.0 μm

Ce: 3.0-6.0 μm

Note that the erbia particles grew less than the others and maintained a spherical shape, while many of the lanthanum and ceria particles became rod-like (Figure 45). Again, the matrices are in all cases a transformed beta structure.

Based on the bend results and other information generated by other workers on RSR rare earth oxide effects, it was clear that there was little benefit of fine dispersion on ductility or toughness. Therefore, at this stage of Task 3, the situation was critically analyzed. To improve toughness, the rare earth additions have to scavenge the oxygen, resulting in low remaining amounts of oxygen in the matrix. The general brittleness of the material with very fine oxide dispersions indicated that any beneficial effect must occur at intermediate particle sizes. Since previous experience with ingot additions of these elements in Task 1 showed that rather coarse dispersoids could be damaging at high temperatures, it was decided to direct the remaining effort in this task to establishing in a systematic way, whether the deoxidation process can effectively increase toughness. The experimental evidence pointed to a rather narrow window for such an approach.

Erbium was selected as the rare earth addition because it appeared to be more thermally stable and result in an alloy with better mechanical properties than the La to Ce as reported in section 3.1.2. The erbium level added was calculated to reduce oxygen in the matrix to <0.05% and not leave 'free' erbium in the lattice. The Ti-25Al-10Nb-3V-1Mo alloy was selected as the base alloy since a fairly extensive data base is available. The PREP process was selected to produce the powder as it was considered the slower rate of cooling would produce intermediate size oxide particles directly and thus avoid some of the problems with very fine precipitates. It was decided to examine six potential process

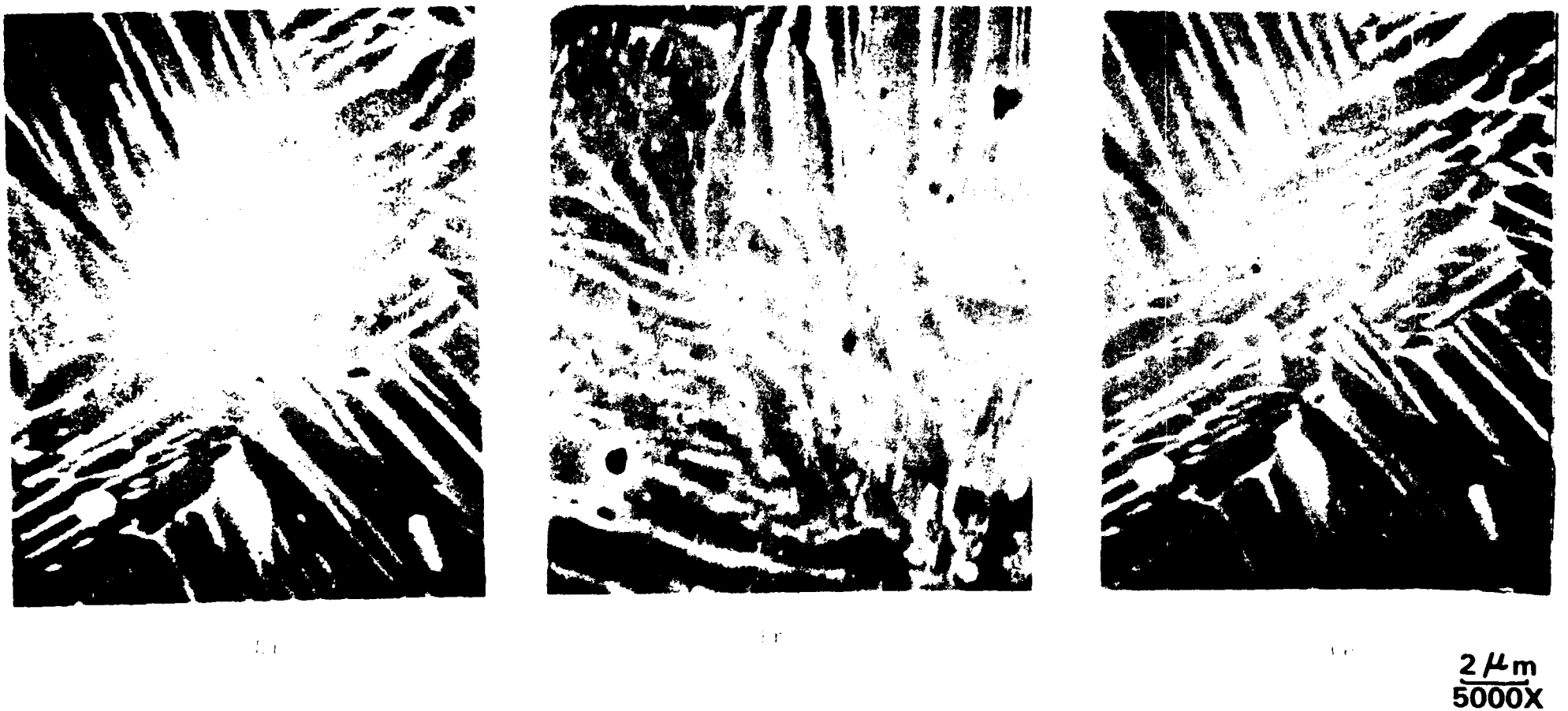

Figure [illegible]

Microstructures of rapidly cooled, dispersoid containing Ti-25Al-10Nb-4V splats after a 1250°C (2282°F) anneal.

cycles to define the variations in oxide dispersions that could be produced. Based on this screening, sufficient material was processed to permit determination of the tensile, creep and toughness properties.

3.3.3 Evaluation of Alloy Deoxidation

Two VAR ingots of the Ti-25Al-10Nb-3V-1Mo-.3Er alloy were melted, processed and machined prior to powder conversion, as previously described in section 3.2.3.1. The ingots were successfully converted to powder using the PREP technique. Chemical composition of the powder is given in Table 23. Examination of the remaining ingot stubs showed no segregation or other abnormalities (Figure 46). The powder was examined using the scanning electron microscope. Unmounted powder particles showed the characteristic dendritic appearance and exhibited a relatively uniform particle size (Figure 47). SEM examination of the polished cross section of typical -80 mesh particles revealed the presence of erbia particles varying in size from 0.2 μm to 1 μm concentrated in the dendrite boundaries (Figure 48). Sizes were significantly larger than those measured in splats but finer than the dispersoid size in the erbium containing ingot metallurgy product. HIP consolidation trials were conducted using the powder sealed in commercially pure titanium alloy containers as previously described. Three temperatures were evaluated. Samples were held at 900°C (1650°F), 1010°C (1850°F) and 1120°C (2050°F) for two hours at a pressure of 105 MPa (15 ksi) and subsequently examined metallographically.

After HIP at 900°C (1650°C) prior particle boundaries were quite distinct and the presence of unhealed porosity was apparent (Figure 49a). After 1010°C (1850°F) prior particle boundaries were less distinct and no porosity was detectable (Figure 49b). At 1120°C (2050°F) the structure exhibited a fine grained Widmanstatten appearance, typical of material annealed above the beta transus. No porosity was apparent (Figure 49c). Using SEM it was found that dispersoids showed no significant change in size for the three HIP temperatures (Figures 50-52) and, in fact, were

Table 23

Chemical Composition of Nuclear Metals Inc.
PREP Powders for Task 3
(In Weight Percent)

Alloy	Task		Average Composition Al	Nb	V	Mo	Er	O	N
148-86	3	Aim	14.0	19.0	3.2	2.0	1.0	0.10*	0.04*
		Actual	12.8	18.9	3.3	2.06	0.77	0.08	0.008

*Maximum

Figure 46

Ingot stubs of Ti-25Al-10Nb-3V-1Mo-.3Er alloy after PREP processing.

Figure 4-7

SEM photos of Ti-25Al-10Nb-3V-1Mo-.3Er alloy PREP powder.

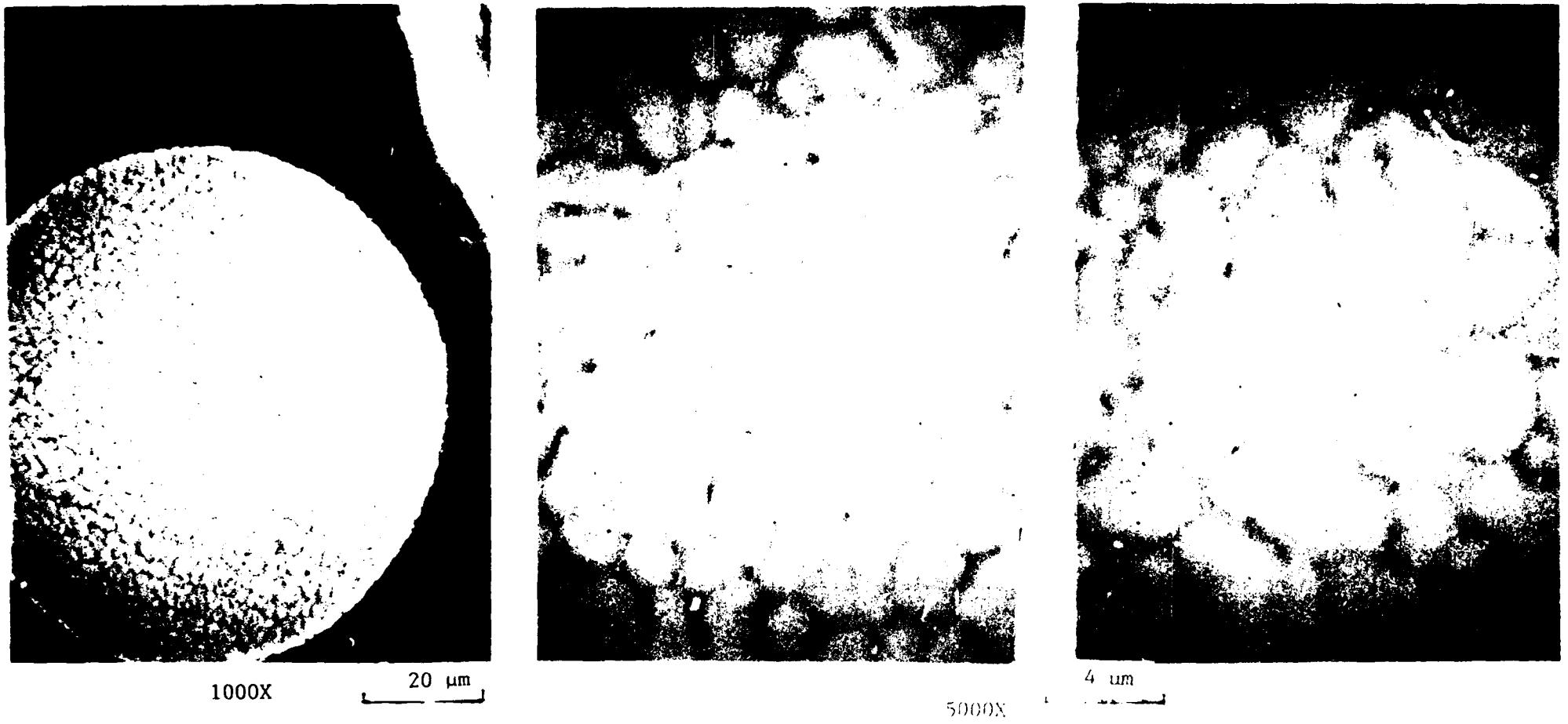

Figure 18

Microstructure of Ti-25Al-10Nb-3V-1Mo-.3Er PREP powder particle cross section. White flecks are erbia particles. Center, small particle; right, large particle.

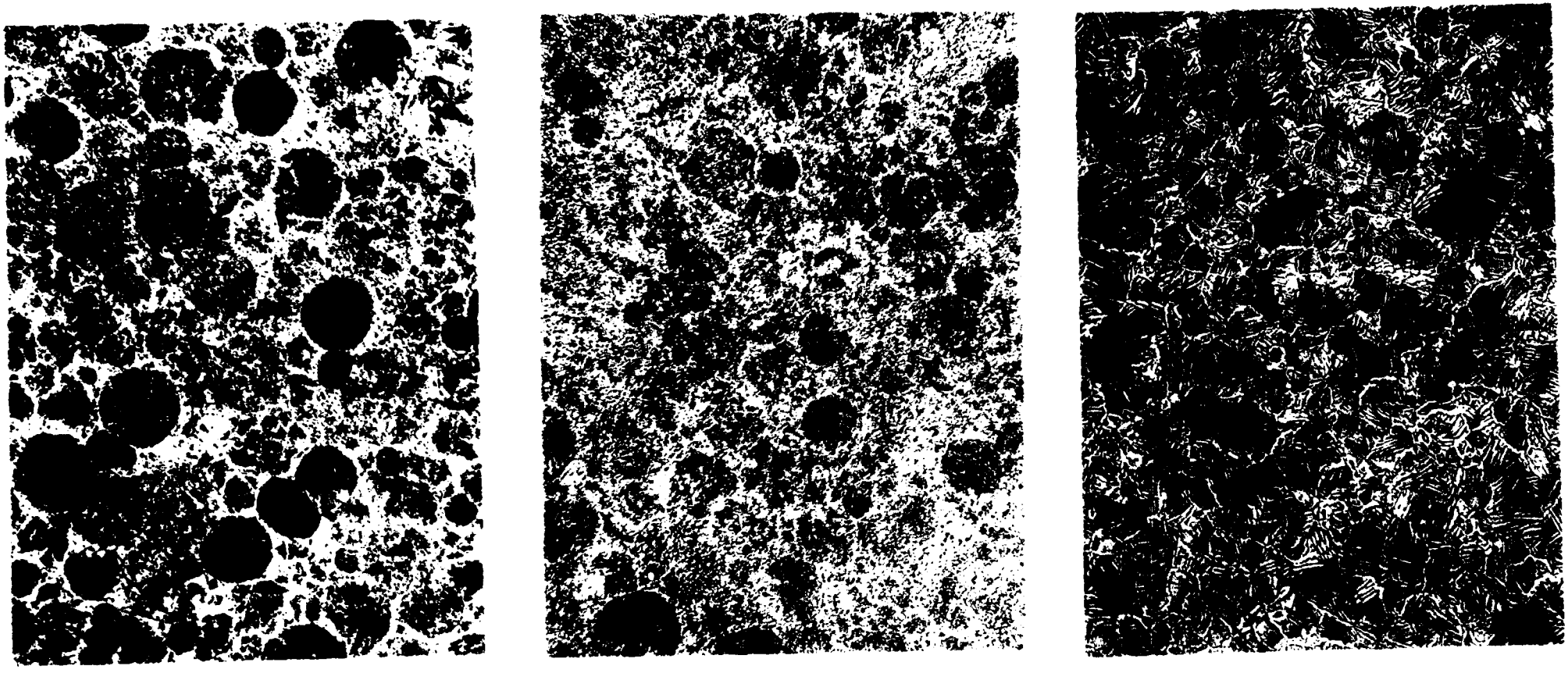

Figure 49

Effect of HIP temperature on the microstructure of Ti-25Al-10Nb-3V-1Mo-.3Er. a) 900°C (1650°F); b) 1010°C (1850°F); c) 1120°C (2050°F). All samples were held at 105 MPa (15 ksi) for 2 hours.

1000X

3000X

Figure 50

Microstructures of Ti-25Al-10Nb-3V-1Mo-.3Er after 900°C (1650°F)/105MPa (15ksi)/ 2 hour HIP. Note fine erbia dispersoids (white) in the grains.

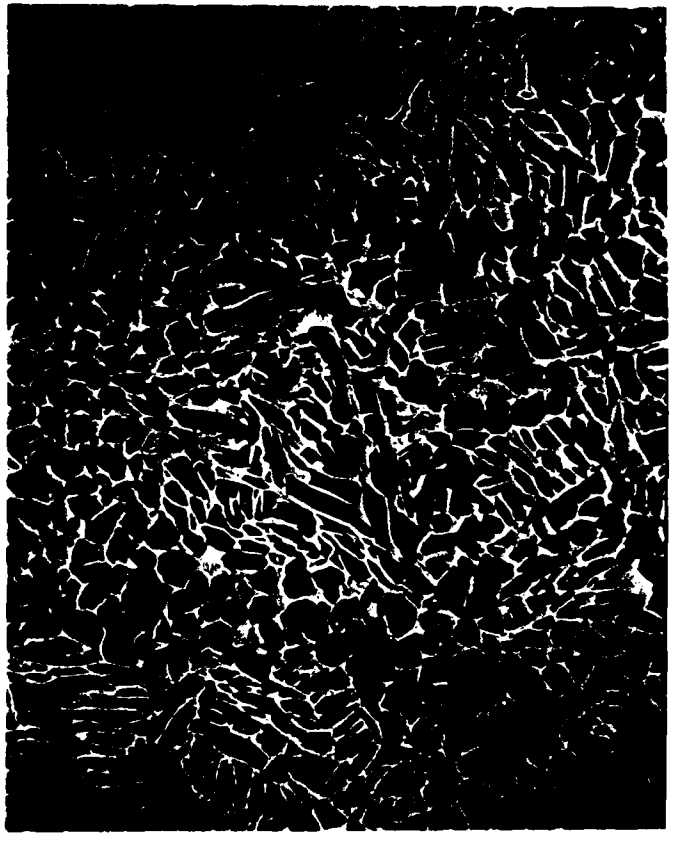

1000X

5000X

Figure 51

Microstructures of Ti-25Al-10Nb-3V-1Mo-.3Er after 1010°C(1850°F)/103MPa (15 ksi)/ 2 hour HIP. Note fine erbia dispersoids (white) in the grains.

1000X

20 μm

Figure 52

Microstructures of Ti-25Al-10Nb-3V-1Mo-.5Fr after 1120°C [illegible]
2 hour HT. Note fine erbia dispersoids (white) in [illegible].

unchanged from the atomized powder of 0.2μ to 1μ. This indicates that the erbia dispersoids are stable to quite high temperatures. Based on these observations, HIP at 1010°C (1850°F) and 1120°C (2050°F) were selected as consolidation temperatures for mechanical property testing.

The consolidations were prepared in a similar manner to those used in the Task 2 phase blending evaluation. Powder was introduced into commercially pure titanium pipe cans which were evacuated, sealed and HIP. Selected containers were isothermally side upset ≈60% using the P&W 4.5 MN (500 ton) press. The specific processing conditions are listed in Table 24. An example of the consolidations are shown in Figure 53.

Material HIP at 1010°C (1850°F) was fully dense although prior particle boundaries were still visible at low magnification (Figure 54). Average hardness was 291 Hv. Solution treating and aging increased the hardness to 360 Hv. The microstructure did not change significantly except a needle-like transformed phase was now visible in the alpha-two (white) regions; no change in dispersoid size was observed (Figure 55). The material showed an uneven etching behavior indicative of some chemical variation, but EDAX analysis could detect no significant difference in composition. Material HIP at 1120°C (2050°F) exhibited a coarsened transformed colony type alpha-two phase structure with grain boundary alpha-two present. Dispersoid size was in the 0.1-1 μm range as before (Figure 56) and hardness was 275 Hv. Solution treating and aging increased the hardness to 360 Hv. Grain size and dispersoid size were unchanged but a Widmanstatten structure was formed due to the faster cooling rate (Figure 57). Some material HIP at 1010°C (1850°F) was isothermally side upset about 60% at 927°C (1750°F) and other material HIP at 1120°C (2050°F) was forged ≈60% at 1120°C (2050°F). Forging at the lower temperature resulted in a microstructure and hardness very similar to that of as-HIP material (Figure 58), while the beta HIP + forged material had a fine Widmanstatten needle-like appearance due to relatively rapid cooling from the press (Figure 59). Solution treating and aging of the forgings resulted in microstructures virtually identical to the HIP counterparts, with hardnesses in the 300-330 Hv range (Figures 60 and 61).

Table 24

Processing Conditions for Task 3
Alloy Ti-25Al-10Nb-3V-1Mo-.3Er

α-β HIP @ 1010°C (1850°F)/105 MPa (15 Ksi)/2 Hours;

β HIP @ 1120°C (2050°F)/105 MPa (15 Ksi)/2 Hours;

α-β HIP + STA 1010°C (1850°F)/1/AC + 815°C (1500°F)/8/AC;

α-β HIP + Forge 927°C (1750°F) + STA as above;

β HIP + STA 1010°C (1850°F)/1/AC + 815°C (1500°F)/8/AC;

β HIP + Forge 1120°C (2050°F) + STA as above

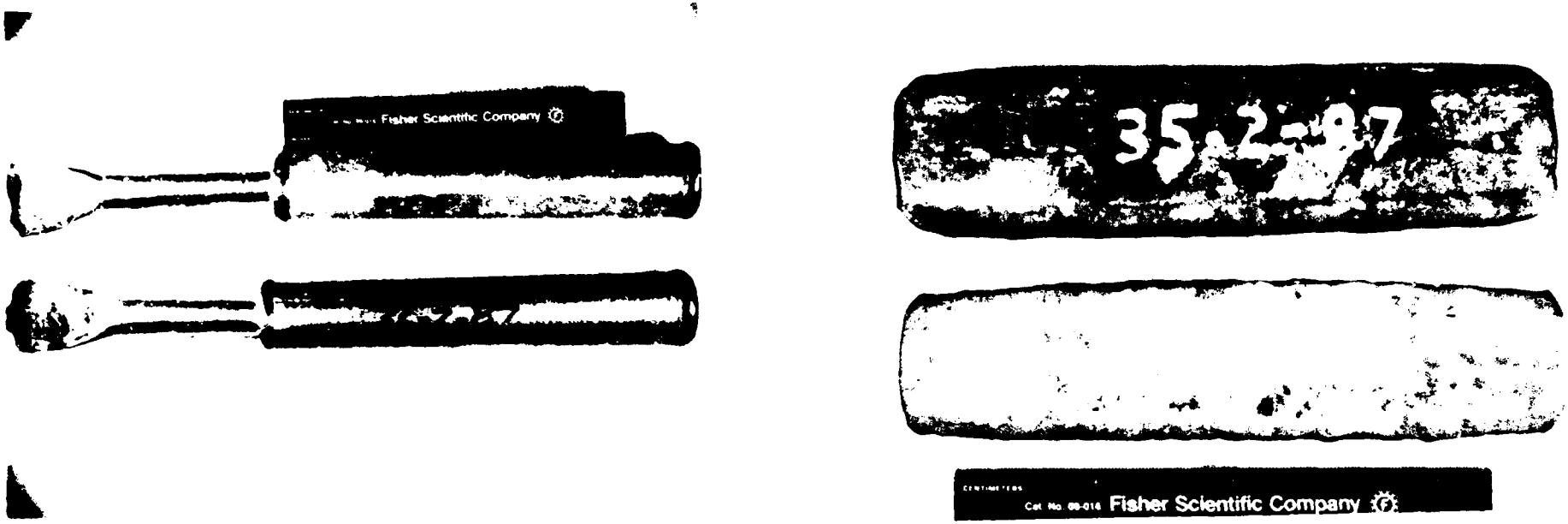

a) b)

Figure 33

Examples of Ti-25Al-10Nb-3V-1Mo compacts produced for Task 3. a) HIP'ed cans; b) side upset HIP cans. 35 series was processed below the beta transus, 36 series above the beta transus.

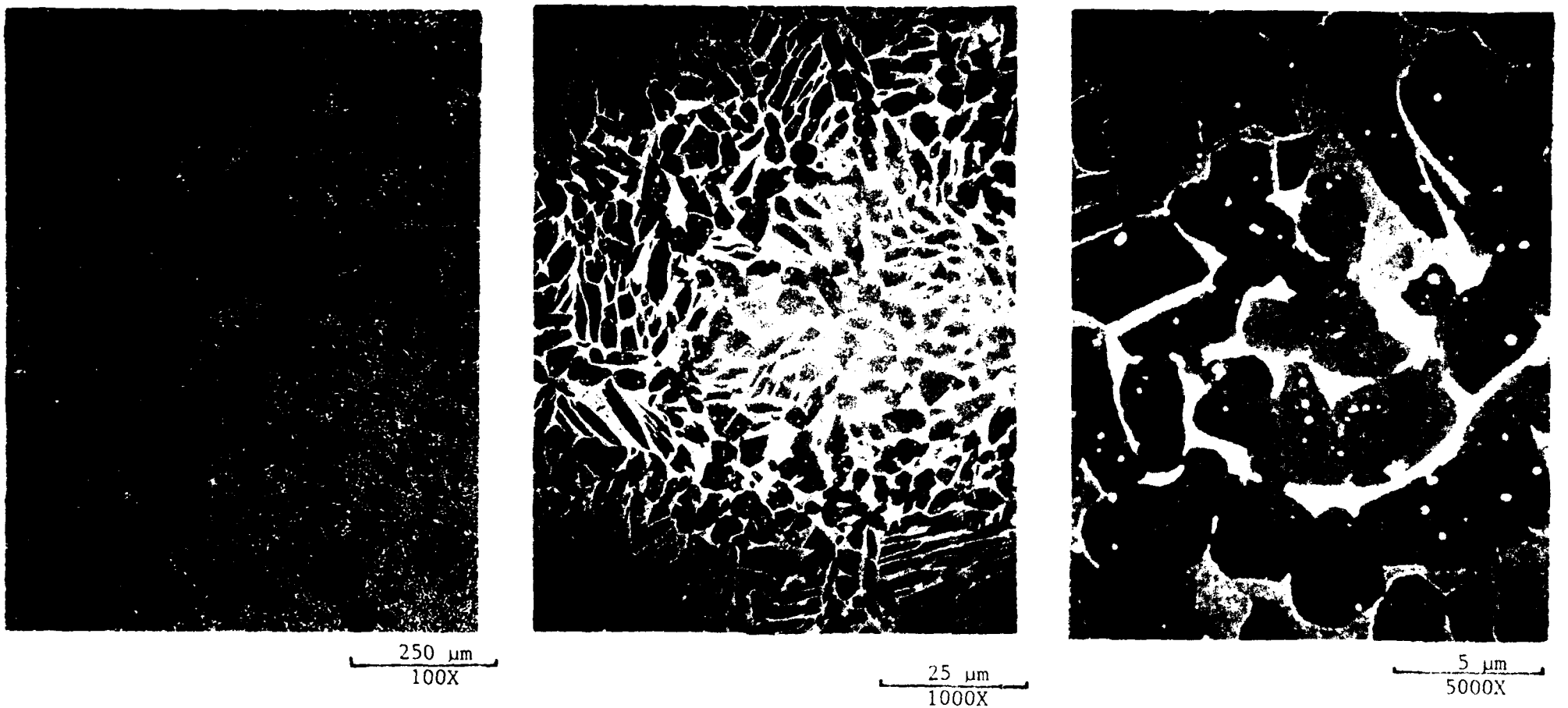

Figure 54

Typical microstructure of Ti-25Al-10Nb-3V-1Mo-0.3Er powder HIP'ed at 1010°C (1850°F)/105 MPa (15 ksi)/2 hours.

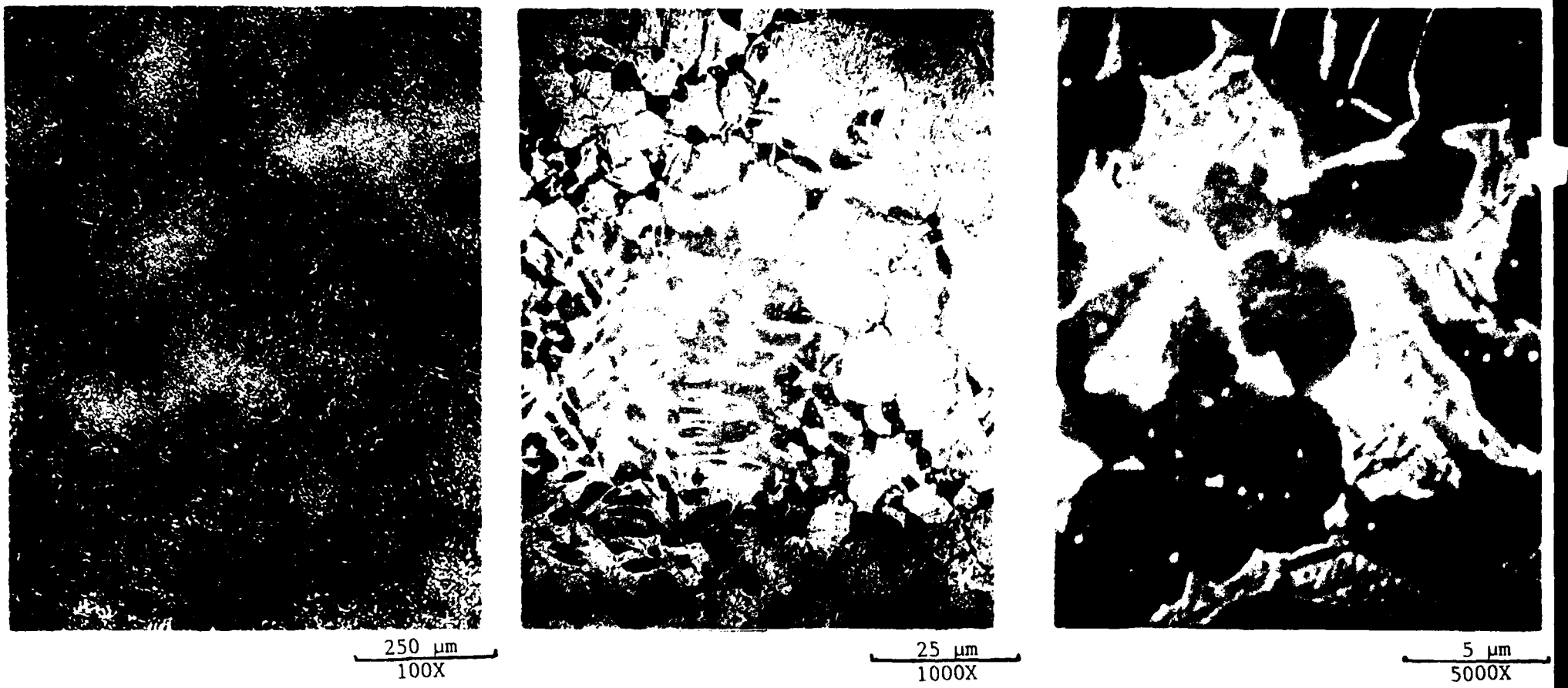

Figure 55

Typical microstructure of Ti-25Al-10Nb-3V-1Mo-0.3Er powder HIP'ed at 1010°C (1850°F)/105 MPa (15 ksi) followed by solution treated and aging at 1010°C (1850°F)/1 hour/AC + 815°C (1500°F)/8 hours/AC.

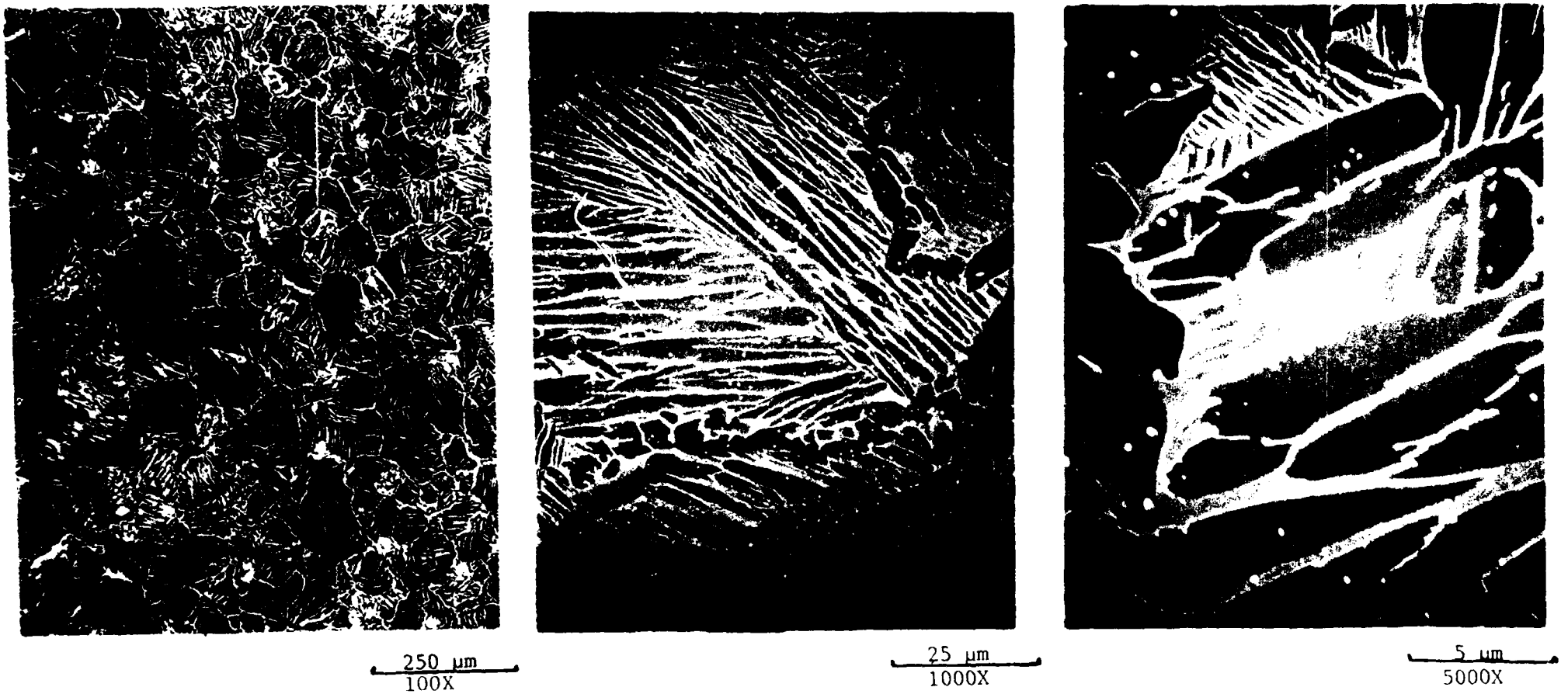

Figure 56

Typical microstructure of Ti-25Al-10Nb-3V-1Mo-0.3Er powder HIP'ed at 1120°C (2050°F)/105 MPa (15 ksi) for 2 hours.

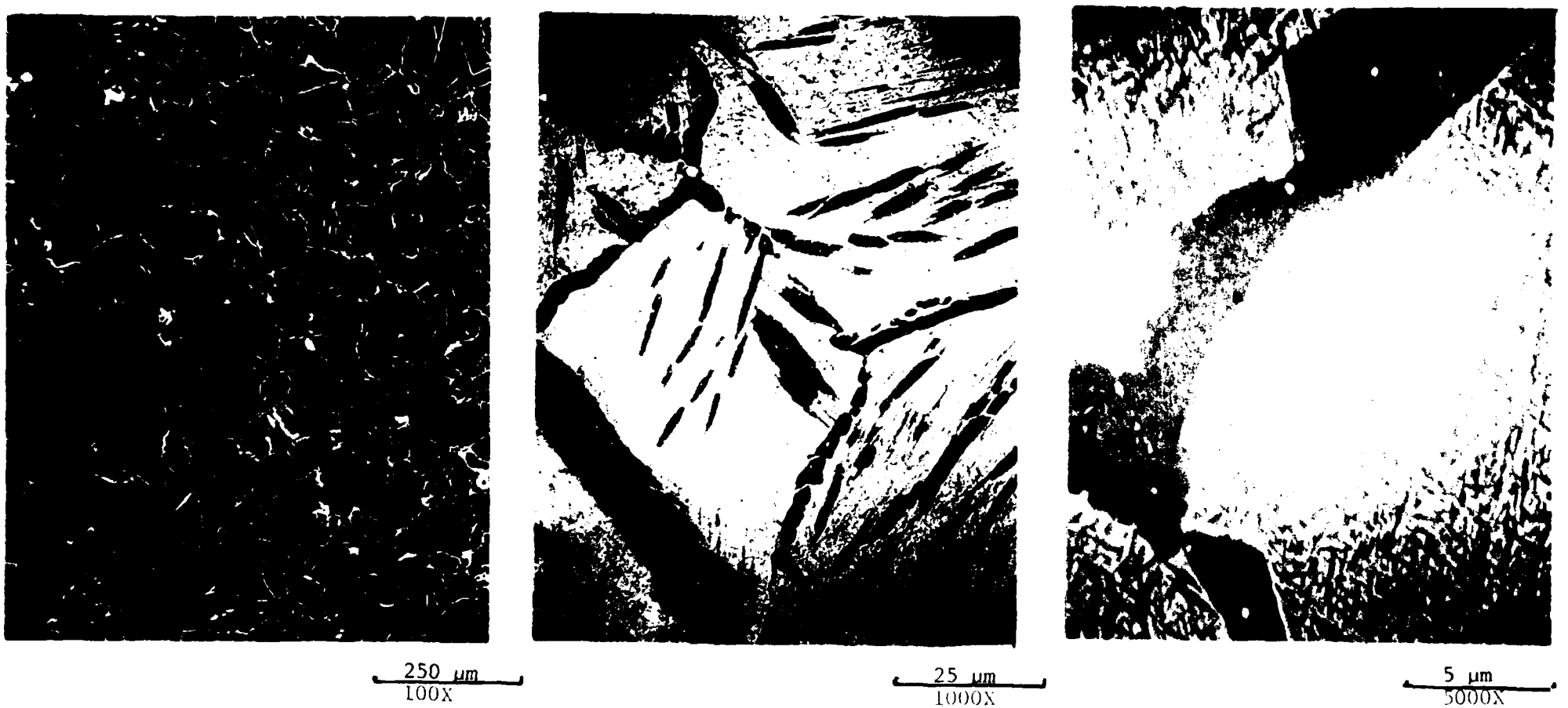

Figure 57

Typical microstructure of Ti-25Al-10Nb-3V-1Mo-0.3Er powder HIP'ed at 1120°C (2050°F)/105 MPa (15 ksi) and solution treated and aged at 1010°C (1850°F)/1 hour/AC + 815°C (1500°F)/8 hours/AC.

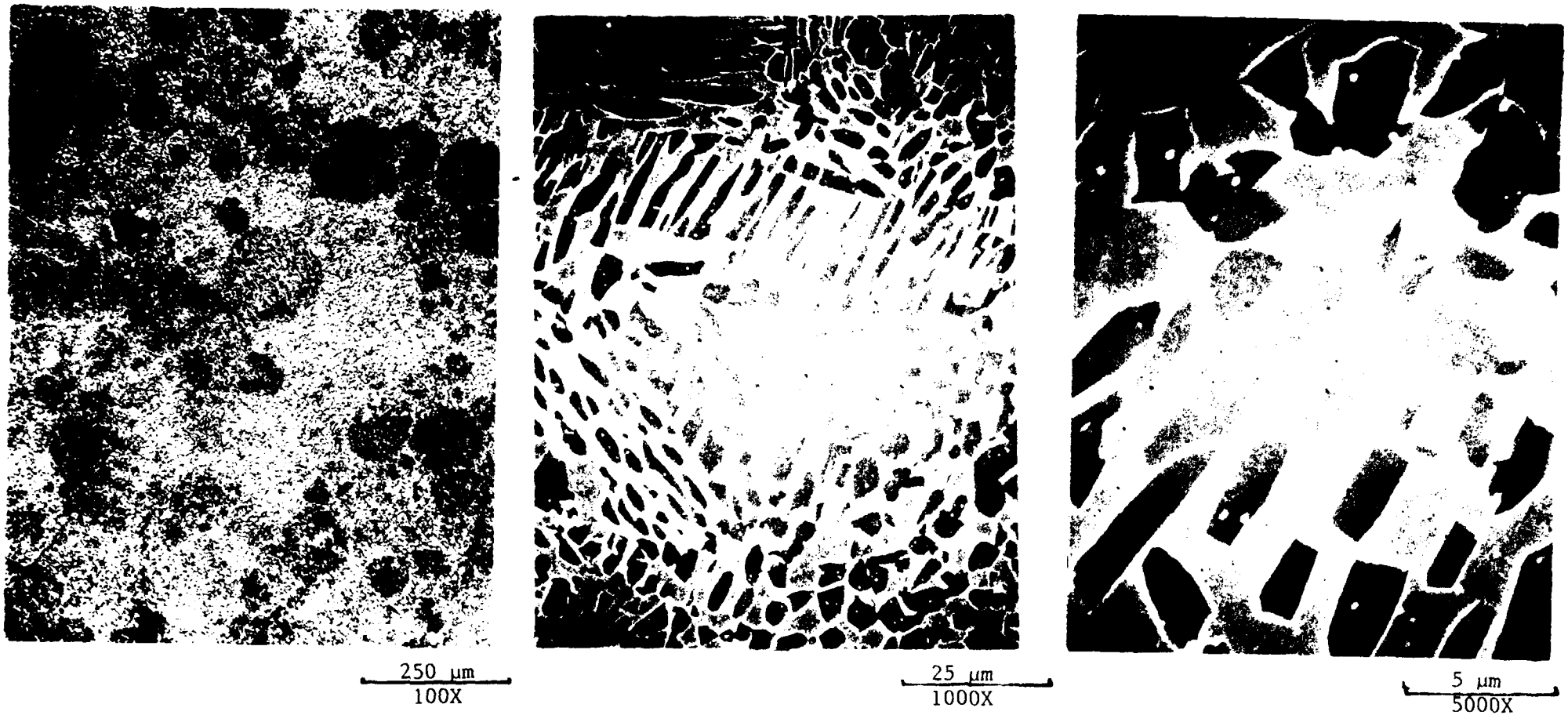

Figure 58

Typical microstructure of Ti-25Al-10Nb-3V-1Mo-0.5Er powder HIP'ed at 1010°C (1850°F)/105 MPa (15 ksi)/2 hours and isothermally forged at 927°C (1750°F).

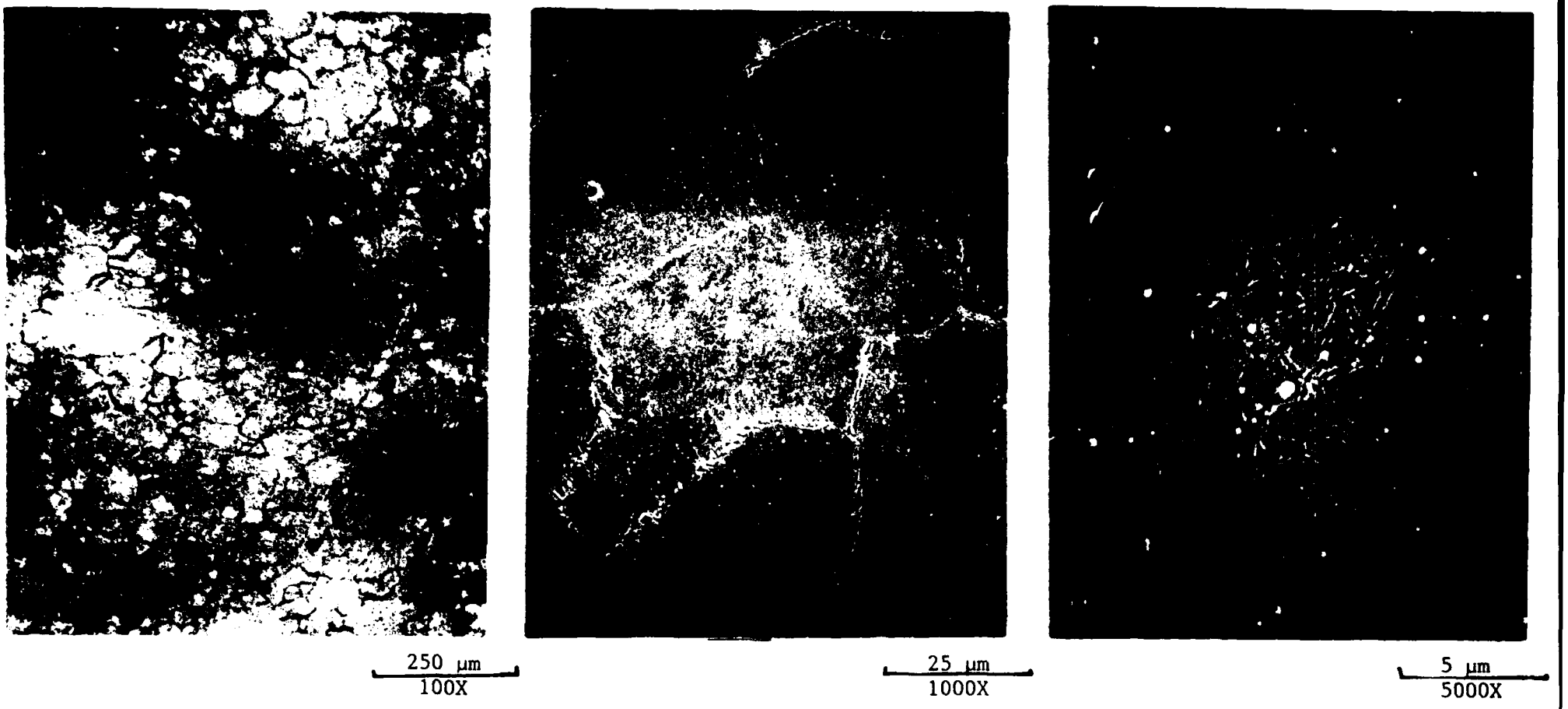

Figure 59

Typical microstructure of Ti-25Al-10Nb-3V-1Mo-0.3Er powder HIP'ed at 1120°C (2050°F)/105 MPa (15 ksi)/2 hours and isothermally forged at 1120°C (2050°F).

250 µm
100X

25 µm
1000X

5 µm
5000X

Figure 60

Typical microstructure of Ti-25Al-10Nb-3V-1Mo-0.3Er powder HIP'ed at 1010°C, forged at 927°C (1750°F) and solution treated and aged at 1010°C (1850°F)/1 hour/AC + 815°C (1500°F)/8 hours/AC.

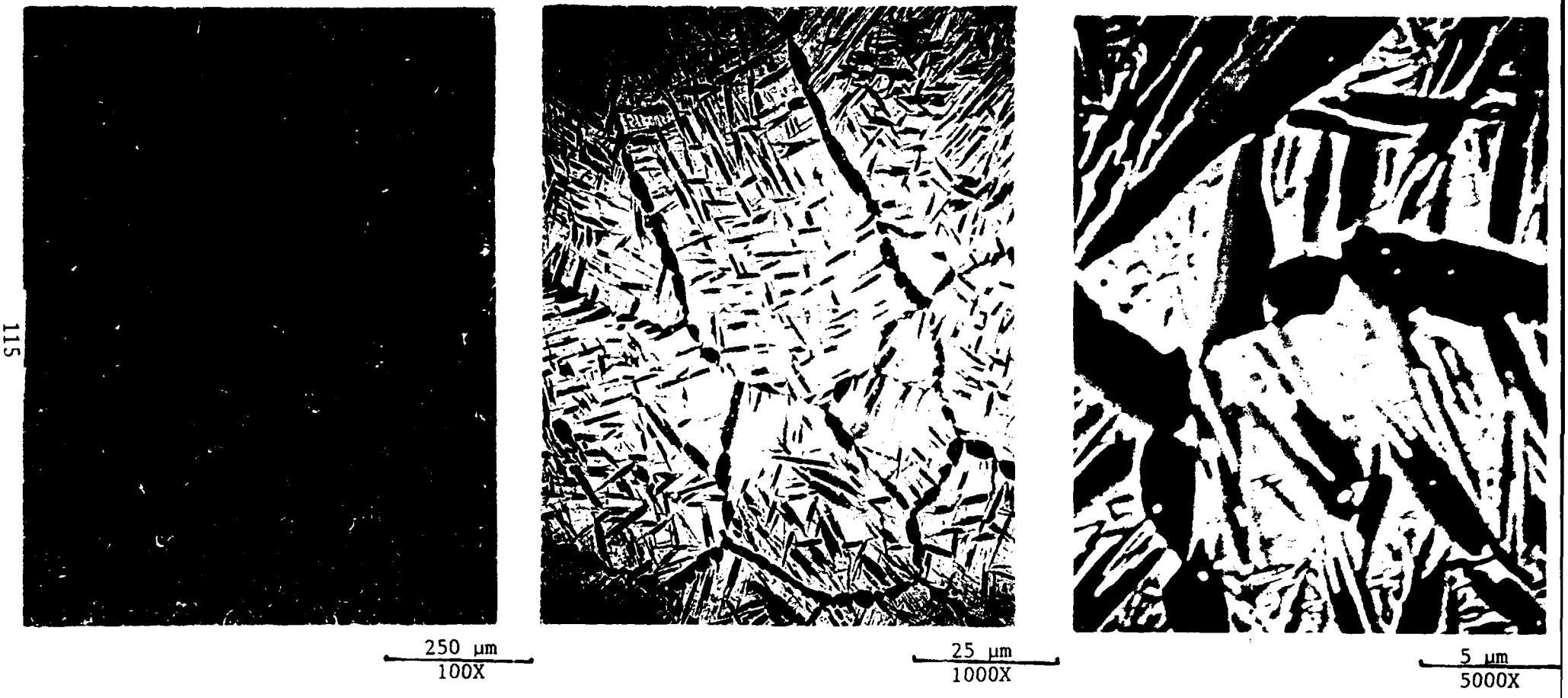

Figure 61

Typical microstructure of Ti-25Al-10Nb-3V-1Mo-0.3Er powder HIP'ed at 1120°C (2050°F), forged at 1120°C (2050°F) and solution treated and aged at 1010°C (1850°F)/1 hour/AC + 815°C (1500°F)/8 hours/AC.

Mechanical property evaluation consisted of tensile tests from ambient to 650°C (1200°F), RT fracture toughness tests and stress-rupture testing at 650°C (1200°F)/385 MPa (55 ksi). The property data are summarized in Tables 25 and 26. We can conclude that the best strength and toughness resulted from beta forging and solution treating; however, none of the processes yielded properties equivalent to wrought baseline alloy. It was noted that the dispersion containing alloy tended to strain harden more than the unmodified alloy because, at elevated temperatures, the gap between yield and ultimate strength was large, but did not result in a corresponding increase in ductility. Creep-rupture lives were very poor, similar to those measured for forged ingot metallurgy specimens containing very large oxides.

Based on these data, it is apparent that the presence of rare earth oxides offered little contribution to either improved tensile or toughness properties in the alpha-two alloy system under the conditions evaluated. Further pursuit of dispersoid strengthening or deoxidation appeared to be unwarranted by the results obtained. Accordingly, it was decided not to incorporate dispersion-forming elements in Task 4 alloys.

3.4 Task 4 - Combination Alloys

3.4.1 Alloy/Process Selection

After completion of the first three tasks of Phase 1, a total of eight conditions, combining the best alloys and/or processes developed in these tasks, were selected for further study. Based on a critical review of the data, it was decided to examine two ingot metallurgy alloy conditions and six phase blended conditions (Table 27). The ingot metallurgy alloys were modifications of the Ti-24.5Al-17Nb (Alloy 19) alloy from Task 1. This alloy exhibited excellent tensile properties and toughness but marginal creep-rupture capability. Thus, the two modifications were made that were intended to increase high temperature properties without degrading the ductility and toughness. The two alloys had the

Table 25

Tensile Properties and RT Fracture Toughness of Task 3 Dispersion Containing Ti-25Al-10Nb-3V-1Mo-.3Er Alloy

Consolidation Method	Heat Treatment	Test Temp. °C	Test Temp. °F	0.2% YS MPA	0.2% YS Ksi	UTS MPA	UTS Ksi	EL (%)	RA (%)	RT K_C MPa $\sqrt{M}$eter (Ksi $\sqrt{I}$nch)
HIP 1010°C/105 MPa/2 Hours (1850°F/15 ksi/2 Hours)	None	21	70	634	91.9	659	95.6	0.5	None	
		21	70	680	98.7	703	101.9	0.75	None	
		427	800	463	67.2	579	84.0	3.5	2.7	17.3
		427	800	471	68.3	595	86.3	3.2	4.0	(15.7)
		650	1200	400	58.1	449	65.1	5.0	5.8	
		650	1200	417	60.5	471	68.3	4.15	5.8	
HIP 1010°C/105 MPa/2 Hours (1850°F/15 Ksi/2 Hours)	1010°C (1850°F)/1 Hour/AC + 815°C (1500°F)/8 Hour/AC	21	70	494	71.7	557	80.8	0.2	None	16.9
		21	70	361	52.3	409	59.3	0.2	None	(15.5)
		427	800	534	77.4	601	87.2	1.0	None	
		427	800	532	77.1	637	92.4	0.1	None	
		650	1200	445	64.5	459	66.6	0.7	1.3	
		650	1200	425	61.6	461	66.9	0.7	1.3	
HIP 1120°C/105 MPa/2 Hours (2050°F/15 Ksi/2 Hours)	None	21	70	565	82.0	629	91.3	0.8	None	16.6
		21	70	581	84.3	669	97.1	1.1	None	(15.1)
		427	800	376	54.5	649	94.2	5.9	4.5	
		427	800	391	56.7	605	87.8	4.3	5.8	
		650	1200	330	47.9	459	66.6	4.2	5.3	
		650	1200	356	51.6	450	65.2	1.9	4.5	
HIP 1120°C/105 MPa/2 Hours (2050°F/15 Ksi/2 Hours)	1010°C (1850°F)/1 Hour/AC + 815°C (1500°F)/8 Hour/AC	21	70	682	98.9	842	122.1	0.8	2.6	20.4
		21	70	691	100.2	782	113.4	0.8	1.3	(18.5)
		427	800	493	71.5	551	80.8	0.9	4.0*	
		427	800	329	76.7	690	100.0	1.4	1.33	
		650	1200	441	63.9	523	75.8	0.7	None	
		650	1200	471	68.3	504	73.1	0.8	2.6	

*Not at fracture

Table 25

Tensile Properties and RT Fracture
Toughness of Task 3 Dispersion
Containing Ti-25Al-10Nb-3V-1Mo-.3Er Alloy
(Continued)

Consolidation Method	Heat Treatment	Test Temp. °C	Test Temp. °F	0.2% YS MPA	0.2% YS Ksi	UTS MPA	UTS Ksi	EL (%)	RA (%)	RT K_{IC} MPa $\sqrt{Meter}$ (Ksi $\sqrt{Inch}$)
HIP 1010°C/105 MPa/2 Hours (1850°F/15 Ksi/2 Hours) + Forge 954°C (1750°F)	1010°C (1850°F)1 Hour/AC + 815°C (1500°F)/8 Hour/AC	21	70	601	87.2	635	92.1	0.6	None	19.8 (18.0)
		21	70	692	100.3	718	104.1	0.6	None	
		427	800	498	72.3	693	93.2	2.2	3.9	
		427	800	517	75.0	634	91.9	1.2	None	
		650	1200	463	67.2	502	72.8	0.98	None	
HIP 1120°C/105 MPa/2 Hours (2050°F/15 Ksi/2 Hours) + Forge 1120°C (2050°F)	1010°C (1850°F)/1 Hour/AC + 815°C (1500°F)/8 Hour/AC	21	70	701	101.7	888	128.8	2.2	2.6	20.9 (19.0)
		21	70	701	101.7	632	120.7	1.3	1.3	
		427	800	512	74.2	634	91.9	1.2	None	
		427	800	522	75.7	776	112.6	4.2	4.5	
		650	1200	475	68.9	560	81.2	1.2	1.3	
Beta Forged Wrought Baseline (No Er)	815°C (1500°F)/1/2 Hour/AC + 593°C (1100°F)/8 Hours AC	21	70	700	101.0	915	132.0	3.3	5.5	15.0 (16.5)
		427	800	508	73.3	948	136.9	21.8	27.5	
		650	1200	434	62.7	708	102.1	11.3	22.3	

Table 26

Stress-Rupture Properties of Task 3 Dispersion
Containing Ti-25Al-10Nb-3V-1Mo-.3Er Alloy*

Consolidation Method	Heat Treatment	650°C/380 MPa Rupt. Life, Hrs	(1200°F/ 55 Ksi) %EL	%RA
HIP 1010°C/105 MPa/2 Hours (1850°F/15 Ksi/2 Hours)	None	0.3	2.1	3.3
HIP 1120°C/105 MPa/2 Hours (2050°F/15 Ksi/2 Hours)	None	Rupt. on Loading	1.2	0
HIP 1120°C/105 MPa/2 Hours (2050°F/15 Ksi/2 Hours)	1010°C (1850°F)/1 Hour/AC	Rupt. on Loading	0.4	0
HIP 1010°C/105 MPa/2 Hours (1850°F/15 Ksi/2 Hours + Forge 954°C (1750°F)	1010°X (1850°F/1 Hour/AC + 815°C (1500°F)/8 Hours/AC	0.2	0.9	0
HIP 1120°C/105 MPa/2 Hours (2050°F/15 Ksi/2 Hours) + Forge 1120°C (2050°F)	1010°C (1850°F/1 Hour/AC + 815°C (1500°F)/8 Hours/AC	1.3	1.3	1.1
Beta Forged Wrought Baseline (No Er)	815°C (1500°F)/1/2 Hour/AC + 593°C (1100°F)/8 Hours/AC	54.0	-	NA

*Only specimens available

Table 27

Improved Toughness Titanium Aluminide
Task 4: Process Conditions

1)	Ti-25Al-18Nb Ingot	β Forge + Salt Quench off the Press to 815°C (1500°F)
2)	Ti-25Al-17Nb-1Mo Ingot	
3)	Ti-25Al-17Nb-1Mo Powder	
4)	Ti-25Al-17Nb-1Mo + 10% Ti-25Al-10Nb-4Mo Powder	
5)	Ti-25Al-17Nb-1Mo + 20% Ti-25Al-10Nb-4Mo Powder	
6)	Ti-25Al-10Nb-4Mo + 5% Ti-6242 Powder	
7)	Ti-25Al-10Nb-4Mo + 10% Ti-6242 Powder	
8)	Ti-25Al-10Nb-4Mo + 20% Ti-6242 Powder	

compositions Ti-25Al-18Nb (Alloy 23) and Ti-25Al-17Nb-1Mo (Alloy 24). It was hoped that the slightly higher aluminum contents, combined with increased niobium or molybdenum would give the necessary property boost. The aim of the phase blending in this task was to exploit the increased toughness potential but also to improve on the extremely poor creep rupture behavior found in blended material in Task 2. Although this appears to be a simple goal, it became clear, based on this work and that in another contract[10] that phase blending was (and remains) a most complex area with a large number of variables that play a role in overall property balance. Rather than just "fine tuning" the Task 2 approach, it was decided to strike out in different directions in order to evaluate a broader range of phase blended systems. The first approach was to pick the same Task 2 Ti-25Al-10Nb-4Mo (Alloy 15) as a matrix, but to add the commercial Ti-6Al-2Sn-4Zr-2Mo-.1Si (w/o) alloy as the second phase. Ti-6242 has a higher creep rupture capability than the Ti-15Al-22.5Nb (Alloy 21) used as a second phase in Task 2 and is at least as tough. Amounts added were 5 v/o, 10 v/o and 20 v/o. In the second approach, it was decided to reverse course and use a tough and ductile alloy as the matrix while adding the high creep resistant alloy as the second phase. Alloy 15 (Ti-25Al-10Nb-4Mo) was selected. Amounts added were 10 v/o and 20 v/o. The processing sequence selected was based on the results of Tasks 1-3. Isothermal forging and quenching to an intermediate temperature and holding at that temperature to permit transformation resulted in the best balance of properties. This processing method was used for all alloys and blends in Task 4.

3.4.2 Alloy Composition and Processing

Material preparation was conducted using techniques developed in Tasks 1-3. Alloy ingots weighing approximately 5.5 Kg (12 pounds) were prepared by blending titanium sponge and master alloy. The compacts were double consumably arc melted as previously described and were machined to the size required for PREP atomization at Nuclear Metals Inc., Concord, MA. The Ti-6242 alloy was atomized from available barstock. Analyzed

and aim compositions are shown in Table 28. PREP parameters were adjusted during atomization to yield a greater volume fraction of coarse particles for the Ti-6242 and Alloy 15 ingots. The -35+180 mesh fraction was used for the ductile second phase additions. The atomized powder was blended and sealed in CP titanium pipe cans and hot isostatically pressed (HIP) at 1093°C/105 MPa (2000°F/15 ksi) for three hours. An ingot of Alloy 24 powder was consolidated to serve as baseline for the Alloy 24/ Alloy 15 blend. Alloy 15 baseline information was generated in Task 2. SEM examination of the powder showed it to be spherical and exhibit the typical "soccer ball" appearance with coarse dendrites visible. Metallographic examination of powder cross sections revealed that the alpha-two powders were equiaxed and consisted of a single phase ordered beta (B2) structure while the Ti-6242 powder was a fully transformed martensitic alpha prime hexagonal structure (Figure 62).

The six blended consolidations listed in Table 27 were HIP at Howmet Thermatech HIP Division in Whitehall, MI. The two ingots were HIP by Pratt & Whitney. HIP conditions were 1093°C (2000°F) at 105 MPa (15 ksi) for 2 hours. All pieces were isothermally forged at Wyman-Gordon Co., Millbury, MA at 1176°C (2150°F) and quenched into an 815°C (1500°F) salt bath. Forgings were crack-free and showed excellent deformation and flow characteristics.

3.4.3 Results and Discussion

Microstructural examination of the Alloy 15 matrix/Ti-6242 HIP consolidated blends revealed that particle distribution was uniform, but a substantial reaction between the two alloys had occurred (Figure 63). Some of the Ti-6242 areas exhibited a coarse blocky transformed structure while other locations exhibited fine structure (Figure 64). Microhardness testing revealed that the matrix hardness was Hv 531; the dark reaction zone was Hv 454 and the particle centers were Hv 480 and 454 for the fine and blocky areas, respectively. The matrix hardness level is comparable to that measured in the TMP study for ingot

Table 28

Improved Toughness Titanium Aluminide
Task 4: Combination Alloy Chemical Composition

Compositions (w/o)

Alloy Number		Ingot* Al	Nb	Mo	O	N	Powder Al	Nb	Mo	O	N
15	Aim	13.7	19.0	7.8	0.10**	0.02**	13.7	19.0	7.8	0.10**	0.02**
	Actual	14.4	18.0	7.2	0.045	0.006	14.0	18.6	7.5	0.055	0.010
23	Aim	13.3	32.9	-	0.10**	0.02**					
	Actual	13.4	30.5		0.05	0.008	No powder made for this alloy				
24	Aim	13.3	31.0	1.9	0.10**	0.02**					
	Actual	12.8	28.6	1.8	0.07	0.008	No powder made for this ingot				
24	Aim	13.3	31.0	1.9	0.10**	0.02**	13.3	31.0	1.9	0.10**	0.02**
	Actual	14.1	29.4	1.8	0.05	0.006	13.1	30.7	1.88	0.15	0.002
Ti-6242		-	-	-	-	-	Al: 5.90		O: 0.050		
							Sn: 1.80		N: <0.001		
							Zr: 2.8				
							Mo: 2.01				

*Ingot average of six locations
**Maximum

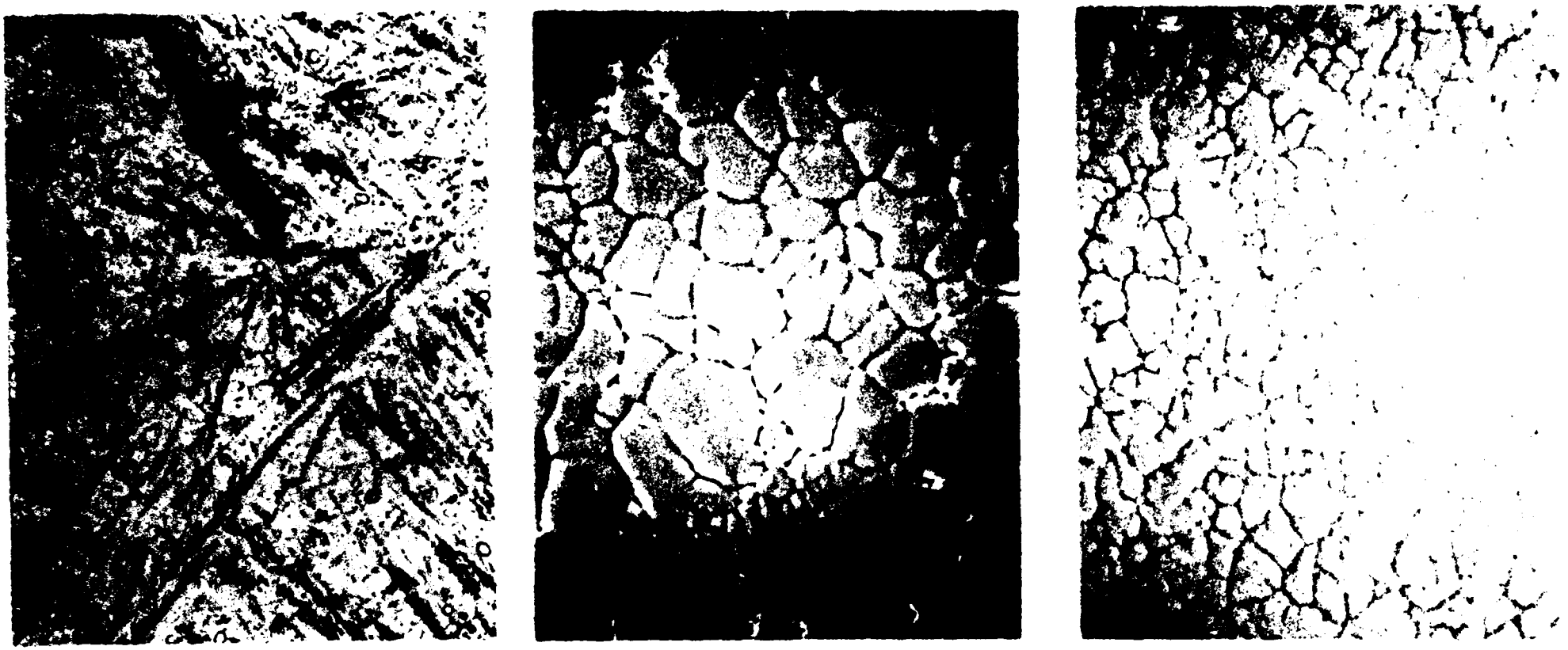

Figure 62

Microstructure of PREP powders used for Task 4 combination alloys. a) Ti-6242; b) Alloy 15; c) Alloy 24.

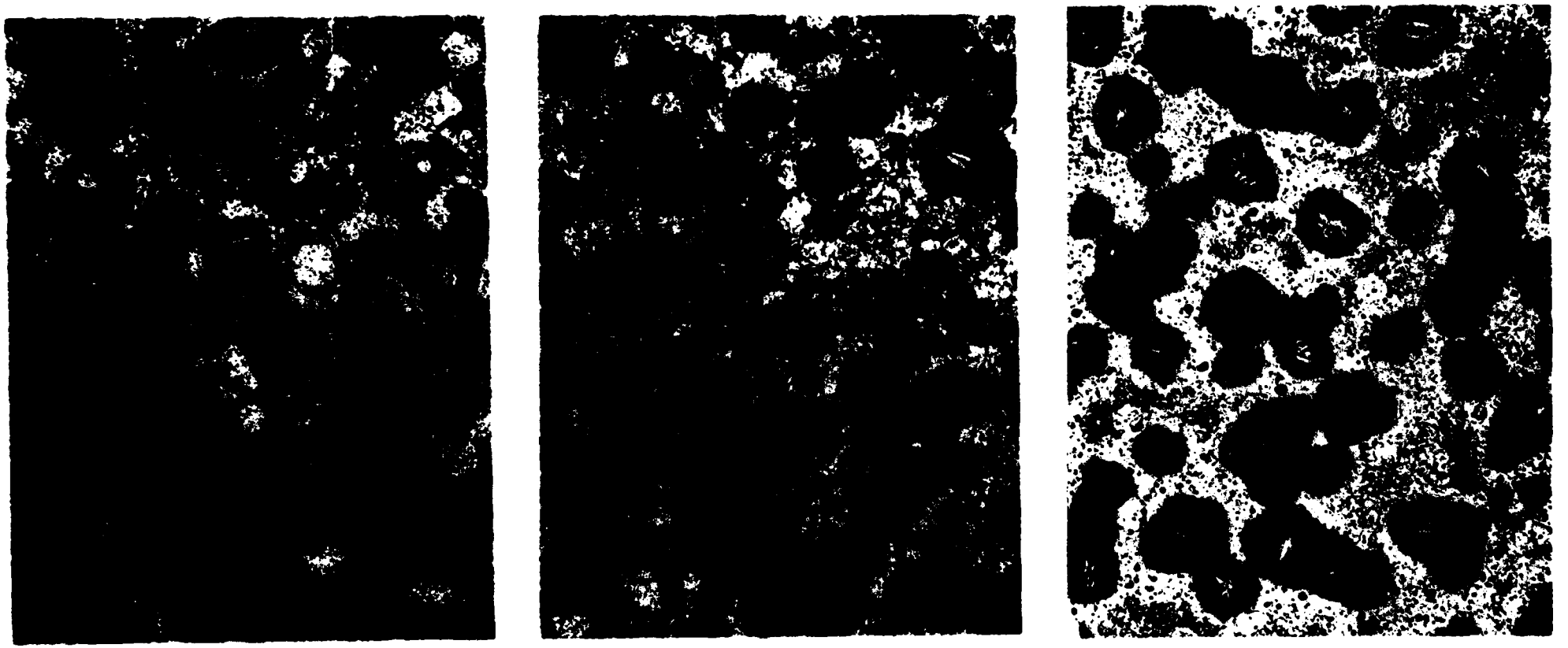

(a) (b) (c)

25X

Figure 63

Microstructure of the Alloy 15 matrix/Ti-6242 blends after HIP at 1093°C (2000°F)/105 MPa (15 ksi)/2 hours. a) 5 v/o Ti-6242; b) 10 v/o Ti-6242; c) 1520 v/o Ti-6242.

200μm

100X

Figure 64

Microstructure of the Ti-6242 particles in HIP consolidated Alloy 15 matrix showing both 'blocky' and fine Ti-6242 microstructures.

metallurgy Alloy 15. The high hardness of the Ti-6242 phase was attributed to the extensive reaction. In contrast, the Alloy 15 (Ti-25Al-10Nb-4Mo) second phase particles in the Alloy 24 matrix showed less reactivity, more comparable to that seen in section 3.2.3.2 (Figures 65 and 66). In this system, the HIP consolidation had a hardness of Hv 348, 436 and 500 for the matrix, reaction zone and second phase core, respectively.

After forging and salt quenching, microstructural examination revealed that continued reaction had occurred between the two phases in both alloy systems. In particular, it was observed that the Ti-6242 particles were almost fully dissolved in the Alloy 15 (Figure 67). The two alpha-two compositions also underwent more extensive reaction (Figure 68) than was observed on the Task 2 blend experiments (note that forging temperatures below the beta transus were used in Task 2). Mechanical property data of the phase blended systems are summarized in Table 29. All six blends had virtually no ductility, even at high temperature. The Alloy 24 baseline powder consolidation did exhibit some yield strength and ductility at 427°C (800°F) and higher. The higher than aim oxygen content of 0.15% resulted in poor RT ductility. In the all alpha-two system (Alloy 24 + Alloy 15 second phase), toughness remained unchanged or decreased slightly compared to baseline as increased second phase was added. Values were about midway between the highest and lowest measured in Task 2. On the positive side, the phase blends showed much better high temperature behavior in the form of increased creep rupture life. However, as second phase content increased, life decreased, a similar trend to Task 2 behavior. In the Alloy 15 matrix + Ti-6242 second phase, toughness was about 12-14 MPa$\sqrt{\text{meter}}$ (11-13 ksi$\sqrt{\text{inch}}$), which is roughly comparable to the lowest Task 2 data. Creep rupture life did increase as the amount of second phase was increased in this case; however, the rupture specimens had low ductility.

In retrospect, it is likely that the beta forge salt quench approach for phase blends was not the correct one. Improved toughness seems to depend upon reasonably large discrete regions that can act as crack stoppers or

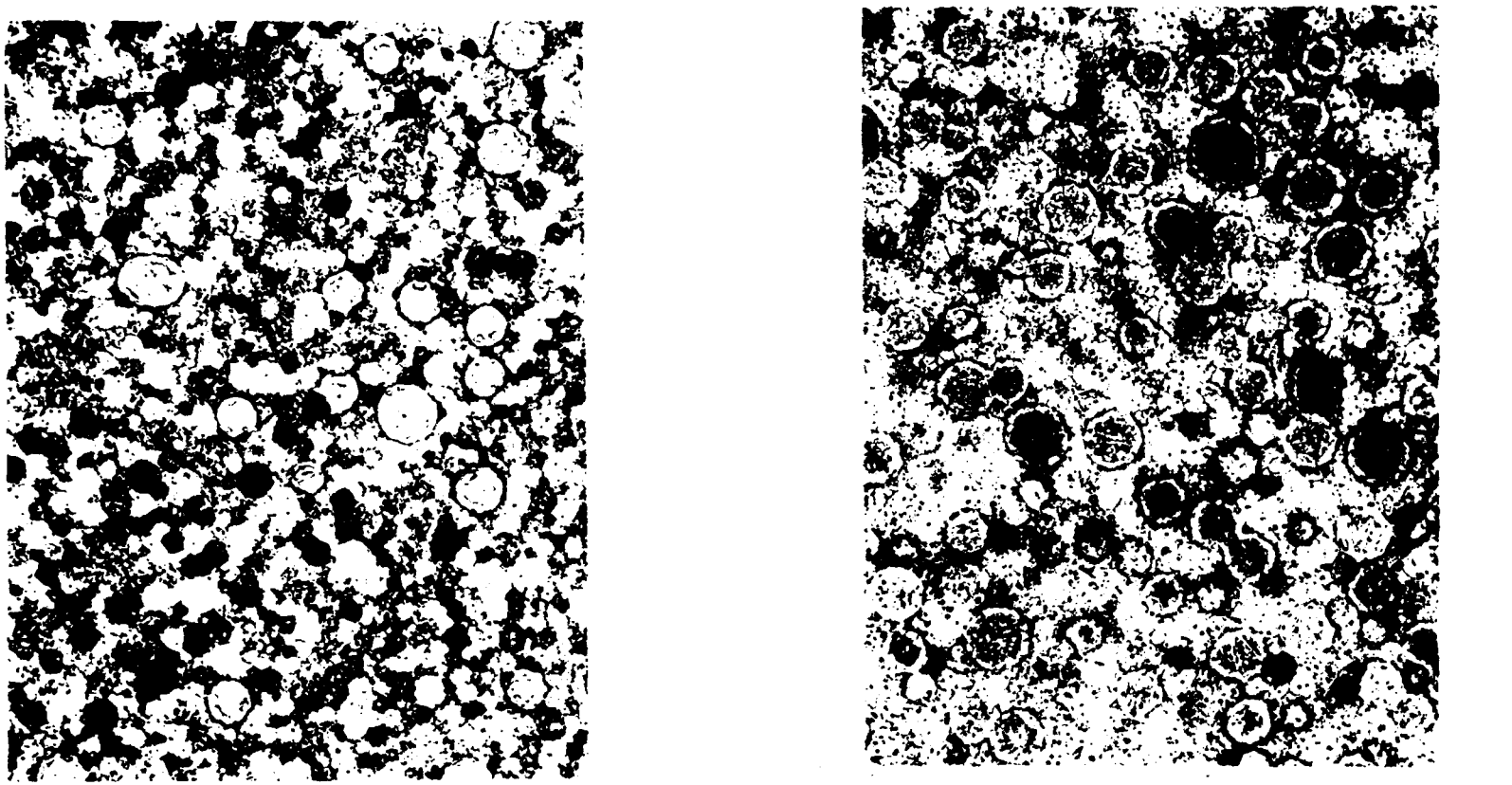

Figure 65

Microstructure of Alloy 24 matrix with a) 10 v/o Alloy 15 and b) 20 v/o Alloy 15 as a second phase (spherical particles). HIP conditions: 1093°C (2000°F)/105 MPa (15 ksi)/2 hours.

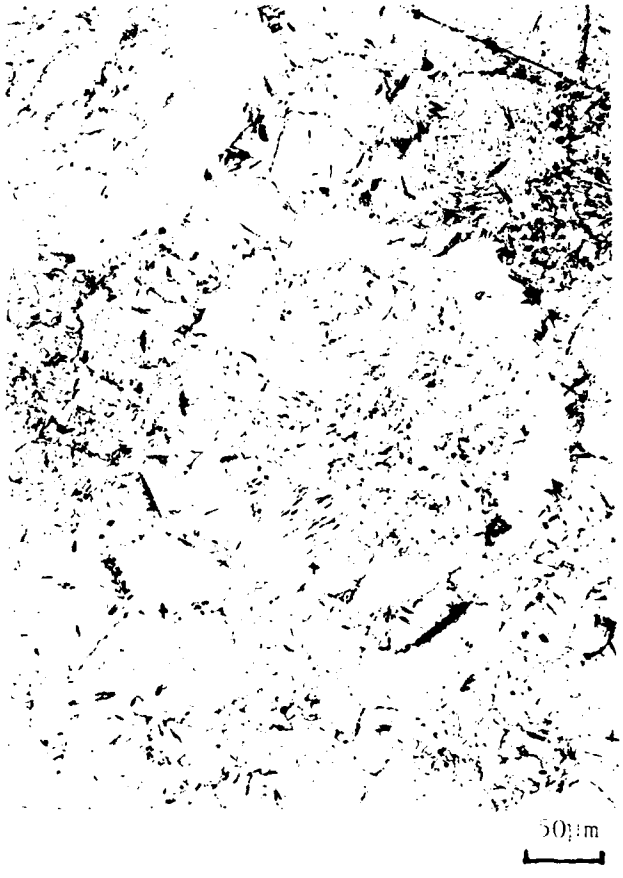

Figure 66

Microstructure of HIP'ed PREP powder Ti-25Al-17Nb-1Mo alloy powder with additions of PREP Ti-25Al-10Nb-4Mo showing some interaction.

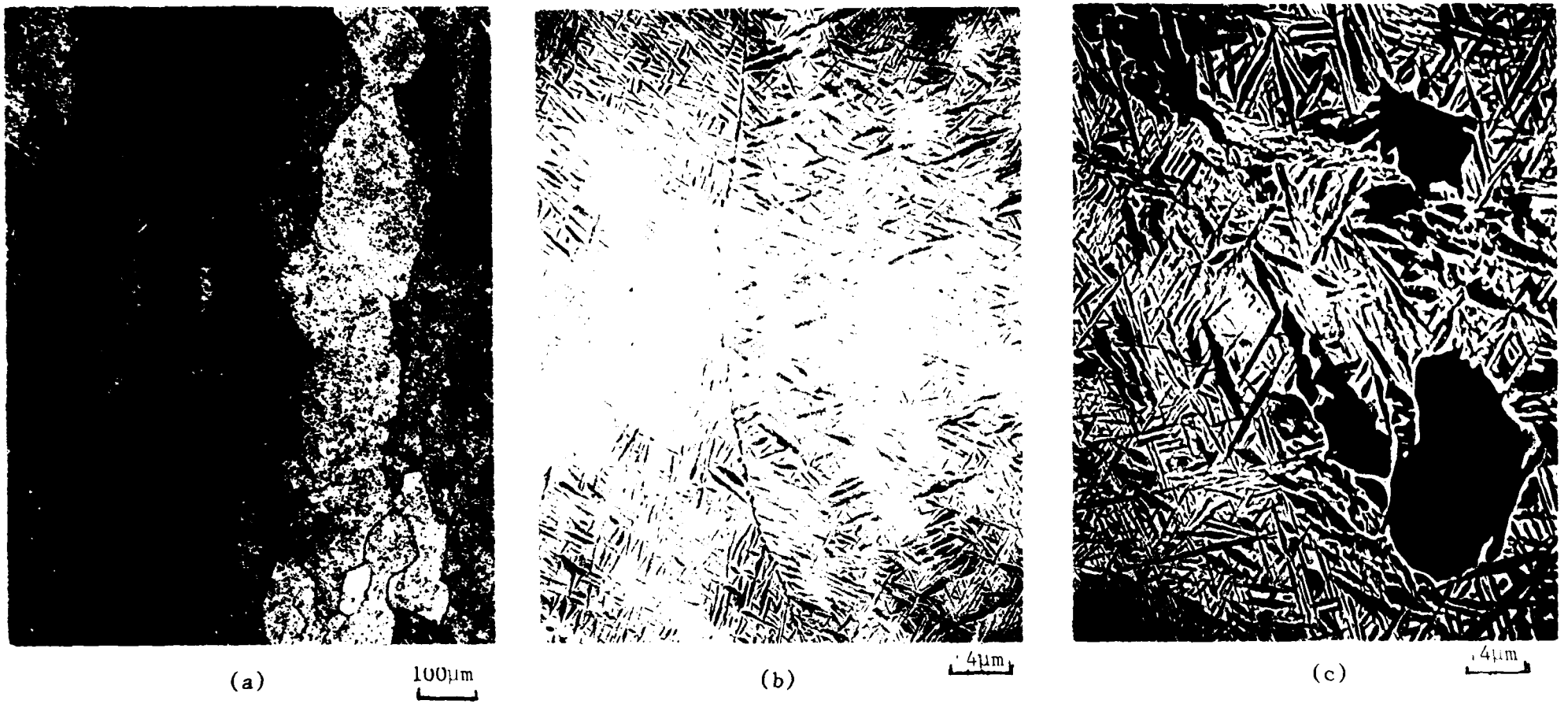

Figure 67

Microstructure of Ti-25Al-10Nb-4Mo + 10 v/o Ti-6242 forged and salt quenched powder consolidation. a) optical microstructure, Ti-6242 in center of photo; b) matrix; c) Ti-6242.

(a)

(b)

(c)

Figure 68

Microstructure of Ti-25Al-17Nb-1Mo + 20% Ti-25Al-10Nb-4Mo forged and salt quenched powder consolidation. a) optical microstructure; b) matrix; c) second phase.

Table 29

Mechanical Summary of Properties
of Task 4 Blended Powder Alloys

Alloy Blend	Test Temp. °C	°F	YS MPa	YS Ksi	UTS MPa	UTS Ksi	EL (%)	RA (%)	RT Fracture MPa√Meter	RT Fracture Ksi√Inch	650°C/380 MPa (1200°F/55 Ksi) Hours	EL (%)	RA (%)
Ti-25Al-17Nb-1Mo	21	70	-	-	1082	157.0	0	0	16.2	14.7	236.2	5.2	4.0
HIP + Forged	21	70	-	-	800	116.0	0	0					
Powder													
	427	800	882	127.9	1028	149.1	2.7	5.4					
	427	800	-	-	902	130.8	0	0					
	650	1200	865	125.4	1003	145.5	3.7	10.7					
	650	1200	858	124.4	954	138.4	2.4	6.6					
Ti-25Al-17Nb-1Mo +	21	70	-	-	1036	150.2	0	0	16.3	14.8	152.2	3.5	2.7
10% Ti-25Al-10Nb-4Mo	21	70	-	-	611	88.6	0	0					
	427	800	-	-	800	116.0	0	0					
	427	800	-	-	722	104.7	0	0					
	650	1200	-	-	787	114.1	0	0					
	650	1200	880	127.6	958	138.9	1.8	4.2					
Ti-25Al-17Nb-1Mo +	21	70	-	-	873	126.6	0	0	13.2	12.0	137.4	5.0	3.7
20% Ti-25Al-10Nb-4Mo	21	70	-	-	956	138.7	0	0					
	427	800	914	132.6	924	134.0	0.9	4.0					
	427	800	944	136.9	963	139.6	0.8	4.0					
	650	1200	882	127.9	945	137.1	1.6	5.2					
	650	1200	858	124.4	880	127.6	1.4	6.6					
Ti-25Al-10Nb-4Mo +	21	70	-	-	634	91.9	0	0	12.2	11.1*	1.5	0.4	0
5% Ti-6242	21	70	-	-	589	85.4	0	0					
	427	800	-	-	687	99.7	0	0					
	427	800	-	-	561	81.4	0	0					
	650	1200	796	115.5	813	117.9	0.7	2.7					
	650	1200	-	-	710	103.0	0	0					

Table 29

Mechanical Summary of Properties
of Task 4 Blended Powder Alloys (Continued)

Alloy Blend	Test Temp. °C	°F	YS MPa	Ksi	UTS MPa	Ksi	EL (%)	RA (%)	RT Fracture MPa√Meter	Ksi√Inch	Stress-Rupture 650°C/380 MPa (1200°F/55 Ksi) Hours	EL (%)	RA (%)
Ti-25Al-10Nb-4Mo +	21	70	-	-	443	64.2	0	0	14.6	13.3*	6.1	0.8	0
10% Ti-6242	21	70	-	-	523	75.9	0	0					
	427	800	857	124.3	890	129.1	0.6	4.0					
	427	800	-	-	769	111.5	0	0					
	650	1200	818	118.6	902	130.8	0.9	2.7					
	650	1200	882	127.9	940	136.3	1.1	5.3					
Ti-25Al-10Nb-4Mo +	RT	70	-	-	543	78.7	0	0	11.0	10.0*	57.4	1.3	1.3
20% Ti-6242	RT	70	-	-	565	82.0	0	0					
	427	800	-	-	709	102.8	0	0					
	427	800	-	-	790	114.6	0	0					
	650	1200	803	116.4	847	122.9	0.9	4.0					
	650	1200	793	115.0	859	124.6	1.1	5.4					

*Baseline: Forge + SQ Ingot 13.7 Ksi√Inch
HIP + STA Powder 6.3 Ksi√Inch

deflectors. Minimal interfacial reaction is also desirable, not only to maintain particle size, but also to avoid the creation of potentially brittle interfacial regions. The extended periods at high temperatures, and in the case of Ti-6242, the larger chemical difference with the matrix combined to dissolve the particles. Thus, to build upon the results obtained in Task 2, considerably more work on alloy selection and the process cycle is needed before a useful system can emerge.

In contrast to the phase blended material the forged ingot metallurgy, Alloy 24 showed an excellent property balance. High tensile strength, 3% elongation at room temperature, a fracture toughness of 20.9 MPa$\sqrt{\text{meter}}$ (19 ksi$\sqrt{\text{inch}}$) and a stress-rupture life of 476 hours were measured (Table 30). The HIP + forged powder of the same aim composition used for powder blend baseline was somewhat less ductile and tough, but slightly stronger. Chemical analysis revealed that the consolidated powder was about actually 1.8% weight percent higher in aluminum and niobium, while the forged ingot was closer to a 24% Al composition. The powder also exhibited a higher interstitial level. Alloy 23 (Ti-25Al-18Nb) was less strong and creep resistant than Alloy 24 with no corresponding advantage in toughness.

3.4.4 Phase II Recommendations

Based on a careful review of the data generated in this program and a previous study(*), it was concluded that a delicate balance exists in obtaining a tough alpha-two alloy without degrading high temperature capability.

It was apparent that the most effective compositional change affecting toughness was to decrease aluminum content while increasing niobium content. Molybdenum up to 1 atomic percent tended to reduce toughness, slightly, but had a more detrimental effect at 2-4 a/o level. However,

*AFWAL-TR-81-4046

Table 30

Mechanical Property Comparison of Mechanical Properties Task 4
Forged Ingot Metallurgy Alloys with Consolidated + Forged Powder

Alloy Blend	Test Temp. °C	°F	YS MPa	Ksi	UTS MPa	Ksi	EL (%)	RA (%)	RT Fracture MPa√Meter	Ksi√Inch	Stress-Rupture 650°C/380 MPa (1200°F/55 Ksi) Hours	EL (%)	RA (%)
Ti-25Al-17Nb-1Mo	21	70	-	-	1082	157.0	0	0	16.2	14.7	236.2	5.2	4.0
HIP + Forged Powder	21	70	-	-	800	116.0	0	0					
	427	800	882	127.9	1028	149.1	2.7	5.4					
	427	800	-	-	902	130.8	0	0					
	650	1200	865	125.4	1003	145.5	3.7	10.7					
	650	1200	858	124.4	954	138.4	2.4	6.6					
Ti-25Al-17Nb-1.0Mo	21	70	998	144.8	1134	164.5	3.4	6.6	20.9	19.0	476.0	5.6	5.3
Forged Ingot	21	70	980	142.1	1131	164.1	3.3	6.1					
Forged Ingot	427	800	891	129.3	1102	159.8	12.0	13.9					
	427	800	944	137.0	1151	167.0	14.7	26.0					
	650	1200	789	114.5	903	131.0	4.7	17.8					
	650	1200	774	112.3	932	135.2	7.6	25.2					
Ti-25Al-18Nb	21	70	831	120.5	952	138.1	2.4	5.5	23.1	21.0	36.0	6.9	13.0
	21	70	820	119.0	958	139.0	3.1	9.8					
	427	800	661	95.9	874	126.7	12.9	42.7					
	427	800	640	92.9	886	128.5	11.6	28.5					
	650	1200	642	93.1	719	104.3	5.2	30.0					
	650	1200	618	89.7	714	103.5	5.7	24.0					

some molybdenum is required to produce a useful alloy with high tensile and creep strengths. Therefore, the three alloys that were proposed for more extensive study were:

24: Ti-25Al-17Nb-1Mo (a/o)
25: Ti-24Al-17Nb-.5Mo
26: Ti-22Al-17Nb-1Mo

Alloy 24 is based on the result cited above which demonstrated the best combination of properties yet obtained on an alpha-two alloy. We should emphasize that careful control of the aluminum content appears critical and this variable is included in the three alloys selected. The other two alloys were designed to establish higher toughness levels with acceptable rupture life. Alloy 25 was expected to show increased toughness but sacrificing some stress-rupture capability, while Alloy 26 with lower aluminum content should have the highest toughness of the three while still meeting minimum rupture life. The proposed processing approach was to continue the use of isothermally beta forging followed by salt quenching (815°C/1500°F) to produce refined grain size with a fine transformed structure.

While phase blending showed potential, it was considered that not enough screening trials had been conducted to establish the optimum combination of processing and compositional variables that could yield a high temperature system with good ductility and toughness.

4.0 PHASE II - SCALE-UP

4.1 Introduction

The objectives of Phase II of the program were to 1) select the three best alloy compositions and scale them up to a minimum 9 Kg (20 lb) heat for each alloy and 2) consolidate or forge the alloys using the optimized processing procedure/heat treatment developed in Phase I. Extensive mechanical property evaluation of the selected alloys to include tensile, impact, fracture toughness, creep rupture and fatigue testing was conducted.

4.2 Alloy Composition and Processing

As discussed previously, the three alloys selected for Phase II were as follows:

Ti-25Al-17Nb-1Mo (Alloy 24)
Ti-24Al-17Nb-.5Mo (Alloy 25)
Ti-22Al-17Nb-1Mo (Alloy 26)

Six ingots, each weighing approximately 4.5 Kg (10 lb) were made using vacuum arc remelt techniques detailed in section 3.1.3. After melting, the ingots were HIP at 1010°C/103 MPa/3 hours (1850°F/15 ksi/3 hours) to seal pipe and any internal porosity. The use of two 4.5 Kg (10 lb) ingots per alloy was necessary due to size limitations of the Wyman-Gordon isothermal press and salt pot, which can accommodate a maximum 18 cm (7 in) diameter pancake.

Analysis of the six ingots was conducted and the results are shown in Table 31. The aluminum content of the Alloy 24 ingots varied from the aim by about ±1.0 a/o. The ingot designated 73-1-88 was about 1.0% higher than aim while 73-1A-88 was about 1.0% lower. It was decided to use the ingots as formulated for the following reasons. The two

Table 31

Chemical Analysis Results for Phase II Ingots
Two Ingots Per Alloy

Alloy Number	Ingot ID	Composition w/o Al Aim	Al Actual[1]	Nb Aim	Nb Actual[1]	Mo Aim	Mo Actual[1]	O_2 Actual
24	73-1-88	13.3	14.0	31.1	29.7	1.9	1.88	0.08
24	73-1A-88	13.3	12.5	31.1	30.2	1.9	1.82	0.10
25	73-2-88	12.7	12.5	31.0	30.1	0.95	0.96	0.11
25	73-2A-88	12.7	12.5	31.0	29.5	0.95	0.91	0.09
26	73-3-88	11.5	11.6	30.7	29.8	1.9	1.83	0.09
26	73-3A-88	11.5	11.9	30.7	29.6	1.9	1.80	0.10

[1]Average of three locations within the ingot.

chemistries would provide an additional set of data and would also give a measure of the effect of a possible aluminum variation in a large production size heat. With this exception, chemical composition of the ingots were essentially on target.

Forging was conducted at Wyman-Gordon in Millbury, MA. Six ingots were machined to 7.9 cm (3.125 in) diameter by 14.6 cm (5.75 in) long with generous machined corner radii. Identification numbers 1, 1A, 2, 2A, 3 and 3A were assigned together with the prefix 73- and the suffix -88. The forging plan was to heat each to 1176°C (2150°F) and flatten across the diameter from 7.9 cm (3.125 in) to 2.59 cm (1 in) thick and immediately quench into 815°C (1500°F) salt and hold for 30 minutes followed by air cooling. However, a trial run using a Ti-6Al-4V billet machined to the above dimensions flowed over the end of the die assembly and caused the dies to stick together. To avoid this problem, the alpha-two billets were shortened to 12 cm (4.75 in) and rechamfered. A flat, approximately 2.5 cm (1 in) wide with a 25 cm (10 in) chord, was ground the length of each billet for stability on the flat die. The ingots were blasted to roughen their surface slightly and coated with boron nitride to minimize die sticking. Forging data are given in Table 32. After forging, the ingots were transferred to 815°C (1500°F) molten salt within 20 seconds and held in the salt for 30 minutes.

Five of the ingots were processed to the above schedule. During the last five minutes of the forging of the ingot designated 73-2-88 (Alloy 25), a water leak developed in the induction coil of the press which cooled both the die stack and forging, causing the high flow stress noted in the table. The pressing had begun at 1176°C (2150°F) but fell to approximately 1038°C (1900°F) at the end of the cycle. This meant that part of the deformation had occurred below the beta transus. Since replacement of the ingot would have caused a major program delay, it was deemed necessary to reheat treat the forging in such a manner to simulate the processing of the remaining five. One obvious reheat treatment would

Table 32

Forging Parameters for Phase II Pancakes

Alloy	ID	Heating Time (Hours)	Die Temp. Start °C	Die Temp. Start °F	Forge Duration Minutes	Die Temp. End °C	Die Temp. End °F	Pressure Max. T	Pressure MPa	Pressure Unit[2] Ksi
24	73-1-88	5	1168	2135	12	1188	2170	50.3	21.4	3.1
24	73-1A-88	2-1/2	1176	2150	12	1183	2161	58.0	21.7	3.0
25	73-2-88	2-1/2	1172	2143	12	1038	1900[1]	144.0	51.8	7.5
25	73-2A-88	4-1/2	1168	2135	13	1174	2146	43.3	15.2	2.2
26	73-3-88	3-1/4	1173	2144	10	1175	2148	40.7	17.9	2.6
26	73-3A-88	4-3/4	1175	2148	10	1167	2134	43.3	15.2	2.2

[1]Water leak in induction coil cooled dies and pancake. S/N 2 was later solutioned at 1107°C (2025°F) for one hour and quenched into 815°C (1500°F) salt for 30 minutes.

[2]Unit pressure approximate based on 17.8 cm (7 in) circle.

have been to beta anneal the pancake and salt quench; however, work during the development of the Ti-25Al-10Nb-3V-1Mo[4] alloy found that beta annealing caused extensive grain growth which had a detrimental effect on ductility and notched properties. Therefore, it was decided that the best approach would be to solution anneal this forging just below the beta transus in order to minimize grain size changes but still result in a transformed beta microstructure. Thus, the procedure used was as follows: anneal for one hour at 1107°C (2025°F) and quench into the 815°C (1500°F) salt bath for 30 minutes. Subsequent metallographic examination revealed that the microstructure was essentially the same as the other pancake. Apparently, the amount of alpha-beta working applied was not enough to cause recrystallization.

Metallographic examination of each pancake forging was conducted at various locations. The Ti-26Al-17Nb-1Mo alloy (73-1-88) revealed an equiaxed appearance with a typical prior beta grain diameter of 0.7-0.8 mm (0.025-0.030 in); some occasional grains as large as 1.6 mm (0.060 in) were observed (Figure 69a). The transformed alpha-two platelets were extremely fine (Figure 69b). The Ti-24Al-17Nb-1Mo alloy (73-1A-88) alloy exhibited more elongated grains, typically 0.2 mm x 0.4-0.6 mm (0.010 in x 0.020in-0.040 in) with occasional grains as large as twice the size of the typical grains present (Figure 70). The alpha-two platelets were somewhat coarser in comparison to those of the 26% aluminum alloy.

Specimens from the Ti-24Al-17Nb-.5Mo (73-2-88), which had been solution treated below the beta transus and salt quenched, exhibited a duplex structure with alternating bands of fine and coarse transformed alpha-two platelets. Prior beta grains were heavily deformed and were approximately the same size as those in 73-1A-88 (Figures 71a,b). A small amount (<1%) of globular alpha-two phase was present in some areas of the forging, especially near the edge where the effect of cooling was stronger (Figure 71c). It is unclear if the duplex structure exhibited by this forging merely resulted from the high temperature solution treatment and subsequent transformation of coarser alpha-two platelets

Figure 69

Microstructure of Ti-26Al-17Nb-1Mo forged and quenched tensile specimen (73-1-88).

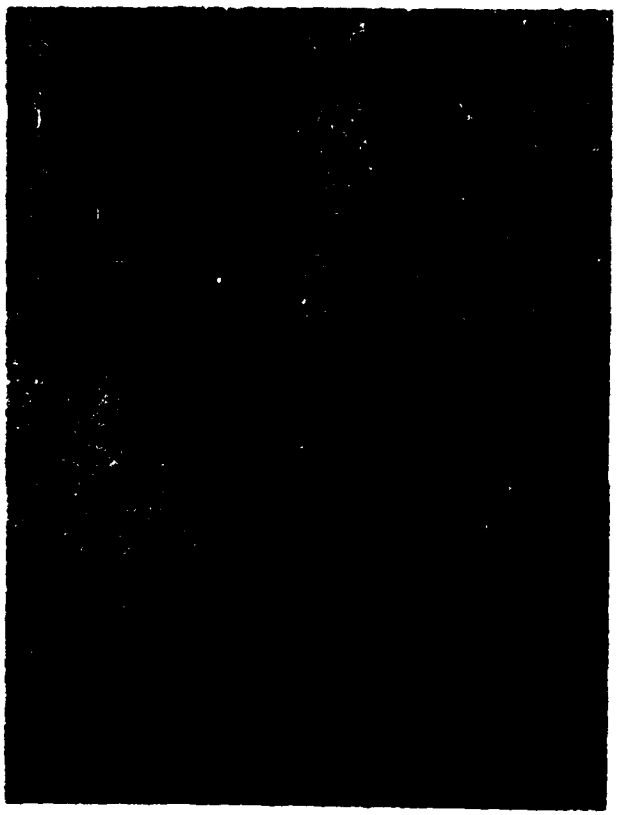

Figure 70

Microstructure of Ti-24Al-17Nb-1Mo forged and quenched tensile specimen (73-1A-88).

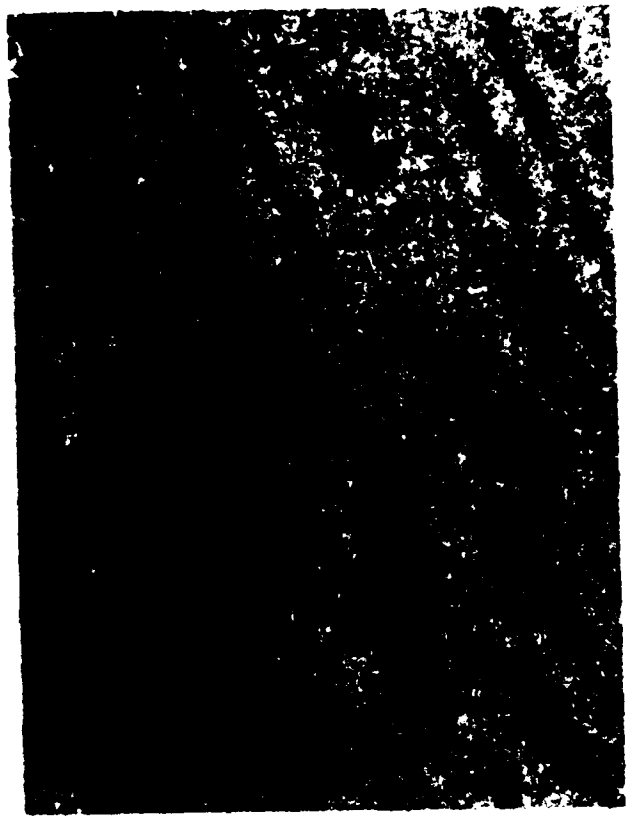

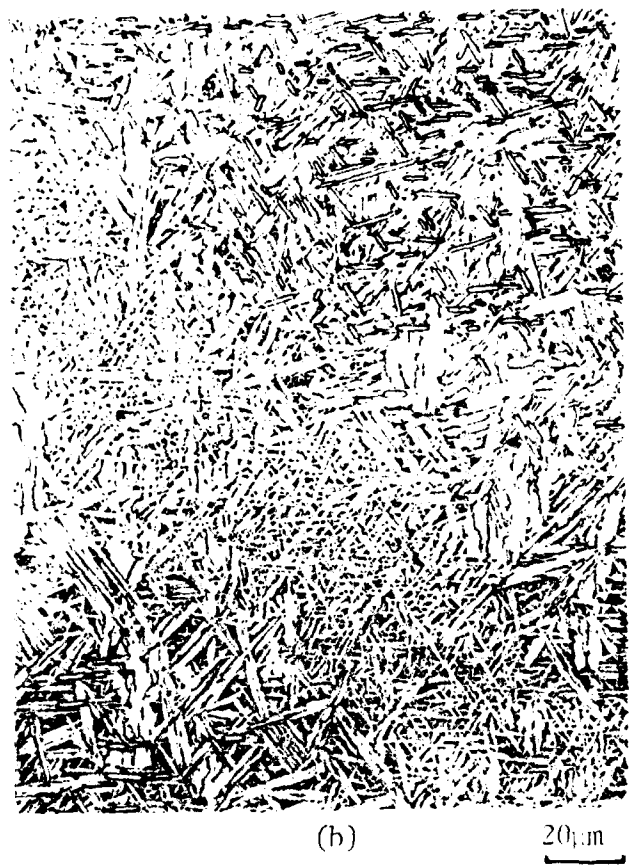

Figure 71

Microstructure of Ti-24Al-17Nb-0.5Mo forged and quenched + solution treated tensile specimen (73-2-88).

during the isothermal hold or could be related to the "beta fleck" type segregation encountered in alloys with large amounts of beta stabilizing elements. However, an EDAX analysis of the material showed no significant difference in the composition of the two types of structures (Figure 72). Microstructure of specimens from the Ti-24Al-17Nb-.5Mo alloy quenched from the press (73-2A-88) was virtually identical to the Ti-24Al-17Nb-1Mo alloy (73-1A-88) in all respects, including prior beta grain size and platelet size (Figure 73).

Specimens from both forgings of Alloy 26 (Ti-22Al-17Nb-1Mo) exhibited similar microstructures so only one photomicrograph is shown. It was observed that the prior beta grains were not as heavily deformed and elongated as other forgings and typical diameter was approximately 0.3-0.4 mm (0.01-0.015 in) (Figure 74a). Alpha-two platelets were coarse and many of the prior beta grain boundaries had spawned subcolonies of alpha-two platelets giving them a "fish bone" appearance (Figure 74b).

4.3 Mechanical Property Testing

4.3.1 Tensile Testing

4.3.1.1 Experimental Details

Six tensile specimens were machined from each of the forgings and tested over the range of 21°C (70°F) to 815°C (1500°F). One specimen from each forging was tested at each temperature.

4.3.1.2 Results and Discussion

The data for the nominal Alloy 24 compositions are given in Tables 33 and 34. Visual representation of the data is shown in Figures 75 and 76. The Ti-26Al-17Nb-1Mo composition (73-1-88) showed excellent strength over the temperature range tested, well in excess of the program goals. Room temperature ductility was only 1-1.5%; however, the ductility rose quickly with temperature to 5-7% at 204°C (400°F). Specimens from the

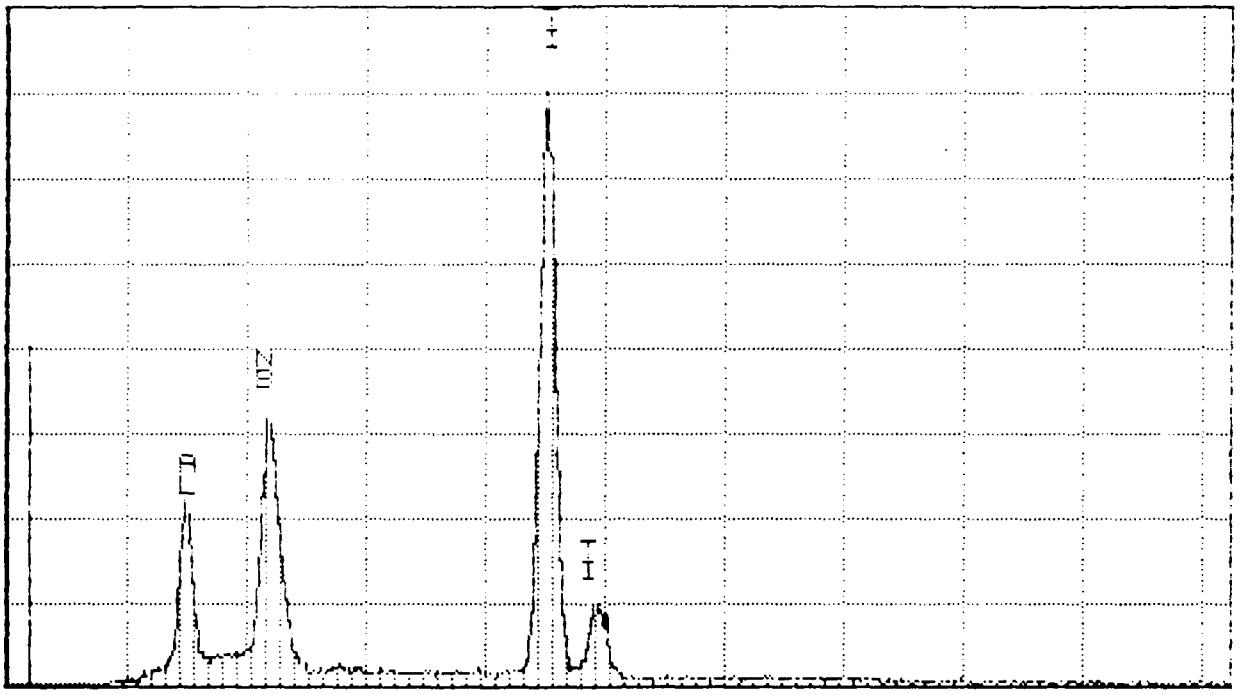

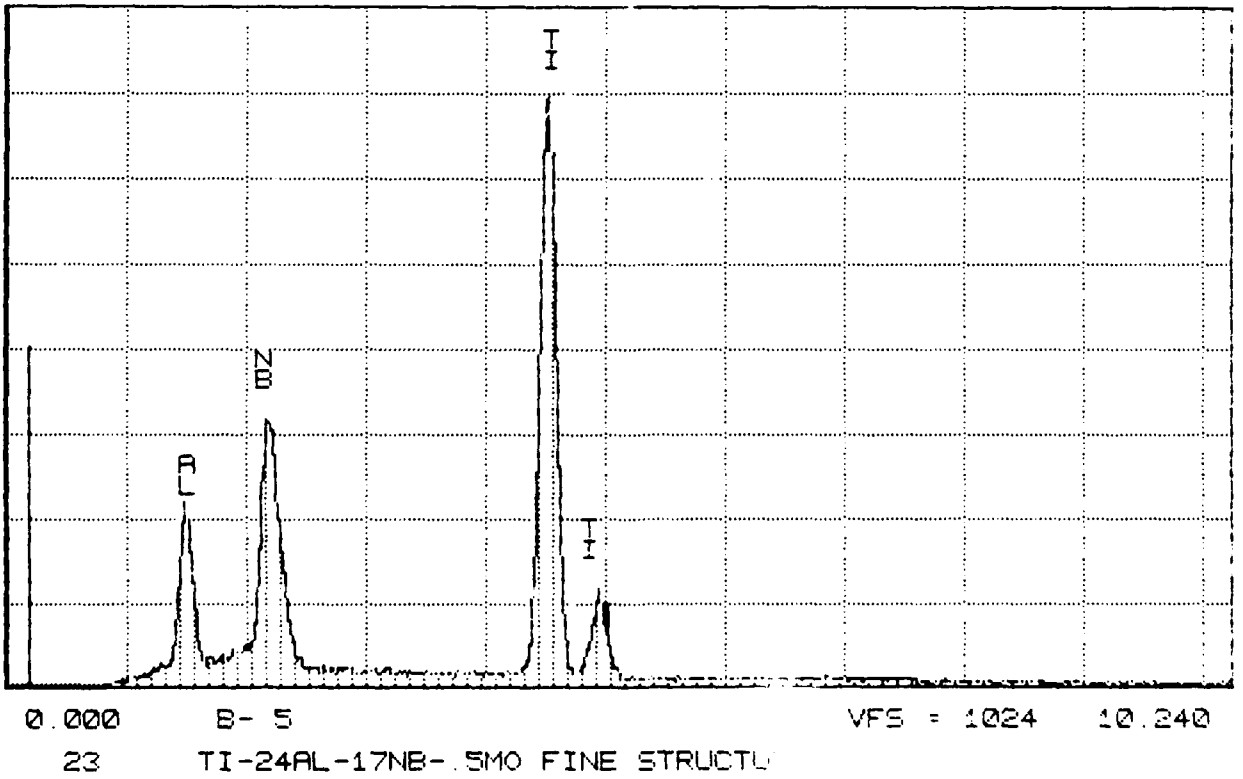

Figure 72

EDAX analysis of Ti-24Al-17Nb-.5Mo alloy specimens with duplex structure

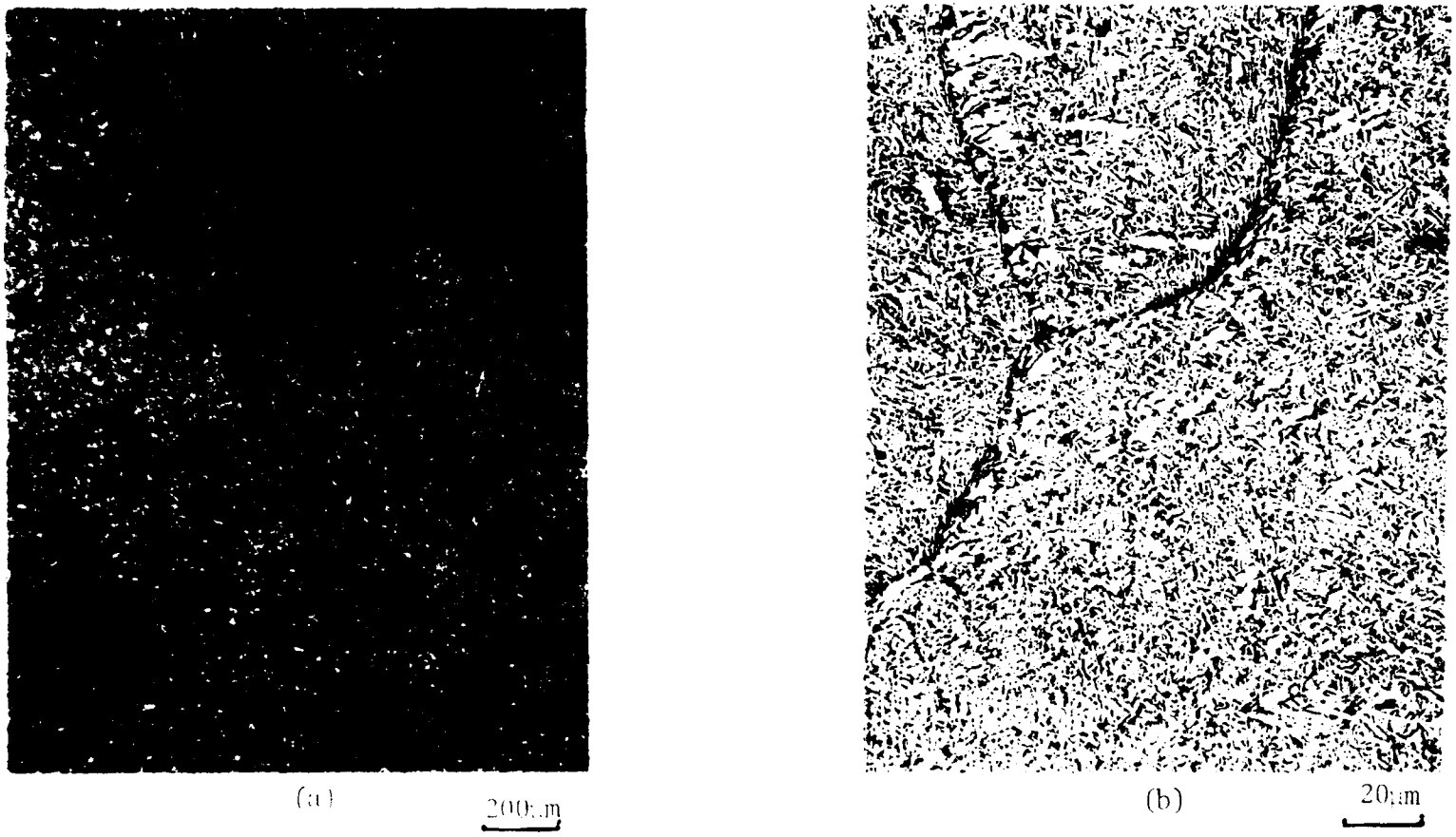

Figure 73

Microstructure of Ti-24Al-17Nb-.5Mo forged and quenched tensile specimen (73-2A-88).

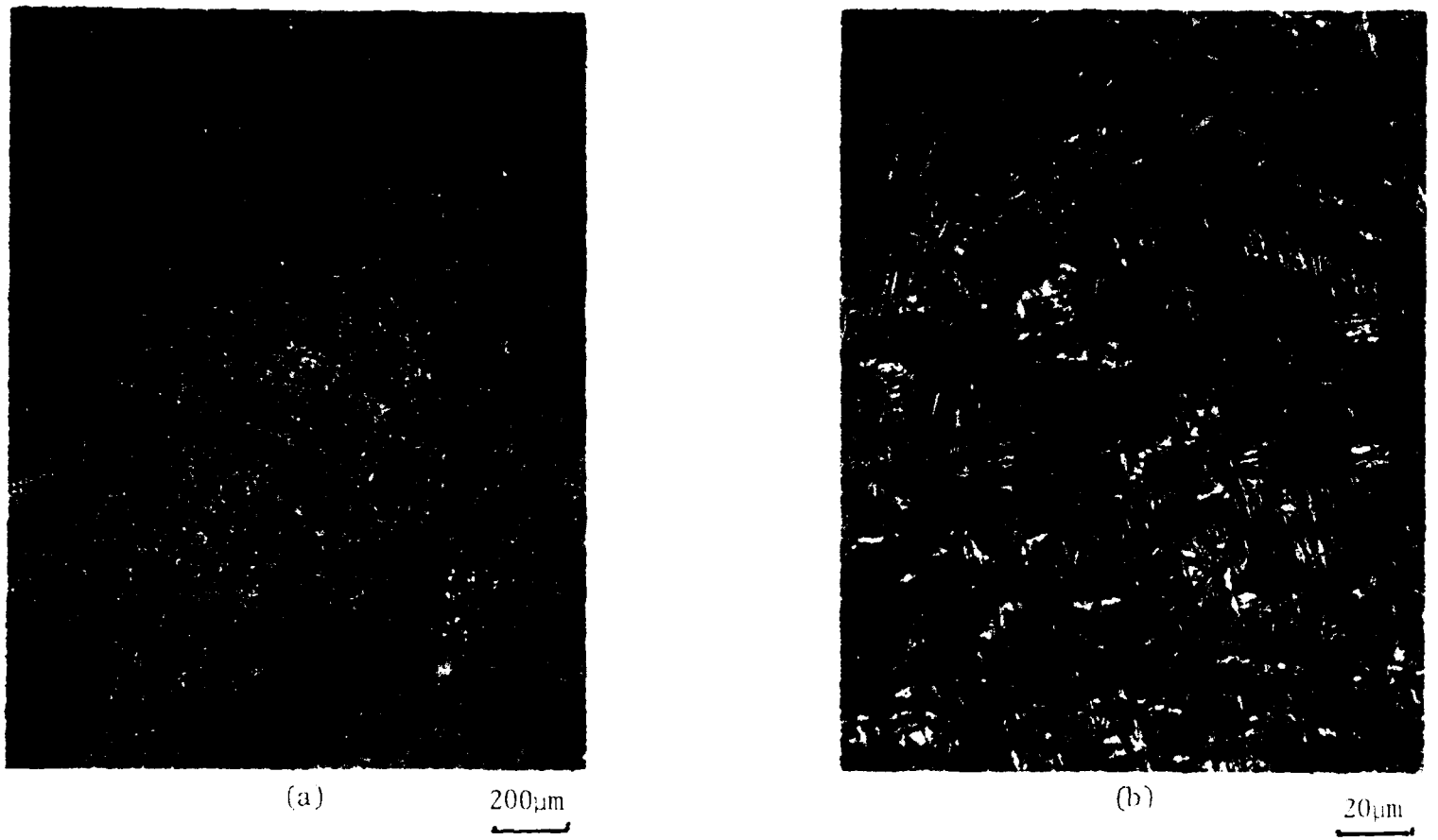

Figure 74

Microstructure of Ti-22Al-17Nb-1Mo forged and quenched tensile specimen (73-3-88).

Table 33

Tensile Properties of Forged + Salt Quenched
Ti-26Al-17Nb-1Mo (73-1-88)

Specimen Number	Test Temp. °C	°F	0.2% Yield Str. MPa	Ksi	Ult. Tens. Str. MPa	Ksi	%EL	%RA
1	21	70	1034	149.2	1107	159.7	0.94	1.4
5	204	400	863	124.5	1031	148.8	5.0	6.7
6	427	800	809	116.8	1037	149.6	13.3	36.2
19	650	1200	791	114.2	923	133.2	4.4	8.0
2	760	1400	735	106.1	888	128.2	5.3	13.1
20	815	1500	466	67.2	545	78.7	4.9	15.7

Table 34

Tensile Properties of Forged + Salt Quenched
Ti-24Al-17Nb-1Mo (73-1A-88)

Specimen Number	Test Temp. °C	°F	0.2% Yield Str. MPa	Ksi	Ult. Tens. Str. MPa	Ksi	%EL	%RA
41	21	70	902	130.1	1021	147.3	2.3	6.7
42	204	400	732	105.7	943	136.1	6.6	13.1
45	427	800	755	108.9	972	140.2	11.2	34.4
46	650	1200	694	100.1	1007	145.3	7.2	16.9
49	760	1400	657	94.8	739	106.7	2.3	8.0
50	815	1500	489	70.6	665	96.0	2.8	8.6

Figure 75

TENSILE PROPERTIES OF FORGED + SALT QUENCHED Ti-26Al-17Nb-1Mo (Alloy 24)

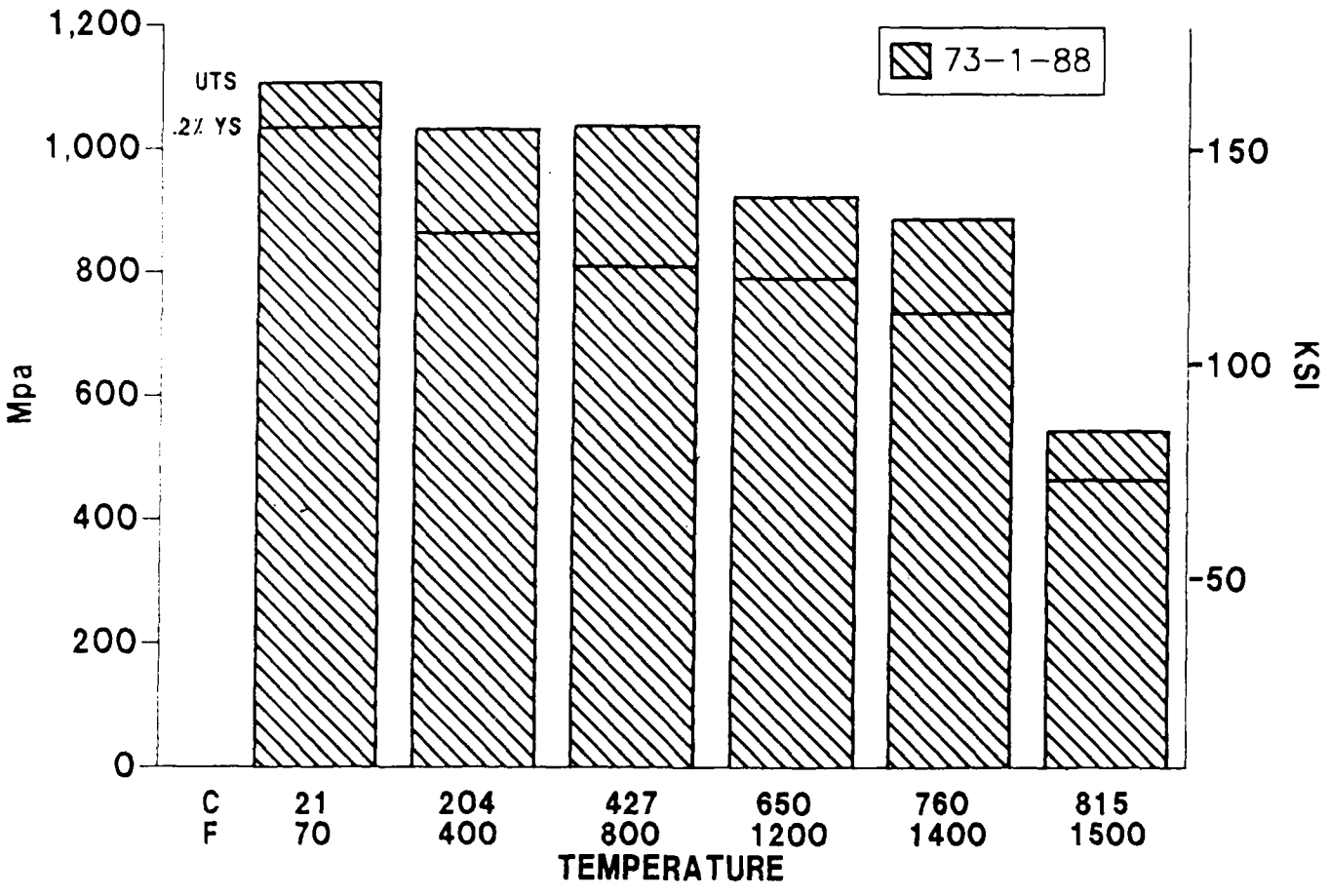

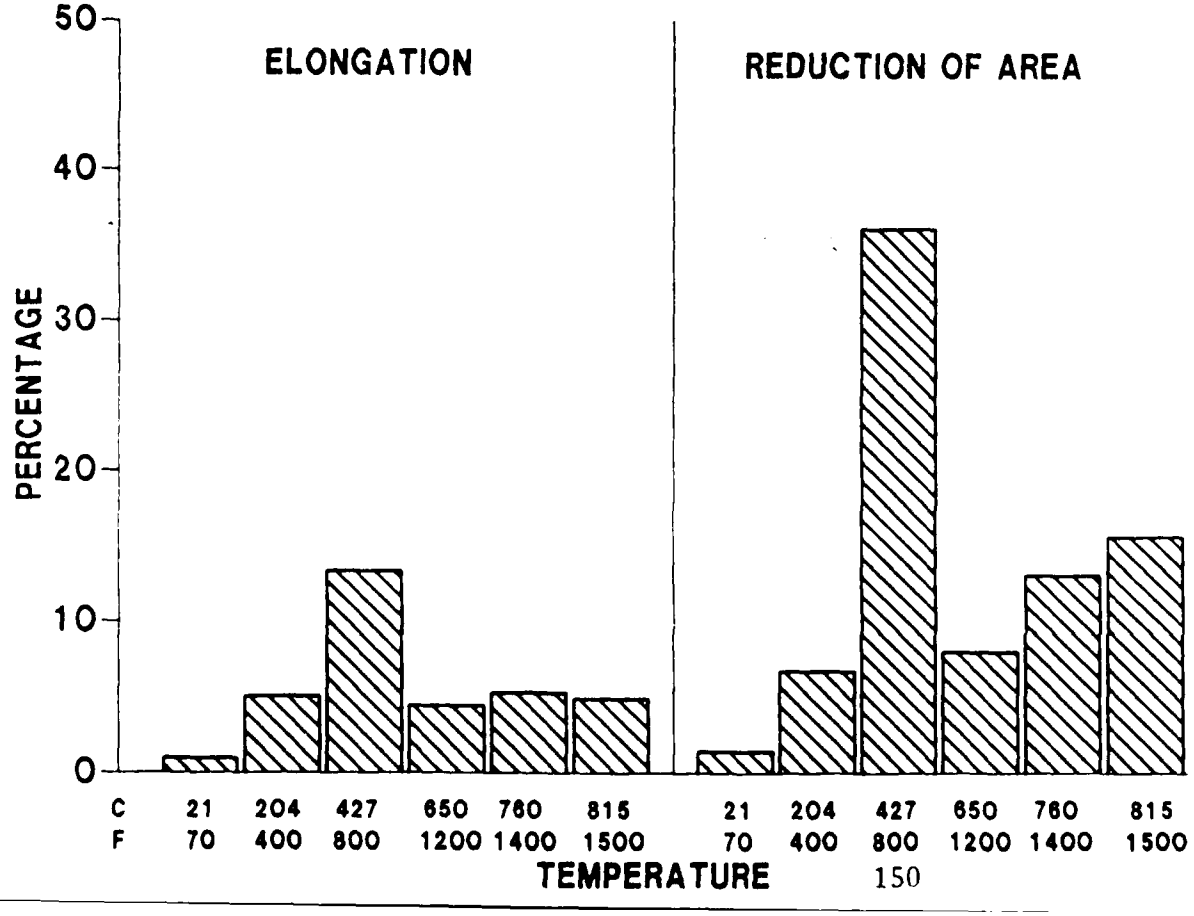

Figure 76

TENSILE PROPERTIES OF FORGED + SALT QUENCHED Ti-24Al-17Nb-1Mo (Alloy 24)

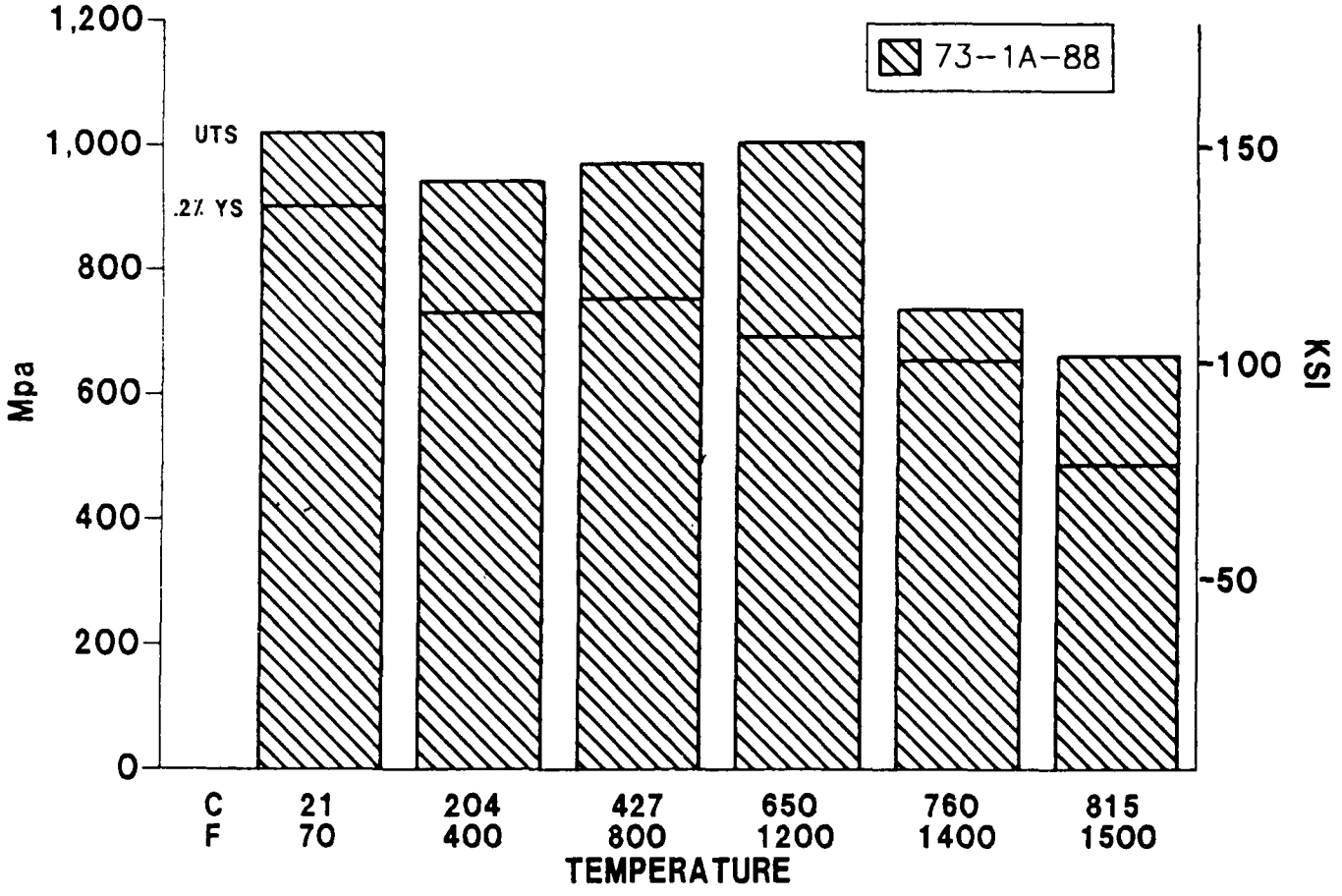

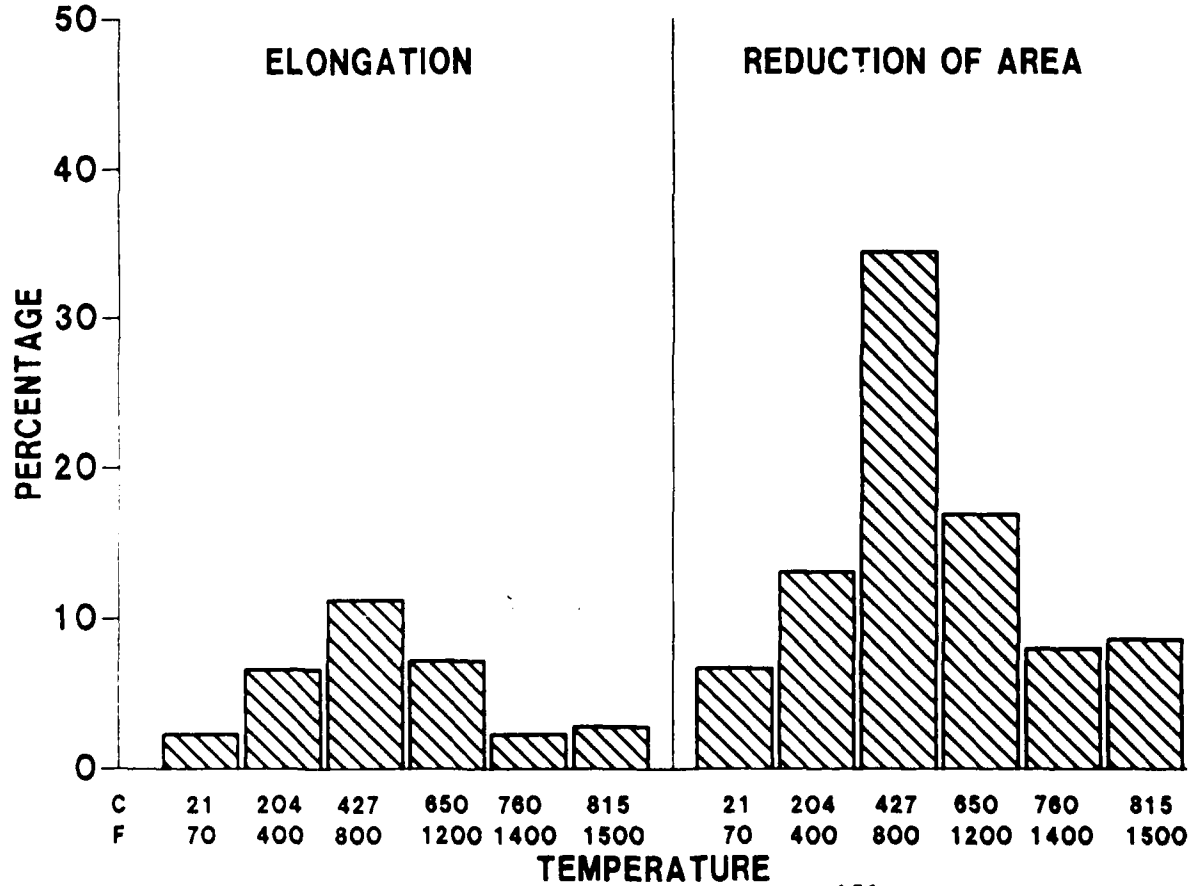

73-1A-88 forging with 24% Al were 69-100 MPa (10-15 ksi) less strong but exhibited twice the ductility at room temperature. Even at this lower strength level, program goals were comfortably met.

Tensile properties of the Ti-24Al-17Nb-.5Mo alloy are given in Tables 35 and 36. Bar chart plots are shown in Figures 77 and 78. Specimens which had been solution treated below the beta transus and quenched were 138-207 MPa (20-30 ksi) lower in strength at room temperature than the Alloy 24 forgings above. As temperature increased, the strength differential became only about 69 MPa (10 ksi). The 73-2A-88 forging, which was beta forged and quenched off the press, exhibited strength levels identical to the Ti-24Al-17Nb-1Mo composition (73-1A-88). Again, both of the forging processes used for the Ti-24Al-17Nb-.5Mo composition resulted in strength and ductility levels at or above goal.

Test results for Alloy 26 (Ti-22Al-17Nb-1Mo) are presented in Table 37 and Figure 79. These are duplicate data for this alloy as no processing or chemistry variations existed between the two forgings. We know that the room temperature strength is equal to the Ti-24Al-17Nb-.5 or 1Mo compositions, but ductility is 1-3% higher. Elevated temperature properties paralleled the higher aluminum content alloys up to 815°C (1500°F) where they fell approximately 138 MPa (20 ksi) lower. These strength levels were somewhat surprising considering that lower aluminum content placed the composition well into the two phase alpha + alpha-two region.

A common characteristic of alpha-two alloys is the peak in tensile ductility which occurs around 427°C (800°F), followed by a 50% drop in ductility at about 650°C (1200°F). Alloys in this program behaved in a similar manner and exhibited this ductility trend. However, as test temperatures were raised to 760°C (1400°F) and higher, the ductility continued to drop to surprisingly low levels. At 815°C (1500°F), in some instances, the elongation values were not much different than those measured at room temperature. No comparable high temperature tensile data for similar alpha-two alloys was generated in previous studies, so

Table 35

Tensile Properties of Forged + Solution Treated and Salt Quenched Ti-24Al-17Nb-0.5Mo (73-2-88)

Specimen[1] Number	Test Temp. °C	°F	0.2% Yield Str. MPa	Ksi	Ult. Tens. Str. MPa	Ksi	%EL	%RA
1	21	70	787	113.6	895	129.1	1.7	2.6
5	204	400	609	87.9	931	134.3	14.3	24.0
6	427	800	579	83.6	847	122.2	15.0	43.2
19	650	1200	563	81.3	692	99.9	3.4	6.7
2	760	1400	554	79.9	686	99.0	8.3	9.1
20	815	1500	442	63.8	559	80.6	6.2	14.5

[1]Solution treated at 1107°C (2025°F)

Table 36

Tensile Properties of Forged + Salt Quenched Ti-24Al-17Nb-0.5Mo (73-2A-88)

Specimen Number	Test Temp. °C	°F	0.2% Yield Str. MPa	Ksi	Ult. Tens. Str. MPa	Ksi	%EL	%RA
41	21	70	822	118.6	997	143.9	4.7	5.3
42	204	400	686	99.0	895	129.1	8.5	20.6
45	427	800	656	94.6	839	121.1	10.0	43.5
46	650	1200	600	86.6	726	104.7	4.3	14.3
49	760	1400	520	75.0	649	93.6	5.9	9.2
50	815	1500	485	70.0	617	89.0	5.3	8.0

Figure 77

TENSILE PROPERTIES OF FORGED + SALT QUENCHED AND RESOLUTION TREATED Ti-24Al-17Nb-.5Mo (Alloy 25)

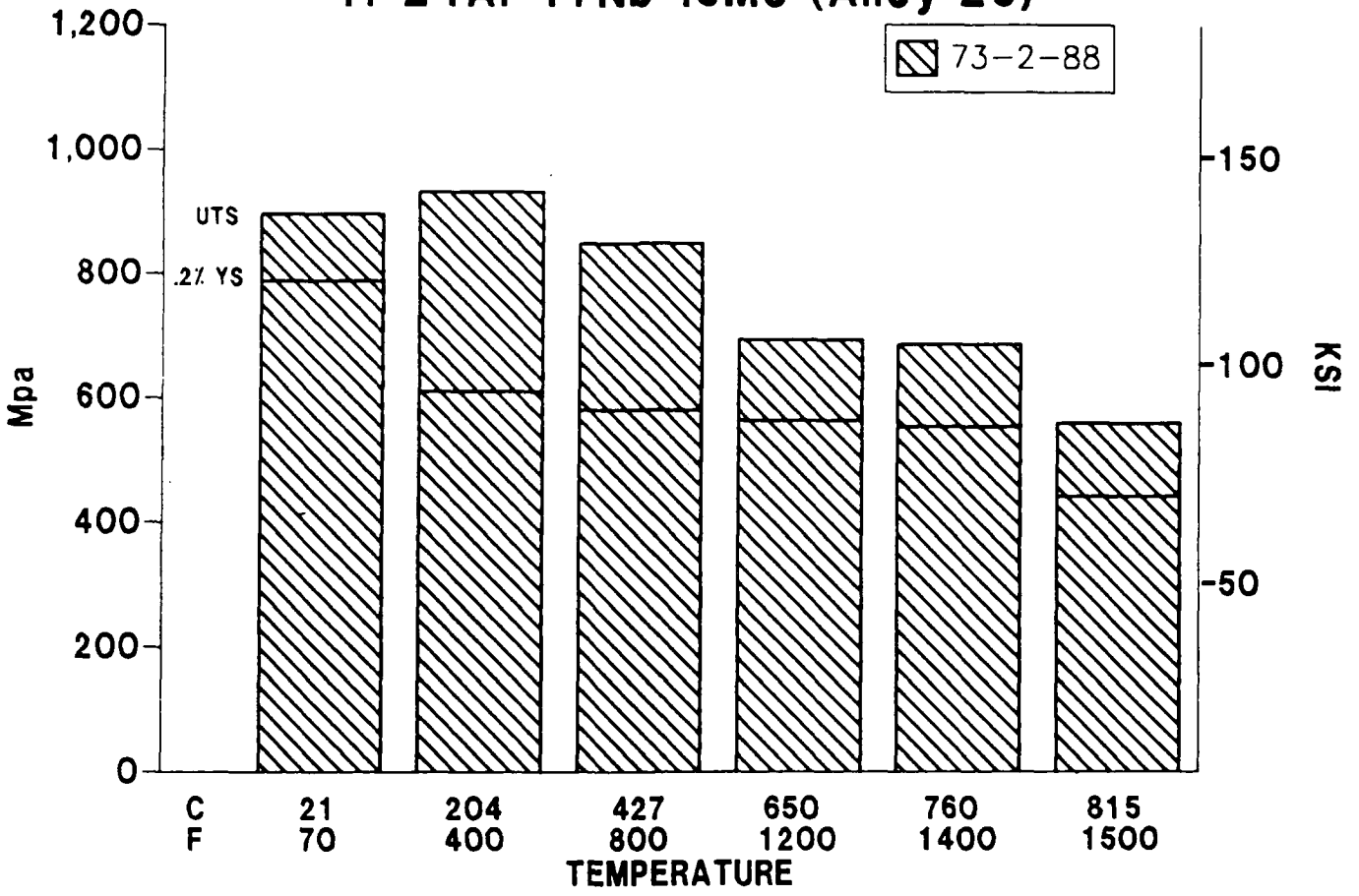

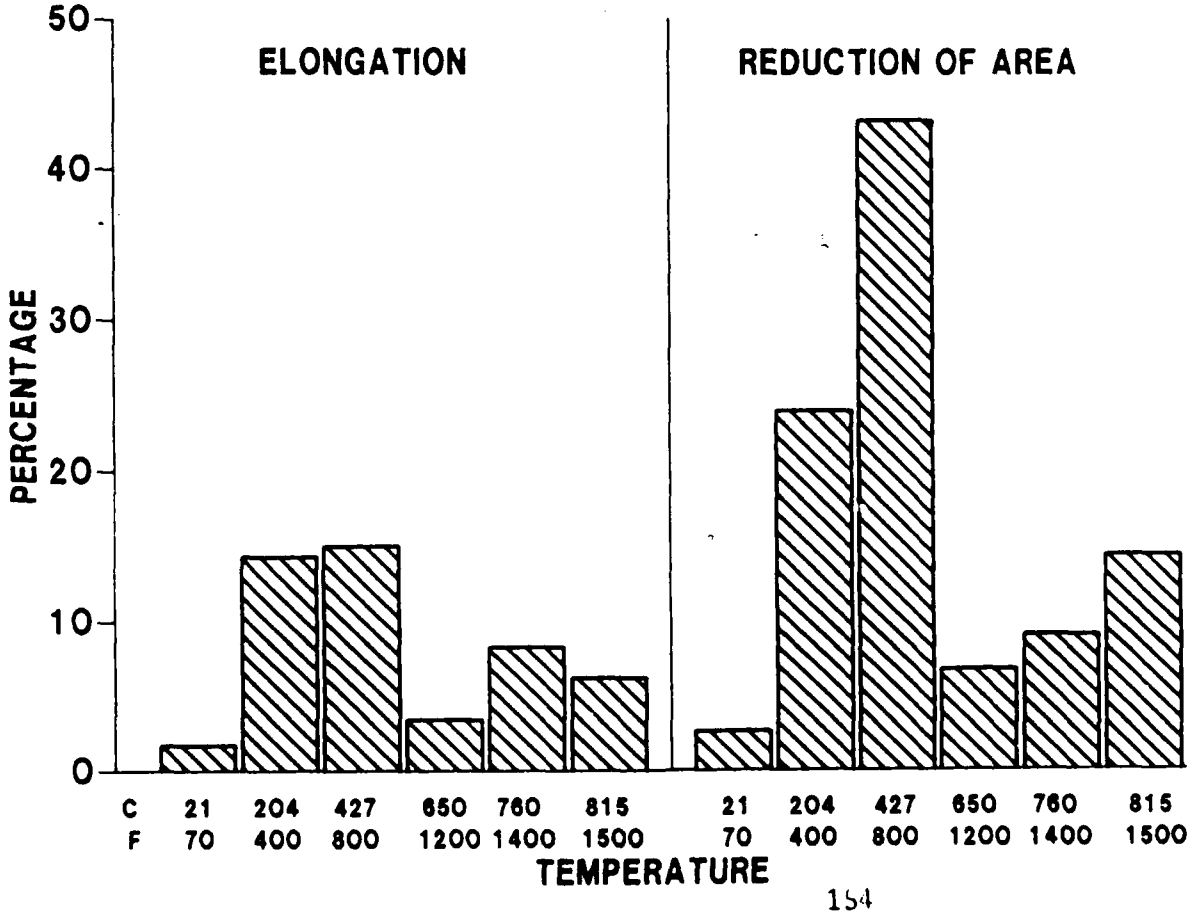

Figure 78

TENSILE PROPERTIES OF FORGED + SALT QUENCHED Ti-24Al-17Nb-.5Mo (Alloy 25)

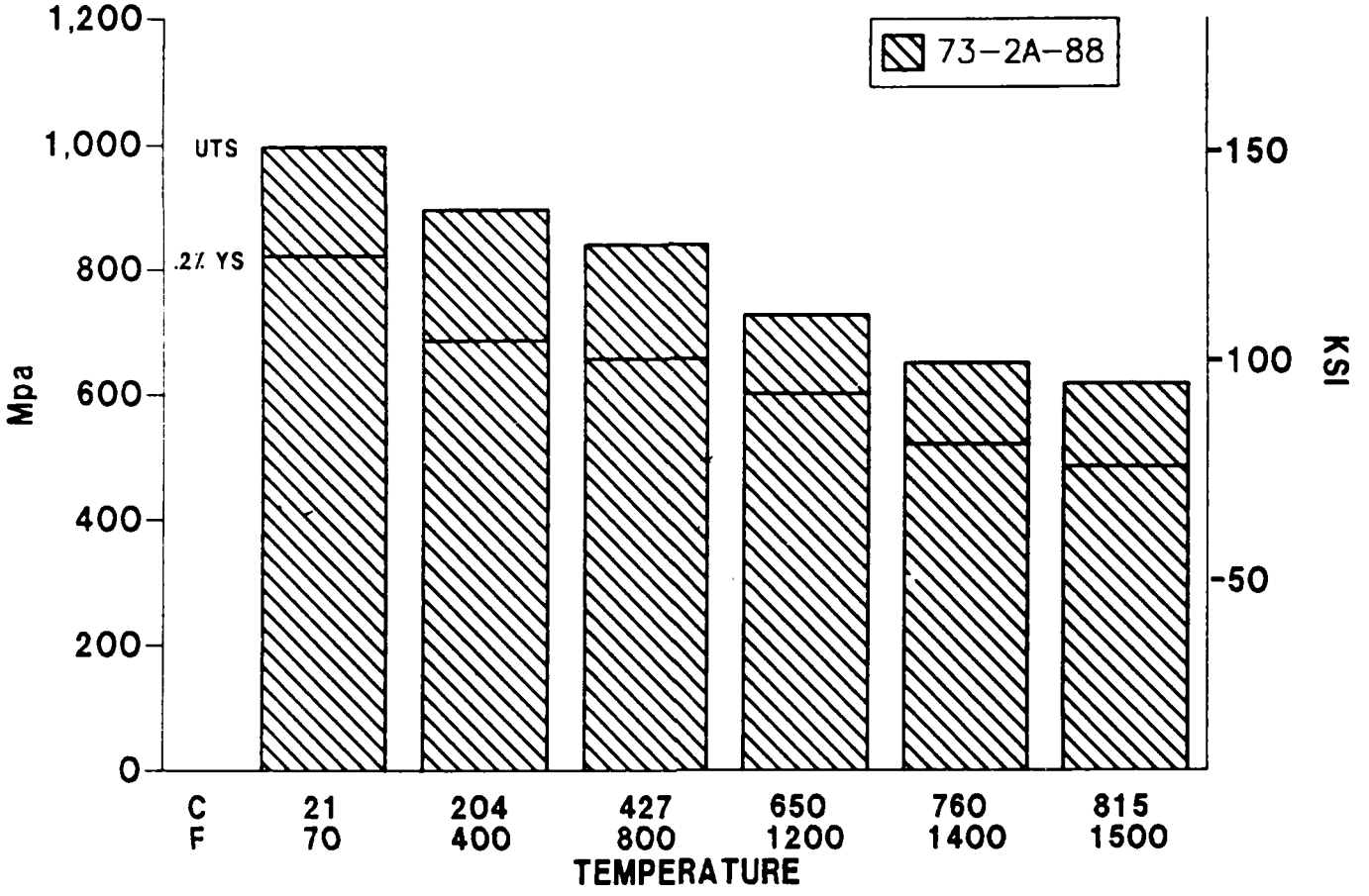

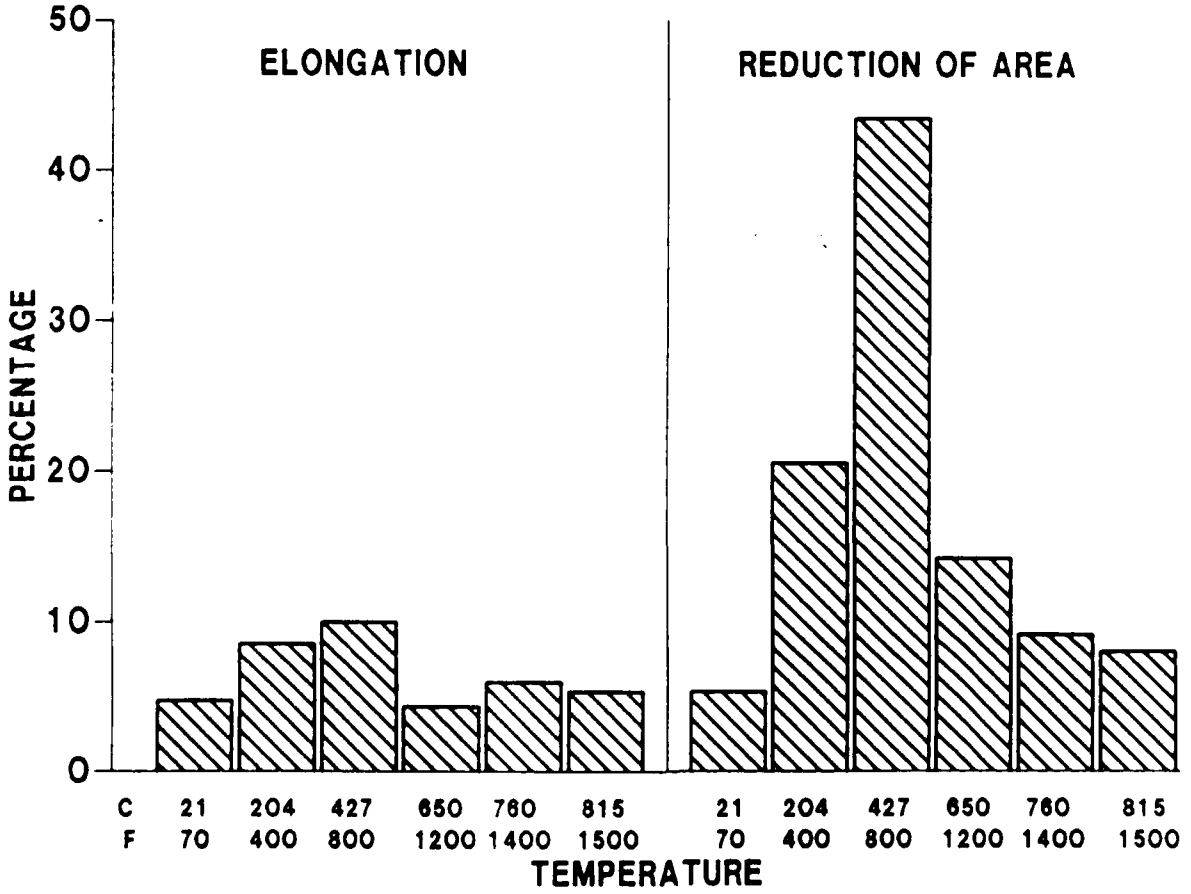

Table 37

Tensile Properties of Forged + Salt Quenched
Ti-22Al-17Nb-1Mo (Alloy 26)

Specimen Number	Test Temp. °C	°F	0.2% Yield Str. MPa	Ksi	Ult. Tens. Str. MPa	Ksi	%EL	%RA
1	21	70	822	118.6	989	142.1	4.5	6.6
41	21	70	870	125.5	1023	147.6	4.5	8.0
5	204	400	692	99.8	948	136.8	12.7	30.2
42	204	400	763	109.9	1006	145.2	11.3	20.7
6	427	800	653	94.3	845	121.9	11.0	30.7
45	427	800	712	102.7	886	127.8	9.3	43.2
19	650	1200	610	88.4	716	103.8	4.5	12.6
46	650	1200	655	94.9	753	109.2	5.6	32.0
2	650	1200*	598	86.7	705	102.2	6.0	19.5
49	760	1400	493	71.4	606	87.8	4.9	9.3
20	815	1500	309	44.8	418	60.6	8.2	8.1
50	815	1500	288	41.7	509	73.8	9.3	12.4

*Intended to be tested at 760°C (1400°F)

Figure 79

TENSILE PROPERTIES OF FORGED + SALT QUENCHED Ti-22Al-17Nb-1Mo (Alloy 26)

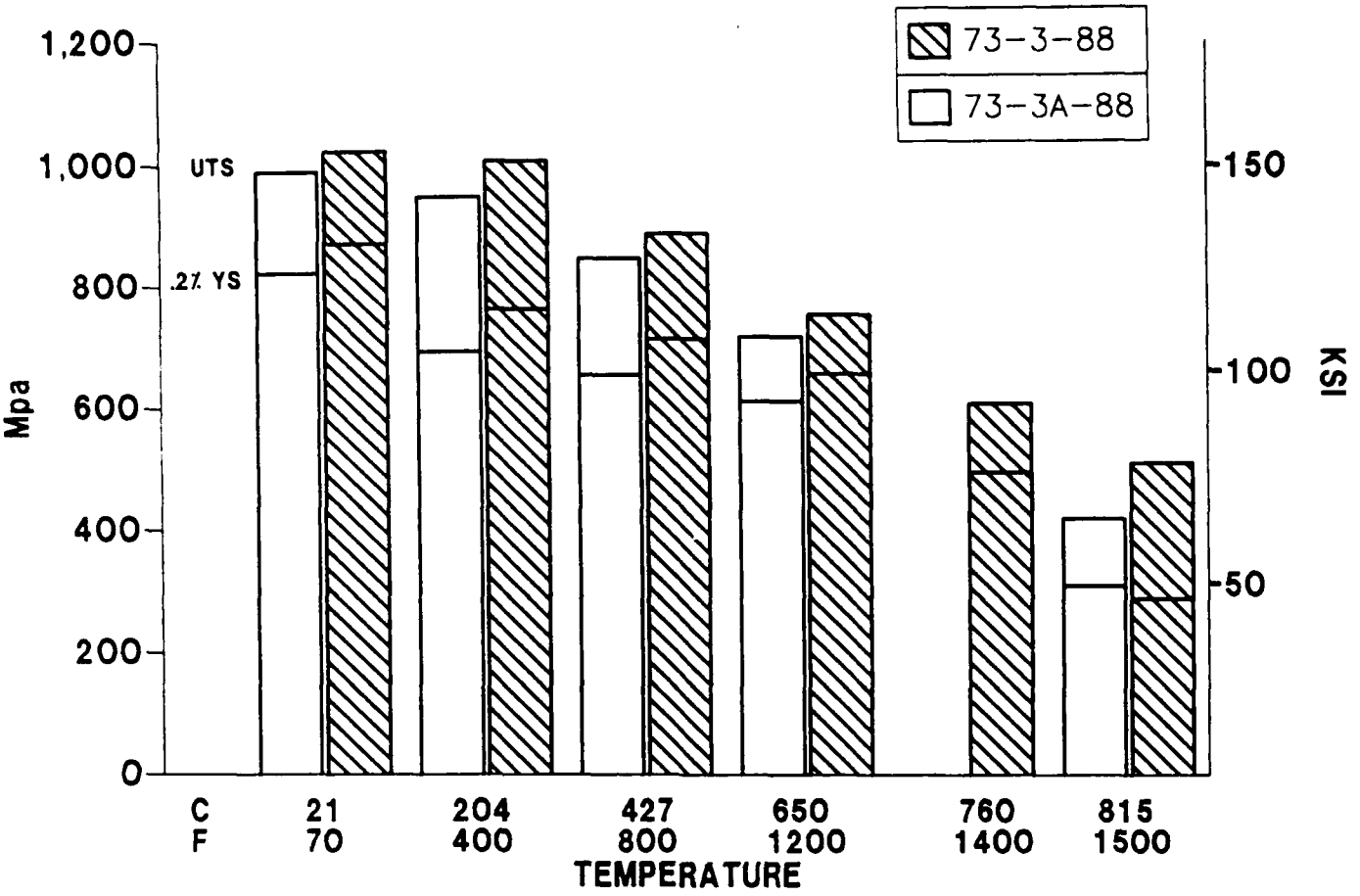

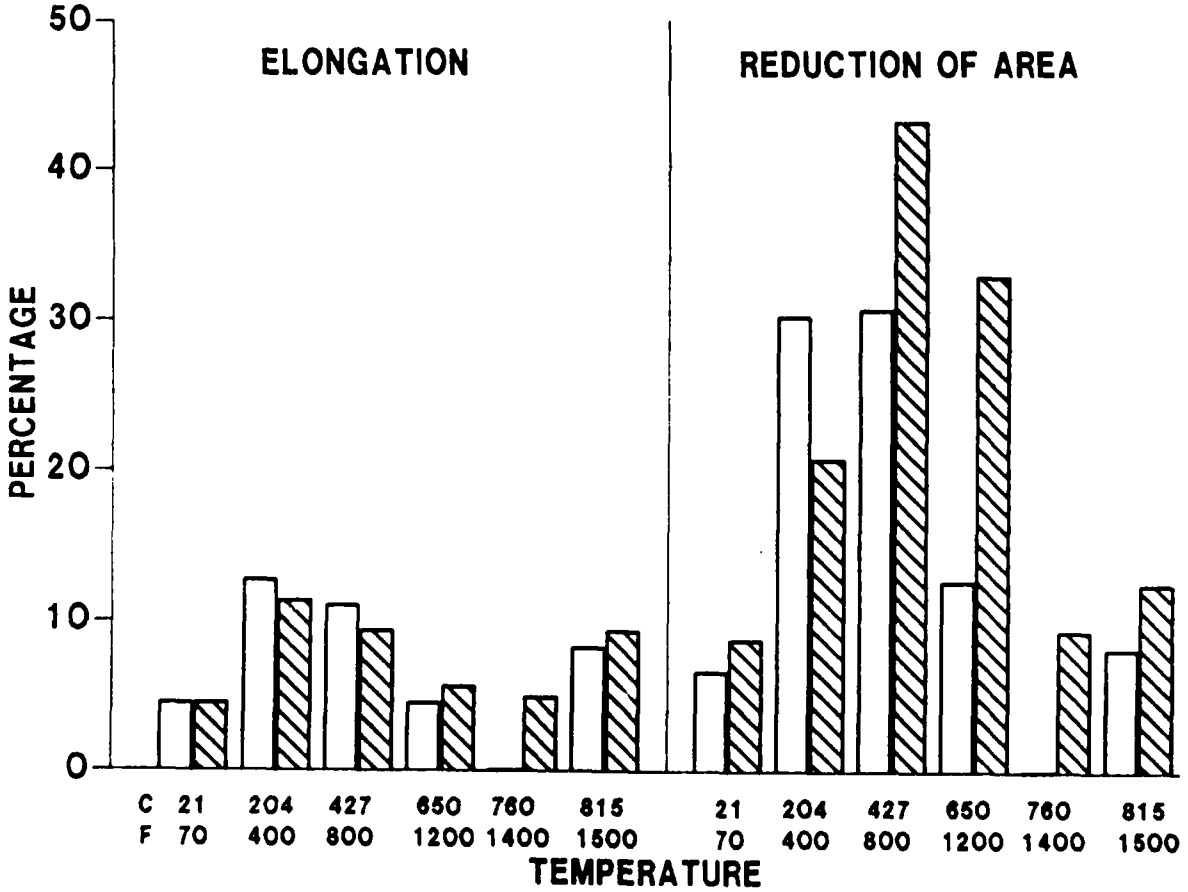

it is not known if this behavior is typical of all alpha-two alloys. While use at 760°C (1400°F) and higher is probably not possible for these alloys, it is a matter of concern for future development and should be the subject of further study.

Limited metallographic and fractographic examination of selected Ti-25Al-17Nb-1Mo specimens was conducted. Specimens selected had been tested at 21°C (70°F), 427°C (800°F) and 815°C (1500°F) prior to examination. At 21°C (70°F), the fracture mode was brittle transgranular cleavage resulting in a very flat fracture surface (Figure 80). At 427°C (800°F), the surface was more textured and shear lips, characteristic of a ductile cup-cone fracture, were observed (Figure 81). Crack progression was still transgranular. At 815°C (1500°F), the fracture surface was heavily sheared, exhibiting a near 45° angle to the applied stress direction, but no shear lips were apparent. Crack progression was not predominantly intergranular (Figure 82). This somewhat cursory examination revealed that significant changes in fracture mode were occurring with increasing temperature, but a more detailed examination was beyond the scope of this program.

While the number of combinations and processing variables make analysis more complex, some observations were made as follows:

- All conditions tested met program goals for strength but not ductility.
- The Ti-26Al-17Nb-1Mo alloy exhibited the highest strength and lowest ductility.
- Specimens with 24% aluminum and 0.5-1% Mo had the optimum combination of strength and ductility.
- Lowering the aluminum content from 24 to 22% did not affect tensile and ultimate strength at temperatures of 650°C (1200°F) and lower, but did substantially increase ductility.

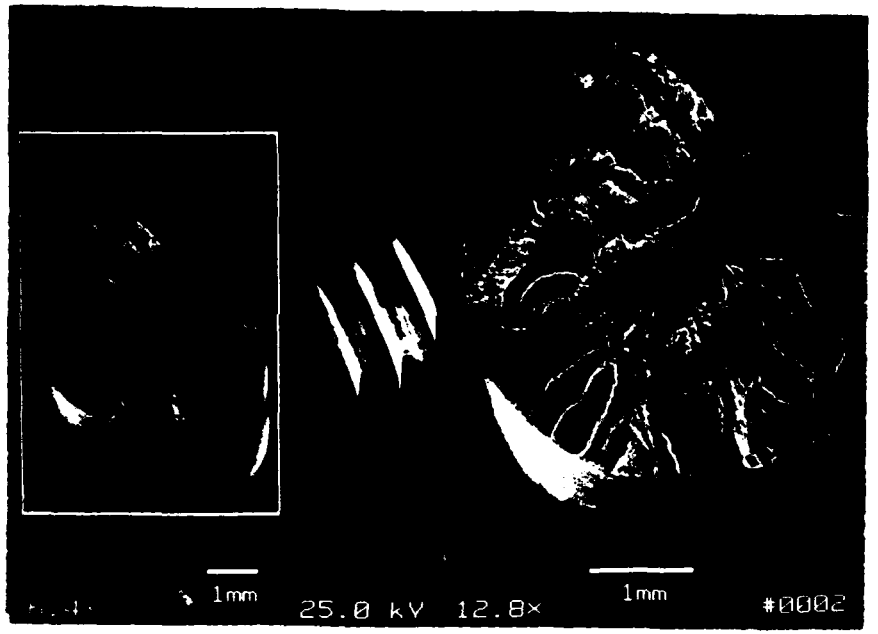

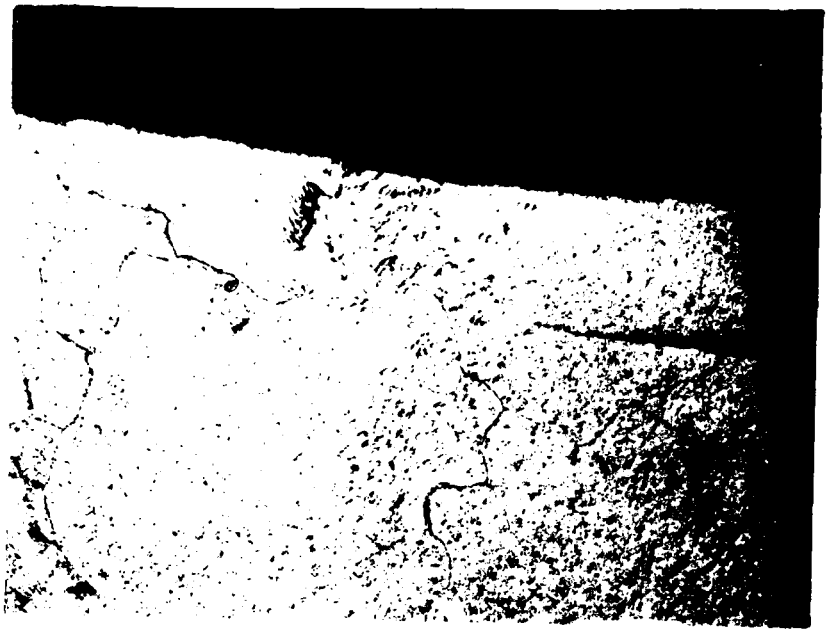

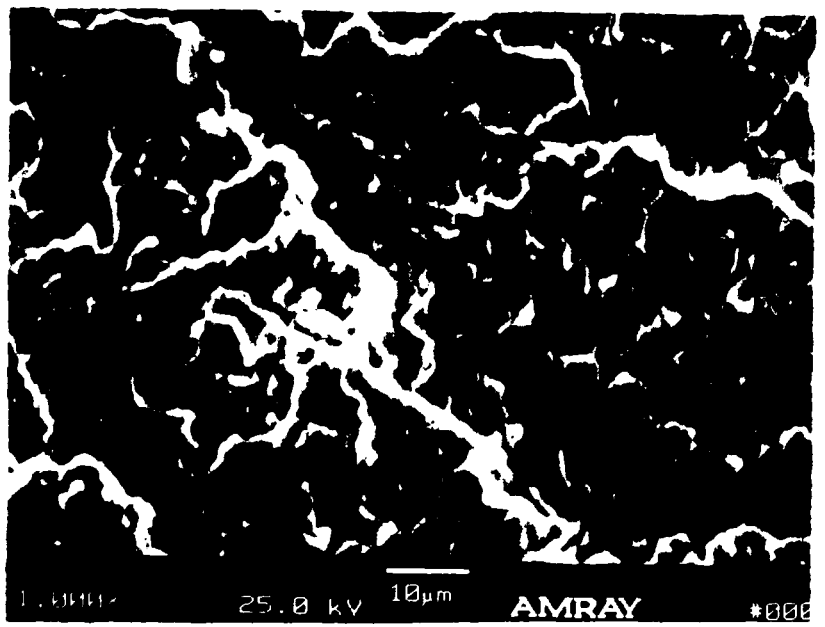

Figure 80

Fracture mode in Ti-26Al-17Nb-1Mo tensile specimen tested at 21°C (70°F). Note flat fracture and secondary cracking below fracture surface. Crack progression is transgranular.

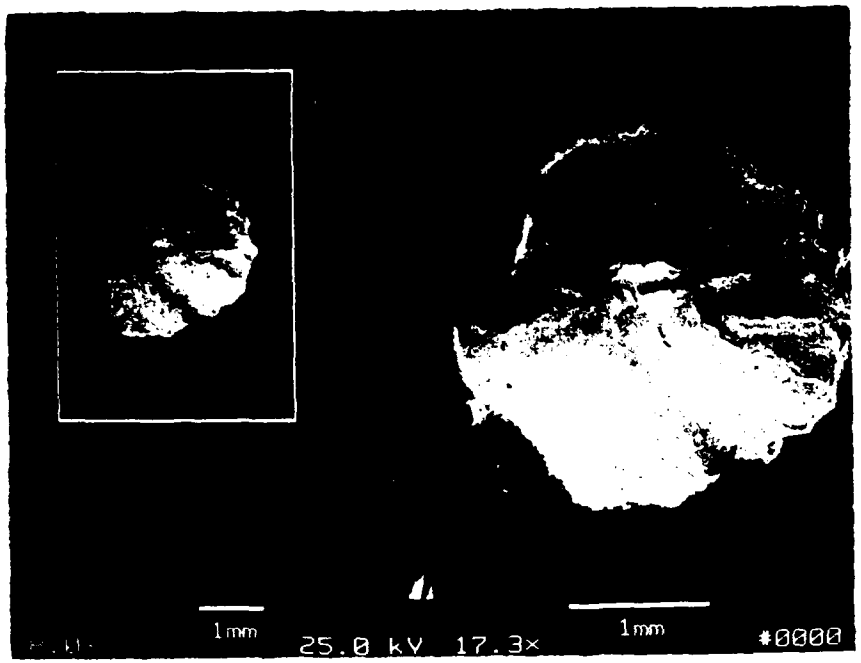

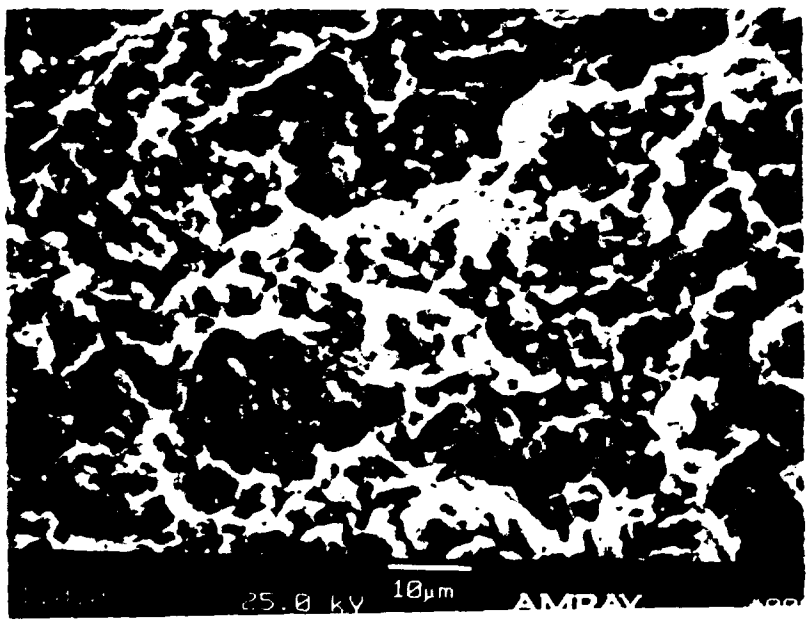

Figure 81

Fracture mode in Ti-26Al-17Nb-1Mo tensile specimen tested at 427°C (800°F). Note transgranular crack progression, shear lip around fracture surface.

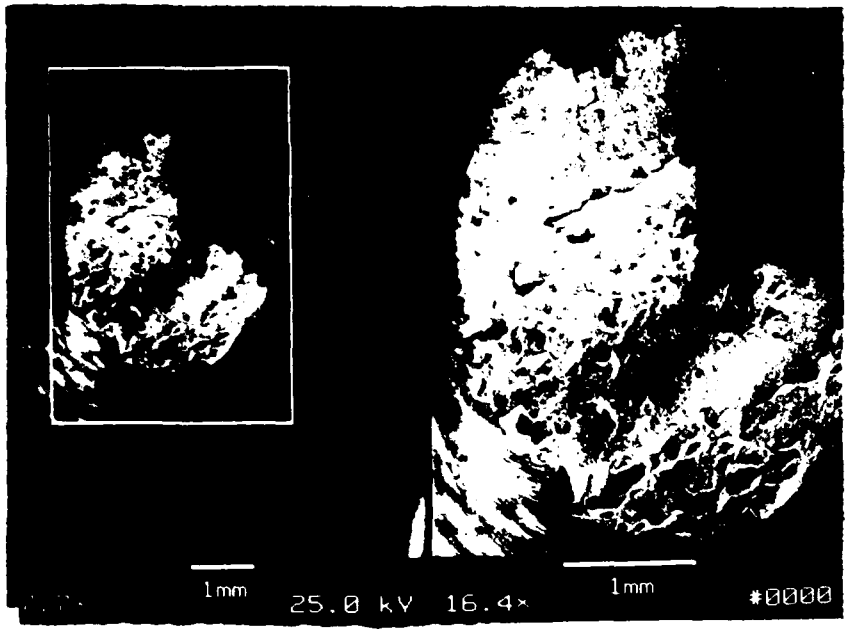

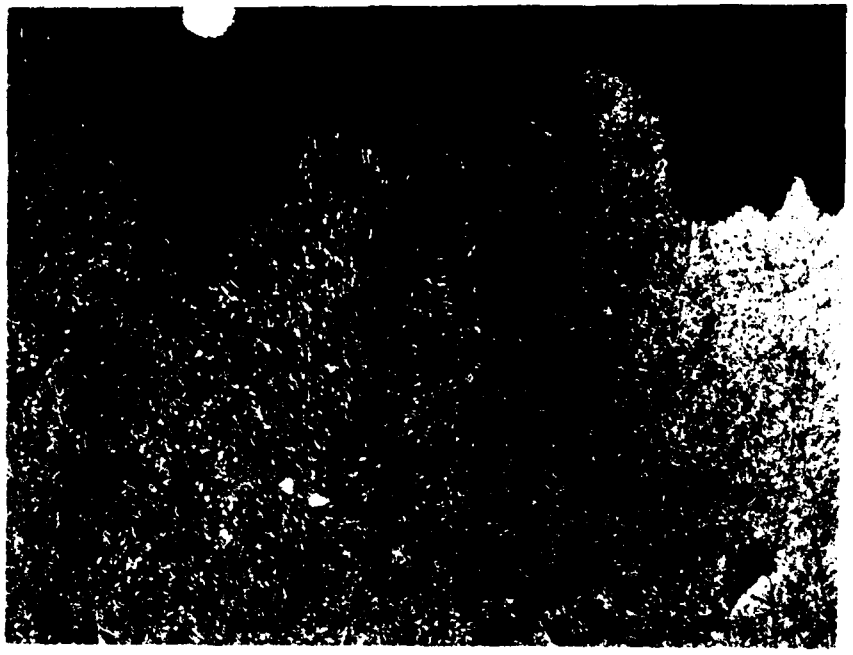

Figure 82

Fracture mode in Ti-26Al-17Nb-1Mo tensile specimen tested at 815°C (1500°F). Note change in crack progression to intergranular and heavy, shear nature of fracture surface.

- o Both niobium and molybdenum additions have a substantial effect on increasing tensile strength in alpha-two alloys. When the sum of Nb + Mo is 17-18 a/o, the resulting alloys range from 30 to 100% stronger than alloys such as Ti-24Al-11Nb or Ti-25Al-10Nb-3V-1Mo.

- o Niobium is the preferred strengthener from a tensile standpoint. Not only does it increase strength, but it improves toughness and ductility. It results in alloys less sensitive to processing than those containing molybdenum.

- o The high temperature (>650°C/1200°F) fracture mode became grain boundary dependent.

4.3.2 Fracture Toughness Testing

4.3.2.1 Experimental Details

Rectangular notched specimens were machined from each of the alloys. Notch orientation was in the plane of the forging for all specimens the including the Charpy Impact specimens to be discussed in 4.3.3. All specimens were machined from the first forging in each alloy (i.e. 73-1-88, 73-2-88, 73-3-88). In the case of Alloy 24, this means all specimens contained 26% aluminum; for Alloy 25, all specimens had been solution treated and quenched rather than quenched from the press.

Testing was conducted per ASTM E-399-83 for three point bend specimens. Prior to testing, the notched specimens were precracked by reverse bending in a high frequency fatigue machine to the required precrack depth. Calculations made after completion of testing showed that all results met plain strain criteria based on yield strength and specimen size.

4.3.2.2 Results and Discussion

Test data for all alloys are listed in Table 38 and presented visually in Figure 83. None of the alloys or conditions met the 33 MPa $\sqrt{\text{meter}}$ (30 ksi $\sqrt{\text{inch}}$) goal. Ti-26Al-17Nb-1Mo (73-1-88) specimens averaged 18.7 MPa $\sqrt{\text{meter}}$ (17 ksi $\sqrt{\text{inch}}$) at room temperature. At 204°C (400°F), the toughness doubled to 41 MPa $\sqrt{\text{meter}}$ (37.3 ksi $\sqrt{\text{inch}}$), while at 427°C (800°F), it rose to 74.8 MPa $\sqrt{\text{meter}}$ (68 ksi $\sqrt{\text{inch}}$). The Ti-22Al-17Nb-1Mo (73-3-88) alloy averaged 25.2 MPa $\sqrt{\text{meter}}$ (23.1 ksi $\sqrt{\text{inch}}$) at room temperature and paralleled behavior of the other beta processed material (73-1-88) by rising much more quickly with increasing temperature. Maximum toughness obtained at 427°C (800°F) was 82.6 MPa $\sqrt{\text{meter}}$ (75.1 ksi $\sqrt{\text{inch}}$). The Ti-24Al-17Nb-.5Mo (73-2-88) alloy which had been solution treated and quenched, averaged 25.3 MPa $\sqrt{\text{meter}}$ (23 ksi $\sqrt{\text{inch}}$) at room temperature; however, this process condition showed a slower increase in toughness with temperature, achieving a maximum toughness of 50.8 MPa $\sqrt{\text{meter}}$ (46.2 ksi $\sqrt{\text{inch}}$) at 427°C (800°F).

Since the main aim of the program was to develop tougher alpha-two based alloys, additional analysis techniques were employed to more fully understand the data and characterize selected test specimens. It was decided to increase the data base by including some selected Phase I toughness data from Ti-Al-Nb and Ti-Al-Nb-Mo alloys in the analysis. Specific data selected included Alloys 15 and 19 from the Task 1 thermomechanical processing study, Alloys 14 and 15 from Task 2 screening trials and Alloys 23 and 24 from Task 4. The assumption was made that, while not all alloys were processed by salt quenching from the press, they all exhibited a transformed microstructure which would behave in a similar manner during toughness testing. Initial analysis consisted of simply plotting observed toughness values against tensile yield strength and ductility to determine if any relationships or trends existed. For example, conventional high strength titanium alloys usually show that the fracture toughness has a inverse relationship with yield strength. These plots are presented in Figures 84 and 85. It can be seen that ductility values correlate more closely with fracture toughness than yield strength

Table 38

Fracture Toughness of Forged + Salt Quenched Alpha-Two Alloys

Alloy	Specimen Number	Test Temp. °C	°F	Fracture Toughness MPa$\sqrt{M}$	Ksi$\sqrt{In}$
Ti-26Al-17Nb-1Mo (Alloy 24)	3	21	70	19.2	17.5
	9	21	70	15.4	14.0
	23	21	70	21.9	19.9
	4	204	400	41.0	37.3
	10	315	600	44.2	40.2
	24	427	800	74.8	68.0
Ti-24Al-17Nb-.5Mo[1] (Alloy 25)	3	21	70	21.6	19.6
	9	21	70	29.4	26.7
	4	315	600	43.2	39.3
	10	427	800	50.8	46.2
Ti-22Al-17Nb-1Mo (Alloy 26)	3	21	70	26.3	23.9
	9	21	70	20.5	18.6
	23	21	70	28.8	26.2
	4	204	400	39.6	36.0
	10	315	600	60.8	55.3
	24	427	800	82.6	75.1

[1] All specimens forged 1038°C; re-solution treated at 1107°C (2025°F) and salt quenched.

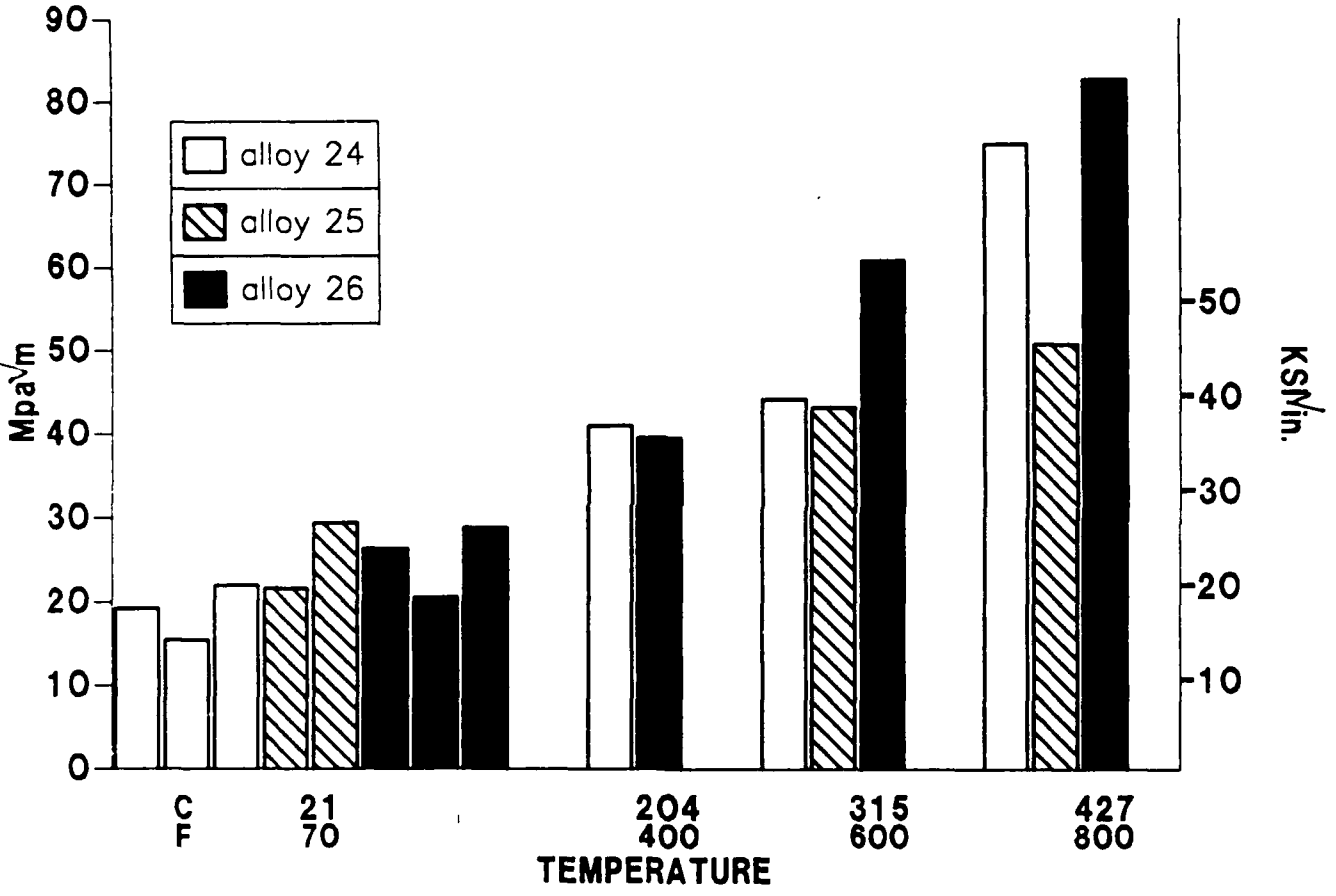

Figure 83

Fracture toughness of forged and salt quenched alpha-two.

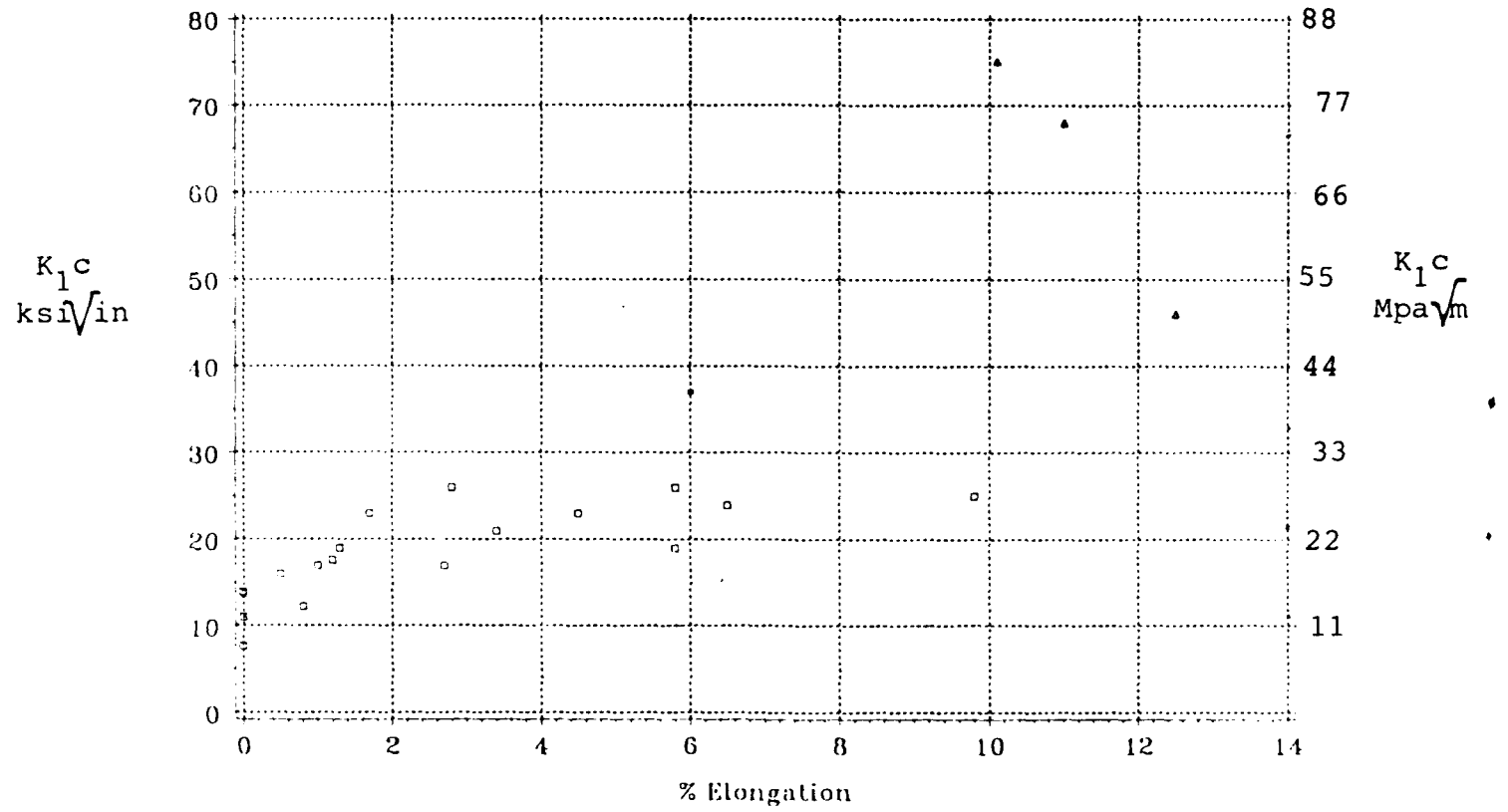

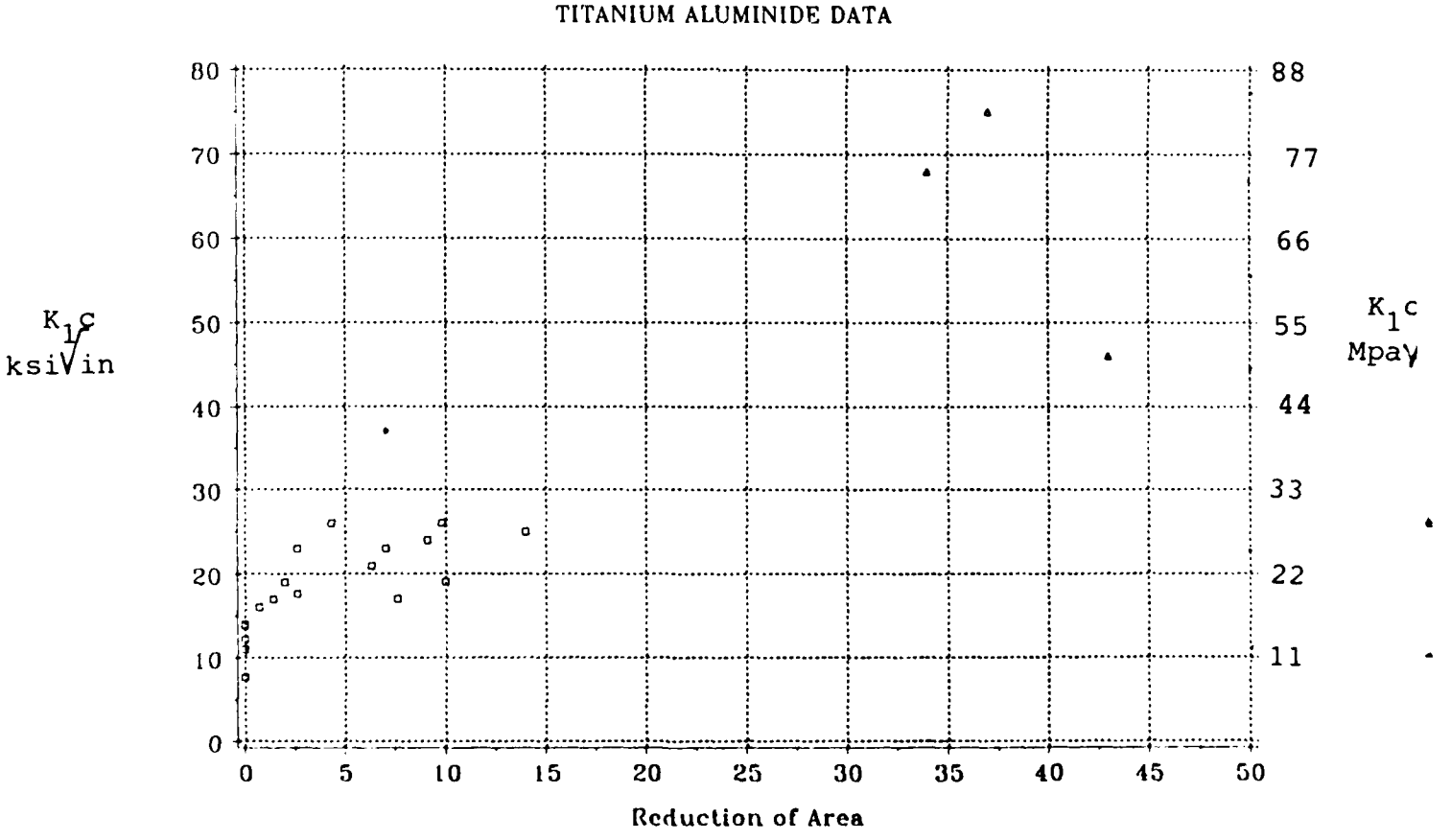

Figure 84

Correlation of tensile ductility with fracture toughness for Ti-Al-Nb and Ti-Al-Nb-Mo alloys.

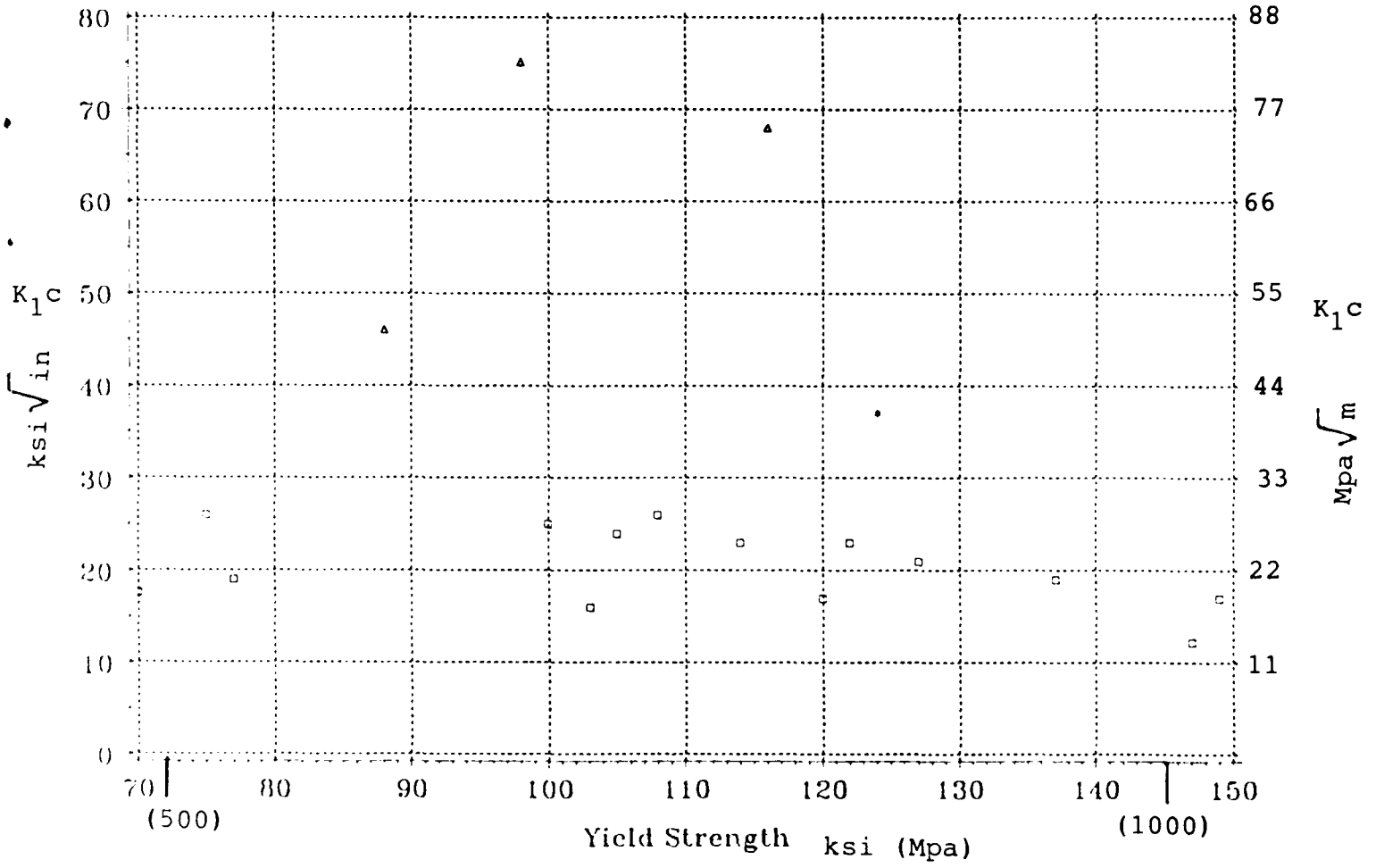

Figure 85

Correlation of yield strength with fracture toughness for Ti-Al-Nb and Ti-Al-Nb-Mo alloys.

which showed no correlation. More scatter exists at the high ductility range, but these numbers are from a relatively few elevated temperature tests where other factors such as oxidation could come into play.

In an attempt to more fully understand the relationship between compositional variables and tensile properties and their effect on fracture toughness, regression analyses were conducted. The regression variables chosen were yield strength, % elongation, % Al, % Mo and % Nb. Two runs were made. First, only room temperature values were analyzed; secondly, elevated and room temperature values were analyzed. The results are plotted in the response graphs (Figure 86). At room temperature, aluminum content and molybdenum content appear to be key factors in controlling toughness and the equation shown provides the best fit for the five variable model. When elevated temperature data are included, different variables become more important. First, temperature itself is a major effect and niobium content becomes a stronger compositional factor than aluminum or molybdenum. Thus, a different equation was generated. It should be noted that the plots, while interesting, may not provide the most accurate possible prediction. While all samples had a transformed beta microstructure, different heat treatments and process sequences were used, however, these equations do point out some general compositional effects which may be valuable in future alloy planning.

Fractographic examination was conducted by examining a typical room temperature and a 427°C (800°F) specimen of the Ti-26Al-17Nb-1Mo alloy. Both specimens exhibited a relatively rough surface with little evidence of smooth cleavage which occurs at higher strain rates as will be shown in the next section. The major difference between the two specimens is that more ductile dimpling and tearing occurs at high temperature (Figure 87) whereas at room temperature fracture seemed to be along platelet boundaries (Figure 88). There was no evidence of intergranular failure along prior beta grain boundaries.

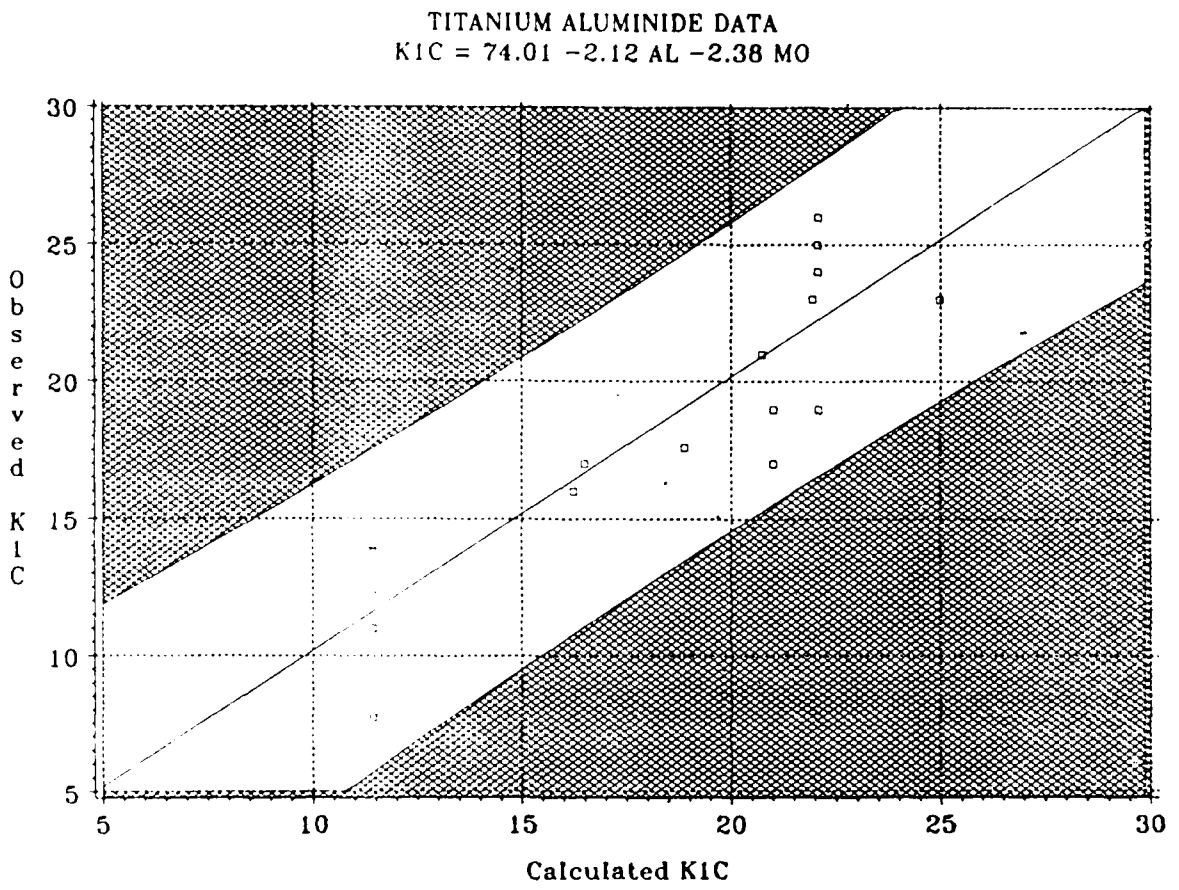

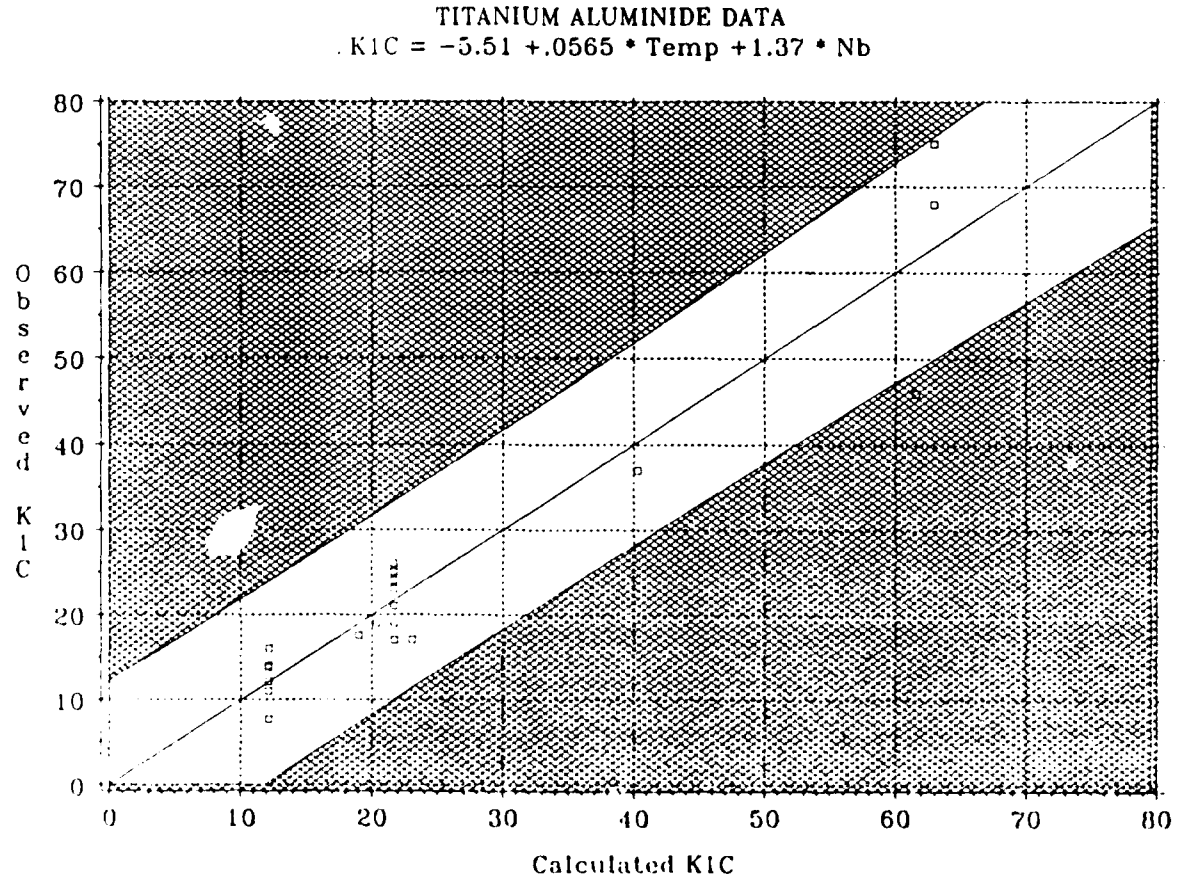

Figure 86

Plots of regression analysis showing empirical equations to predict fracture toughness for Ti-Al-Nb and Ti-Al-Nb-Mo alloys. Top plot is for 21°C (70°F) data; bottom contains elevated temperature data.

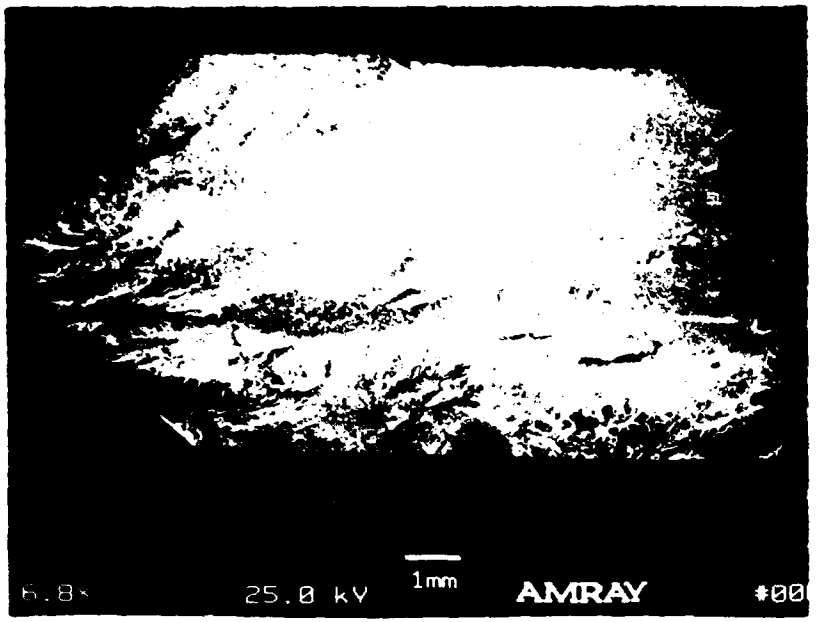

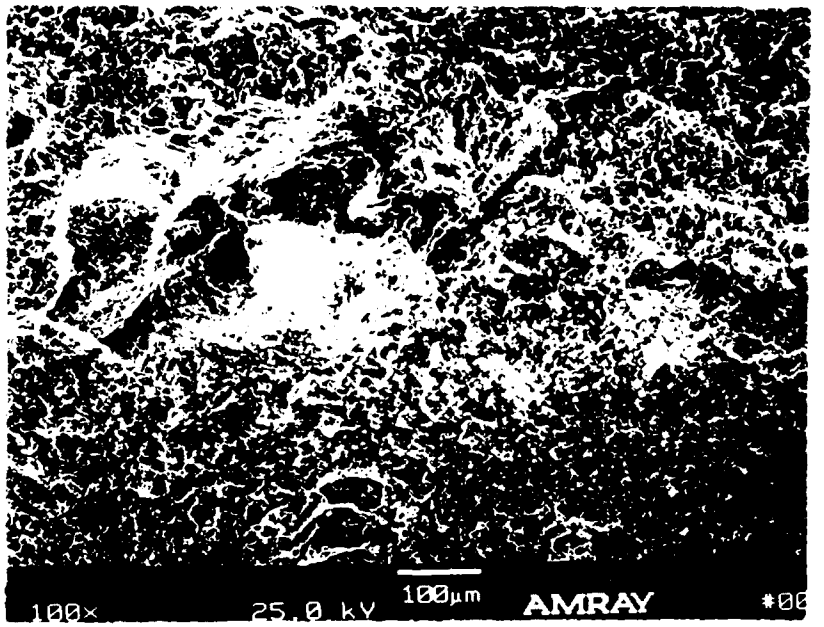

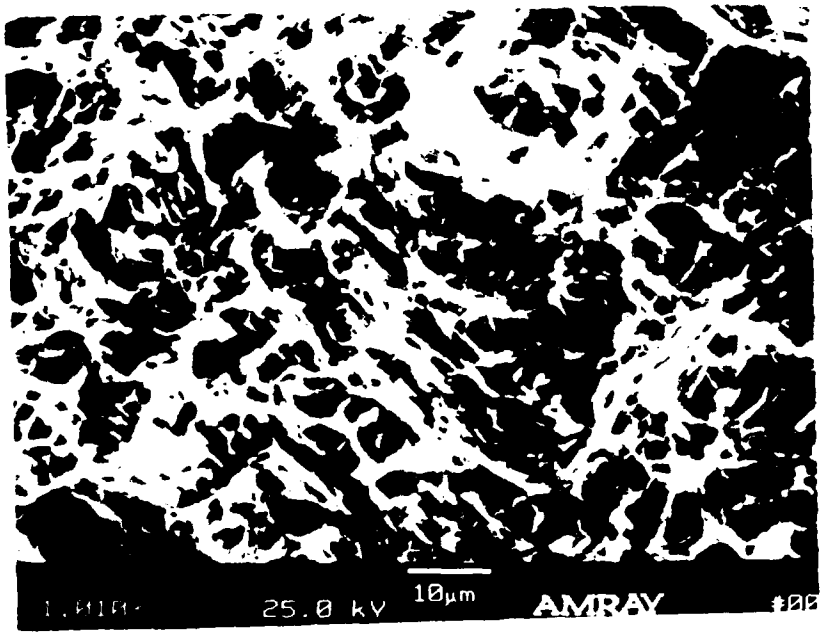

Figure 87

Fracture surface of Ti-26Al-17Nb-1Mo (Alloy 24) fracture toughness specimen tested at 427°C (800°F). Note ductile tearing (left). Toughness = 75 MPa$\sqrt{m}$ (68 ksi$\sqrt{inch}$).

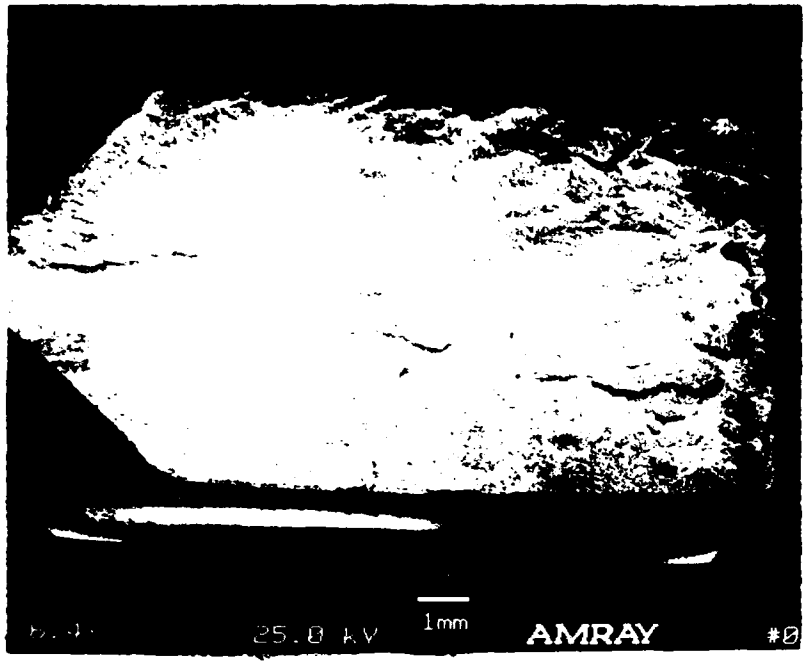

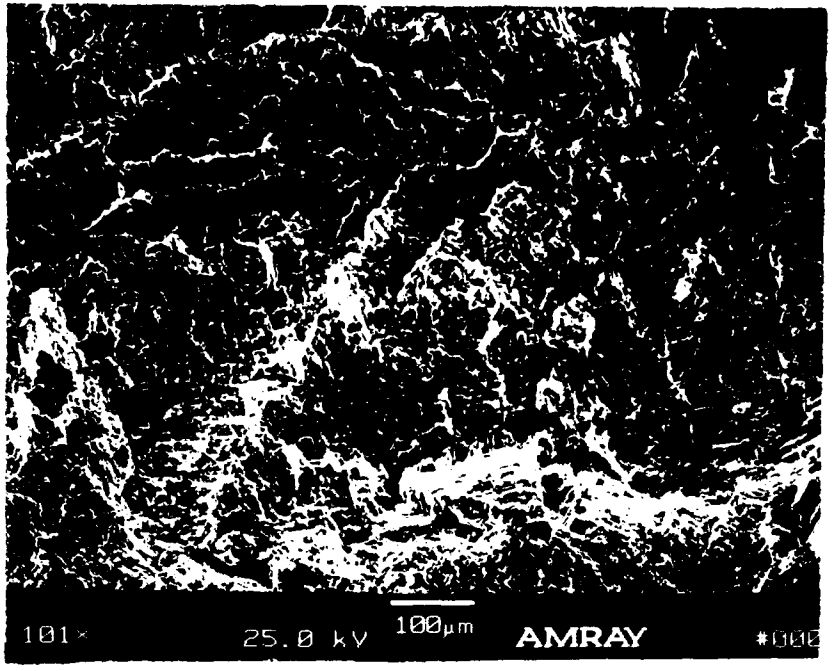

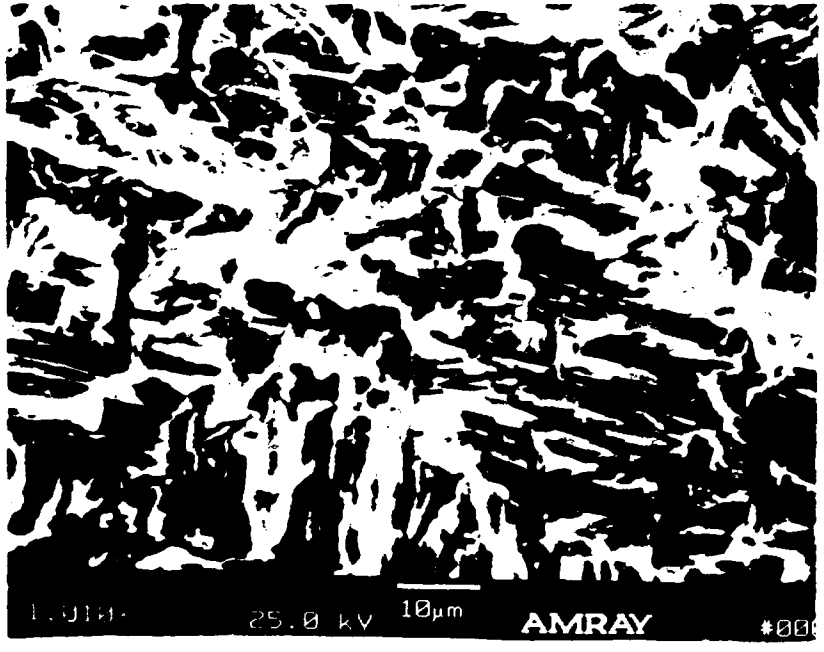

Figure 88

Fracture surface of Ti-26Al-17Nb-1Mo (Alloy 24) fracture toughness specimen tested at 21°C (70°F). Note fracture along platelet boundaries (left). Toughness = 19.8 MPa$\sqrt{m}$ (18 ksi$\sqrt{inch}$).

Since the goal to develop an alpha-two type alloy system/process procedure with room temperature fracture toughness of 33 MPa$\sqrt{meter}$ (30 ksi$\sqrt{inch}$) while maintaining an acceptable level of elevated temperature properties was not achieved, it is fair to ask what progress has been made as a result of the program efforts. By comparing the data from this program with alpha-two titanium aluminide alloys developed in earlier programs (Table 39), it can be shown that substantial progress has been made. The only alpha-two alloy with comparable room temperature fracture toughness is the venerable Ti-24Al-11Nb composition. This alloy is far inferior to the Phase II alloys in tensile strength, ductility and elevated temperature capability (including toughness). The widely used high strength "super" alpha-two, Ti-25Al-10Nb-3V-1Mo, which was developed by P&W in the early 1980's[4], has only about half the fracture toughness of the Phase II alloys at roughly equivalent property levels. Therefore, it can be concluded that real progress has been made, but the actual levels achieved are still not high enough to engender a totally comfortable feeling about use of alpha-two alloys in notched, high stress applications.

4.3.3 Notched Charpy Impact Testing

4.3.3.1 Experimental Details

Standard notched Charpy impact specimens were machined from the forgings. Notch orientation was constant for all specimens and was identical to the fracture toughness specimens. Testing was conducted over the range 21°C (70°F) to 650°C (1200°F).

4.3.3.2 Results and Discussion

Charpy impact values are summarized in Table 40 and shown visually in the bar chart plot of Figure 89. While all 21°C (70°F) numbers were low, the test was sensitive enough to sort out differences in composition or processing. The Ti-26Al-17Nb-1Mo composition (73-1-88) had the lowest impact strength (0.8 Joules/0.6 ft-lb) while the Ti-24Al-17Nb-1Mo

Table 39

Comparison of Fracture Toughness in
MPa M (Ksi In) For Various Titanium Alloys

Alloy	Reference	Test Temperature °C (°F) 21 (70)	315 (600)	427 (800)
Ti-24Al-11Nb	12	21.0 (19)	31.0 (28)	48.4 (44)
Ti-25Al-10Nb-3V-1Mo β Anneal AC	13	15.4 (14)	31.3 (33)	43.0 (39)
Ti-25Al-10Nb-3V-1Mo β Anneal + SQ	4	13.2 (12)	33.0 (30)	48.4 (44)
Alloy 24	-	18.7 (17)	48.4 (44)	75.0 (68)
Alloy 25 (Alpha-Two Beta Sol.)	-	25.3 (23)	47.3 (43)	50.6 (46)
Alloy 26	-	25.3 (23)	60.8 (55.3)	82.0 (75)

Table 40

Charpy Vee Notch Impact Strength of
Forged + Salt Quenched Alpha-Two Alloys

Alloy	Specimen Number	Test Temp. °C	Test Temp. °F	Impact Str. Joules	Impact Str. Ft-Lbs.	Process Condition
Ti-26Al-17Nb-1Mo	25	21	70	0.8	0.6	Beta Forge & SQ
Ti-24Al-17Nb-1Mo	31	21	70	1.22	0.9	↓
Ti-26Al-17Nb-1Mo	26	204	400	3.5	2.6	
Ti-24Al-17Nb-1Mo	27	427	800	13.6	10.0	
Ti-24Al-17Nb-1Mo	30	650	1200	36.7	27.0*	
Ti-24Al-17Nb-.5Mo (Alloy 25)	25	21	70	1.09	0.8	α2-β Solution & SQ
↓	31	21	70	1.5	1.1	Beta Forge & SQ
	26	204	400	3.8	2.8	↓
	27	427	800	13.3	9.8	
	30	650	1200	53.7	39.5	
Ti-22Al-17Nb-1Mo (Alloy 26)	25	21	70	1.9	1.4	Beta Forge & SQ
↓	31	21	70	1.8	1.3	↓
	26	204	400	3.4	2.5	
	27	427	800	26.4	19.4	
	30	650	1200	67.3	49.5	

*Estimated: specimen did not break

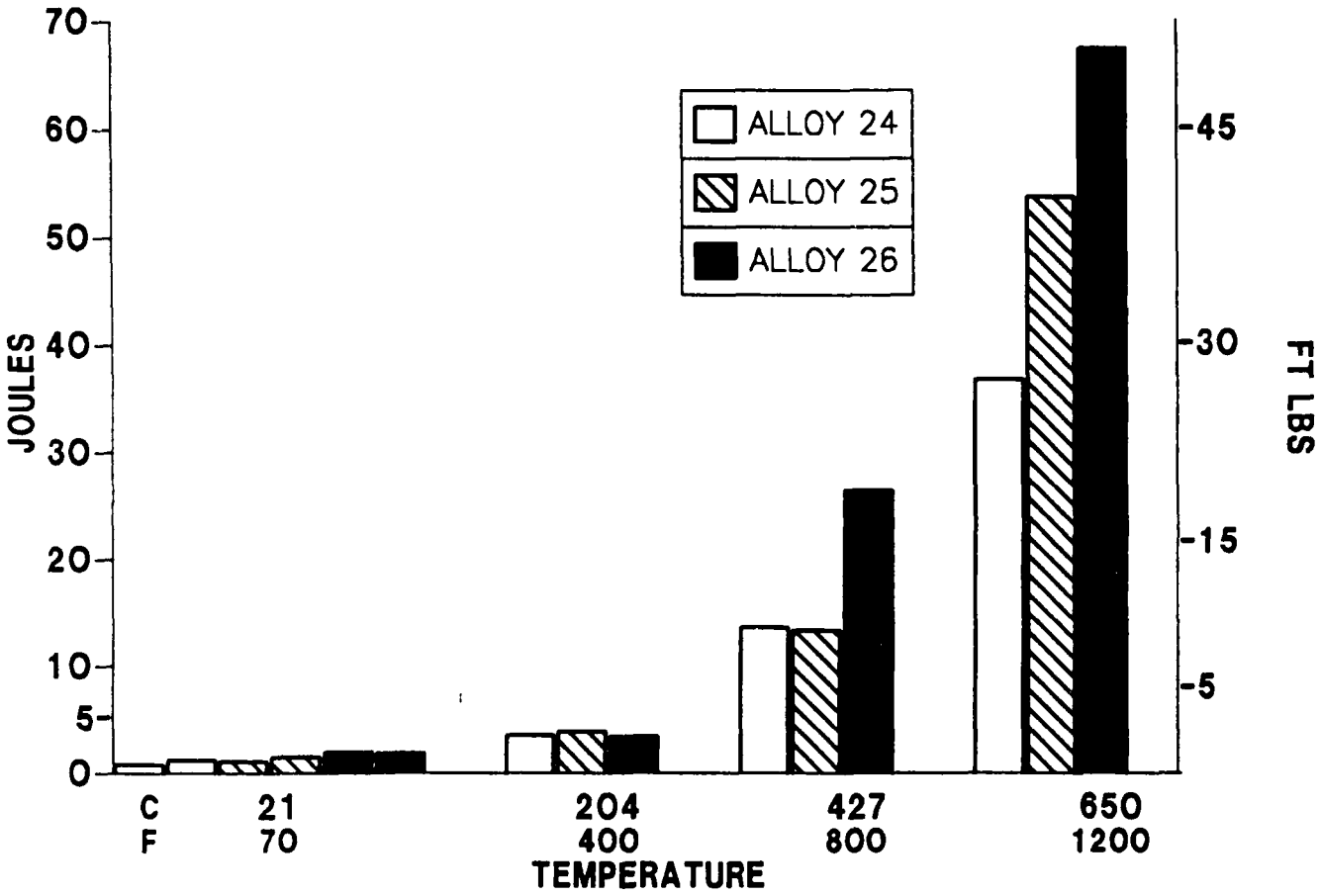

Figure 89

Charpy Vee notch impact strength of forged and salt quenched alpha-two alloys.

alloy (73-1A-88) had an impact strength of 1.22 Joules (0.9 ft-lb) in the forged and quenched condition. Impact strength rose gradually with temperature, but did not achieve a level typical of conventional alloys at room temperature until between 427-650°C (800-1200°F). The forged and quenched Ti-24Al-17Nb-.5Mo (73-2A-88) had a room temperature impact strength of 1.5 Joules (1.1 ft-lb); in the solution treated and quenched condition, it was yet lower at 1.09 Joules (0.8 ft-lb). Elevated temperature strengths were comparable to the 1% Mo alloys. Highest impact strength was achieved by the Ti-22Al-17Nb-1Mo alloy. Average RT impact strength was 1.8 Joules (1.3 ft-lb) and elevated temperature data were substantially higher at 427°C (800°F) and above.

SEM and metallographic examination was conducted on the two Ti-26Al-17Nb-1Mo room temperature and 427°C (800°F) specimens. At room temperature, the fracture surface exhibited a rather smooth appearance with large areas of cleavage apparent (Figure 90). In contrast, the room temperature fracture toughness specimen had a much more textured and rough surface with some cleavage occurring but on a much smaller scale. At 427°C (800°F) the impact specimen was rougher and more textured and exhibited ductile tearing (Figure 91). It did not differ significantly in appearance when compared to the fracture toughness specimen tested at the same temperature. Metallographic examination revealed that the fracture path was intragranular at both temperatures (Figure 92).

A search of earlier and current titanium aluminide programs yielded only a very limited data base for Charpy impact strength[1,4,11]. There was insufficient data to use regression analysis, but the information found is listed in Table 41 for comparison to the Phase II data from this report. (It should be noted at this time that, while all data was from specimens with an acicular transformed microstructure, different processing was used.) At room temperature, impact values are very similar. However, differences in capability are clearly seen at 650°C (1200°F). At this temperature, niobium has a strong influence, for example, the Ti-25Al-5Nb alloy had an impact strength of 6.6 Joules (4.9 ft-lb); the Ti-24Al-11Nb had an impact strength of 33.8 Joules (25.0

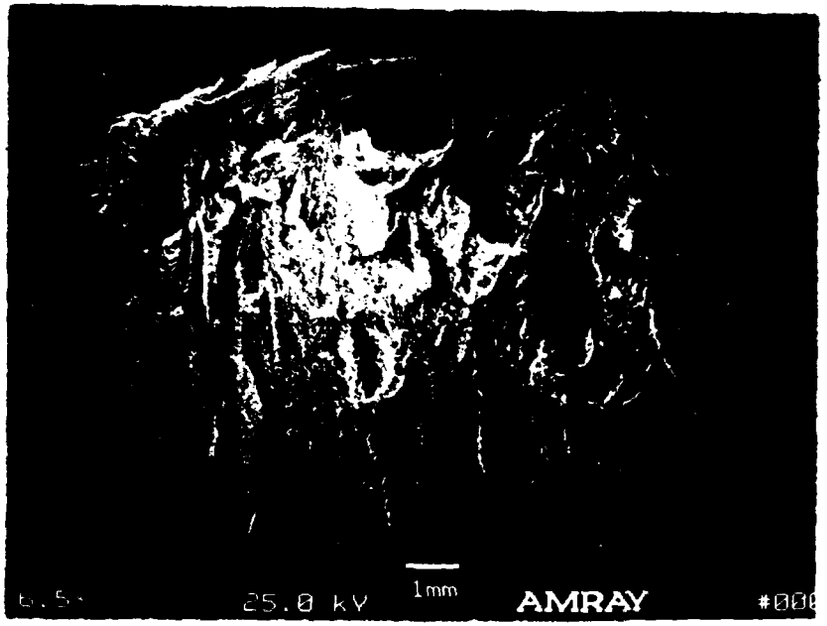

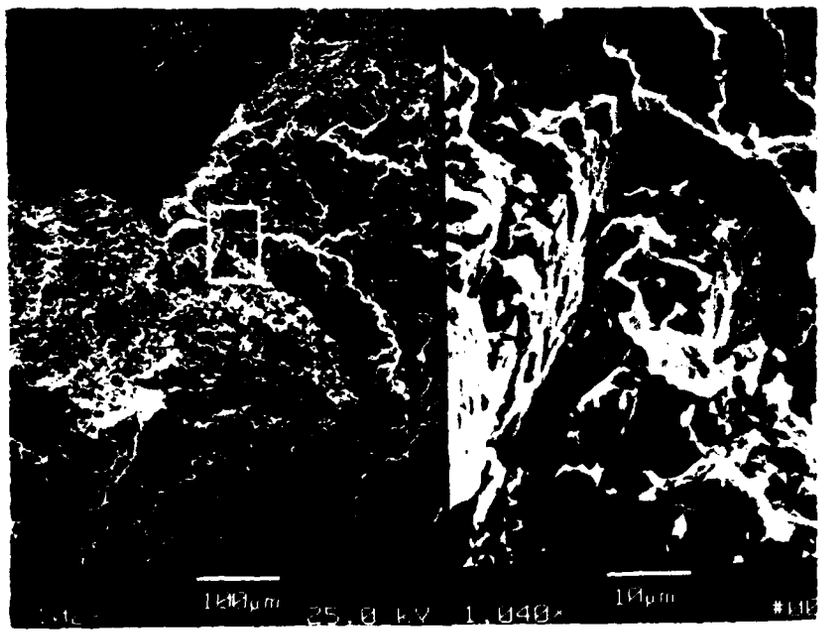

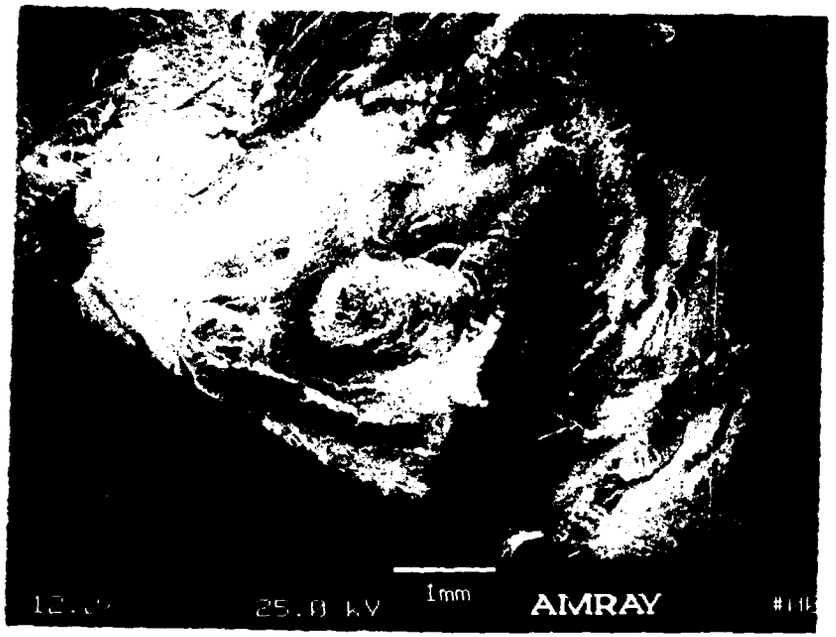

Figure 90

Fracture surface of Ti-26Al-17Nb-1Mo (Alloy 24) Charpy impact specimen tested at 21°C (70°F).

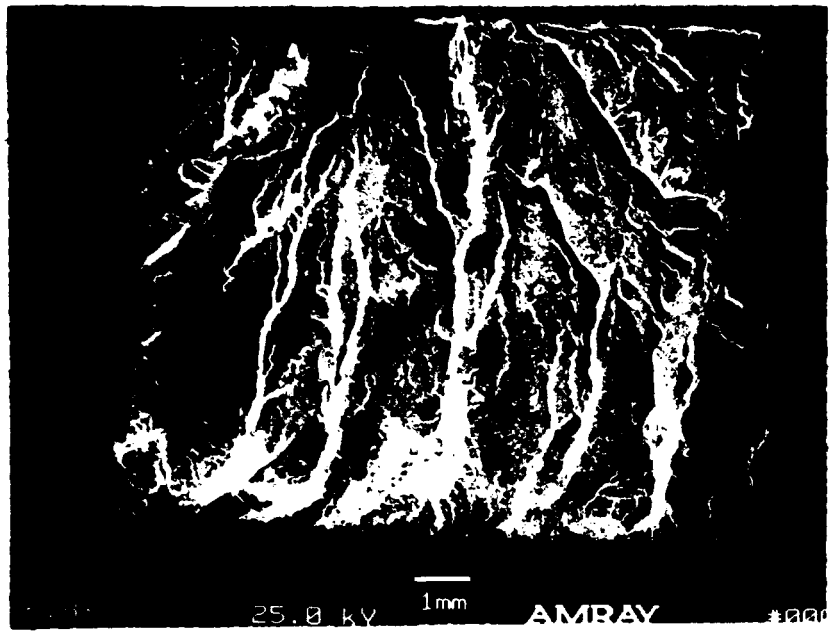

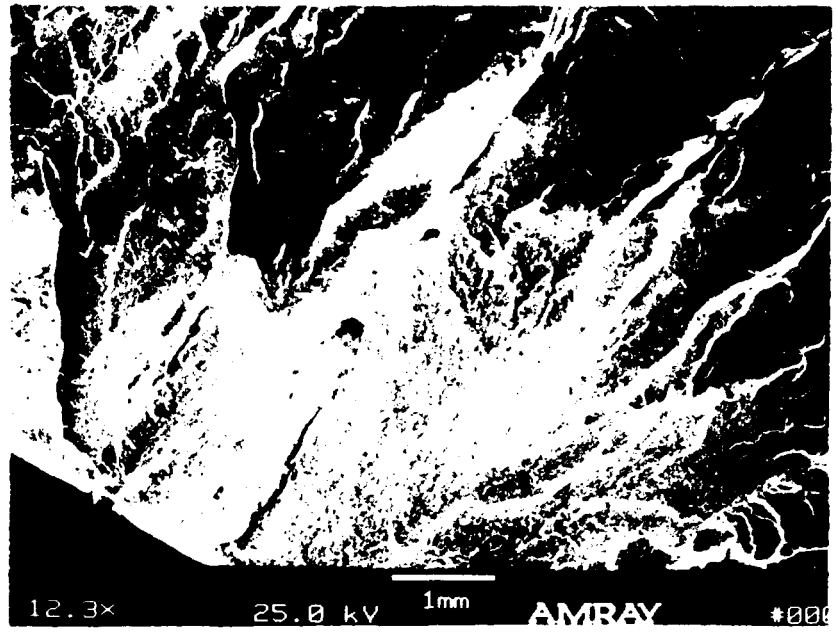

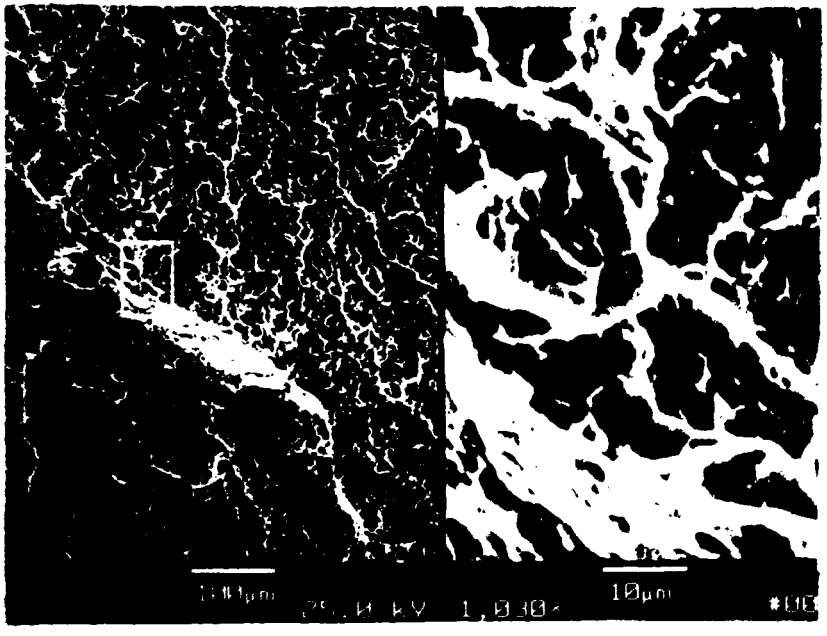

Figure 91

Fracture surface of Ti-26Al-17Nb-1Mo (Alloy 24) Charpy impact specimen tested at 427°C (800°F). Note ductile appearance compared with faceted cleavage of RT specimen.

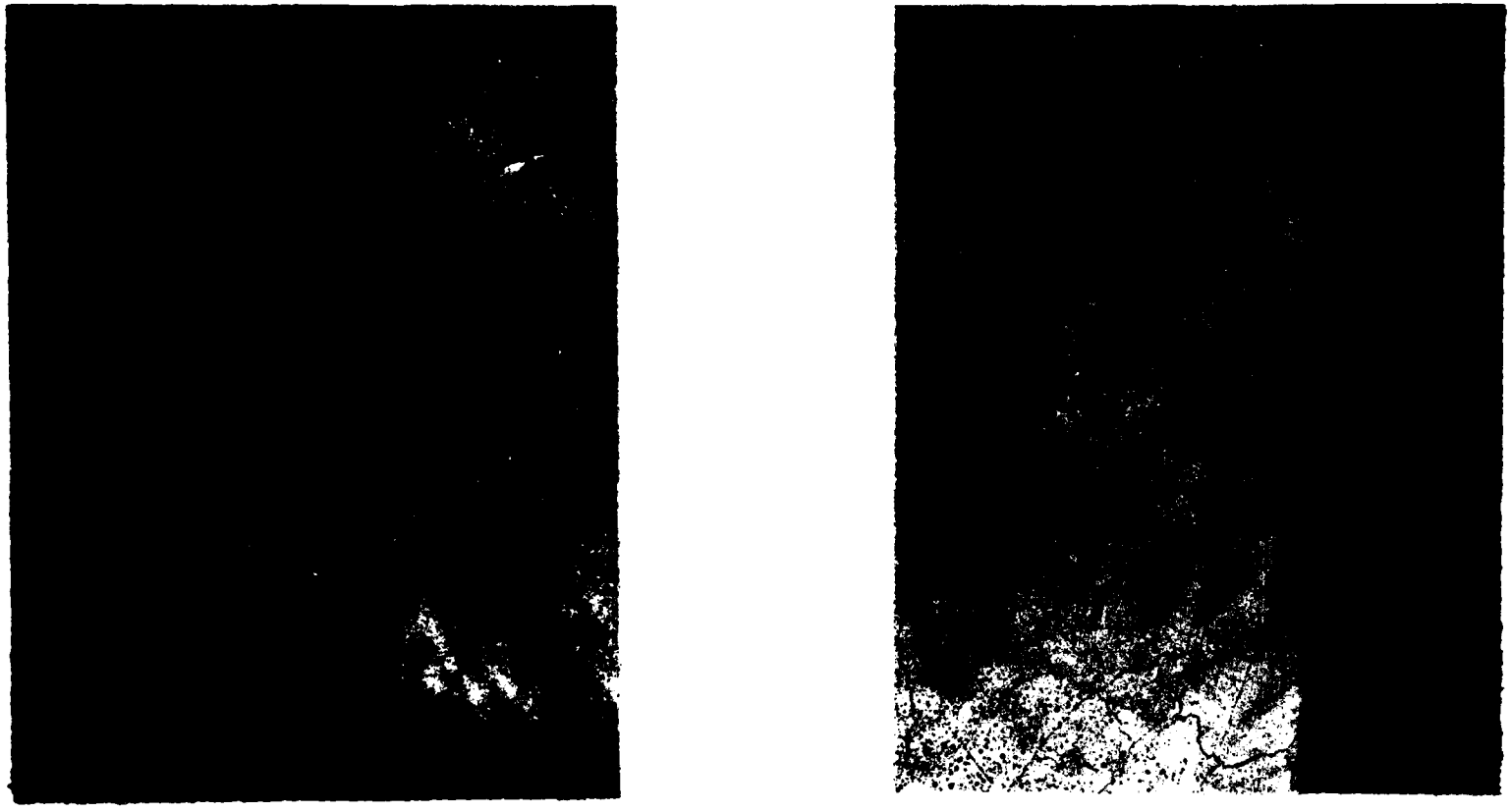

(a) (b)

12X

Figure 92

Cross section of Ti-26Al-17Nb-1Mo (Alloy 24) Charpy impact specimens. a) 21°C (70°F) test; b) 427°C (800°F) test. Note both show transgranular failure mode.

Table 41

Comparison of Notched Charpy Impact Strength in Joules (Ft-Lbs) For Various Titanium Alloys

Alloy	Reference	Test Temperature °C (°F) 21 (70)	204 (400)	427 (800)	650 (1200)
Ti-25Al-5Nb	1	1.35 (1.0)	1.8 (1.3)	2.7 (2.0)	6.6 (4.9)
Ti-24Al-11Nb	12	1.5 (1.1)	4.0 (3.0)	14.9 (11.0)	33.8 (25.0)
Ti-25Al-10Nb-3V-1Mo Beta Anneal AC	12	2.3 (1.7)	3.6 (2.7)	5.9 (4.4)	22.3 (16.5)
Ti-25Al-10Nb-3V-1Mo Beta Anneal + SQ	4	2.2 (1.6)	2.3 (1.7)	-	-
Ti-26Al-17Nb-1Mo	-	0.8 (0.6)	-	-	-
Ti-24Al-17Nb-1Mo	-	1.1 (0.8)	3.5 (2.6)	13.5 (10.0)	36.4 (27.0)
Ti-24Al-17Nb-.5Mo β	-	1.5 (1.1)	3.8 (2.8)	13.3 (9.8)	53.7 (39.5)
α-β		1.09 (0.8)	-	-	-
Ti-22Al-17Nb-1Mo	-	1.8 (1.35)	3.4 (2.5)	26.2 (19.4)	67.3 (49.5)
Ti-6Al-2Sn-4Zr-2Mo		20-27 (15-20)	-	-	-

ft-lb) and the Ti-24Al-17Nb-1Mo alloy had an impact strength of 53.3 Joules (39.5 ft-lb). Molybdenum appears to have an influence at the 11% Nb level. For example, at 650°C (1200°F), the Ti-24Al-11Nb alloy had an impact strength of 33.8 Joules (25 ft-lb) compared to 22.3 Joules (16.5 ft-lb) for Ti-25Al-10Nb-3V-1Mo.

Based on the data generated, it is apparent that the progress made in improving toughness was also beneficial to the rapid impact capability of alpha-two alloys, but at temperatures below 204°C (400°F), notched Ti_3Al alloys are still "delicate" in comparison with conventional titanium. Components without notches are much less of a problem as smooth impact data generated on the Ti-25Al-10Nb-3V-1Mo composition[4] showed approximately an order of magnitude increase over notched specimens.

4.3.4 Creep Rupture Testing

4.3.4.1 Experimental Details

An equal number of creep specimens was machined from each forging of the three alloys. Generally, a duplicate test condition was run with a specimen from each forging. Time to various percent plastic deformation was recorded. Stresses were set at relatively high levels in order to achieve rupture in approximately 100 hours.

4.3.4.2 Results and Discussion

The results of this part of the development program are most confusing and disappointing. All previous work had pointed to molybdenum as a major enhancer of creep and stress-rupture capability. If all the results of these alloys are examined, the anticipated improvements are not seen and, in fact, property levels appear to be reduced by at least a factor of five (Figure 93).

The data in Tables 42-46 for each of the alloys show that the creep and rupture properties do vary in a reasonably systematic way. Properties increase with aluminum and molybdenum level, but the Ti-26Al-17Nb-1Mo

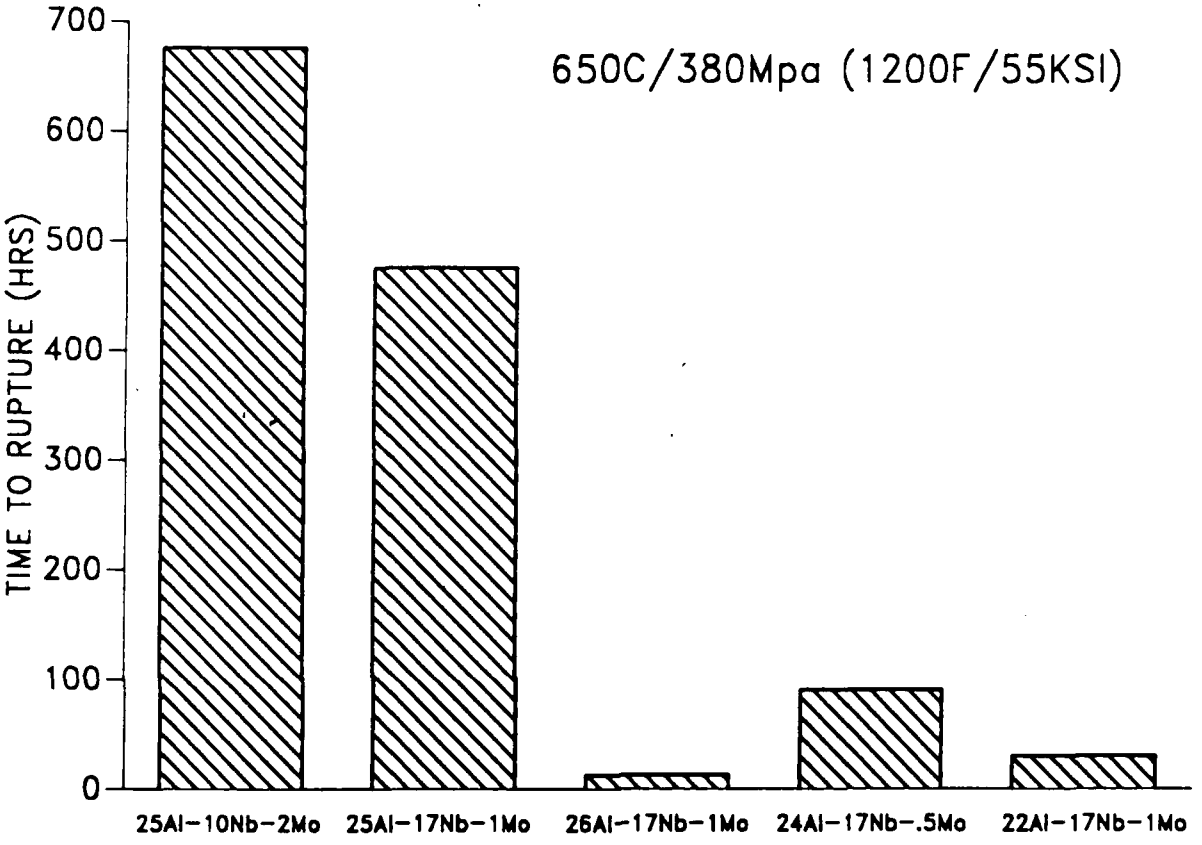

Figure 93

Comparison of stress-rupture life of various alpha-two titanium aluminide alloys.

Table 42

Creep Rupture Data for Forged and
Salt Quenched Ti-26Al-17Nb-1Mo (73-1-88)

Specimen Number	Test Temp. °C	°F	Test Stress MPa	Ksi	Time, Hours 0.2%	1%	Rupture	%EL	%RA
7	650	1200	380	55	0.6	7.2	9.7	5.1	10.9
8	650	1200	414	60	0.1	2.0	6.1	5.4	10.7
12	760	1400	207	30	0.1	1.4	8.9	10.0	18.9
21	760	1400	242	35	0.1	0.8	3.3	8.0	14.1
22	815	1500	104	15	0.3	3.0	17.5	22.2	(1)

(1) Radius failure

Table 43

Creep Rupture Data for Forged and
Salt Quenched Ti-24Al-17Nb-1Mo (73-1A-88)

Specimen Number	Test Temp. °C	°F	Test Stress MPa	Ksi	Time, Hours 0.2%	1%	Rupture	%EL	%RA
28	650	1200	380	55	2.0	33.0	67.8	4.1	3.1
29	704	1300	276	40	1.1	12.2	94.8	8.8	7.4
43	704	1300	276	40	0.9	10.8	71.7	8.7	8.3
44	760	1400	207	30	0.3	4.0	46.3	14.3	10.2
47	815	1500	104	15	0.8	10.6	137 (1)	14.6	12.6
48	815	1500	172	25	0.1	1.0	14.4	20.2	14.2

(1) Discontinued, did not rupture

Table 44

Creep Rupture Data for Solution Treated and Salt Quenched Ti-24Al-17Nb-.5Mo (73-2-88)

Specimen Number	Test Temp. °C	°F	Test Stress MPa	Ksi	Time, Hours 0.2%	1%	Rupture	%EL	%RA
7	650	1200	380	55	0.8	17.2	119.8	4.8	4.5
8	650	1200	380	55	0.7	10.5	71.8	10.5	10.5
11	704	1300	276	40	0.4	14.2	135.7	8.1	6.6
12	760	1400	207	30	0.3	4.5	56.5	15.7	11.7
21	760	1400	276	40	0.1	0.4	37.0	11.0	11.7
22	815	1500	104	15	0.3	3.9	59.0	42.5	79.7

Table 45

Creep Rupture Data for Forged + Salt Quenched Ti-24Al-17Nb-.5Mo (73-2A-88)

Specimen Number	Test Temp. °C	°F	Test Stress MPa	Ksi	Time, Hours 0.2%	1%	Rupture	%EL	%RA
8	650	1200	380	55	1.0	13.6	68.0	8.1	8.7
28	650	1200	380	55	0.6	8.8	23.3	5.1	7.9
29	704	1300	276	40	0.8	3.8	20.7	7.3	7.8
43	704	1300	276	40	0.3	3.5	28.3	8.7	9.4
44	760	1400	207	30	0.1	1.5	12.1	11.0	14.4
47	815	1500	104	15	0.3	2.7	33.9	28.8	(1)
48	815	1500	69	10	1.2	23.6	138.9	3.6	2.6

(1) Could not measure due to nature of fracture; %RA >50

Table 46

Creep Rupture Data for Forged + Salt Quenched
Ti-22Al-17Nb-1Mo (Alloy 26)

Specimen Number	Test Temp. °C	°F	Test Stress MPa	Ksi	Time, Hours 0.2%	1%	Rupture	%EL	%RA
7	650	1200	380	55	0.2	3.5	14.1	4.4	6.7
28	650	1200	380	55	0.3	4.8	17.9	5.6	10.6
29	704	1300	276	40	0.2	2.6	9.9	7.4	13.7
11	704	1300	276	40	0.5	5.4	29.6	10.6	13.6
43	704	1300	242	35	0.5	6.6	55.5	11.0	10.5
12	760	1400	207	30	0.2	1.0	10.5	25.1	28.0
44	760	1400	207	30	0.1	1.3	14.1	24.4	27.4
21	760	1400	172	25	0.3	3.3	43.8	30.7	27.0
47	815	1500	104	15	0.2	3.0	38.9	42.8	(1)
22	815	1500	104	15	0.3	3.5	46.2	36.1	(1)
48	815	1500	138	20	0.1	0.7	5.4	23.2	63.5

(1) Could not measure due to nature of fracture; %RA >50 (est.)

does not fit the pattern showing very poor rupture capability. Once before we have encountered low properties in higher aluminum content alloys[3]. In this case, two alloys containing 27% Al showed very low lives which have never been explained satisfactorily.

In an attempt to explain the lower properties of this alloy set, a series of additional analyses were performed. First, records of Phase I and II tests were examined for errors in stress or temperature. No errors were detected. Detailed fractography was performed to determine if some change in fracture mechanism had occurred. (For example, if grain boundary sliding and separation may have contributed to more rapid creep and rupture.) No difference between long and short lived specimens was apparent. It has been shown in internal studies that the presence of small amounts of beta eutectoid formers such as Fe, Ni, Cr, Co or Cu can dramatically lower creep rupture capability at relatively low levels in conventional alloys and possibly by analogy in alpha-two alloys. Commercial titanium specifications limit these elements to 0.05% maximum or at most, 0.1%). Selected specimens exhibiting short lives from the Phase II Ti-24Al-17Nb-1Mo alloy and the long lived Task 4 Ti-25Al-17Nb-1Mo specimen were analyzed. Except for iron, all elements were much less than 0.05% in all specimens. Iron contents were quite high (≈0.10-0.12%) but there were no differences between short and long life specimens. Thus, the role of chemistry or test error seems to be ruled out as possible causes for the low lives of the Phase II specimens. Metallographic examination revealed that microstructure of all specimens was similar (Figure 94). Thus, the low numbers cannot be explained at this time, but they seem to be atypical based on earlier results obtained in both this program and others.

4.3.5 Fatigue Testing

4.3.5.1 Experimental Details

Fifteen smooth fatigue specimens, of the type shown in Figure 95, were machined from each alloy. All testing was conducted using axial loading at a rate of 30 Hz (1800 cpm) and an R ratio of zero, i.e. a

Figure 94

Microstructure of Alloy 24 creep specimens. a) 73-1-88 with 26% aluminum (10 hours); b) 73-1A-88 with 24% aluminum (70 hours); Alloy 24 from Task 4 which contained 24.5% aluminum (476 hours).

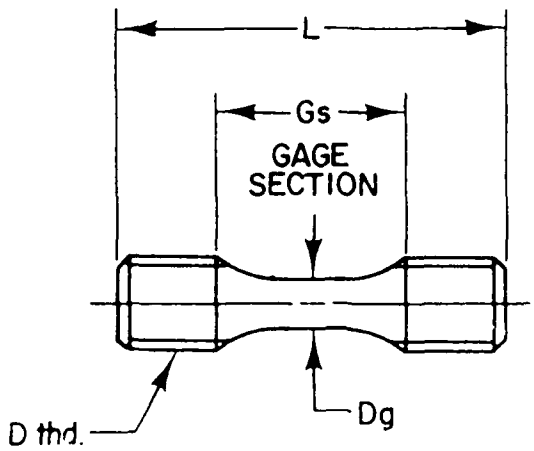

DRWG. NO.	REF. PRINT	L ref.	Gs	Dg	D thd.
MERL 2	MDL 4725	2.000	.960-.980	.249-.251	.500-20UNJF

Figure 95

Smooth fatigue specimen used to evaluate titanium aluminide alloys. Dg reduced to 0.198-0.202 after initial testing.

tension-release mode where the maximum stress is as shown and the minimum stress is zero. Most testing was conducted at 427°C (800°F) and 650°C (1200°F) but a limited number of specimens were run at RT and 815°C (1500°F). The majority of the specimens were machined from the "A" forgings. In the case of Alloy 24, this means that most of the specimens had an aluminum content of 24%; for Alloy 25, most of the specimens were beta forged and salt quenched, not solution treated and salt quenched. Several failures occurred in the specimen grips during the initial round of testing. To eliminate this problem, the gage diameter of the remaining specimens was reduced 1.3 mm (0.050 in). This approach was successful in preventing additional grip failures. Specimens which did not fail at the 10^6 cycle limit were uploaded in stress or temperature and tested under a different condition.

4.3.5.2 Results and Discussion

Prior to conducting the fatigue test program, the number of available specimens from the various alloy forgings and the aim of the testing were taken into consideration. Based on this evaluation, it was decided to establish a stress vs. cycles (S/N) curve for each major alloy at a minimum of two test temperatures. Primary temperatures selected were 427°C and 650°C (800°F and 1200°F). If a reasonable curve could be established at each temperature using four or five specimens, remaining specimens would be tested at 815°C (1500°F) and 21°C (70°F). Since previous attempts to test threaded alpha-two specimens at RT usually resulted in a high incidence of grip failures[4], room temperature testing was assigned low priority. In spite of the problems with the aluminum variation and heat treatment variation in Alloys 24 (73-1-88, 73-1A-88) and Alloy 25 (73-2-88, 73-2A-88), it was felt that treating each alloy as the group would give valid results. This was important because if these two alloys were tested as separate entities, the small number of specimens in 73-1-88 and 73-2-88 would severely limit testing flexibility and would allow only one curve to be established. When dealing with previously untested alloys, the approach used in establishing S/N curves is to select a stress and temperature at which

tensile strength is known, run the specimen to fracture or runout and adjust the next specimen accordingly. (Thus, it usually takes at least five specimens to delineate an S/N curve.) First, a review of available fatigue data for related alpha-two alloys with transformed beta microstructures revealed that there was little difference in runout stress for a wide range of compositions (Table 47). Thus, it was probable that the 2% aluminum difference between the Ti-26Al-17Nb-1Mo and Ti-24Al-17Nb-1Mo would have little or no effect on runout stress. Second, in the case of the alpha-two beta solution treated Ti-24Al-17Nb-.5Mo material, independent work conducted on conventional alloys at P&W showed that fatigue properties of alloys forged and annealed above the beta transus had similar fatigue lives as those forged above or at the beta transus and subsequently solution annealed below the transus. Thus, for Alloy 25, it was felt that testing all specimens as one group would be valid.

Complete test data for individual specimens of each alloy are presented in Tables 48, 49 and 50, respectively. Stress vs. cycle (S/N) curves for each alloy are plotted in Figures 96, 97 and 98. These curves do not reflect any grip failures and are plotted as a minimum line, i.e. all data points lie above the lines shown. It can be seen that there is little significant difference between the three alloys at the test temperatures evaluated. Also, in Alloys 24 and 25, the difference in aluminum content or heat treatment had no effect on fatigue lives. Existing fatigue data from alpha-two alloys are limited[1,3,4] but the comparison showed that the previous results had 10^6 cycle runout stress about 69 MPa (10 ksi) lower than Alloys 24, 25 and 26. This slight debit is most likely attributable to processing differences as the older data are from beta annealed and air cooled forgings, which exhibited a coarser platelet/colony type of microstructure in contrast to the finer Widmanstatten matrix of salt quenched alloys. Colony microstructures have been shown to be lower in fatigue capability than fine Widmanstatten structures. Conventional Ti-6Al-2Sn-4Zr-2Mo (w/o) alloy shown for comparison had similar runout stresses at least up to 427°C (800°F). It is likely that the conventional alloy would fall rapidly in capability above this temperature, however.

Table 47

Comparison of Fatigue Stress in MPa (Ksi)
to Reach 10^6 Cycles for Various Titanium Alloys

Alloy	Reference	Test Temperature °C (°F)			
		21 (70)	427 (800)	650 (1200)	815 (1500)
Ti-24Al-11Nb	1	-	414 (60)	-	-
Ti-25Al-5Nb	1	-	414 (60)	380 (55)	-
Ti-25Al-9Nb-2V	3	-	-	380 (55)	-
Ti-25Al-8Nb-1Hf	3	-	448 (65)	-	-
Ti-25Al-10Nb-3V-1Mo	4	-	-	518 (75)	-
Ti-25Al-17Nb-1Mo	-	690 (100)	483 (70)	470 (68)	-
Ti-24Al-17Nb-.5Mo	-	621 (90)	552 (80)	483 (70)	345 (50)
Ti-22Al-17Nb-1Mo	-	621 (90)	552 (80)	483 (70)	290 (42)
Ti-6242 Sheet*	-	552 (80)	483 (70)	-	-

*Aerospace Handbook

Table 48

Smooth Fatigue Test Results for Forged + Salt Quenched Ti-25Al-17Nb-1Mo (Alloy 24)(1)

Specimen Number(2)	Test Temp. °C	Test Temp. °F	Maximum Test Stress MPa	Maximum Test Stress Ksi	Specimen Life Cycles	Remarks
16	21	70	690	100	$>10^6$	Disc.; prev. tested to 10^6 cyc. @ 650°C (1200°F)
37	21	70	690	100	444,200	Grip failure; prev. tested to 10^6 @ 427°C (800°F)
14	427	800	483	70	908,800	Grip failure
17	427	800	483	70	$>10^6$	Broke on unloading from rig
33	427	800	552	80	304,100	Grip failure
35	427	800	690	100	171,200	
37	427	800	483	70	$>10^6$	Retested @ RT
38	427	800	690	100	294,700	
40	427	800	586	85	270,500	
16	427	800	828	120	5,300	Prev. tested to 10^6 cyc. @ RT and 650°C (1200°F)
13	650	1200	448	65	136,450	Grip failure
16	650	1200	483	70	$>10^6$	Retested @ RT & 650°C (1200°F)
18	650	1200	518	75	9,950	
32	650	1200	466	67.5	69,800	Grip failure
34	650	1200	518	75	70,300	Grip failure
36	650	1200	552	80	$>10^6$	Uploaded and rerun
36	650	1200	690	100	5,200	
39	650	1200	621	90	6,400	

(1) R = 0; Freq. = 30 HZ

(2) Specimens numbered 18 and lower from Ti-26Al-17Nb-1Mo composition (73-1-66); others from Ti-24Al-17Nb-1Mo composition (73-1A-88)

Table 49

Smooth Fatigue Test Results for Forged +[1] Salt Quenched Ti-24Al-17Nb-.5Mo (Alloy 25)

Specimen Number[2]	Test Temp. °C	Test Temp. °F	Maximum Test Stress MPa	Maximum Test Stress Ksi	Specimen Life Cycles	Remarks
33	21	70	690	100	855,900	Prev. tested to 10^6 cyc. @ 427°C (800°F)
16	427	800	518	75	469,700	Grip failure
18	427	800	552	80	$>10^6$	Uploaded
18	427	800	828	120	5,200	
33	427	800	586	85	$>10^6$	Retested @ RT
35	427	800	483	70	110,000	
36	427	800	552	80	$>10^6$	Retested @ 815°C (1500°F)
39	427	800	690	100	449,700	
13	650	1200	518	75	7,300	
14	650	1200	448	65	$>10^6$	Retested @ 815°C (1500°F)
15	650	1200	497	72	$>10^6$	Retested @ 815°C (1500°F)
17	650	1200	552	80	377,200	
32	650	1200	586	85	6,500	
34	650	1200	345	50	$>10^6$	Retested @ 815°C (1500°F)
37	650	1200	518	75	0	FOL. - cracked THD
38	650	1200	518	75	1,800	
40	650	1200	690	100	1,000	
36	815	1500	448	65	39,400	
14	815	1500	345	50	$>10^6$	
15	815	1500	345	50	669,400	

[1] R = 0; Freq. = 30 HZ

[2] Specimens numbered 18 and lower forged at 1038°C (1900°F); resolution treated at 1107°C (2025°F)/1/SQ to 815°C (1500°F)/30 min. Others forged 1176°C (2150°F) and salt quenched

Table 50

Smooth Fatigue Test Results for Forged + Salt Quenched Ti-22Al-17Nb-1Mo (Alloy 26)(1)

Specimen Number	Test Temp. °C	Test Temp. °F	Maximum Test Stress MPa	Maximum Test Stress Ksi	Specimen Life Cycles	Remarks
36	21	70	690	100	15,700	
16	427	800	621	90	194,600	Grip failure
33	427	800	483	70	$1,993_{6}400$	
34	427	800	552	80	$>10^6$	Uploaded
34	427	800	828	120	10,200	
37	427	800	690	100	0	FOL. cracked THD
38	427	800	690	100	1,500	
39	427	800	586	85	612,900	
40	427	800	518	95	$406_{6}400$	
13	650	1200	448	65	$>10^6$	Retested @ 815°C (1500°F)
14	650	1200	483	70	152,300	Grip failure
15	650	1200	518	75	$9_{6}000$	
17	650	1200	483	70	$>10^6$	Retested @ 815°C (1500°F)
18	650	1200	621	90	2,200	
32	650	1200	518	75	$10_{6}300$	
35	650	1200	552	80	$>10^6$	Retested @ 815°C (1500°F)
38	650	1200	690	100	1,500	
13	815	1500	448	65	55,400	
17	815	1500	380	55	21,400	
35	815	1500	483	70	14,500	

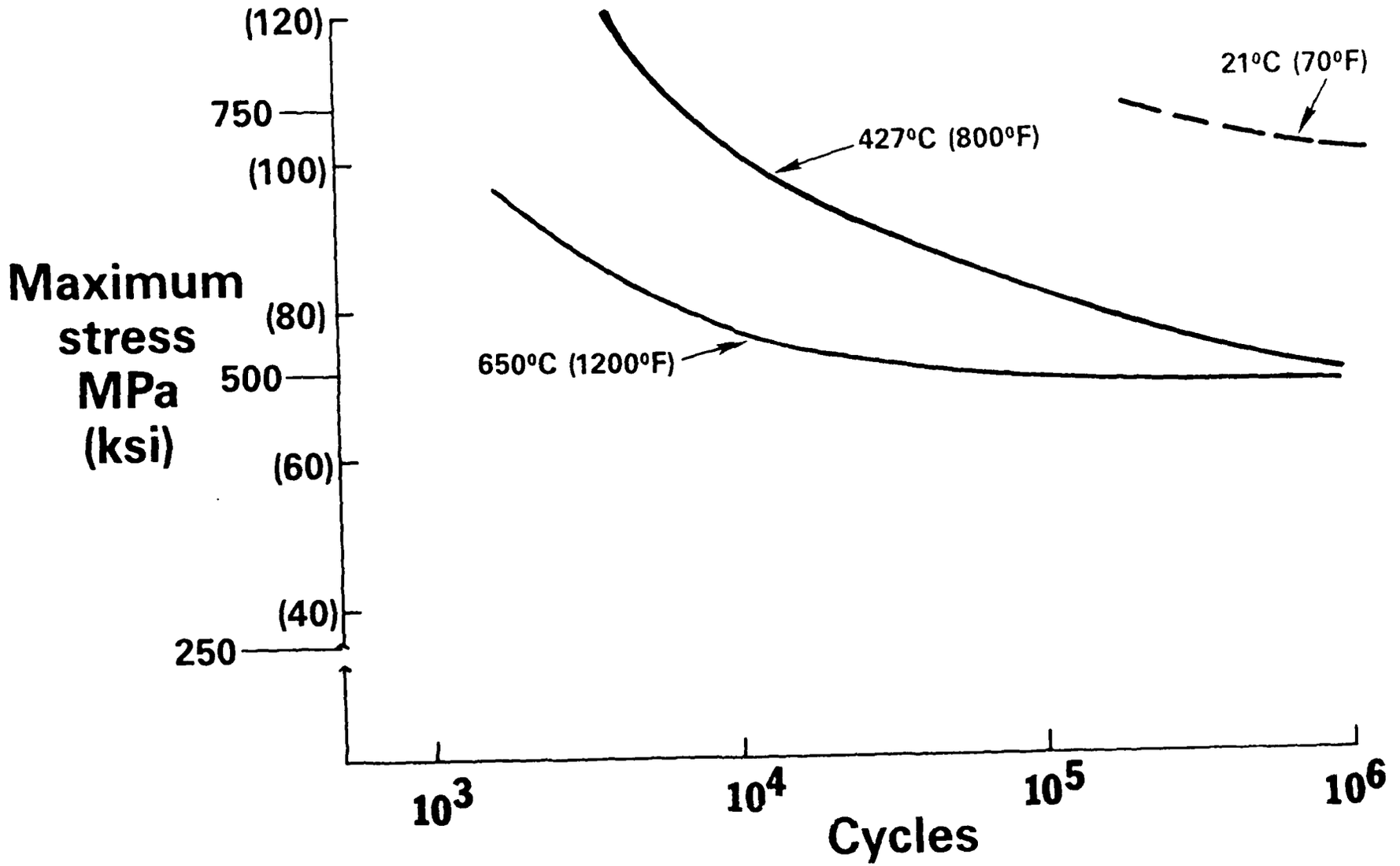

Figure 96

Smooth fatigue (S/N) curves for Ti-25Al-17Nb-1Mo Alloy 24 specimens.

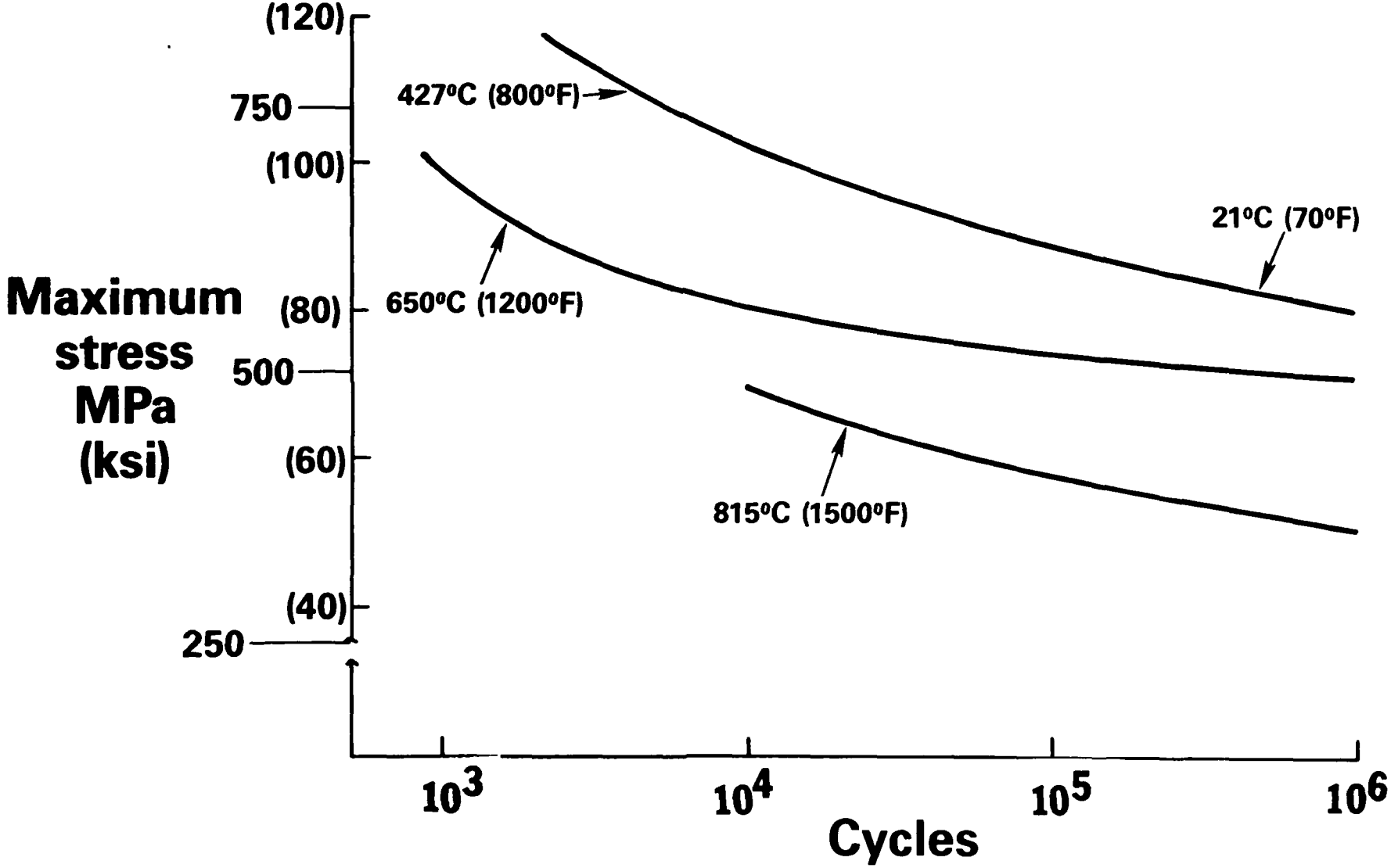
(120)
750
(100)
(80)
500
(60)
(40)
250
Maximum stress MPa (ksi)
427°C (800°F)
650°C (1200°F)
815°C (1500°F)
21°C (70°F)
10^3
10^4
10^5
10^6
Cycles

Figure 97

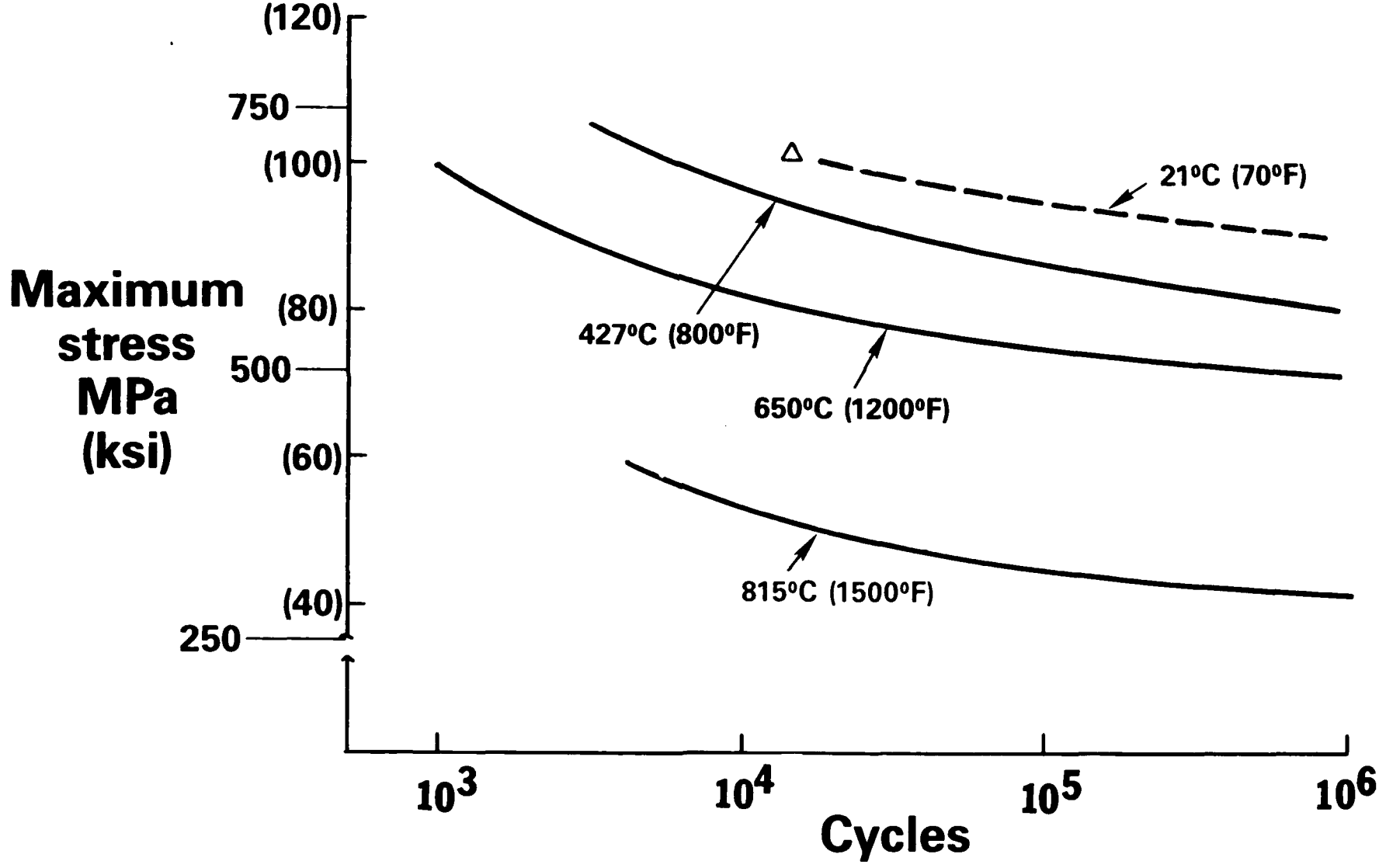

Figure 98

Smooth fatigue (S/N) curves for Ti-22Al-17Nb-1Mo Alloy 26 specimens.

In summary, it was found that the fatigue lives of the Phase II alloys were not substantially different than previous alloys, and that fracture toughness at room temperature does not have a strong effect on smooth fatigue life. It is probable that fracture toughness might have a stronger effect on notched fatigue capability. Most grip failures, which are indicative of notch sensitivity and low toughness, occurred in Alloy 24 specimens, which had the lowest toughness. Fatigue capability is probably adequate in these alloys to allow use in gas turbine components such as blades.

5.0 CONCLUSIONS AND RECOMMENDATIONS

And so we come to the end of an era. This is probably the last contribution by the authors to a series of programs on titanium aluminide alloy development, programs that date back to the mid 1970's. We do not mean to imply that there will be no further progress in titanium aluminide technologies, rather that we will no longer be participants. In the last part of this report, recent results are compared with the property levels achieved in alloys developed in the earlier studies. One can see from these comparisons that steady rather than spectacular progress has been made. We can note that although we have come close to achieving the rather simplistic goals, set over ten years ago, an alloy that meets all goals simultaneously remains elusive. Further, for a true engineering material, there is much additional characterization needed. Regretfully, there has been a tendency to devote quite large fractions of available resources to characterize non-optimum alloys.

Analysis of the data in this report leads to the following conclusions from Phase I of the project:

- Higher niobium levels (17-20%) increase ductility and toughness but tend to reduce creep rupture capability.

- Addition of lanthanum or rare earth elements resulted in the formation of large oxide particles often at primary beta grain boundaries. Slight gains in room temperature ductility are offset by major reductions in high temperature properties.

- In attempt to demonstrate definitively that toughness could be increased by deoxidation using rare earth element as a getter, a modified Ti-25Al-10Nb-3V-1Mo alloy containing 0.3% Er was converted to powder, consolidated and tested. A variety of process and heat treatment variations produced only marginal increases in toughness. In addition, the high temperature properties [650°C (1200°F)] were greatly reduced.

- In the first part of Task 1, addition of 2-4% molybdenum was found to be extremely effective in raising tensile and creep rupture strength. Fracture toughness was equivalent but room temperature ductility was poor compared to previously developed alloys such as Ti-25Al-10Nb-3V-1Mo.

- Chromium additions led to some gain in rupture properties, tungsten produced very little change while copper reduced lives.

- For a Ti-24.5Al-17Nb alloy, a fine transformed beta structure gave a better balance of properties than a coarser acicular structure. Strength increases of almost a factor of two were accompanied by no loss in ductility, toughness or creep strength.

- For a Ti-25Al-10Nb-4Mo alloy, isothermal beta forging followed by direct isothermal transformation at 815°C (1500°F) gave superior properties to a beta solution treat and age. In the latter condition, the alloy was brittle to 650°C (1200°F), while isothermal transformation gave good strength and creep capability with some ductility. The improvement was due, in part, to the finer grain size of the isothermally transformed material.

- A more radical approach to increase toughness was by the introduction of ductile crack stoppers in a more brittle aluminide matrix. Candidate ductile alloys were screened and Ti-15Al-22Nb was selected. This alloy, when blended in powder form with Ti-25Al-10Nb-4Mo powder and consolidated, produced toughness increases of up to 16.5 MPa$\sqrt{\text{meter}}$ (15 ksi$\sqrt{\text{inch}}$). Although the toughness of the blended powder mixtures was increased, major reductions in tensile and creep properties over the baseline alloy were measured.

In the final part of Phase I, an attempt was made to combine the several factors identified that improved toughness. Conclusions from Task 4 are as follows:

- Various combinations of alloys were blended in powder form to determine whether improved toughness could be coupled with adequate high temperature properties. Extensive interdiffusion between the particles pointed to the need for better chemical matching between the blended alloys. The large reaction zones probably caused the rather poor property levels found.

- A balanced set of properties was obtained for the Alloy 24 composition (Ti-24.5Al-17Nb-1Mo) isothermally forged from ingot and transformed in 815°C (1500°F) salt. Excellent strength and creep rupture levels were combined with intermediate toughness and ductility. The same alloy fabricated from powder had slightly less attractive properties which can be traced to the higher aluminum content.

Phase II of the program selected three alloys with varying aluminum, niobium and molybdenum levels for detailed evaluation. The alloys were prepared as VAR ingot, isothermally forged to pancakes in the beta field and quenched directly into salt. Based on the results, we conclude:

- Tensile properties met or exceeded goal requirements in all alloys. Ductility, at room temperature, generally exceeded two percent and increased as aluminum content was reduced.

- None of the alloys achieved the goal toughness level of 33 MPa$\sqrt{\text{meter}}$ (30 ksi$\sqrt{\text{inch}}$). The highest value was 29.4 MPa$\sqrt{\text{meter}}$ (26.7 ksi$\sqrt{\text{inch}}$). Toughness increased quite rapidly with temperature and the low aluminum alloys would probably achieve goal levels at 200°C (400°F). There is a strong correlation between tensile ductility and toughness. Empirical relationships were developed to describe the toughness result as a function of composition and temperature.

- Charpy impact results paralleled those for fracture toughness. While improved over earlier alloys, the initial values at temperatures less than 260°C (500°F) remain quite low.

- Creep rupture lives of Phase II alloys underwent a major, as yet unexplained, decrease compared to those measured for similar alloys in Phase I or in earlier development programs. It remains clear that rupture capability increased with increasing molybdenum and aluminum content. For aluminum, the optimum rupture resistance seemed to occur between 24-25% while a molybdenum level of about 2% offered a high rupture life with a good balance of other properties.

Recommendations:

- There is no simple approach for further alloy development. Some factors that should be included in any future program include:

  - A more detailed study of thermomechanical processing.
  - Clarification of the molybdenum effect.
  - Evaluation of elemental additions that can improve creep properties at intermediate temperatures.

- Prospects for useful rapidly solidified dispersion containing alpha-two alloys look bleak. It does not seem that further work on rare earth (and related) elements or oxides is warranted.

- "Phase blending" as a toughening approach appears to have some merit. Any futher evaluation should concentrate on minimizing interface reaction and establishing the property characteristics needed to retard or arrest cracks. Obviously, it is also essential to find additions that do not degrade other desirable characteristics of the host phase (creep, modulus, etc.).

REFERENCES

1. Blackburn, M. J. and Smith, M. P., "Research to Conduct an Exploratory Experimental and Analytical Investigation of Alloys," AFML TR-78-18, March 1978.

2. Blackburn, M. J. and Smith, M. P., "Research to Conduct an Exploratory Experimental and Analytical Investigation of Alloys," AFWAL-TR-80-4175, November 1980.

3. Blackburn, M. J. and Smith, M. P., "Research to Conduct an Exploratory Experimental and Analytical Investigation of Alloys," AFWAL-TR-81-4046, June 1981.

4. Blackburn, M. J., Hill, J. T. and Smith, M. P., "R&D on Composition and Processing of Titanium Aluminide Alloys for Turbine Engines," AFWAL-TR-82-4086, July 1982.

5. Blackburn, M.J. and Smith, M. P., "The Understanding and Exploitation of Alloys Based on the Compound TiAl (Gamma), AFML-TR-79-4056, May 1979.

6. Rhodes, C. G., Evans, A. G. and Paton, N. E., "Study of Intermetallic Compounds," AFML TR-76-105, June 1976.

7. Sastry, S.M.L., et al, "Rapid Solidification and Powder Metallurgical Processing of Titanium Alloys," Paper Presented at 1984 International Powder Metallurgy Conference, 17-22 June.

8. Sastry, S.M.L., et al, "Rapid Solidification Processing of Titanium Alloys," Journal of Metals, V35, No. 9, September 1983, pp. 21-28.

9. Sastry, S.M.L., et al, "Structure and Properties of Rapidly Solidified Dispersion Strengthened Titanium Alloys (Part 1 and 2)," Met Trans A Vol. 15A, July 1984, pp. 1451-1474.

REFERENCES

(Continued)

10. Rowe, R. C., et al, "Dispersion Modification of Ti_3Al-Nb Alloys," Mat. Res. Soc. Symp. Proc., Vol. 48 (1986).

11. Anderson, R. E., et al, "High Temperature Titanium Alloys," Contract F33657-86-C-2211, Final Report to be Published.

12. Cowles, B. A. and Deluca, D. P., "Fatigue and Fracture of Titanium Aluminides," Contract F33615-85-C-5029, Final Report to be Published.